DIPARTIMENTO SCIENZE DELLA VITA

DOTTORATO DI RICERCA IN SCIENZE DELLA VITA

CICLO XXXIV

COORDINATORE Prof. Massimo Valoti

NUTRACEUTICAL PROPERTIES OF EXTRA-VIRGIN OLIVE OILS AND LEAVES EXTRACTS FROM AUTOCHTHONOUS TUSCAN OLIVE TREES

SETTORE SCIENTIFICO-DISCIPLINARE: CHIM/08

TUTOR: Prof. Marco Macchia

DOTTORANDA: Dott.ssa Jasmine Esposito Salsano

Jasmine Esposito Salsano

A.A. 2021-2022

Table of Contents

List of Abbreviations

ACE	Angiotensin Converting Enzyme
AD	Alzheimer's Disease
AKT	Protein Kinase B
AT	Adipose Tissue
CAT	Catalase
COL1A1	Collagen Type I Alpha 1 Chain
COX	Cyclooxygenase
CXCL	C-X-C Motif Ligand
DPPH	1,1-diphenyl-2-picrylhydrazyl
DSS	Dextran Sodium Sulfate
DW	Dry Weight
DXR	Doxorubicin
EAE	Experimental Autoimmune Encephalomyelitis
ECM	Extracellular Matrix
EFSA	European Food Safety Authority
EGF	Epidermal Growth Factor
eNOS	Endothelial Nitric Oxide Synthase
EPCs	Endothelial Progenitor Cells
ERK	Extracellular Signal-Regulated Kinases
EtOAc	Ethyl Acetate
EVOO	Extra-Virgin Olive Oil
FAs	Fatty Acids
FAMEs	Fatty Methyl Esters
FCR	Folin-Ciocalteu's Phenol Reagent
FT-IR	Fourier-Transform Infrared Spectroscopy
GAE	Gallic Acid Equivalent
GDX	Glutathione Reductase
GHS	Glutathione
GM-CSF	Granulocyte-Macrophage-Colony-Stimulating Factor
GPX	Glutathione Peroxidase
GSH	Reduced Glutathione
HBD	Human Beta Defensin
HDACs	Histone Deacetylases
HSCs	Hepatic Stellate Cells
Hsp	Heat Shock Protein
HT	Hydroxytyrosol
HUVECs	Human Umbilical Vein Endothelial Cells
IL	Interleukin
iNOS	Inducible Nitric Oxide Synthase
IOC	International Olive Council
IP	Itraperitoneal
IRI	Ischemia Perfusion Injury
IS	Internal Standard
KDR	Kinase Insert Domain Receptor
KOH	Potassium Hydroxide
LC-MS	Liquid Chromatography-Mass Spectrometry

LOD	Limit Of Detection
LOQ	Limit Of Quantification
LOX	Lipoxygenase
LPS	Lipopolysaccaride
LRP	Lipoprotein Receptor-Related Protein
M-CSF	Macrophage Colony-Stimulating Factor
MCP	Monocyte Chemoattractant Protein
MIP	Macrophage Inflammatory Protein
miRNA	microRNA
MMP	Matrix Metalloproteinase
mRNA	Messenger RNA
mTOR	Mammalian Target of Rampicin
MUFA	Mono-Unsaturated Fatty Acid
NF	Nuclear Factor
NMR	Nuclear Magnetic Resonance
NMSC	Non-Melanoma Skin Cancer
NO	Nitric Oxide
NOX	Nicotinamide Adenine Dinucleotide Phosphate (NADPH) Oxidase
OA	Oleocanthalic Acid
OC	Oleacein
OL	Oleuropein
OLE	Olive Leaves Extract
OO	Oleocanthal
ORE	Oleuropein-Rich Extract
oxLDL	Oxidized Low Density Lipoprotein
P-gp	P-glycoprotein
P(VDF-TrFE)	Poly(vinylidenefluoride-co-trifluoroethylene)
PARP	Poly(ADP-ribose) Polymerase
PBS	Phosphate Buffered Saline
PHB/PHOHD	Polyhydroxybutyrate/poly(hydroxyoctanoate-co-hydroxydecanoate)
PHBHV	Poly(3-hydroxybutyrate-co-3-hydroxyvalerate)
PPARγ	Peroxisome Proliferator-Activated Receptor-γ
PUFA	Poly-Unsaturated Fatty Acid
RNS	Reactive Nitrogen Species
ROO$^{\bullet}$	Peroxyl Radical
ROS	Reactive Oxygen Species
SEM	Scanning Electron Microscopy
SFA	Saturated Fatty Acid
SGBS	Simpson-Golabi-Behmel Syndrome
SOD	Superoxide Dismutase
STAT	Signal Transducer and Activator of Transcription
T	Tyrosol
TE	Trolox Equivalent
TGF	Transforming Growth Factor
TIMP	Tissue Inhibitor of Metalloproteinases
TLC	Thin Layer Chromatography
TNF	Tumour Necrosis Factor
TP	Total Polyphenols

TPC	Total Phenolic Content
UC	Ulcer Colitis
VEGF	Vascular Endothelial Growth Factor
VOO	Virgin Olive Oil
α-SMA	α-Smooth Muscle Actin

1 INTRODUCTION

1.1 General Introduction

1.1.1 Botanical Description of *Olea europaea* L.

Olea europaea L. is a small tree belonging to the *Oleaceae* family and typical of Mediterranean Basin (Figure 1).

Figure 1 - Illustration of Olea europaea L. (Köhler's Medizinal-Pflanzen, 1887, Franz Eugen Köhler).

Olive tree is a very long-lived plant that can easily live several hundreds of years thanks to its ability to regenerate the damaged epigeal and hypogeal systems, and it can reach 8-15 meters in height (Figure 2**A**). It is an evergreen plant, in facts, its vegetative phase is almost continuous throughout the year, with only a slight decrease in the winter period. The greyish trunk is cylindrical in shape and very straight initially, but over the years becomes more irregular and gnarled, forming cavities (Figure 2**B**). Olive leaves are persistent and leathery with an opposite arrangement and an internal margin slightly revolute (Figure 2**C**). They are dark green on the front side (Figure 2$\mathbf{C_1}$) and whitish or silvery on the back side due to the presence of scaly, lanceolate or oval-oblong hairs (Figure 2$\mathbf{C_2}$). The flowers, arranged in axillary racemes, are small and white, they have a persistent calyx and gamopetaly and deciduous corolla (Figure 2**D**). The indehiscent fruit (olive) is a glossy ellipsoid drupe, green when unripe (Figure 2$\mathbf{E_1}$) and black-purplish when ripe

(Figure 2**E$_2$**). The drupe is characterized by an oily mesocarp and woody endocarp containing mainly one seed (Figure 3).

Olea europaea subsp. *europaea,* includes the var. *sylvestris*, which represents the wild olive tree characterized by branches and small fruits which produce low amount of oil and the var. *europaea*, constituted by the cultivated olive tree, which produces edible fruits.

Despite *Olea europaea* L. is a widespread cultivation, about 98% of the world total crops are in the Mediterranean Basin. Spain, Italy, Greece and Portugal are the main producers of olive oil, as reported by International Olive Council (IOC).[1]

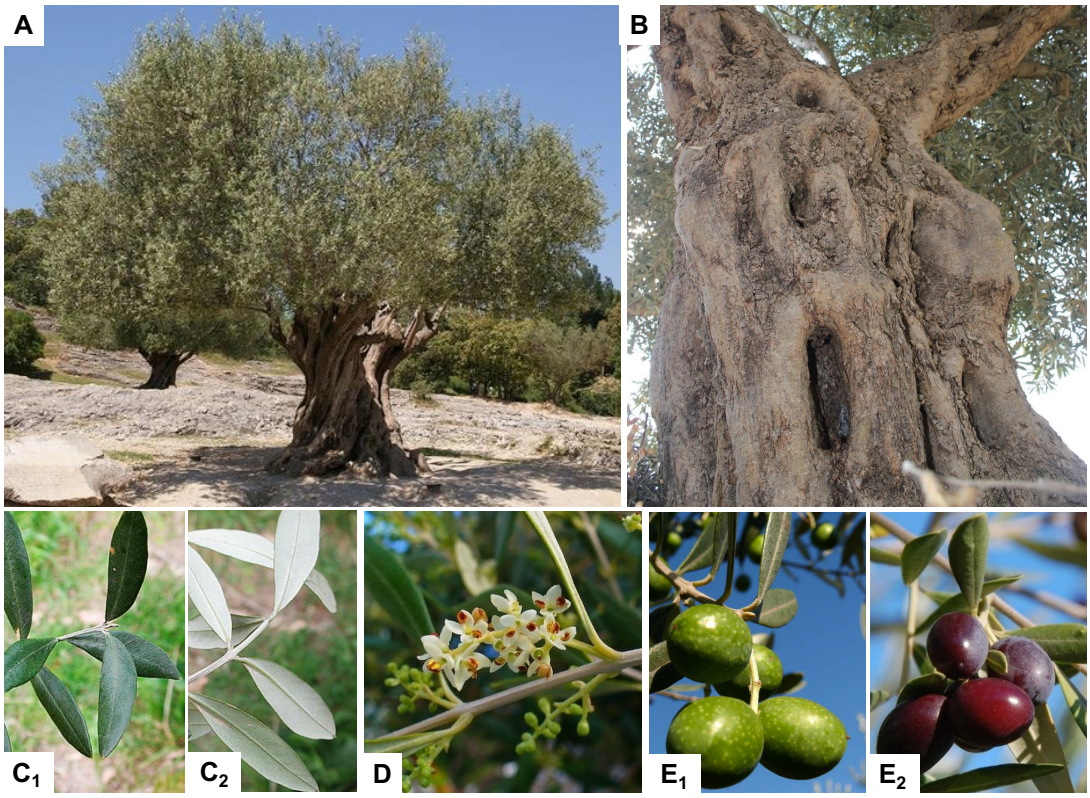

*Figure 2 – Olive tree (**A**), trunk (**B**), leaves front side (**C$_1$**) and back side (**C$_2$**), flowers (**D**), unripe (**E$_1$**) and ripe (**E$_2$**) olives.*

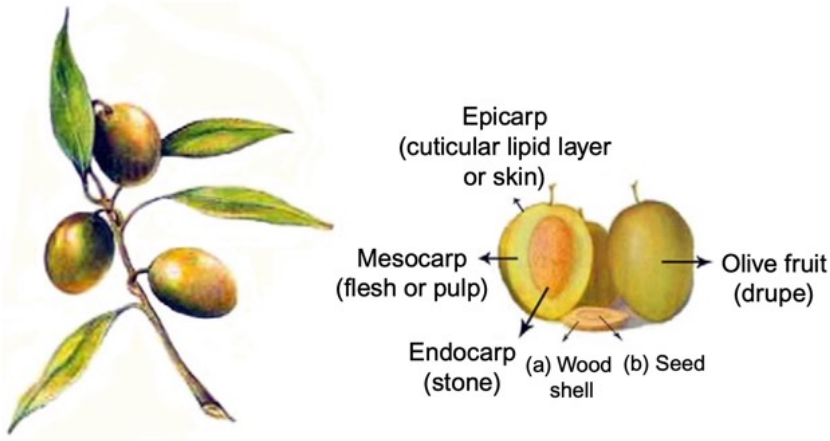

Figure 3 – Cross-section of olive tree fruit (Olea europaea L.).[2]

1.1.2 Olive Oils Production

The extraction of olive oil represents an industrial process of agri-food transformation which aims to obtain oil from the drupes of the olive tree. The oil is contained within the mesocarp cells of the olive from which it is extracted and separated. The olive oil production involves several steps as here reported (Figure 4).[3]

- Olive harvesting and cleaning

Identifying the optimal period for harvesting olives is essential to obtain oil with high yield and good quality. Successively, olives are controlled to eliminate damage fruits, leaves, pieces of wood and branches, and then washed, to remove dust and soil.

- Olive milling

During the milling process, olives are broken to provoke the release of oil from their pits, skins, pulp cells and vacuoles. The product of this phase, called “olive paste”, is a semiliquid mixture which contains a solid fraction (from pit shell and pulp) and a liquid fraction constituted by two immiscible liquids: water and oil.

- Olive paste malaxation

Malaxation consists of a slow and continuous mixing of the olive paste to break the water-oil emulsions and to make the separation of the oil in the next phase easier. Time and temperature influence this operation which typically is performed for 20-40 minutes at 27°C.

- Centrifugal separation

After the milling and the malaxation processes, olive paste is made of three phases characterized by different density, *i.e.* solid phase, aqueous phase and oil phase, which need to be separated in order to obtain oil. The separation was performed by using three-phase or two-phase decanter.

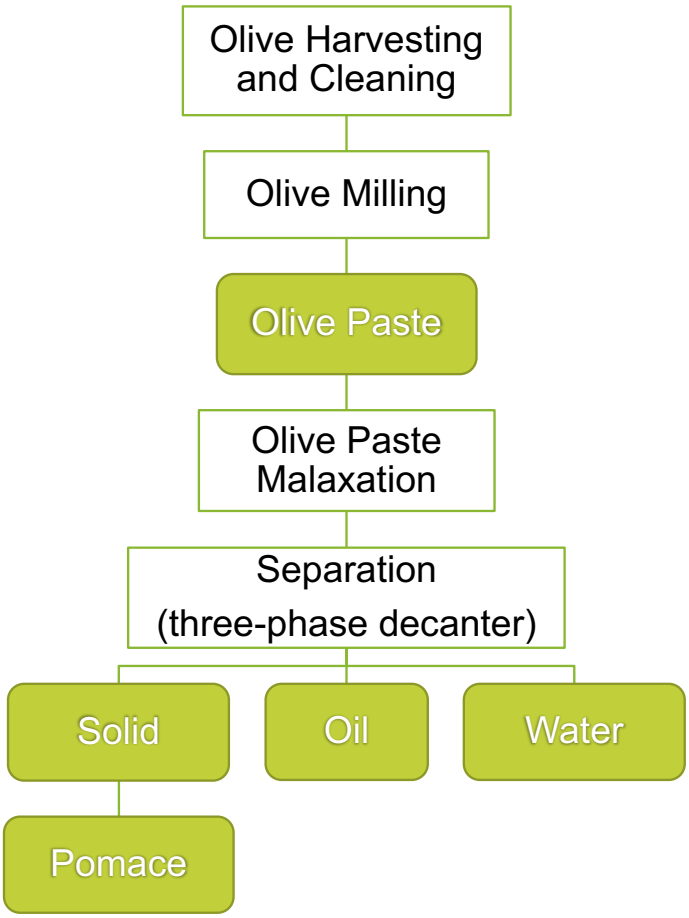

Figure 4 – Scheme of olive oils production (by using three-phase decanter).

1.1.3 Olive Oils Classification

Olive oils are classified in different categories, as reported in Figure 5.

Virgin olive oils are distinguished from other oils by main prerogatives concerning the quality and type of the raw materials, which must be exclusively pulp of the olives, and the extraction method, which must be represented by an exclusively mechanical process without use of any chemical method and a conspicuous increase in temperature. These kinds of oils are distinguished by European Legislation, in three types based on chemical and sensory standards:

- Extra-virgin olive oil (EVOO) is a flavourful and tasty oil, and sometimes it has bitter and pungent notes. It represents the oil with the highest quality and the lowest free acidity compared with other oils. Its free acidity level is below 0.8 g for 100 g of oils (0.8%). It is suitable for human consumption, and it is endowed with health and nutraceutical properties.
- Virgin olive oil (VOO) is also suitable for human consumption. This oil can reach a maximum of 2.0% free acidity value.
- Lampante virgin olive oil is an oil derived from bad fruits or careless processing and it is endowed with the lowest quality. Its level of free acidity is more than 2.0% and for this reason this oil is not suitable for human consumption, but it can become edible after refining processes, as “refined olive oil”.

After the milling process, it is possible to also obtain the *pomace,* a residue containing small amounts of oil which could be extracted only though chemical processes, obtaining the “raw pomace olive oil”. This oil can be made suitable for human consumption after a refining process, becoming a “refined pomace olive oil”.

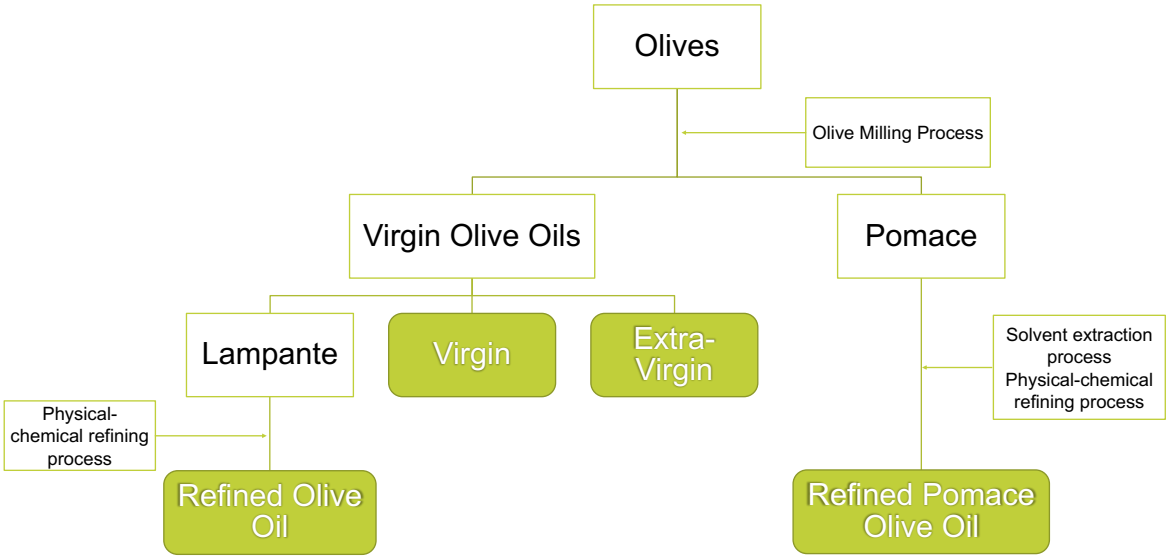

Figure 5 – Different categories of olive oil. In green boxes are reported the olive oils suitable for human consumption.

1.2 Extra-Virgin Olive Oil

EVOO is considered a key food in Mediterranean Diet, and it is placed at the basis of the Mediterranean Diet Pyramid (Figure 6) as main source of lipids and then the nutriment to be daily taken. Its physico-chemical quality and its organoleptic characteristics are strictly defined by European laws.

EVOO consumption in Mediterranean diet has been correlated with beneficial effects on human health including reduction of cardiovascular and related diseases, chemoprevention, modulation of inflammatory and immune responses and reduction of neurological disorders. These properties are linked to its chemical composition, and in particular to its fatty acid (FA) profile and phenolic composition.[4]

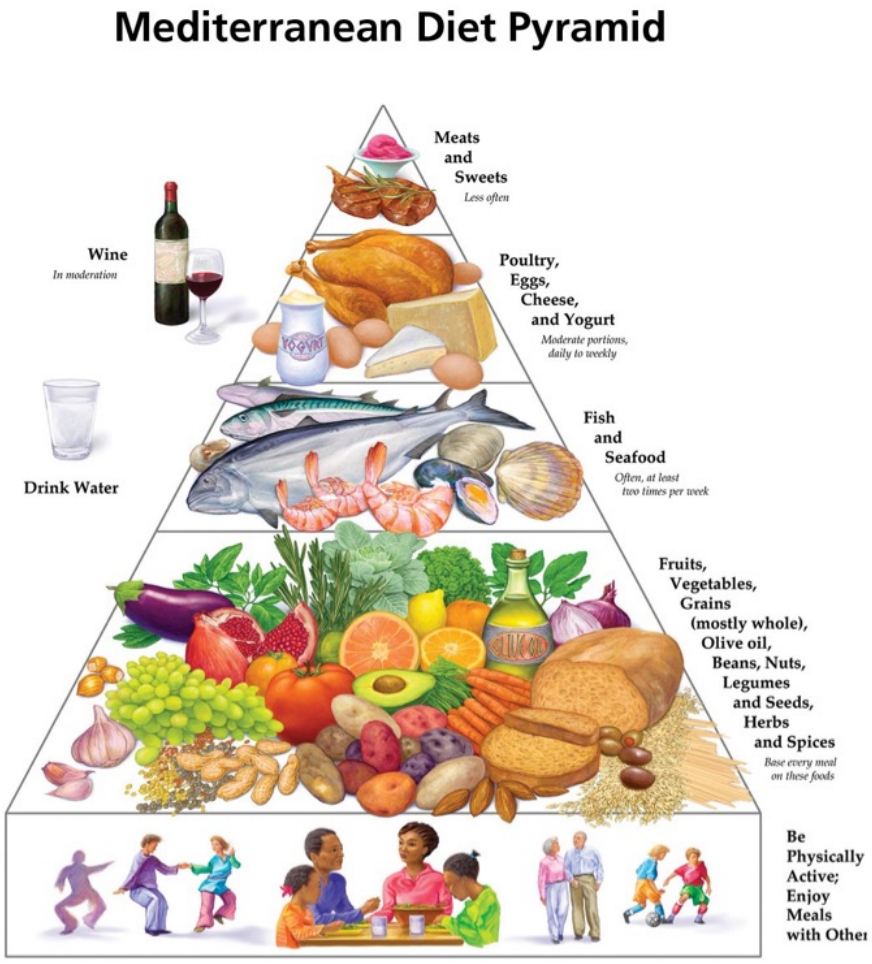

Figure 6 – Mediterranean Diet Pyramid (Make Every Day Mediterranean: An Oldways 4-Week Menu Plan, 2019, E-BOOK).

1.2.1 Chemical Composition

The chemical composition of EVOO is influenced by numerous factors such as variety of the plant (*Cultivar*), climatic conditions, agronomic techniques and reaping and conservation of the fruit. Chemically EVOO consists of a mixture of triglycerides and FAs (97-99%) and of a mixture of minor components which can be liposoluble, amphiphilic or polar compounds (1-3%), in addition to a very small quantity of water. The balanced content in FAs (oleic acid, ω3 and ω9), vitamin E and phenolic compounds is crucial for its beneficial properties in human health.[3]

1.2.1.1 Triglycerides and Fatty Acids

Olive oil consists almost entirely of triglycerides (about 97-99%) which are constituted by glycerol linked to three FAs through an ester bond. Triglycerides are mostly found in the pulp of olive and contain saturated FAs (SFAs), mono-unsaturated FAs (MUFAs) and poly-unsaturated FAs (PUFAs). The most important FAs are the MUFA oleic acid, (~60-80%), the PUFAs linoleic acid (~3-20%), and α-linolenic acid (~0.5-2%), the SFAs palmitic (~15%) and stearic acids (~5%). Moreover, there are small percentages of free FAs directly related to the acidity value of EVOO, as well as diglycerides (~2-3%) and monoglycerides (~0.1-0.2%), all derived from the hydrolysis process of triglycerides. It is possible also to find 1,2-diglycerides which derived from incomplete biosynthesis of triglycerides and 1,3-diglycerides, produced from triglycerides by hydrolysis reaction.

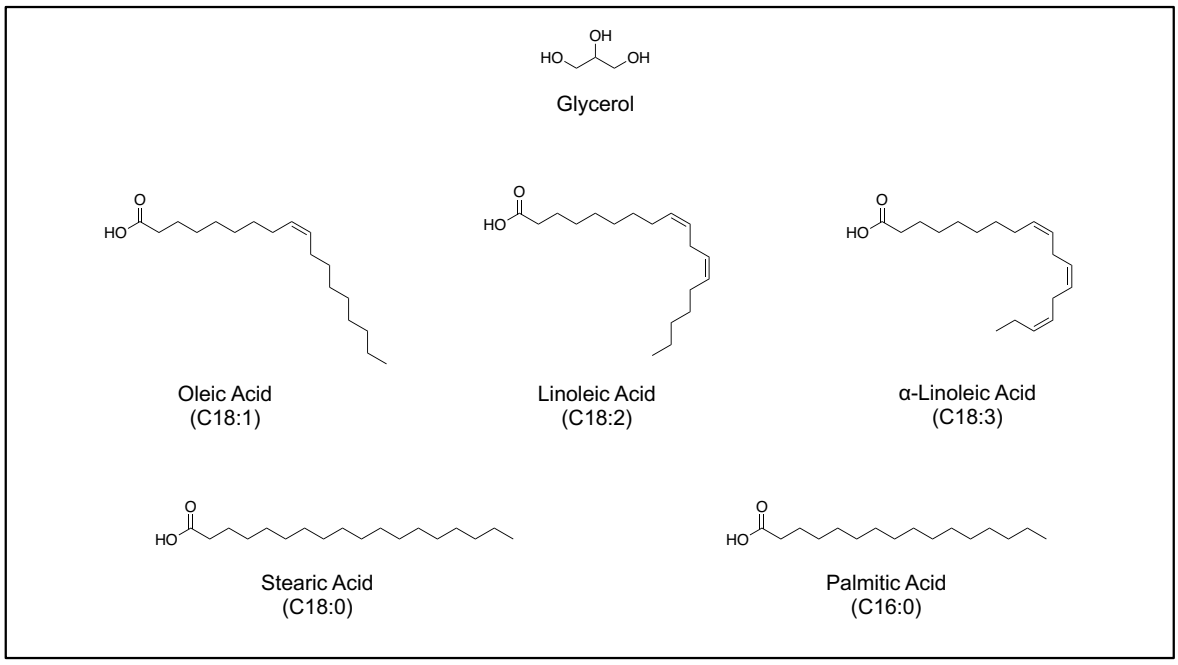

Figure 7 – Chemical structures of glycerol and the main fatty acids which constitute the triglycerides in EVOO.

Unsaturated FAs are essential for the diet and must be provided directly by food, as they cannot be synthesized by our body or can only be synthesized in limited quantities. In particular, linoleic and α-linolenic acids are considered "essential fatty acids". Triglycerides and the products of their transformation after ingestion, carry out a regulatory action of important physiological functions, such as platelet aggregation, maintenance of blood pressure and muscle contraction. They also perform plastic functions in tissues and organs, as constituents of cell membranes; functional actions, as precursors of prostaglandins; structural role (*e.g.* in skin, nervous system); antioxidant action. Moreover, they are precursors of hormones and exert an important role in the intestinal absorption of vitamins. Epidemiological studies, that aimed at identifying correlations between different diets and incidence of coronary heart disease and mortality, highlighted a close relationship between olive oil consumption in the Mediterranean Diet and reduction of cholesterolemia, atherosclerosis and cardiovascular diseases. In particular, oleic acid is considered an ideal food component able to reduce the levels of low-density lipoprotein (also called bad cholesterol) and increase the levels of high-density lipoprotein (also called good cholesterol) preventing the formation of lipid plaques on the arterial walls.[3]

Concerning MUFAs and PUFAs present in EVOO, the European Food Safety Authority (EFSA) approved some health claims providing authorized health indications, conditions and restrictions of use, as reported in Table 1 (Commission Regulation (EU) 432/2012).[5–8]

Table 1 – List of permitted health claims for oleic acid and monounsaturated and/or polyunsaturated fatty acids of olive oil and the relative conditions of use.[5]

Food or Food Constituents	Health Claim	Condition
Oleic acid	Replacing saturated fats in the diet with unsaturated fats contributes to the maintenance of normal blood cholesterol levels. Oleic acid is an unsaturated fat.	The claim may be used only for food which is high in unsaturated fatty acids, as referred to in the claim high unsaturated fat as listed in the Annex to Regulation (EC) No 1924/2006 and subsequent amendments A claim that a food is high in unsaturated fat, may only be made where at least 70 % of the fatty acids present in the product derive from unsaturated fat under the condition that unsaturated fat provides more than 20 % of energy of the product.
Monounsaturated and/or polyunsaturated fatty acids	Replacing saturated fats with unsaturated fats in the diet has been shown to lower/reduce blood cholesterol. High cholesterol is a risk factor in the development of coronary heart disease	The claim may be used only for food, which is high in unsaturated fatty acids, as referred to in the claim high unsaturated fat as listed in the Annex to Regulation (EC) No 1924/2006 and subsequent amendments. The claim may only be used on fats and oils

1.2.1.2 Minor Compounds

Minor compounds present in EVOO represent 1-3% of the oil weight and include about 200 chemical compounds belonging to different classes such as saturated and unsaturated hydrocarbons (~50-60%), aliphatic and triterpenic alcohols (~20-35%), phytosterols (~1-2%), pigments (~1-2%), phenols (~18-37%), tocopherols (~2-3%) and other substances (*e.g.* aldehydes, ketones, esters). These compounds can be polar, non-polar or amphiphilic and they exert mainly antioxidant and scavenging activity of reactive oxygen species (ROS) and reactive nitrogen species (RNS).

Among *hydrocarbons*, the most abundant component in EVOO is squalene (2-7 mg/g), a molecule with a triterpene structure, with numerous unsaturation that plays a key role in biosynthesis, absorption and elimination of cholesterol, exerting an hypocholesterolemic effect.[9] In some studies, the antioxidant and the chemopreventive activities of squalene have been proved.[9,10] Its antiproliferative

capacity in different kinds of cancer cells, such as colon, breast and prostate cancer cells was demonstrated.[9] Squalene exerts also a protective role in skin against UV radiations.[9,10] The chemical structure of squalene is reported in Figure 8.

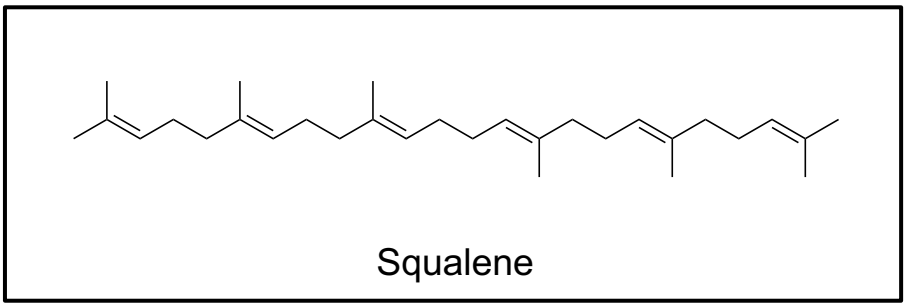

Figure 8 – Chemical structure of squalene.

Vitamin E is a fat-soluble vitamin which exists in different isoforms including tocopherols and tocotrienols. The main isoform, used by human body and contained in EVOO, is represented by α-tocopherol (generally called vitamin E, Figure 9). α-tocopherol is a lipophilic molecule endowed with antioxidant properties and thus involved in neutralizing lipid peroxyl radicals and superoxide anion radicals.[11,12] In particular, it bears an important role in EVOO, decreasing the lipids peroxidation and so maintaining its stability.[12] The health claim relating to vitamin E of olive oil approved by EFSA is reported in Table 2.[5,13]

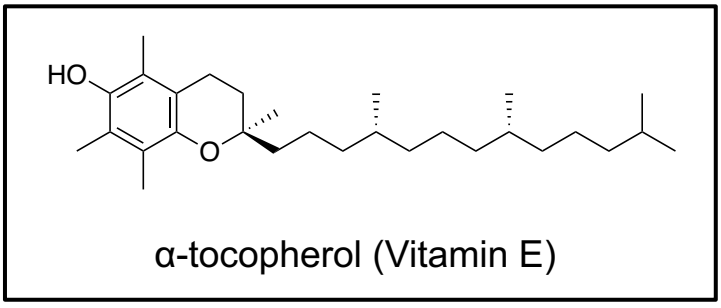

Figure 9 – Chemical structure of α-tocopherol (vitamin E).

Table 2 – List of permitted health claim for vitamin E of olive oil and the relative conditions of use.[5]

Food or Food Constituents	Health Claim	Condition
Vitamin E	Vitamin E contributes to the protection of cells from oxidative stress.	The claim may be used only for food which is at least a source of vitamin E as referred to in the claim source of vitamin e as listed in the Annex to Regulation (EC) No 1924/2006 and subsequent amendments.

Phenolic compounds, even if present in small quantities in EVOO, are endowed with numerous nutraceutical properties. Indeed, EFSA recently approved a health claim on olive oil polyphenols (Commission Regulation (EU) 432/2012), as reported in Table 3.[5,14]

Table 3 – List of permitted health claim for polyphenols of olive oil and the relative conditions of use.[5]

Food or Food Constituents	Health Claim	Condition
Olive oil polyphenols	Olive oil polyphenols contribute to the protection of blood lipids from oxidative stress.	The claim may be used only for olive oil which contains at least 5 mg of hydroxytyrosol and its derivatives (*e.g.* oleuropein complex and tyrosol) per 20 g of olive oil. In order to bear the claim information shall be given to the consumer that the beneficial effect is obtained with a daily intake of 20 g of olive oil.

Among phenolic compounds present in EVOO, secoiridoid derivatives, lignans, phenyl-alcohols (or phenolic alcohols), phenyl-acids (or phenolic acids) and flavonoids, can be distinguished.

Secoiridoids are the most important class of phenolic compounds in EVOO and they are present exclusively in plants belonging to *Oleaceae* family. Secoiridoids derive from an enzymatic degradation that occurs in EVOO during the mechanical extraction process. In particular, the glycoside forms of oleuropein and ligstroside are hydrolysed by the endogenous β-glucosidase producing secoiridoid derivatives. Moreover, phenolic compounds are oxidised by oxidoreductases, like polyphenoloxidases and peroxidases. Indeed, secoiridoids are classified as hydroxytyrosol (HT) and tyrosol (T) derivatives linked to elenolic acid or as oleuropein and ligstroside derivatives. In fresh EVOOs the dialdehydic form of decarboxymethyl oleuropein aglycone (oleacein, OC), and the dialdehydic form of decarboxymethyl ligstroside aglycone (oleocanthal, OO) are the main

representative secoiridoids. Other secoiridoids such as oleuropein aglycone and ligstroside aglycone, could be detectable.

Lignans, such as pinoresinol and 1-acetoxypinoresinol represent, after secoiridoids, the most abundant class of phenolic compounds in EVOO.

Moreover, in EVOO it is possible to found *flavonoids* (*e.g.,* luteolin and apigenin), *phenyl-acid* (*e.g.,* caffeic, ferulic, *p*-coumaric and vanillic acids) and *phenyl-alcohols*, among which HT and T are the most representative.

The chemical structures of the most important molecules cited are reported in Figure 10.

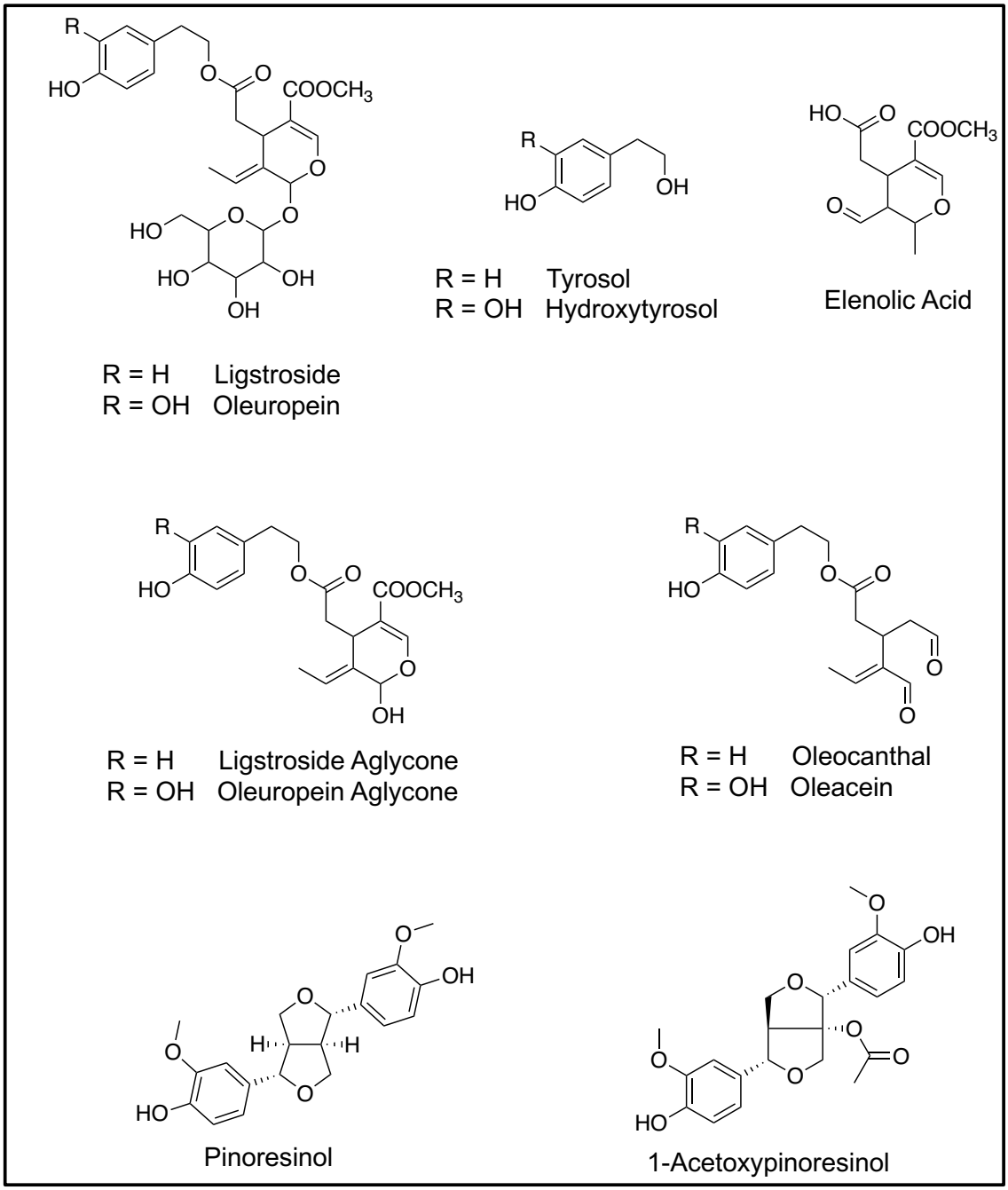

Figure 10 – Chemical structures of the phenolic compounds cited.

1.2.2 Variation of Chemical Composition of Olive Oil

Generally, EVOO shelf-life ranges roughly from 9 to 18 months, as long as its stability is influenced by degradative processes depending on internal factors (chemical composition) and external factors (*e.g.* presence of pro-oxidants agents).[12]

As concerns triglycerides, they are subjected to hydrolytic and oxidative processes.[3,15] The hydrolysis reaction of triglycerides causes the formation of

monoglycerides, diglycerides and, above all, free FAs. This hydrolytic reaction is due to the presence of endogenous and/or exogenous lipases. Endogenous lipases are enzymes naturally present in olives and during the mechanical process of production of the oil, they are released, and they induce lipolysis (this process could be also accelerated by high temperature). Since lipases are hydrophilic compounds, during the water removal phase (decantation and centrifugation), lipases are separated from the oil and the hydrolytic process is reduced or stopped. The release of free FAs is lightly influenced by these endogenous enzymes. However, free acidity could rapidly increase during EVOO storage due to the presence of exogenous lipases produced in very high amounts by micro-organisms. Moreover, the action of lipases is increased in presence of other factors affecting the integrity of the olives.[3] Free acidity, expressed as percentage of oleic acid, is one of the parameters used to verify the quality of oil. Despite the legal limit of free acidity for an EVOO is 0.8%, a good oil should have a value lower than 0.5%, while an excellent oil has values lower than 0.3%. In Table 4 the legal free acidity values for virgin olive oils are reported.[3]

Table 4 – Legal values of free acidity for virgin olive oil.[3]

Olive Oil	**Free Acidity (%)**	
Extra-Virgin	≤ 0.8%	
	≤ 0.5% (Good oil)	≤ 0.3% (Excellent oil)
Virgin	≤ 2.0%	
Lampante	> 2.0%	

The main degradative reaction that affects EVOO triglycerides is represented by the oxidation process which takes place during EVOO storage thus decreasing the sensory and health-promoting qualities of oils because it leads to the formation of rancid-flavour substances, reduces the antioxidants molecules, and induces the accumulation of toxic compounds (*e.g.* free radicals). This negative phenomenon is related to the presence of enzymes (lipoxidases and lipoxygenases), external factors (*e.g.* oxygen, temperature and light), and other pro-oxidant factors (*e.g.* chlorophylls and metals). The oxidative reaction consists of two stages. The first one involves the formation of hydroperoxides from PUFAs through a radical

mechanism, starting from an induction phase moving on a propagation phase that, once triggered, continues to propagate inexorably. In the second one the hydroperoxides formed in the first stage undergo further degradation producing aldehydes, ketones and conjugated dienes, which are the substances responsible of the rancid flavour of oil. The response of EVOO to this oxidation process depends on its chemical composition. In particular, natural antioxidants compounds present in EVOO, such as phenolic compounds and tocopherols (vitamin E), may slow down the oxidative reaction progression.[3,12,15,16] The oxidative reaction is estimated through the determination of peroxide value (expressed as meqO_2/kg of oils), which gives information about the first stage of oxidation, and through specific spectrophotometric absorption (K) measured in the UV region (λ = 232 and 270 nm), which gives information mainly about the second stage of oxidation.[3] The legal values of peroxide index and K are reported in Table 5.

Table 5 – Peroxide index, K_{232} and K_{270} values for virgin olive oils.[3]

Olive Oil	**Peroxide Index (meqO_2/kg)**		**K_{232}**		**K_{270}**
Extra-Virgin	≤ 20		≤ 2.50		≤ 0.22
	≤ 12 (Good oil)	≤ 8 (Excellent oil)	≤ 2.10 (Good oil)	≤ 1.90 (Excellent oil)	
Virgin	≤ 20		≤ 2.60		≤ 0.25

Moreover, during EVOO storage, also the phenolic compounds could be affected by hydrolytic and oxidative processes which lead to chemical composition transformation.[12,15,17,18] In particular, during storage it is possible to observe an increase in simple phenols, such as HT and T, due to the hydrolytic process that affect OC and OO, respectively, which at the same time tend to decrease.[15,18] These degradative processes are influenced by several factors, such as the exposition to light, temperature and oxygen and depend on storage time and conditions. Moreover, the degradation processes are closely related to the initial phenolic composition.[12,15] Indeed, EVOO with higher initial amount of phenols, showed a lower decrease in phenolic content during storage, than EVOOs characterized by a lower initial amount of phenolic compounds.[12]

1.3 Olive Leaves

Olive leaves are considered a by-product of olive oil production. They are collected and accumulated during olive tree pruning and olives harvesting and cleaning. Annually pruning produces 25 kg of by-products per tree, including leaves (about 25%), thin branches (about 50%) and thick branches or wood (about 25%). Moreover, leaves represent 10% of the weight of olives collected for oil production.[19,20] Therefore, olive leaves are abundant vegetable waste-material, which must be removed, stored and eliminated thus increasing the cost for the producers and the farms. Generally, olive by-products, including olive leaves, have no practical application. In particular, leaves are exploited as animal feed for small ruminants (goats and sheep), cows and non-ruminants, or more often used for direct combustion and burned, potentially causing environmental damage.[19,20] Throwing away olive leaves may also represent a waste of resources because they are a source of bioactive substances, such as phenolic compounds endowed with nutraceutical properties.[20]

Reducing agro-industrial waste and biomass accumulation and thus the negative environmental impact, represent a challenge for the producers and food industries. Bioeconomy, circular economy, and sustainable resource policy promote practical strategy and models of green technologies in order to valorize the waste products and to recover active and/or bioactive compounds from by-products. In particular, olive leaves may be useful in agronomic, food, nutraceutical and cosmetic fields as well as for biomedical applications.[19,21,22]

1.3.1 Chemical Composition of Olive Leaves

Chemically, olive leaves contain several bioactive substances such as *sugars*, *triterpenic acids* and *phenolic compounds*.[20,23–25]

Among *sugars*, olive leaves contain high amount of mannitol (Figure 11) endowed with several health properties and largely used in the pharmaceutical formulation.[23,24]

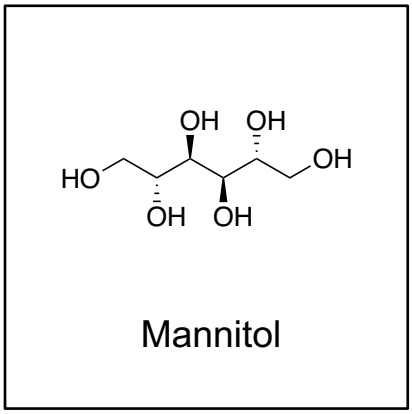

Figure 11 – Chemical structure of mannitol.

The main *triterpene* present in olive leaves is oleanolic acid, followed by maslinic acid. These compounds (Figure 12) possess several biological properties such as anti-inflammatory, anti-microbial and anti-tumour effects.[23,24] Moreover, in olive leaves ursolic acid, erythrodiol, and uvaol can also be found, in minor concentrations.[24]

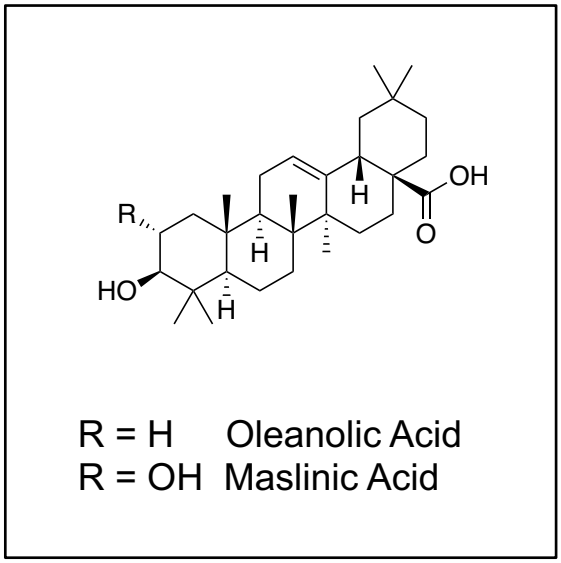

Figure 12 – Chemical structures of oleanolic acid and maslinic acid.

Concerning *phenolic compounds*, the most abundant is represented by oleuropein (OL), a secoiridoid. Therefore, in olive leaves it is possible to find other classes of phenolic compounds such as oleuropeosides (*e.g.* verbascoside and ligstroside); flavones (*e.g.* luteolin-7-O-glucoside, apigenin-7-O-glucoside, diosmetin-7-O-glucoside, luteolin, apigenin and diosmetin); flavonols (*e.g.* rutin);

flavan-3-ols (*e.g.* catechin); phenyl-alcohols (*e.g.* T and HT); phenyl-acids (*e.g.* vanillic acid, caffeic acid, *p*-coumaric acid, ferulic acid); other (*e.g.* vanillin). [20,23–25]

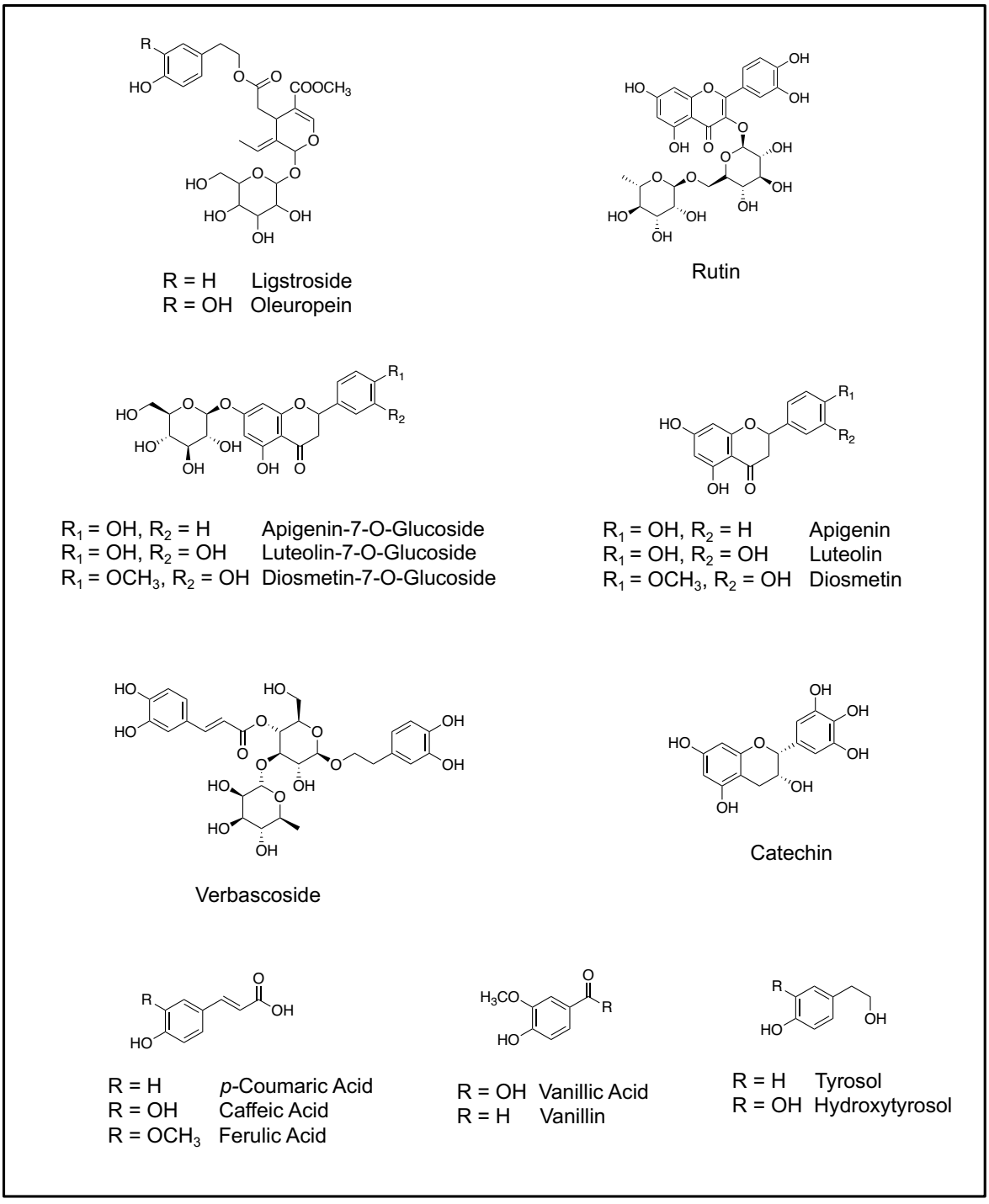

Figure 13 – Chemical structures of the main phenolic compounds in olive leaves.

1.4 Phenolic Compounds

Several studies demonstrated that phenolic compounds possess antioxidant, anti-inflammatory, antidiabetic, anti-tumoural, anti-angiogenic, hypolipidaemic, antiatherosclerotic and platelet anti-aggregate properties. The most important nutraceutical properties of OO, OC and OL are here reported.

1.4.1 Oleocanthal

OO was discovered for the first time in olive oil in 1993 by Montedoro *et al.*[26] and corresponds to the dialdehydic form of decarboxymethyl ligstroside aglycone. It is considered the molecule responsible of the pungency and the irritative sensation in the throat. In fact, the word *"oleocanthal"* derived from the union of the terms *"oleo-"* for olive, "-canth-" for sting, "-al" for aldehyde. In Figure 14 the chemical structure of OO is reported.

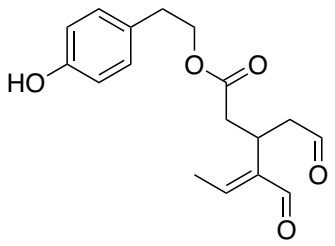

Oleocanthal (OO)

Figure 14 – Chemical structure of oleocanthal (OO).

In 2005, the anti-inflammatory activity was attributed to OO by Beauchamp *et al*.[27] In particular, these researchers demonstrated that OO acts as a natural anti-inflammatory compound showing a potency and a profile similar to that of ibuprofen, a well-known nonsteroidal anti-inflammatory drug (NSAID). Indeed, OO and ibuprofen are able to inhibit the cyclooxygenase (COX)-1 and COX-2 involved in the prostaglandin-biosynthesis pathway and thus reducing inflammation.[27] However, OO is a more potent anti-inflammatory agent than ibuprofen.[27]

Inflammation and chronic inflammatory processes are involved in several disorders such as arthritis, atherosclerosis, cancer and neurodegenerative diseases, including Alzheimer's disease (AD). Considering the anti-inflammatory

activity attributed to OO, its health potential on inflammatory-mediated pathologies was thus investigated.[28]

1.4.1.1 Anti-Inflammatory, Anti-Microbial and Antioxidant Properties of Oleocanthal

OO displayed anti-inflammatory effects, in *in vitro* and *in vivo* studies, by inhibiting COX-1 and COX-2 involved in synthesis of prostaglandins and 5-lipoxygenase (5-LOX), responsible for biosynthesis of pro-inflammatory leukotrienes.[27,29,30] Moreover, it was demonstrated that OO is able to reduce the production and the expression of inducible nitric oxide synthase (iNOS) and endothelial nitric oxide synthase (eNOS), and to down-regulate the expression of proinflammatory molecules, including interleukin (IL)-1β, IL-6, tumour necrosis factor-α (TNF-α), granulocyte-macrophage-colony-stimulating factor (GM-CSF) and macrophage inflammatory protein-1α (MIP-1α).[31]

OO exhibits anti-microbial activities against *Escherichia coli*, *Salmonella enterica*, *Listeria monocytogenes* and *Helicobacter pylori*.[32–34]

Although, more studies to investigate the antioxidant capacity of OO are needed,[35] this molecule is able to inhibit the nicotinamide adenine dinucleotide phosphate oxidase (NOX) thus reducing the superoxide anion radical ($O_2^{\bullet -}$) levels.[36]

1.4.1.2 Oleocanthal and Cancer

Cancer is a disease characterized by uncontrolled cells growth and proliferation. Moreover, cancer cells can spread from the first site they formed to other parts of the body by invading nearby tissues or traveling to distant places and then promoting metastasis formation. Recent studies demonstrated that OO reduces cancer cells proliferation and promotes cancer cells death. In particular, OO demonstrated promising anticancer properties against *in vitro* and/or *in vivo* models of several cancers cells such as adeno-carcinoma (HeLa and Caco-2),[37] breast cancer (MDA-MB-231, MCF-7, BT-474, MDA-MB-231 and T-47D),[37–41] colon cancer (HCT-116 and HT-29, JB6 Cl41, SW480, HT29),[42,43] hepato-carcinoma (Huh-7, HepG2, HCCLM3, Male BALB/c athymic nude mice, Hep3B, and PLC/PRF/5),[43,44] leukemia (HL60),[45] multiple myeloma (RH-77 human and MOPC-31C murine),[31] pancreas and prostate cancers (BxPC3 and PC3, respectively),[38,40] skin cancers, both melanoma and non-melanoma (NMSC) (A375, 501Mel and A431)[46–48] and

actinic keratosis (HaCaT cells stimulated with epidermal growth factor, EGF)[47], a lesion that can cause squamous cell carcinoma (a kind of NMSC). The mechanisms of action attributed to OO include the modulation and/or the inhibition of several signalling pathways. In particular, OO is able to inhibit the mammalian target of rapamycin (mTOR) thus inducing apoptosis by blocking mitotic cells in the G1 phase (in adeno-carcinoma and breast cancer)[37], to reduce the c-Met receptor expression decreasing tumour growth, survival and angiogenesis (in breast cancer)[38,39] and to block the transcription factor STAT3 (signal transducer and activator of transcription 3) inhibiting cancer cells growth and metastasis (in hepato-carcinoma and skin cancer).[44,48] Moreover, OO seems to be able to downregulate the extracellular signal-regulated kinases (ERK) 1/2 and the protein kinase B (AKT) cell signalling pathways, inhibiting cells proliferation (both in melanoma and NMSC, in multiple myeloma and in breast cancer).[31,39,46,47] Furthermore, OO demonstrated apoptosis-promoting effects by inducing the activation of apoptotic mechanisms such as the cleavage of poly (ADP-ribose) polymerase (PARP) and caspase-3, causing DNA fragmentation in tumour cells (breast, colon, prostate, pancreas and multiple myeloma),[31,39,40,42] by decreasing the antiapoptotic protein Bcl-2 expression (skin cancer),[46] or inhibiting COX-2, resulting in the activation of AMP-activated protein kinase (colon cancer).[42]

1.4.1.3 Oleocanthal and Neuroprotection

In *in vitro and in vivo* studies, OO demonstrated promising neuroprotective properties by reducing oxidative stress and by preventing apoptosis of neuronal cells. The neuroprotective property of OO was mainly evaluated on AD. This disorder is characterized by a misfolding, aggregation and an increase in toxicity of β-amyloid peptide and tau protein in the brain leading to an increase of inflammatory signals and to neuronal apoptosis. OO reduces the negative phenomena that involved both β-amyloid peptide and tau protein in AD by exploiting different mechanisms of action. In particular, OO is able to increase the expression and the activity of the efflux transporter P-glycoprotein (P-gp) and to up-regulate the low-density lipoprotein receptor-related protein 1 (LRP1), inducing efflux and clearance of β-amyloid peptide.[49–51] Moreover, OO induced degradation of β-amyloid peptide and promotes a change in its structure transforming the peptide into a protein which could be easier to eliminate.[49,52–54] In addition, OO prevents the aggregation into

fibrillary structures of tau protein, modifying and stabilizing its conformation in a more stable secondary structure.[55,56] Furthermore, it was demonstrated that OO reduces the synthesis of both β-amyloid peptide and tau protein by inhibiting mTOR.[37]

It is well known that the progression of neurodegenerative diseases such as AD and Parkinson's disease is associated with oxidative stress. In this context, OO is able to protect neurological cells from apoptosis, by counteracting oxidative stress. In particular, OO reduces ROS production, increases the reduced glutathione (GSH) intracellular level and up-regulated proteins involved in the maintenance of cell proliferation and cell survival such as the chaperone heat shock protein 90 (Hsp90) and AKT.[57]

1.4.1.4 Oleocanthal and Arthropathy

The most common forms of arthropathy are osteoarthritis and rheumatoid arthritis. The first one represents a disorder that affects joints and it is caused by a cartilage damage which wears down over time, while the second one is considered an auto-immune disorder which can not only affect the joints, but also skin, eyes, lungs, and blood vessels. Both diseases, particularly rheumatoid arthritis, are mainly caused by inflammation promoted by pro-inflammatory cytokines and mediators which induce up-regulation of cartilage-degrading factors. *In vitro* studies demonstrated the ability of OO to down-regulate these pro-inflammatory mediators, ameliorating the osteoarthritis and the rheumatoid arthritis conditions. Iacono *et al.* investigated the effect of OO in chondrocytes (ATDC-5 murine cells line) stimulated with lipopolysaccharide (LPS), in order to induce NO production and thus obtained an *in vitro* model of degenerative joint disease. The researchers demonstrated that OO is able to reduce the production of NO by inhibiting iNOS, responsible of NO production.[58] Moreover, Scotece *et al.* evaluated the effect of OO on ATDC5 murine chondrogenic cells and murine macrophages J774, both stimulated with LPS, demonstrating that OO is able to reduce the production of NO and the expression of pro-inflammatory mediators such as IL-1β and TNF-α, in treated cells.[31]

1.4.1.5 Oleocanthal and Other Effects

OO showed a possible application in cardiovascular diseases. In fact, a clinical trial demonstrated that OO is able to improve the endothelial function in patients with early atherosclerosis. This is probably linked to its capability to reduce vascular inflammation[59] and to prevent platelet activation and aggregation by inhibiting COX, thus limiting endothelial damage.[60]

1.4.2 Oleacein

OC was discovered for the first time in olive oil in 1993 by Montedoro *et al.*[26] and corresponds to the dialdehydic form of decarboxymethyl oleuropein aglycone (Figure 15).

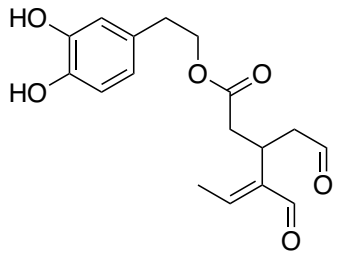

Oleacein (OC)

Figure 15 – Chemical structure of oleacein (OC).

OC represents the main component responsible for the anti-sclerotic effect of EVOO and it possesses, like OO, anti-inflammatory and antioxidant properties as well as anti-cancer effects.[61]

1.4.2.1 Antioxidant, Anti-Inflammatory and Anti-Microbial Properties of Oleacein

The antioxidant activities of OC are well documented. It was proved that OC is a radical scavenger of ROS ($O_2^{\bullet -}$, hydrogen peroxide (H_2O_2)) and hypochlorous acid (HOCl)) and RNS (NO and peroxynitrite ($ONOO^-$)).[62] Moreover, it possesses a DPPH (1,1-diphenyl-2-picrylhydrazyl) radical scavenging activity comparable with those of α-tocopherol. The OC antioxidant activity is not only linked to its free radical scavenging property, but also to its metal ion chelating activity.[63]

OC is able to inhibit many enzymes, such as COX-2 and 5-LO, involved in the synthesis of pro-inflammatory prostaglandins and leukotrienes respectively, thus acting as an anti-inflammatory mediator.[29,30]

Furthermore, OC is endowed with anti-microbial activity showing bactericidal effects against *Listeria monocytogenes* and other Gram-positive and Gram-negative.[33]

1.4.2.2 Oleacein and Cardiovascular Diseases

OC displays beneficial effects on cardiovascular diseases, mainly atherosclerosis, due to its antioxidant and anti-inflammatory properties.[61] Moreover in 1996 Hansen *et al.* described for the first time OC as an inhibitor of the angiotensin converting enzyme (ACE).[64] Acting as ACE inhibitor, antioxidant and anti-inflammatory molecule, OC is able to reduce blood pressure and to prevent the senescence of endothelial progenitor cells (EPCs) induced by angiotensin II.[61] EPCs play a key role in the neovascularization of ischaemic tissue and in the re-endothelization of an injured arterial wall. On the other hand, angiotensin II induces accumulation of ROS in EPCs attenuating their functions and inducing senescence through inhibition of telomerase activity and cell proliferation. Parzonko *et al.* demonstrated that OC is able to increase cell proliferation and telomerase activity as well as to reduce ROS accumulation and the percentage of senescent cells, in angiotensin II-stimulated cells, thus restoring the EPCs regenerative activities.[65] OC may thus reduce atherosclerosis development and plaque destabilization showing a vasculoprotective effect.[65,66]

Circulating neutrophils are detected in coronary artery disease and are associated with high risk of cardiovascular incidences.[67] In inflammatory conditions neutrophils release ROS and enzymes, such as myeloperoxidase, which catalyse the formation of HOCl.[67] The cardioprotective effect of OC is also correlated to its ability to counteract the release of pro-inflammatory mediators and ROS production stimulated by neutrophils.[62] Therefore, OC is able to reduce the neutrophils adhesion inducing them to roll along the vascular wall, by down-regulating the expression of adhesion molecules.[68,69]

Filipek *et al.* in a recent study, demonstrated the ability of OC to inhibit the formation of foam cells, basic components of atherosclerotic plaques, thus suggesting that OC may be useful in the prevention of early and advanced

atherosclerotic lesions. OC mainly acts by decreasing the expression of receptors on the surface of macrophages, which promote an interaction with oxidised low density lipoprotein (oxLDL) leading to the formation of foam cells from macrophages, by switching macrophages from a pro-inflammatory type to an anti-inflammatory type.[70] Furthermore, OC is able to inhibit the macrophages early apoptosis induced by ox-LDL and to directly inhibit LDL oxidation.[70,71]

1.4.2.3 Oleacein and Cancer

The anti-antitumour properties of OC were poorly investigated compared with that of OO. However, OC showed promising properties against several *in vitro* models of cancer cells, such as multiple myeloma (NCI-H929, RPMI-8226, U266, MM1s and JJN3),[72] leukemia (HL60),[45] neuroblastoma (SH-SY5Y)[73], skin cancer, both melanoma and NMSC, and actinic keratosis (A431 and EGF-stimulated HaCaT cells)[47].

Concerning multiple myeloma, Juli *et al.* demonstrated that OC is able to induce cell cycle arrest and apoptosis in tumour cells, without exerting any toxic effect on healthy cells. The researchers evaluated the epigenetic impact of OC on multiple myeloma cells proving that it down-regulates several classes of I/II histone deacetylases (HDACs), whose aberrant expression and/or activity induces malignant transformation of tumour cells, *via* Sp1, a transcriptional activator of HDAC.[72]

In HL60 cells line, OC inhibits cells proliferation and induces apoptosis in tumour cells.[45]

In NMSC, OC is able to decrease A431 cells viability in a concentration-dependent manner and to inhibit EGF-stimulated HaCaT cells growth, by targeting signalling molecules, particularly the B-Raf-Erk pathway involved in cancer progression.[47]

In human neuroblastoma cells lines (SH-SY5Y), OC reduces cells proliferation by blocking the cell cycle in S phase and induces apoptosis by increasing the pro-apoptotic Bax and p53 expression levels, by reducing the anti-apoptotic Bcl2 expression levels as well as STAT3 phosphorylation. Moreover, OC exerts anti-metastatic effects by reducing cells adhesion, migration and invasion.[73]

1.4.2.4 *Oleacein and Other Effects*

OC exhibits a protective effect against the damage/metabolic alterations caused by high-fat diet, in *in vivo* tests (C57BL/6JolaHsd male mice). In particular, Lombardo *et al.* demonstrated that OC reduces abdominal fat accumulation, weight gain and liver steatosis, as well as improves insulin sensitivity in liver and increases lipid metabolism, by modulating the expression levels of several proteins.[74]

The OC effect on the main clinic-pathological features of experimental autoimmune encephalomyelitis (EAE), an *in vivo* model of multiple sclerosis disease, which progression is influenced by oxidative stress and pro-inflammatory cytokines, was also evaluated. As results of this study, OC seems to be able to increase anti-inflammatory cytokines and to down-regulate pro-inflammatory mediators, as well as to reduce oxidative stress. Moreover, OC reduces clinical score and histological signs typical of EAE.[75]

1.4.3 Oleuropein

OL is a secoiridoid which represents a chemotaxonomical marker for the infra-generic classification of *Oleaceae* family.[76] Chemically it consists of a polyphenolic compound, constituted by HT, a secoiridoid, represented by elenolic acid, and a glucose molecule (Figure 16-left). It is the most abundant bioactive compound of olive tree leaves. In olive oil, OL, undergoes enzymatic degradation during the mechanical extraction process, releasing OC, so it is not present in oils, except in small quantities as oleuropein aglycone (Figure 16-right).

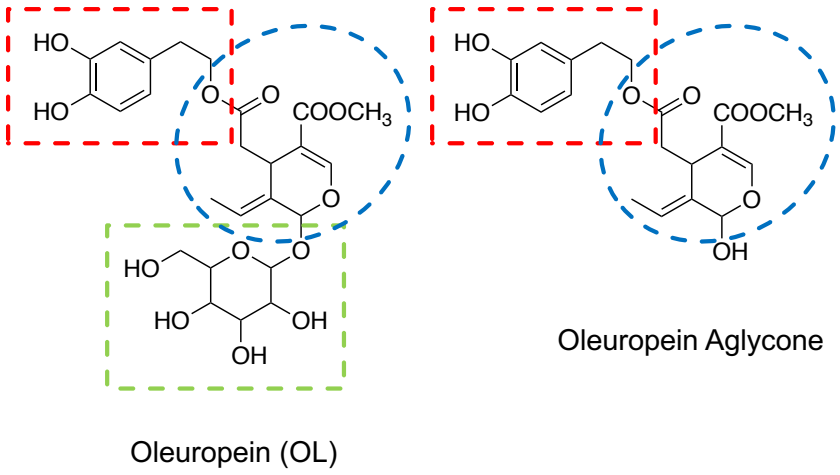

Figure 16 – Chemical structures of oleuropein (OL) (left) and oleuropein aglycone (right). Hydroxytyrosol (HT) (red box); elenolic acid (blue circle); glucose (green box).

Several *in vitro* and *in vivo* studies proved the antioxidant, anti-inflammatory, anti-microbial, antifungal, anti-tumoural, hypolipidemic, hypotensive, anticancer and cardioprotective properties of OL.

1.4.3.1 Antioxidant, Anti-Inflammatory and Anti-microbial Properties of Oleuropein

The antioxidant properties of OL are mainly attributable to the presence of 1,2-dihydroxybenzene moiety in its structure. OL is endowed with strong free radical scavenging and metal-chelating activities.[76] In particular, it was demonstrated its ability to suppress the production of ROS ($O_2^{\bullet-}$, H_2O_2 and HOCl) and RNS (NO and $ONOO^-$), and to reduce *in vitro* the release of myeloperoxidase which catalyses the formation of HOCl.[62] Furthermore, OL induces the activation of human antioxidant defence and enhances the DNA repair system. In particular, *in vivo* tests showed that OL is able to increase the level of antioxidant enzymes, such as superoxide dismutase (SOD), glutathione peroxidase (GPX), glutathione reductase (GRX) and catalase (CAT), and non-enzymatic defence such as glutathione (GHS), α-tocopherol, β-carotene and ascorbic acid.[77–79] These activities are related to the anti-cancer and anti-inflammatory properties of OL.

OL exhibits anti-inflammatory effects by targeting inflammatory cytokines and mediators. Particularly, it reduces nuclear factor (NF)-κB activation and its translocation to the nucleus, iNOS expression and inhibits COX-2.[80] The anti-inflammatory effect of OL is associated with its cardioprotective and anti-cancer properties.

OL is a growth inhibitor of *Salmonella enteritidis*.[81] Moreover, it is demonstrated that also olive leaves extracts (OLEs), rich in OL, exert antimicrobial activities.[81]

1.4.3.2 Oleuropein and Cancer

In vitro and *in vivo* studies proved the anti-tumour effects of OL on several cancerous cell lines, including glioblastoma (LN-18)[82], leukemia (TF-1a)[82], prostate cancer (LNCAP and DU145)[83], breast cancers (T-47D, MCF-7, MDA)[82,84–87] and skin cancer (RPMI-7951 and A375)[82,88]. The mechanisms of action include the inhibition of cell growth, motility, proliferation, invasion and metastasis and the induction of apoptosis.

Concerning MCF-7 cell line (human breast cancer cells), OL is able to inhibit cells proliferation in a concentration-dependent manner. In addition, it can induce apoptosis by blocking cell cycle at G1 phase and by increasing cell mortality,[84] as well as *via* p53-dependent pathway by increasing the pro-apoptotic Bax expression levels and by down-regulating the anti-apoptotic Bcl-2 gene expression.[87] On the same cells line, OL interferes with tumour cells proliferation stimulus induced by oestradiol by inhibiting the oestradiol-dependent activation of ERK1/2, demonstrating chemo-preventive properties. Moreover, Sepporta *et al.* investigated the *in vivo* effect of OL on breast cancer animal model consisting of MCF-7 cells injected into mouse mammary fat pads, thus demonstrating a chemopreventive activity of OL on breast cancer.[85] In addition, the anti-metastatic effect of OL on MDA cells line is also proved by reducing the expression levels of enzymes which induce invasion (matrix metalloproteinase (MMP)-2 and MMP-9), and by up-regulating the expression of tissue inhibitors of metalloproteinases (TIMP)1 and TIMP4 genes, endowed with apoptosis-inducing properties.[86]

OLE enriches in OL (oleuropein-rich extract, ORE) were also evaluated on 4-nitroquinoline 1-oxide-induced rat tongue carcinogenesis in F344 rats, revealing the chemopreventive role of ORE in tongue squamous cell carcinoma.[89]

1.4.3.3 Oleuropein and Cardioprotection

The cardioprotective effect of OL is supported by several *in vitro* and *in vivo* studies.

In *in vivo* tests, the cardioprotective efficacy of OL on hypercholesterolemic rabbits was evaluated. The results of this study demonstrated that OL is able to reduce the infarct size, to confer strong antioxidant protection against oxidative damage during ischemia-reperfusion, to enhance SOD activity and to reduce total cholesterol and triglyceride circulating levels as well as malondialdehyde and protein carbonyl circulating levels.[90] It was also demonstrated that OL exerts a cardioprotective role against doxorubicin (DXR)-induce cardiotoxicity *in vivo* (adult male Wistar rats). This effect is due to the reduction in the serum level alteration and the over-expression of intracellular and peripheral markers induced by DXR and to the decrease in the peroxidation and protein oxidation in the heart tissue after DXR administration.[91] In a recent study, Tsoumani *et al.* elucidated the cardioprotective effect of OL against ischemia reperfusion injury (IRI) assessed on

an animal model (rabbits and mice) of myocardial IRI. The researchers demonstrated the cardioprotective effect of OL administered during ischemia by up-regulating the antioxidant defence systems in the myocardium mediated by the nuclear factor (erythroid-derived 2)-like 2 signalling pathway, which plays a key role in the regulation of cytoprotective systems.[92]

Since OL is an ACE inhibitor, like OC, it exerts a protective role on ECPs preventing their senescence induced by angiotensin II.[65]

Moreover, OL aglycone displays an anti-platelet effect by inhibiting phosphodiesterase thus increasing of intraplatelet cAMP levels.[93]

1.4.3.4 Oleuropein and Hepatoprotection

Several studies demonstrated the potential hepatoprotective effect of OL against liver injury. This secoiridoid can prevent the hepatic cadmium (Cd) toxicity in mice, by reducing the oxidative stress induced by Cd.[94] OL exerts a hepatoprotective activity in male BALB/cN mice with liver injury induced by carbon tetrachloride (CCl_4), which triggered inflammatory response in mice livers and consequently a massive hepatic necrosis and an increase in plasma transaminases. In this context, OL is able to reduce the oxidative and the nitrosative stress and inflammation induced by CCl_4, exerting anti-fibrotic effect.[80] Moreover, OL demonstrated anti-fibrotic effects on high fat diet-induced mouse model of non-alcoholic steatohepatitis (C57BL/6 mice) by reducing the expression of profibrotic genes, such as α-smooth muscle actin (α-SMA) and collagen type I alpha 1 chain (COL1A1). These results suggest that OL may be a promising therapeutic agent in the prevention of steatohepatitis and fibrosis.[95]

1.4.3.5 Oleuropein and Gastroprotection

OL displays gastroprotective effects mainly due to its antioxidant and anti-inflammatory properties. Several studies supported that OL may be useful in treatment of ulcer colitis (UC). In particular, Larussa *et al.* demonstrated that OL is able to reduce the expression of COX-2 and IL-17 as well as the infiltration of CD3, CD4 and CD20 cells in the colonic mucosa from patients with UC.[96] In an animal model of chronic colitis (mice exposed to dextran sodium sulfate, DSS), OL is able to reduce the pro-inflammatory cytokines IL-6 and IL-1β in colon tissue, and

increase the production of IL-10, which plays a key role in the resolution of inflammation. Furthermore, OL decreases the expression levels of COX-2 and iNOS in DSS-induced chronic colitis model. The OL molecular mechanism is related to its capability to reduce the phosphorylation of p38 MAPK, which activation induces an increasing of pro-inflammatory mediators in intestinal epithelium.[97]

Moreover, investigating the effect of OLE on two mice models of colitis (DSS and DNBS), Vezza *et al.* showed that OLE treatment reduced the expression of pro-inflammatory mediators (IL-1β, TNF-α, iNOS, MIP-2 and COX-2) and restores the expression of mediators involved in the maintenance of intestinal epithelial barrier integrity and epithelial regeneration. The same authors confirmed that OLE reduces the production of proinflammatory cytokines, such as IL-1β, IL-6, IL-8, and TNF-α in intestinal mucosal samples from Crohn's disease patients compared with *ex vivo* organ cultures of mucosal explants of healthy donors.[98]

1.4.3.6 Oleuropein and Other Effects

In vitro and *in vivo* studies demonstrated that OL is able to protect kidney oxidative damage induced by Cd administration and treatment.[99,100]

Moreover, OL owned anti-gout activity[101], protective effect against osteoporosis[102] and UVB radiations[103] and immunomodulatory properties.[104]

OL also exerts a positive role in regulating diabetes and mitigating diabetes-associated complications, such as cardiovascular diseases, diabetic nephropathy, neuropathy and retinopathy.[105]

Moreover, OL accelerates the re-epithelization process and increases collagen deposition by up-regulating vascular-endothelial growth factor (VEGF) expression levels, thus showing promising skin wound healing effects.[106]

2 AIM OF THE THESIS

Extra-virgin olive oil (EVOO) and olive leaves extract (OLE) represent an important source of nutraceutical compounds including phenolic and polyphenolic compounds such as phenyl alcohols, phenolic acids, lignans, flavones, flavonols and secoiridoids. Secoiridoids are a class of compounds exclusive of *Oleaceae* family. Oleocanthal (OO) and oleacein (OC) are the most important secoiridoids present in EVOO, while oleuropein (OL) is the main representative in OLE (Figure 17). These compounds possess nutraceutical properties, such as antiproliferative, cardioprotective, antioxidant and anti-inflammatory properties.[28,76,107]

My research project was focused on the study of the phenolic and polyphenolic compounds in EVOOs and in OLEs.

In particular my PhD project was aimed to these parallel objectives:

- The development of efficient methods for the extraction and the purification of oleocanthal and oleacein from EVOOs.
- The study of the nutraceutical properties of oleocanthal and oleacein.
- The study of the variations in the phenolic and polyphenolic composition of EVOOs during storage.
- The study of novel components in EVOOs and their potential nutraceutical properties.
- The study of composition of Tuscan EVOOs for the determination of their geographical traceability.
- The development of devices useful in tissue regeneration fields from olive leaves phytoextracts (OLEs) obtained from autochthonous Tuscan olive trees *Cultivars*.

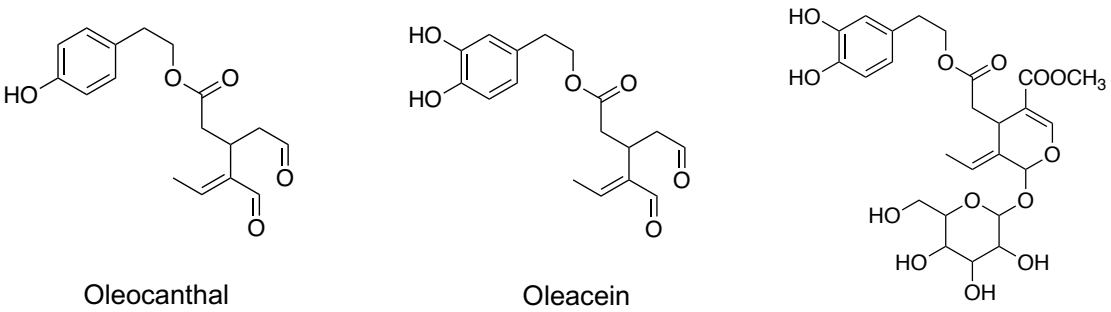

Figure 17 – Chemical structures of the main secoiridoids present in EVOO and in OLE.

3 RESULTS AND DISCUSSION

3.1 Development of efficient methods for the extraction and the purification of oleocanthal and oleacein from EVOOs

A part of my PhD project was dedicated to the development of efficient methods for the extraction and the purification of significant amount of OO and OC with high purity from EVOOs obtained from autochthonous Tuscan olive trees, to submit these compounds to nutraceutical studies.

3.1.1 Method Development

In my PhD thesis' laboratory, the techniques for the extraction and the purification of these two secoiridoids from EVOOs were already developed.[47] The extraction method was based on a liquid-liquid extraction performed by using *n*-hexane:acetonitrile (ACN) (4:5, v/v). The purification of the two compounds involved a double-step process consisting of a direct flash column chromatography, as first step of purification, followed by a preparative thin layer chromatography (TLC), as second step of purification. This procedure required very long purification times, high amounts of solvent, moreover the yield of OO and OC was low. I thus improved the purification procedure of these two compounds.

For this purpose, firstly, I selected a Tuscany EVOO with a high amount of secoiridoids (OO and OC) to be extracted, through high-performance liquid chromatography (HPLC) analysis by using the method described in section 4.2.9.2.2 of the experimental part. In Figure 18 the HPLC chromatogram of the selected EVOO is shown and the peaks corresponding to OO and OC are indicated.

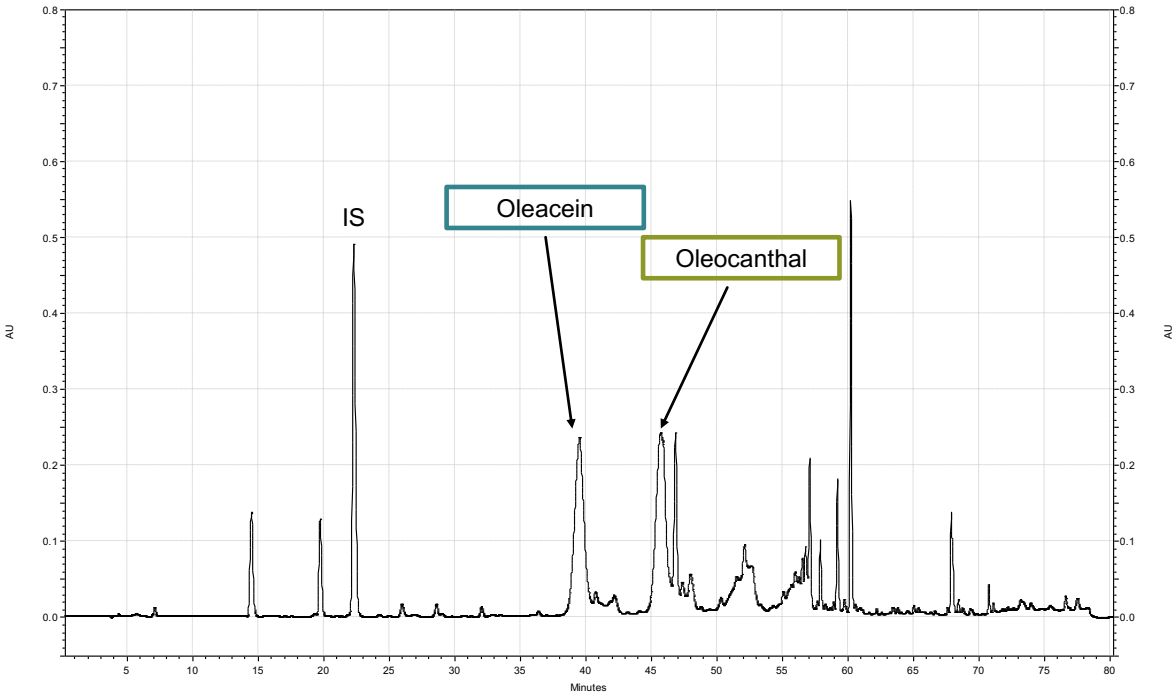

Figure 18 – HPLC chromatogram of the selected EVOO. IS = Internal Standard.

Once EVOO was selected, it was extracted through a liquid-liquid extraction by following the procedure already developed in my PhD thesis' laboratory, as reported in section 4.2.1 of the experimental part.[47] Then the crude residue obtained was subjected to purification.

Initially, the first step of purification was based on the procedure previously developed in my PhD thesis' laboratory,[47] that was adapted to the advanced automated flash purification system (Isolera™ Prime 3.2.2, Biotage®). This method consisted of a direct phase cartridge, as stationary phase, and a mixture of chloroform ($CHCl_3$) and ethyl acetate (EtOAc), as mobile phase, with a gradient reported in section 4.2.2.1 of the experimental part. Through the nuclear magnetic resonance (NMR) spectroscopy the ^{1}H-NMR spectra of the fractions collected containing OC (Figure 20) or OO (Figure 20), were acquired. These spectra showed the diagnostic signal of the two compounds, but they were not sufficiently pure. These fractions were then further purified.

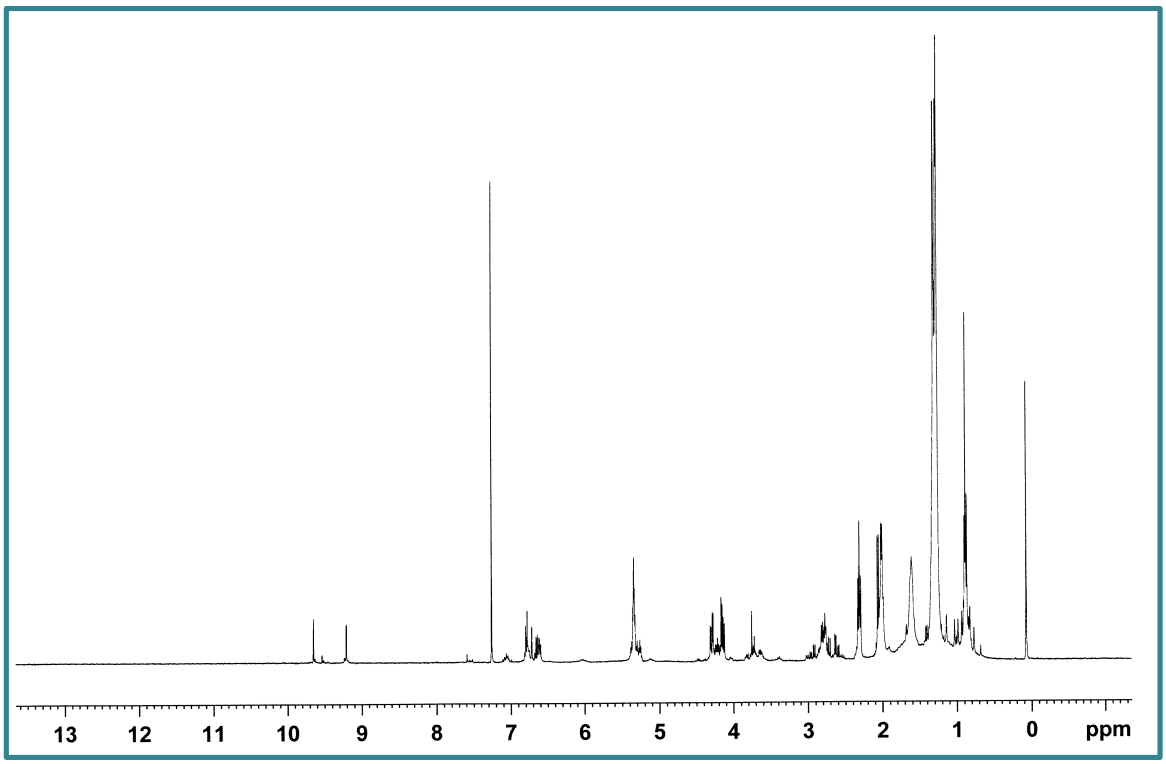

Figure 19 – ^{1}H-NMR ($CDCl_3$ - 400 MHz) of oleacein after the first step of purification.

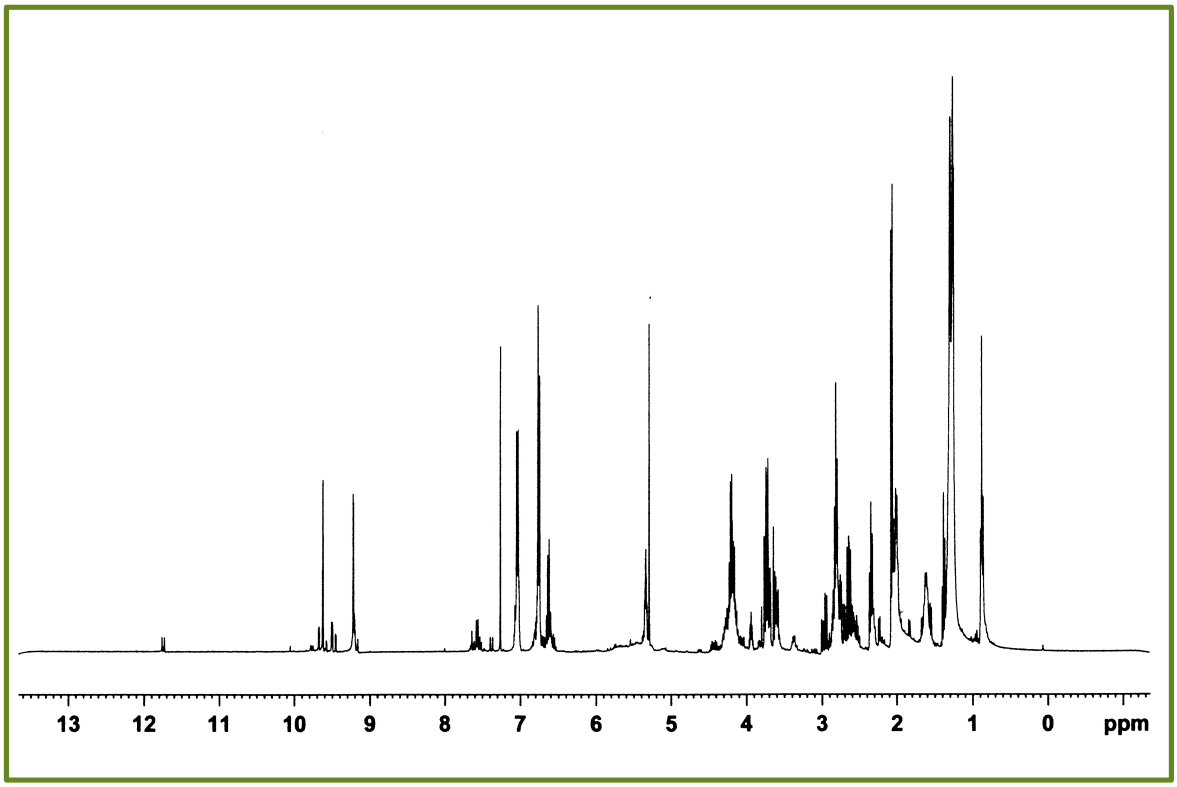

Figure 20 – ^{1}H-NMR ($CDCl_3$ - 400 MHz) of oleocanthal after the first step of purification.

Therefore, the residues contained OC or OO were initially purified by exploiting a preparative TLC, according to the procedure already developed,[47] which consisted of a mixture of *n*-hexane and EtOAc, as mobile phase, as reported in section 4.2.2.2.1 of the experimental part. With this method (Method I) OC and OO were obtained with low yield, and they were not sufficiently pure. In Figure 21 and Figure 22, the ^{1}H-NMR spectra of OC and OO respectively, obtained after purification through preparative TLC, are reported. In these spectra it is possible to observe some impurities.

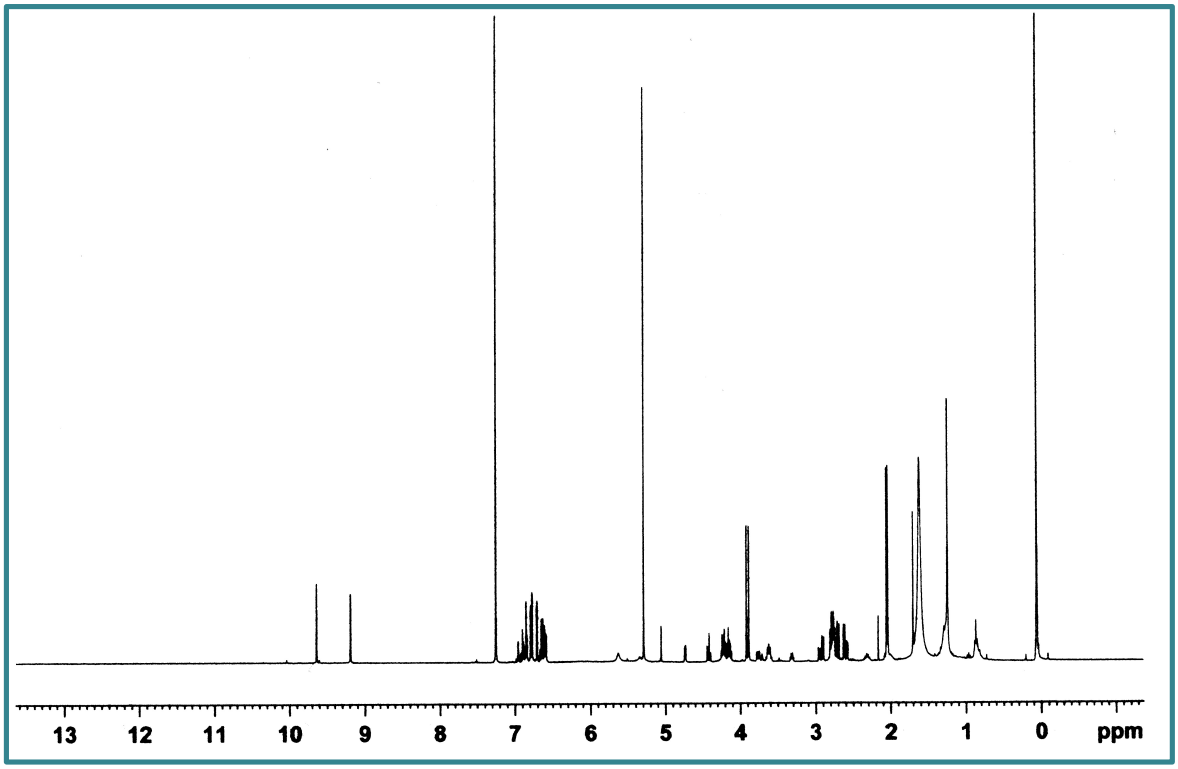

Figure 21 – ^{1}H-NMR ($CDCl_3$ - 400 MHz) of oleacein after the second step of purification performed by exploiting preparative thin layer chromatography.

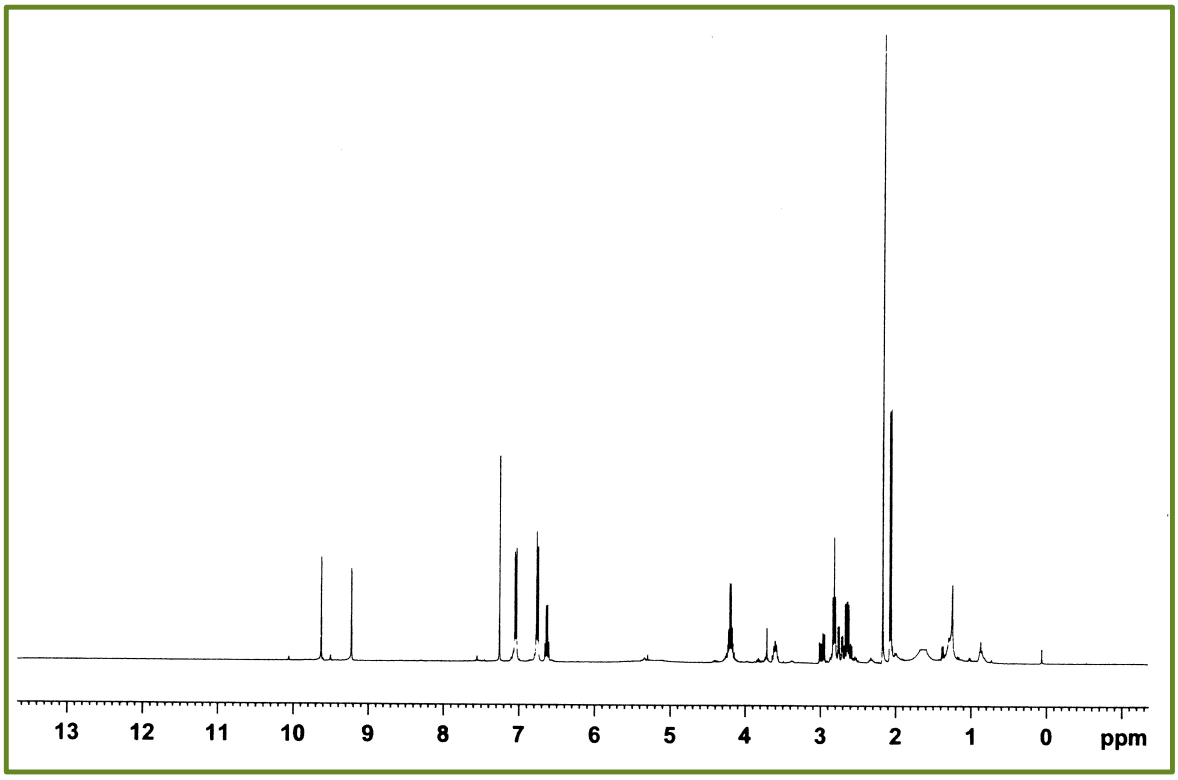

Figure 22 – ^{1}H-NMR ($CDCl_3$ - 400 MHz) of oleocanthal after the second step of purification performed by exploiting preparative thin layer chromatography.

In order to improve the yield and the purity of these two compounds, the residues containing OC and OO derived from the first step of purification were further purified by exploiting a direct flash column chromatography, by using the same mobile phase used for the preparative TLC (a mixture of *n*-hexane and EtOAc). With this method (Method II), extensively described in section 4.2.2.2.2 of the experimental part, the yield increased, but the two compounds thus obtained were still not sufficiently pure, as shown in the ^{1}H-NMR spectra of OC (Figure 23) and OO (Figure 24). Indeed, also in this case the spectra still present some impurities.

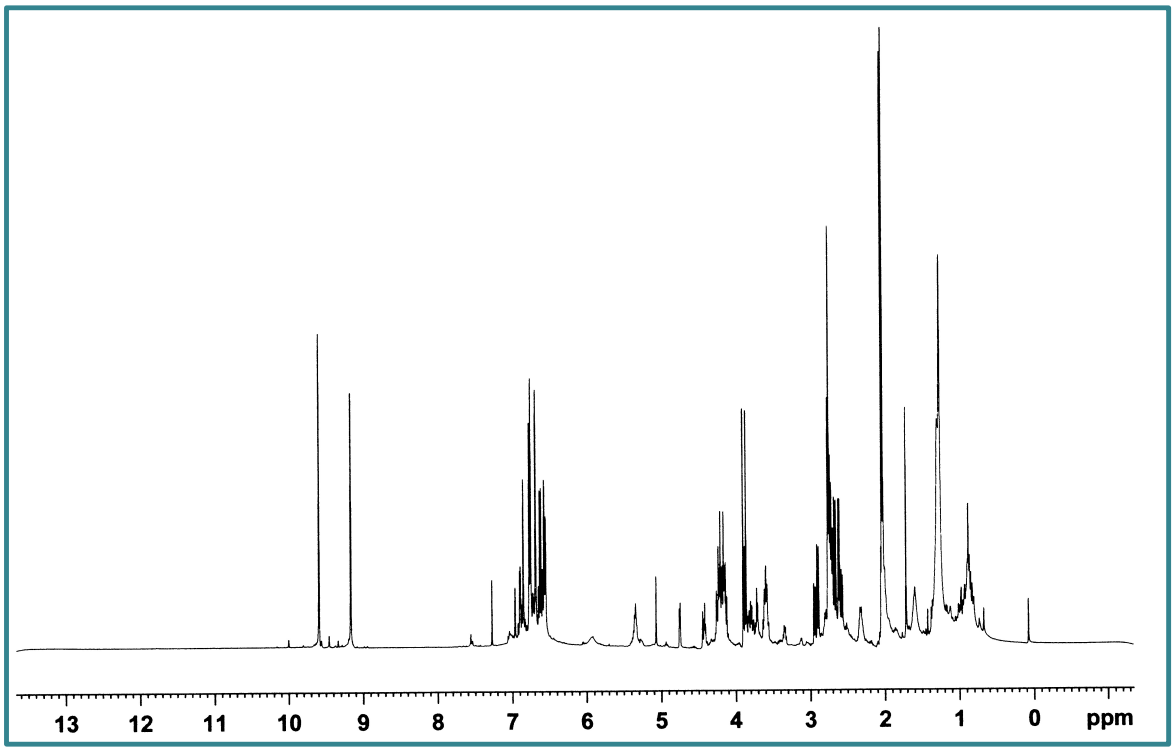

Figure 23 – ^{1}H-NMR ($CDCl_3$ - 400 MHz) of oleacein after the second step of purification performed by exploiting flash column chromatography.

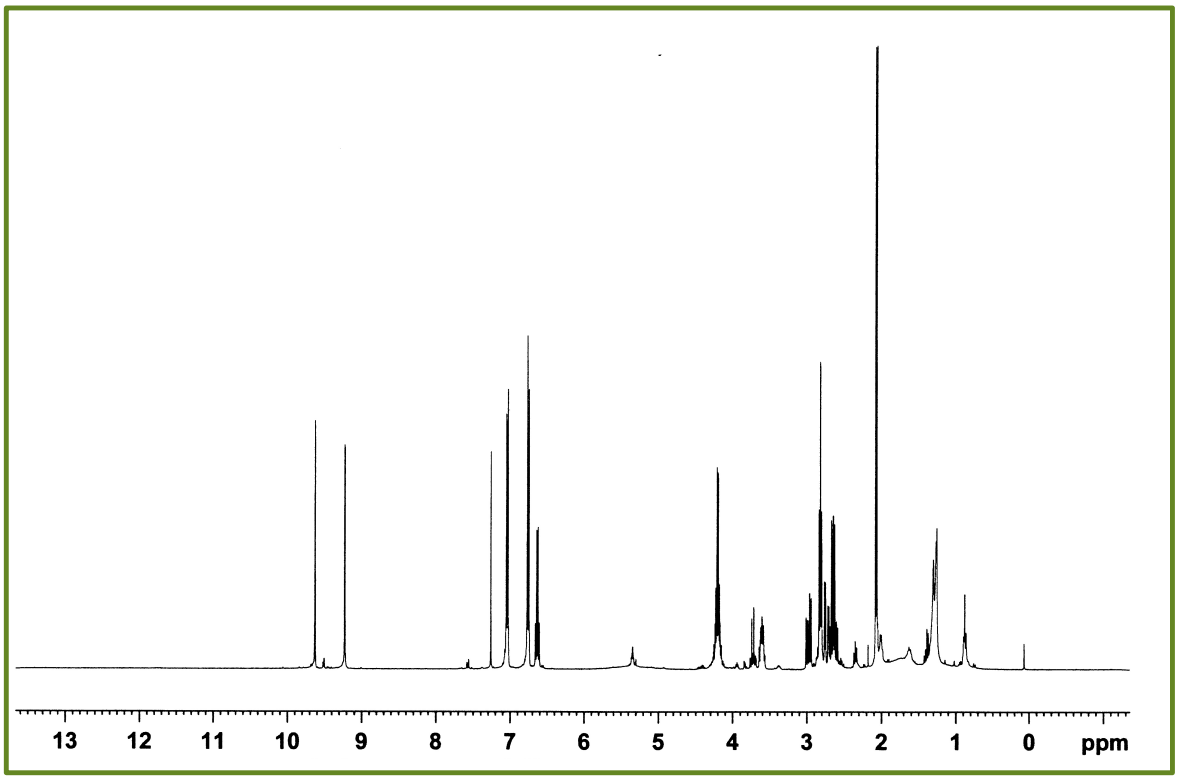

Figure 24 – ^{1}H-NMR ($CDCl_3$ - 400 MHz) of oleocanthal after the second step of purification performed by exploiting flash column chromatography.

Finally, a reverse phase column chromatography was used to perform the second step of purification of OC and OO. In particular, this purification was carried out by advanced automated flash purification instrument and by using a C18 cartridge as stationary phase and a mobile phase similar to that one used in HPLC analysis of EVOOs (section 4.2.9.2.2 of the experimental part), constituted by a mixture of H_2O and ACN with the gradient extensively reported in section 4.2.2.2.3 of the experimental part. With this method (Method III), it was possible to obtain OC and OO with a high yield and good purity (>95%), to be submitted to pharmacological investigations. In Figure 25 and Figure 26 the ^{1}H-NMR spectra of OC and OO respectively, are reported.

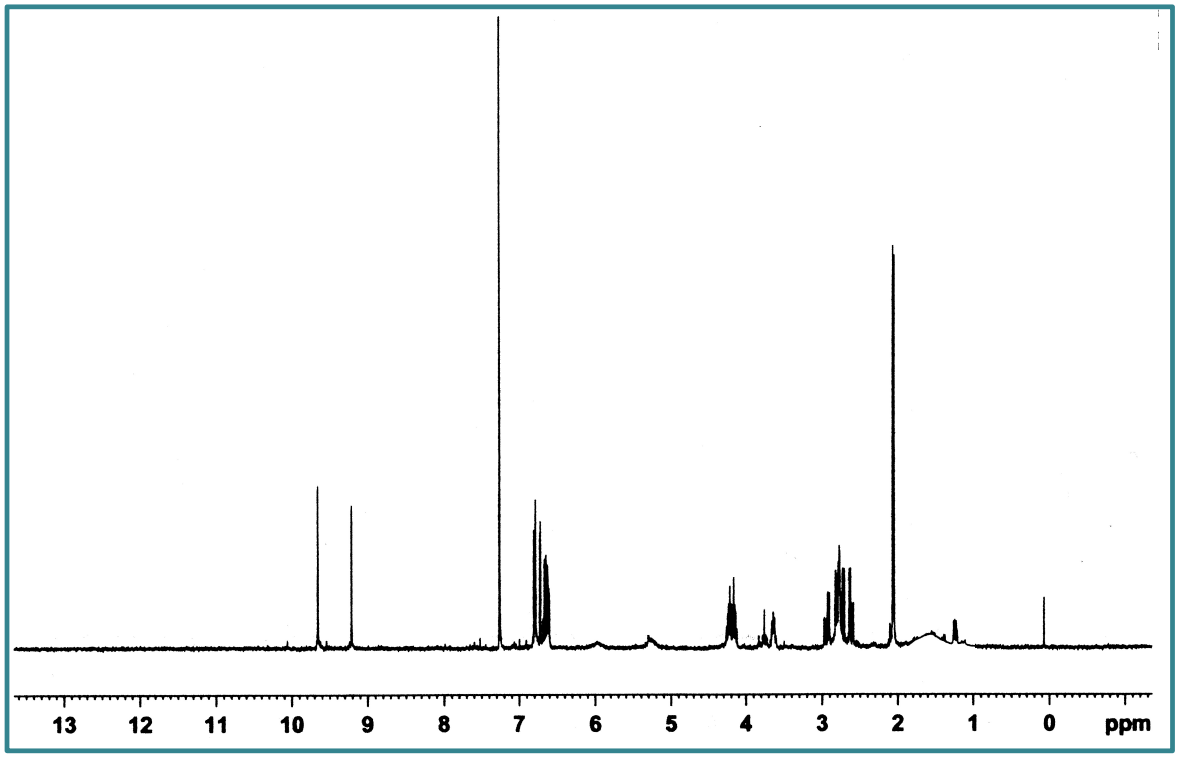

Figure 25 – ^{1}H-NMR ($CDCl_3$ - 400 MHz) of oleacein after the second step of purification performed by exploiting reverse flash column chromatography carried out by automated flash purification instrument.

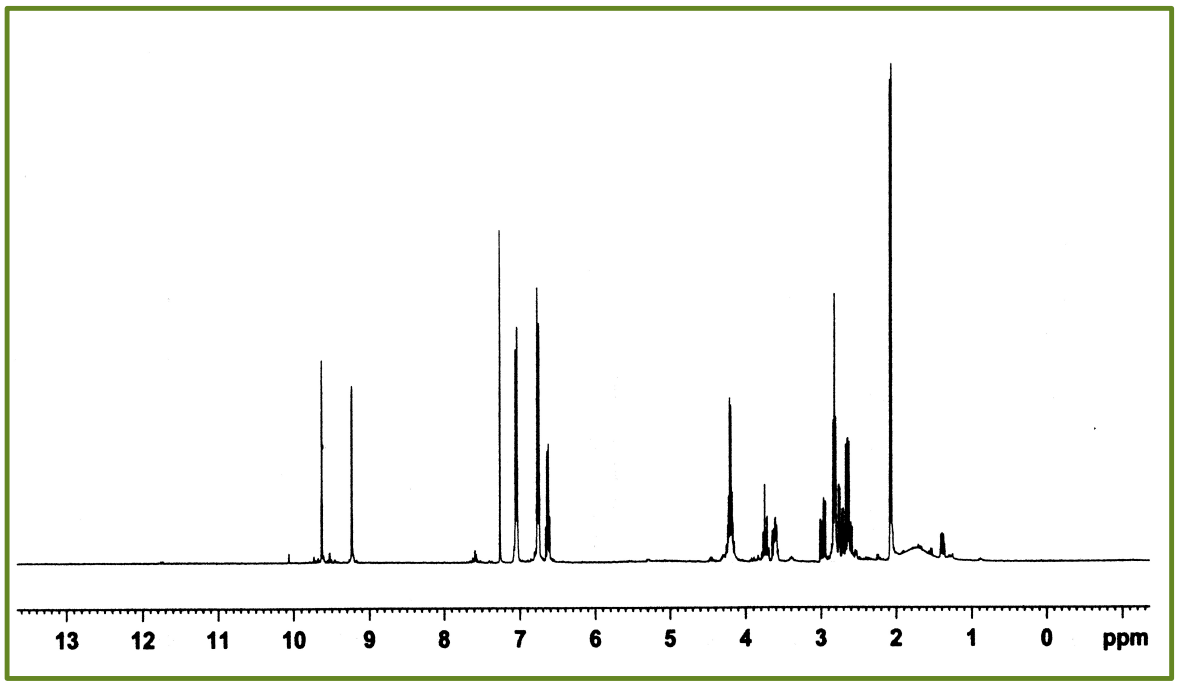

Figure 26 – ^{1}H-NMR ($CDCl_3$ - 400 MHz) oleocanthal after the second step of purification performed by exploiting reverse flash column chromatography carried out by automated flash purification instrument.

3.1.2 Conclusion

The method developed during this PhD for the purification of OC and OO involves the use of advanced automated flash purification system, by exploiting a direct phase chromatography as a first step of purification and a reverse phase chromatography as a second step of purification. With this procedure, it was possible to reduce the amount of solvent used and the time necessary for the purification compared with the procedure previously reported.[47] Moreover, it was possible to increase the yield obtaining significant amount of OC and OO with good purity (>95%), starting from a small amount of fresh EVOO (100g).[108,109]

3.2 Study of the nutraceutical properties of oleocanthal and oleacein

OC and OO extracted and purified from Tuscan EVOOs were then submitted to pharmacological studies, to investigate their nutraceutical properties. In particular, their role in obesity-associated adipocyte inflammation was investigated.[110] Moreover, the anti-tumour effect of OC[108] and the anti-fibrotic effect of OO[109] were evaluated.

3.2.1 Role of Oleacein and Oleocanthal in Obesity-Associated Adipocyte Inflammation

The main cellular components of adipose tissue (AT) are represented by adipocytes which are considered as an energy depot. Recently an important role has been attributed to these cells in the control of energy homeostasis and metabolism in the liver, in the vasculature, in the skeletal muscle, and in the AT itself, through the production of adipo(cyto)kines.[111] The alteration of adipocyte functions, and thus the inflammation of AT that occur in obesity, could lead to the production of inflammatory mediators, metabolic and proliferative factors and consequently could induce disorders such as cardiovascular and respiratory diseases, insulin resistance and type 2 diabetes, osteoarthritis and cancer.

NF-κB and microRNAs (miRNAs) could play an important role in obesity-associated inflammation. In particular, NF-κB is involved in the initiation and progression of metabolic diseases, while miRNAs regulate gene expression.[110]

The role of OC and OO on the activation of NF-κB and the expression of molecules involved in inflammatory and dysmetabolic responses was investigated in collaboration with the research group of Professor Paola Nieri of the Department of Pharmacy (University of Pisa).[110] For these purposes, fully differentiated Simpson-Golabi-Behmel syndrome (SGBS) adipocytes were pre-treated with 25 μmol/L of OC or OO before stimulation with the pro-inflammatory cytokine TNF-α supplemented in the culture medium, thus mimicking the AT inflammation. Indeed, TNF-α is overexpressed in AT inflammation during obesity, representing a prototypic inflammatory stimulus.

The effects of OO and OC on mRNA expression levels of adipokines associated with AT inflammation, oxidative stress, insulin resistance and tissue remodeling, were evaluated. In particular, OO and OC are able to prevent the TNF-α-induced up-regulation of the mRNA levels of the chemokines monocyte chemoattractant protein (MCP)-1 (Figure 27**A**) and C-X-C Motif Ligand (CXCL-10) (Figure 27**B**). Moreover, only for OO, the mRNA levels of the macrophage colony-stimulating factor (M-CSF) was reduced (Figure 27**C**).[110]

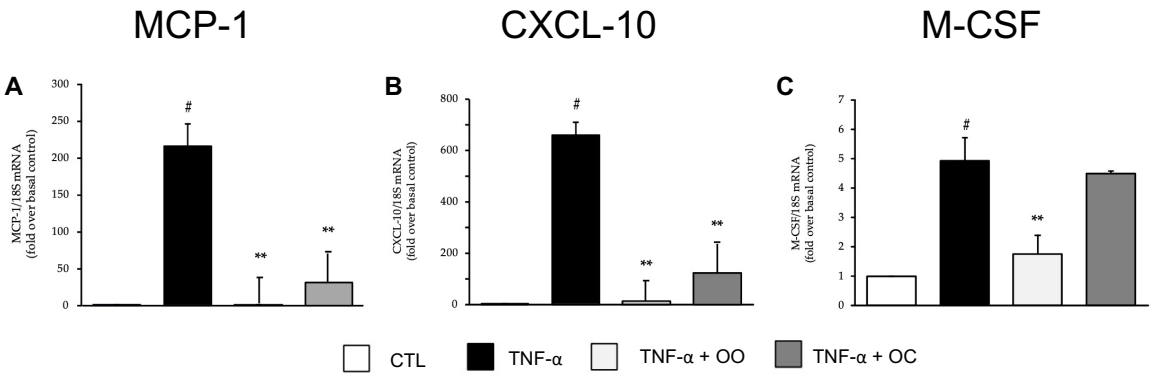

*Figure 27 – Modulation by OO and OC of mRNA expression levels of chemokines associated with adipocyte inflammation. SGBS adipocytes were pretreated with OO or OC 25 µmol/L (6 h) and then treated with 10 ng/mL TNF-α for 18 h. Total RNA was extracted from cells, and mRNA levels of the monocyte chemoattractant protein (MCP-1) (**A**), C-X-C Motif Ligand 10 (CXCL-10) (**B**), and macrophage colony-stimulating factor (M-CSF) (**C**) were measured by qPCR using specific primers and probes and normalized to 18S RNA. Data (means ± SD, n = 3) are expressed as fold induction over unstimulated control (CTL). # p < 0.05 versus CTL. ** p < 0.01 versus TNF-α alone.*[110]

Moreover, the TNF-α-stimulated increase in the mRNA expression of the cytokine IL-1β (Figure 28**A**) and the pro-inflammatory enzyme COX-2 (Figure 28**B**) was mitigated by OC and OO, thus reducing the expression of genes implicated in adipocyte inflammation.[110]

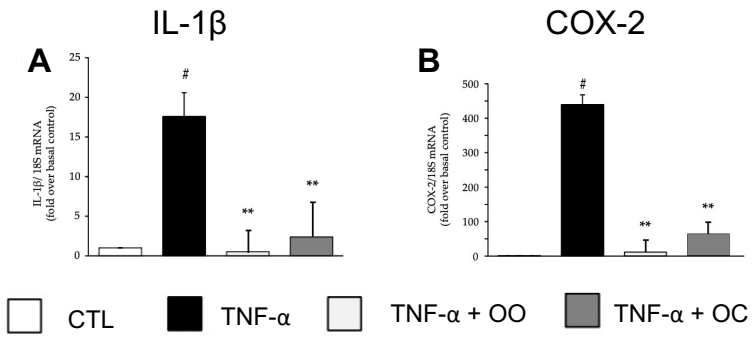

*Figure 28 – Modulation by OO and OC of mRNA expression levels of interleukin-1β (IL-1β) and cyclooxygenase-2 (COX-2). SGBS adipocytes were pretreated with OO or OC 25 µmol/L (6 h) and then treated with 10 ng/mL TNF-α for 18 h. Total RNA was extracted from cells, and mRNA levels of IL-1β (**A**) and cyclooxygenase-2 (COX-2) (**B**) were measured by qPCR using specific primers and probes and normalized to 18S RNA. Data (means ± SD, n = 3) are expressed as fold induction over unstimulated control (CTL). # p < 0.05 versus CTL. * p < 0.05 versus TNF-α alone. ** p < 0.01 versus TNF-α alone.*[110]

A significant inhibitory effect induced by OO and OC was also observed on the mRNA levels implicated in angiogenesis such as the pro-angiogenic VEGF (Figure 29**A**), its receptor kinase insert domain receptor (KDR) (Figure 29**B**) and the matrix-degrading enzyme MMP-2 (Figure 29**C**).[110]

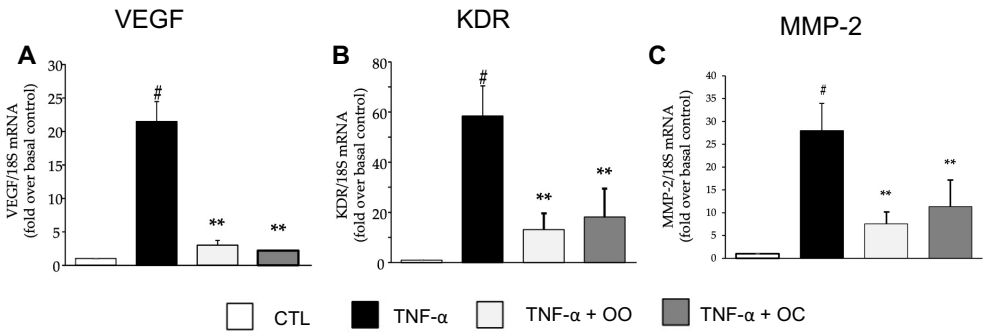

*Figure 29 – Modulation by OO and OC of mRNA expression levels of vascular endothelial growth factor (VEGF), its receptor kinase insert domain receptor (KDR) and the metalloproteinase-2 (MMP-2). SGBS adipocytes were pretreated with OO or OC 25 µmol/L (6 h) and then treated with 10 ng/mL TNF-α for 18 h. Total RNA was extracted from cells, and mRNA levels of VEGF (**A**), KDR (**B**) and MMP-2 (**C**) were measured by qPCR using specific primers and probes and normalized to 18S RNA. Data (means ± SD, n = 3) are expressed as fold induction over unstimulated control (CTL). # p < 0.05 versus CTL. ** p < 0.01 versus TNF-α alone.*[110]

Furthermore, OO and OC significantly reduced the mRNA levels of the pro-oxidant enzyme NOX-4 (Figure 30**A**) and NOX-2 (Figure 30**B**), implicated in oxidative stress and attenuated the increase of mRNA levels of antioxidant enzymes such as SOD-2 (Figure 30**C**) and GPX (Figure 30**D**) in response to TNF-α.[110]

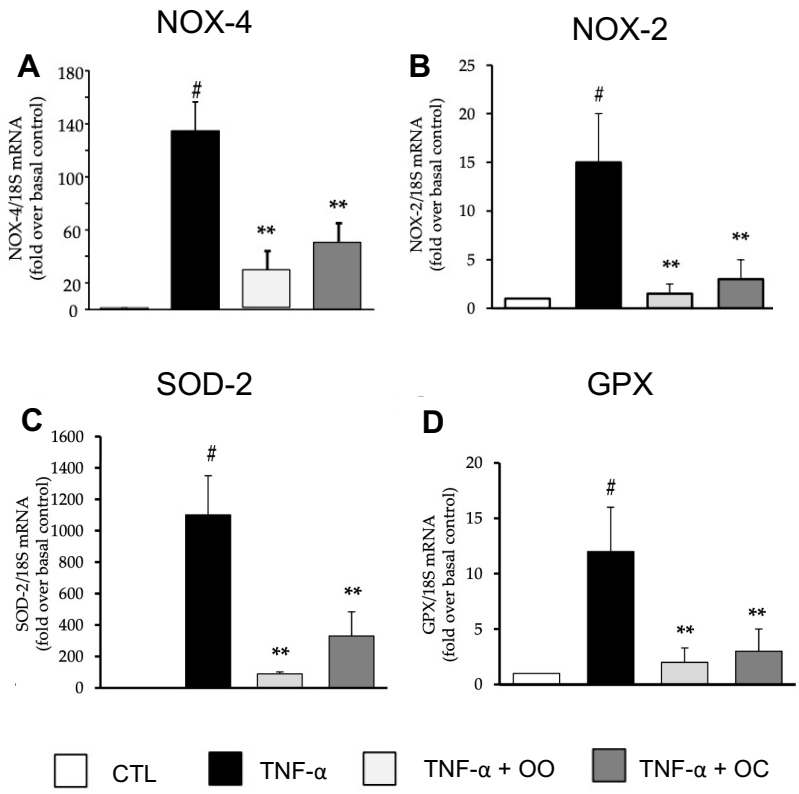

*Figure 30 – Modulation by OO and OC of mRNA expression levels of the pro-oxidant enzyme NADPH oxidase (NOX) (NOX-4 and NOX-2), and the antioxidant enzymes superoxide dismutase-2 (SOD- 2) and glutathione peroxidase (GPX). SGBS adipocytes were pretreated with OO or OC 25 µmol/L (6 h) and then treated with 10 ng/mL TNF-α for 18 h. Total RNA was extracted from cells, and mRNA levels of NOX-4 (**A**), NOX-2 (**B**), SOD-2 (**C**) and GPX (**D**) were measured by qPCR using specific primers and probes and normalized to 18S RNA. Data (means ± SD, n = 3) are expressed as fold induction over unstimulated control (CTL). # p < 0.05 versus CTL. ** p < 0.01 versus TNF-α alone.*[110]

Differently, OO and OC are able to avoid the TNF-α-induced downregulation of peroxisome proliferator-activated receptor-γ (PPARγ) mRNA levels (Figure 31). PPARγ represents a transcription factor which controls the energy metabolism and inflammation in AT.[110]

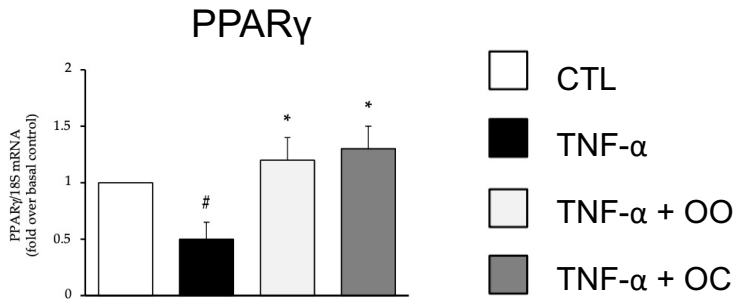

*Figure 31 – Modulation by OO and OC of mRNA expression levels metabolic transcriptional regulator associated with adipocyte inflammation. SGBS adipocytes were pretreated with OO or OC 25 µmol/L (6 h) and then treated with 10 ng/mL TNF-α for 18 h. Total RNA was extracted from cells, and mRNA levels of peroxisome proliferator-activated receptor-γ (PPARγ) were measured by qPCR using specific primers and probes and normalized to 18S RNA. Data (means ± SD, n = 3) are expressed as fold induction over unstimulated control (CTL). # p < 0.05 versus CTL. * p < 0.05 versus TNF-α alone. ** p < 0.01 versus TNF-α alone.*[110]

Moreover, this study has demonstrated that OO and OC are able to significantly counteract the miRNA modulation and NF-κB activation induced by TNF-α.

NF-κB is a transcription factor that regulates the expression of genes and miRNAs, linked to the inflammatory responses. The effect of OO and OC on the activation of NF-κB by TNF-α in human adipocytes, was investigated. For this purpose, SGBS cells after treatment with OO or OC were stimulated with TNF-α for 1h to induce NF-κB activation and its nuclear translocation. Since TNF-α strongly increases the DNA binding activity of the p65 NF-κB subunit, the ability of the p65 subunit of NF-κB to bind to the DNA consensus site, was evaluated. The results of this study showed that OO or OC are able to reduce NF-κB activation in response to TNF-α, by about 35% and 20%, respectively (Figure 32).[110]

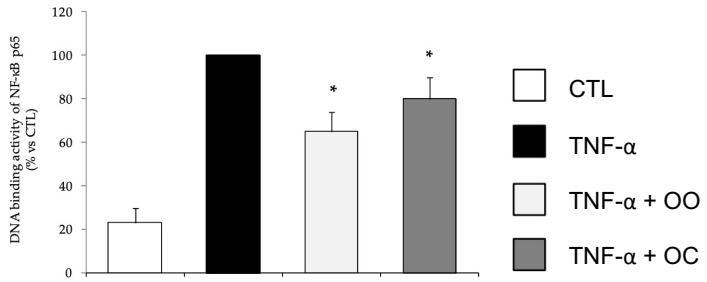

*Figure 32 – Modulation by OO and OC of NF-κB activation. SGBS adipocytes were pretreated with OO or OC 25 µmol/L (6 h) and then treated with 10 ng/mL TNF-α for 1 h. Then, nuclear proteins were extracted and assessed by ELISA to measure the DNA binding activity of the p65 NF-κB subunit. Data (means ± SD, n = 3) are expressed as percent of TNF-α. CTL = unstimulated control. *p < 0.05 versus TNF-α alone.*[110]

In conclusion OO and OC are able to significantly reduce the expression of genes implicated in leukocytes chemotaxis and infiltration (*e.g.* MCP-1, CXCL-10 and MCS-F), adipocyte inflammation (*e.g.* IL-1β and COX-2), angiogenesis (*e.g.* VEGF/KDR and MM-2), oxidative stress (NOXs), antioxidant enzymes (*e.g.* SOD-2 and GPX) and to enhance the expression of the anti-inflammatory/metabolic effector PPARγ.[110] Moreover, OO and OC are able to counteract inflammation by reducing NF-κB activation and the expression of inflammatory cells and exosomal miRNAs. At the same time the two secoiridoids modulate the expression of pro-inflammatory genes. These studies suggested that OO and OC may be useful in the prevention of metabolic inflammation associated with obesity.[110]

3.2.2 Evaluation of the Anti-melanoma Effect of Oleacein

Previously, OC and OO had been studied for their antiproliferative properties on cellular models of skin cancer, by my research group. It was demonstrated that the single phenolic compounds OC and OO as well as EVOO extracts containing significant amount of OC and OO played an important role in the prevention of NMSC.[47,107] Furthermore, the potential anticancer effect of OO in *cutaneous* malignant melanoma was proved.[46]

The activity of OC against *cutaneous* melanoma had not yet been investigated. Therefore, during this PhD, the antimelanoma effect of OC was evaluated, in collaboration with the research group of Professor Paola Nieri of the Department of Pharmacy (University of Pisa).[108]

OC inhibits cell growth in 501Mel cells (human melanoma cells from melanoma metastasis), showing an IC_{50} mean value of 81.9 ± 6.9 μM and 19.1 ± 5.8 μM after 48 h and 72 h of treatment, respectively (Figure 33), with a reduction of cell viability in a time- and concentration-dependent manner.[108]

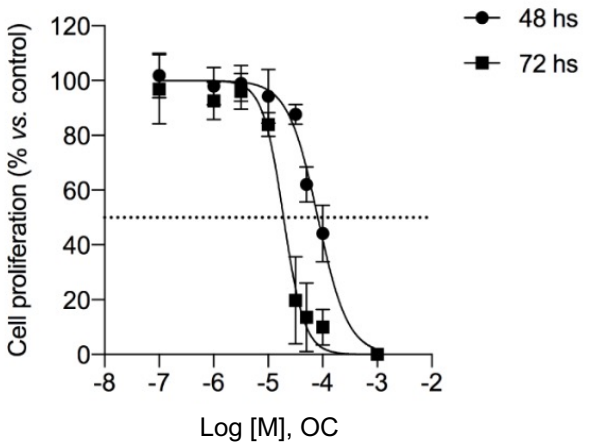

Figure 33 – 501Mel cells were treated with increasing concentration (0.1–200 mM) of oleacein. Growth inhibition was measured at 48 and 72 h using the MTT assay and is expressed as percentage of Ctrl (vehicle-treated cells). Data are presented as means ± SD of three independent experiments, each performed in triplicate.[108]

Moreover, the capability of OC to induce cell cycle arrest, was investigated. In particular, the levels of Histone H3-pSer10 (marker of mitosis) and Cdk2-pTyr15, (marker of the G1/S transition) were evaluated. In late G2 phase and during mitosis the H3 on Ser10 is phosphorylated while it is completely dephosphorylated at the end of mitosis. It was demonstrated that OC at the IC_{50} concentration for 72 h, significantly decreases the H3-pSer10 levels, compared to control cells (Figure 34**A**). OC did not induce cell cycle block in G2/M transition, as suggested by the significant reduction of phosphorylation. In OC treated cells a significant increase of the phosphorylation of Cdk2 on Tyr15 (Figure 34**B**), was observed. As Cdk2 is a master regulator of G1/S transition and the phosphorylation on Tyr15 inactivates this cyclin, this result indicates that OC induces cell cycle arrest in G1/S transition.[108]

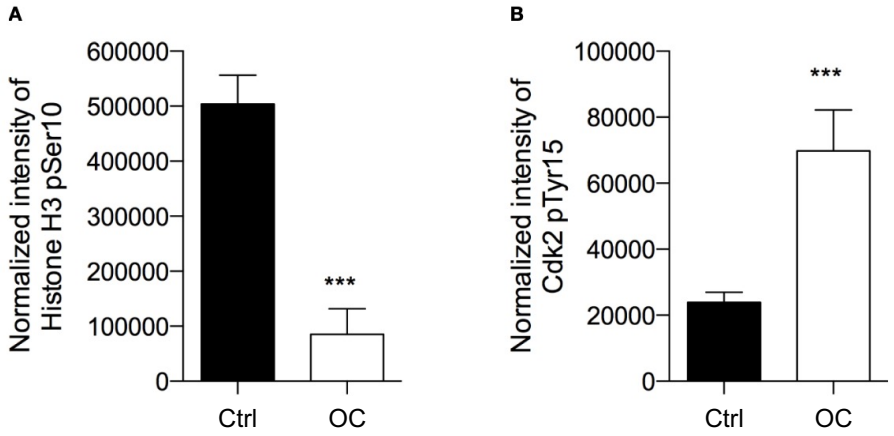

*Figure 34 – Oleacein induces a cell cycle arrest in G1/S phase transition. 501Mel cells were treated with OA 20 μM for 72 h. Phosphorylation levels of Histone H3 at pSer10 (**A**) and Cdk2 at pTyr15 (**B**) were expressed as fluorescence unit normalized on the corresponding cell amount (Normalized intensity). Data are presented as means ± SD of three independent experiments, each performed in triplicate. Student-t test was performed; ***p < 0.001 compared to the corresponding control (vehicle-treated cells, Ctrl).*[108]

In order to investigate the role of OC in apoptosis, the internucleosomal DNA fragmentation, which takes place during late stages of programmed cell death, and the expression levels of genes and miRNAs (short non-coding RNAs able to post-transcriptionally regulate gene expression) involved in the apoptotic process, were evaluated. The results showed that OC increases DNA histone fragments into cell cytoplasm, demonstrating a pro-apoptotic effect (Figure 35**A**). Moreover, it was possible to observe that OC (at the IC_{50} concentration for 72 h) strongly increases the pro-apoptotic BAX mRNA levels and significantly reduces the anti-apoptotic BCL2 and MCL-1 transcriptional levels (Figure 35**B**).[108] In accordance with these results, OC induces a marked upregulation of miR-34a-5p and miR-16-5p (both targeting BCL2) and of miR-193a-3p (targeting MCL-1) and a significant reduction of miR-214-3p (targeting BAX) (Figure 35**C**).[108]

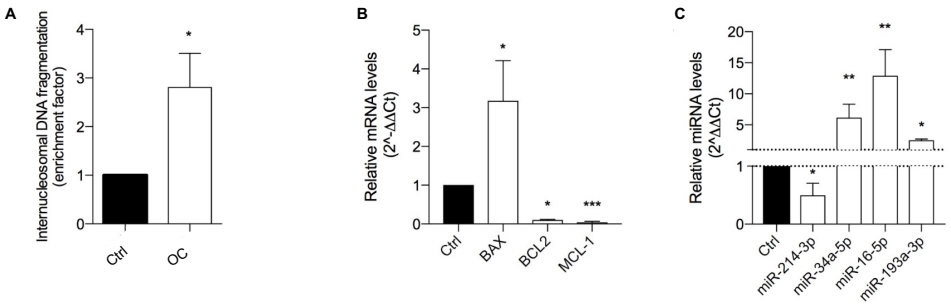

*Figure 35 – Oleacein induces apoptosis in 501Mel cells. (**A**) Internucleosomal DNA fragmentation in cells treated with 20 mM oleacein for 72 h, compared to control (vehicle-treated) cells. Expression levels of mRNAs (**B**) and microRNAs (miRNAs) (C) involved in the apoptosis regulation in cells treated with 20 μM oleacein for 72 h, expressed as fold over control. Data are presented as means ± SD of three independent experiments, each performed in triplicate. Student-t test was performed. *p < 0.05, **p < 0.01, ***p < 0.001, compared to the corresponding control.*[108]

Since mTOR signalling pathway regulates cell proliferation, survival and apoptosis, the expression of genes and miRNAs correlated to this pathway was evaluated after treatment of 501Mel cells with OC (at the IC_{50} concentration for 72h). The results demonstrate that OC is able to down-regulate the expression of C-KIT, KRAS and PIK3R3, important effectors that intensified mTOR activation, and to significantly reduce the mTOR transcriptional levels (Figure 36**A**).[108] Concordantly, OC induces a strongly increase of miR-155-5p (targeting KRAS and PIK3R3) and miR-193a-5p (targeting mTOR) (Figure 36**B**).[108] These results demonstrate, for the first time, that OC can affect the activation of mTOR pathway by targeting the transcriptional level of its main effector proteins.[108]

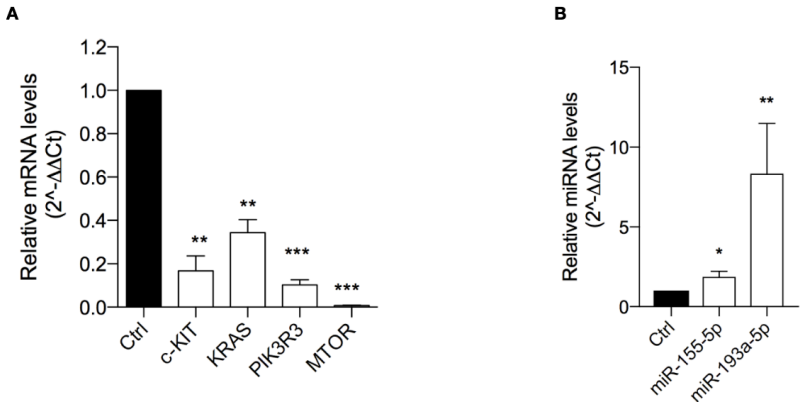

*Figure 36 – Oleacein downregulates genes and miRNAs involved in mammalian target of rapamycin (mTOR) pathway. Expression levels of genes (**A**) and microRNAs (miRNAs) (**B**) related to mTOR pathway in cells treated with 20 μM oleacein for 72 h. Data are presented as means ± SD of three independent experiments, each performed in triplicate. Student-t test was performed, *p < 0.05; **p < 0.01; ***p < 0.001 compared to the corresponding control.*[108]

These studies have established that OC possesses anticancer effect against melanoma, as it is able to inhibit cells viability, to induce G1 cell cycle arrest, to induce apoptosis and to inhibit mTOR signalling pathway in 501Mel cell line.[108] In Figure 37 a schematic summary of the pathways involved in the anti-tumour effect associated with OC in melanoma cells is shown.

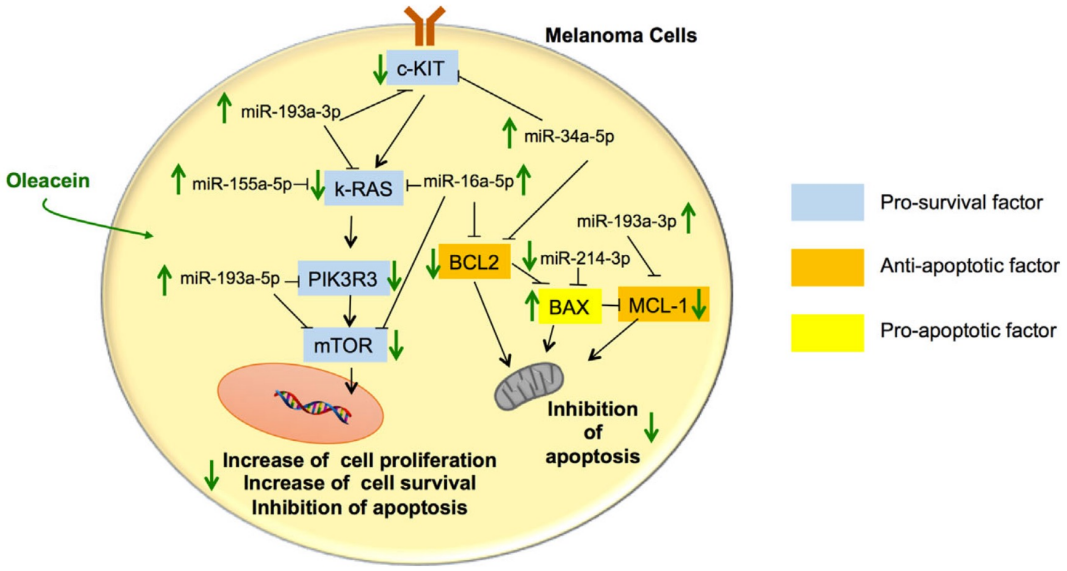

Figure 37 – OC regulates the expression pattern of genes and miRNAs so that to inhibit proliferation, survival and to induce apoptosis of melanoma cells. The black arrows indicate stimulation. The black lines indicate inhibition.[108]

3.2.3 Evaluation of Oleocanthal Antifibrotic Effect in the Liver

Liver fibrosis is considered the outcome of wound-healing response that arises in chronic liver diseases, and it can proceed into liver cirrhosis and subsequently it can progress in liver failure and cancer.

Hepatic stellate cells (HSCs), physiologically dedicated to store lipids, play a key role in the deposition of fibrotic tissue in the liver, by turning from a quiescent state to a pro-inflammatory and pro-fibrotic myofibroblast-like phenotype, due to a prolonged hepatic injury. In particular, HSCs can induce the remodeling of the extracellular matrix (ECM) by up-regulating some MMPs. Furthermore, proinflammatory chemokines and cytokines, such as the transforming growth factor (TGF)-β, can lead to the HSCs activation. Moreover, ROS can induce the activation of HSCs and induce hepatocyte inflammation. Indeed, several evidence suggests that oxidative stress could be related to the disease progression. Consequently, in

order to reduce liver fibrosis progression and to promote its remission, a valid strategy could be represented by targeting redox homeostasis.[109]

Recent studies have demonstrated the hepato-protective action of EVOO characterized by a high OO concentration by decreasing pro-inflammatory cytokines. Considering this evidence, the anti-fibrotic and anti-inflammatory effects of OO in *in vitro* and *in vivo* models of hepatic fibrosis, were studied, in collaboration with Professor Sara De Martin of the Department of Pharmaceutical and Pharmacological Sciences (University of Padova).[109]

3.2.3.1 In vitro evaluation

In *in vitro* studies, LX2 (human hepatic stellate cell line) and HepG2 (human hepatocellular carcinoma cells) were used.

The OO antifibrotic effect was evaluated on LX2 cells which were treated with TGF-β1 (2 ng/mL) with or without 2 μM OO for 24 h. TGF-β1 induces LX2 activation obtaining a model of activated HSCs.

OO counteracted the increase of the expression of the two pro-fibrotic genes α-SMA (Figure 38**A**) and COL1A1 (Figure 38**B**) induced by TGF-β1.[109]

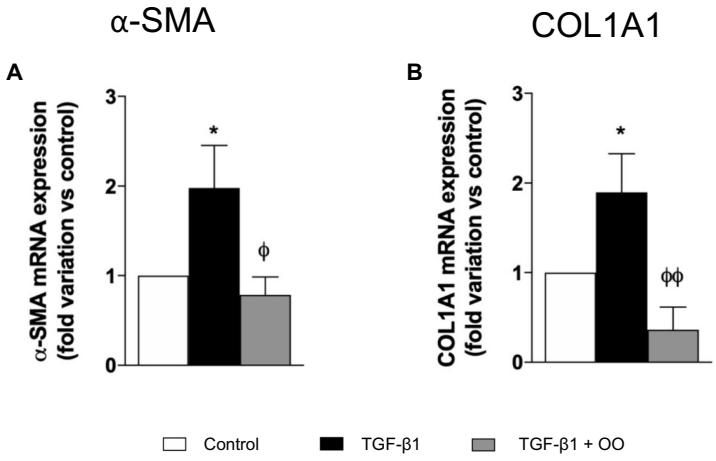

*Figure 38 – Effect of OO on α-SMA (**A**) and COL1A1 (**B**) gene expression in LX2 cell line. *P < 0.05 vs. control, φP < 0.05, φφ, P < 0.01 vs. TGF-β1 treated cells. Results are the mean of 3 independent experiments and have been analyzed by one-way ANOVA followed by the Tukey's post hoc test.*[109]

The effect of OO on the expression of some MMPs involved in the remodeling process of ECM induced by the activation of HSCs, was evaluated. OO counteracts the increase of mRNA expression of the investigated MMPs isoforms stimulated by

TGF-β1. OO is able to strongly down-regulate the mRNA expression of MMP2, 3 and 7, for MMP9 OO only induces a slightly decrease, while the MMP1 mRNA expression did not change.[109]

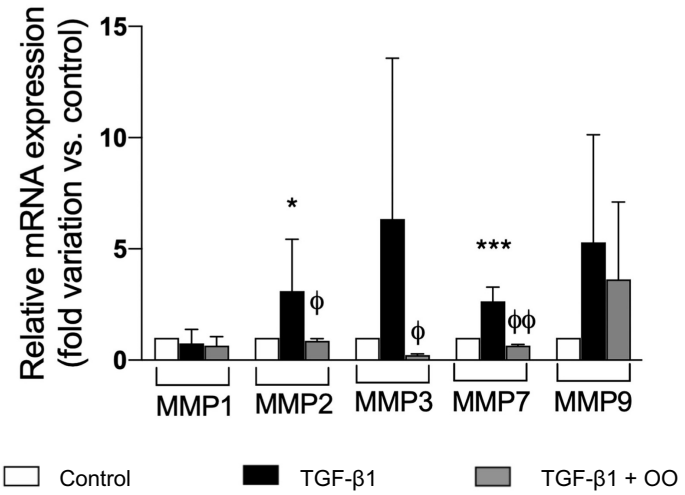

*Figure 39 - Effect of OO on MMPs gene expression in LX2 cell line. *P < 0.05, ***P < 0.001 vs. control, φP < 0.05, φφP < 0.01 vs. TGF-β1 treated cells. Results are the mean of 3 independent experiments and have been analyzed by one-way ANOVA followed by the Tukey's post hoc test.*[109]

Furthermore, the effect of OO on VEGFA, which markedly increases during fibrogenesis, was investigated. OO significantly decreased both the gene expression (Figure 40**A**) and release (Figure 40**B**) of VEGFA from LX2 cells activated by TGF-β1, thus restoring their physiological levels.[109]

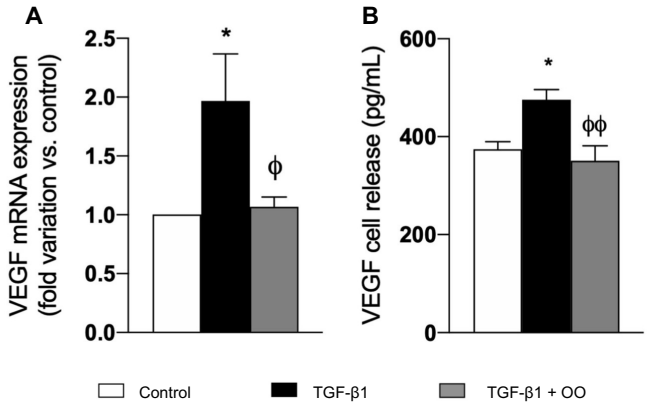

*Figure 40 – Effect of OO on VEGF mRNA expression (**A**) and release (**B**) from LX2 cell line. *P < 0.05 vs. control, φP < 0.05 vs. TGF-β1 treated cells. φφP < 0.01 vs. Results are the mean of 3 independent experiments performed in triplicate (qRT-PCR) or in duplicate (ELISA) and have been analysed by one-way ANOVA followed by the Tukey's post hoc test.*[109]

As oxidative stress is fundamental for fibrogenesis, also the effect on oxidative stress-related pathways of OO was investigated by evaluating the mRNA levels of NOX1 and NOX4, which are associated with hepatic ROS production. In particular, it was demonstrated that OO strongly down-regulates NOX1 and NOX4 gene expression in LX2 cells stimulated with TGF-β1 (Figure 41).[109]

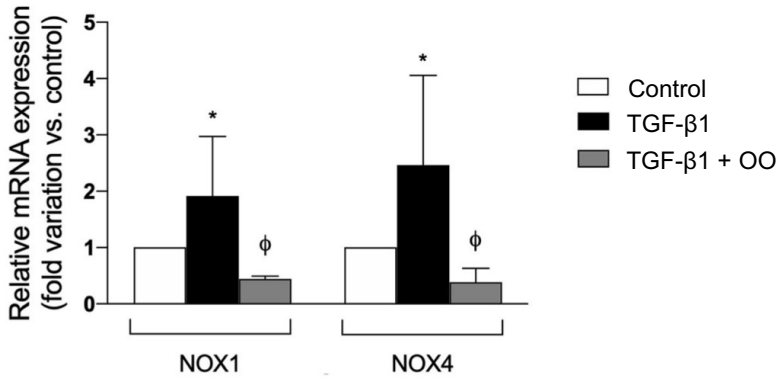

*Figure 41 – Effect of OO on gene expression of NOX1 and NOX4 in LX-2 cells. *P < 0.05 vs. control, φP < 0.05 vs. TGF-β1-treated cells. Results are the mean of 3 independent experiments performed in triplicate and have been analysed by one-way ANOVA followed by the Tukey's post hoc test.*[109]

Moreover, the antioxidant effect of OO on the hepatocyte-like cells HepG2, was explored. OO significantly decreases ROS production in HepG2 cells stimulated with H_2O_2 (Figure 42).[109]

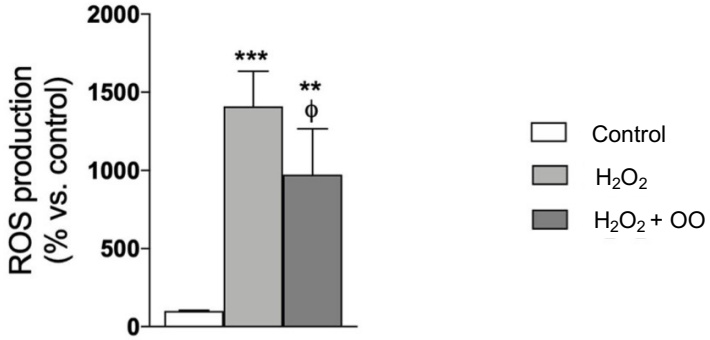

*Figure 42 – Effect of OO on ROS production by HepG2 cells treated with H_2O_2. **P < 0.01, ***P < 0.001 vs. control, φP < 0.05 vs. H_2O_2-treated cells. Results are the mean of 3 independent experiments performed in triplicate and have been analysed by one-way ANOVA followed by the Tukey's post hoc test.*[109]

From the results of these *in vitro* studies, it was possible to conclude that OO decreases HSCs activation, by down-regulating the expression of α-SMA, COL1A1 and of several MMPs associated with ECM remodeling. In addition, OO is able to reduce VEGFA release from HSCs and to counteract the hepatic oxidative stress by decreasing NOX1 and NOX4 expression levels and ROS production.[109]

3.2.3.2 <u>In vivo evaluation</u>

On the basis of the *in vitro* studies performed, the *in vivo* antifibrotic effect of OO was investigated on a murine animal model of liver fibrosis achieved by using Balb/C male mice treated with CCl_4 in corn oil by intraperitoneal (IP) injection performed three times a week for 4 weeks. After the first week 12 mice were randomized into 2 experimental groups: one ("fibrotic mice") was treated with CCl_4 IP; the other one ("fibrotic mice + OO") was treated with both CCl_4 and OO. CCl_4 represents an hepatotoxicant generally exploited to obtain rodent models of liver fibrosis.

The treatment with CCl_4 induced a strongly up-regulation of the mRNA expression of both α-SMA and COL1A1. The administration of OO induces a marked reduction of both α-SMA and COL1A1 expression, thus restoring their physiological levels (Figure 43).[109]

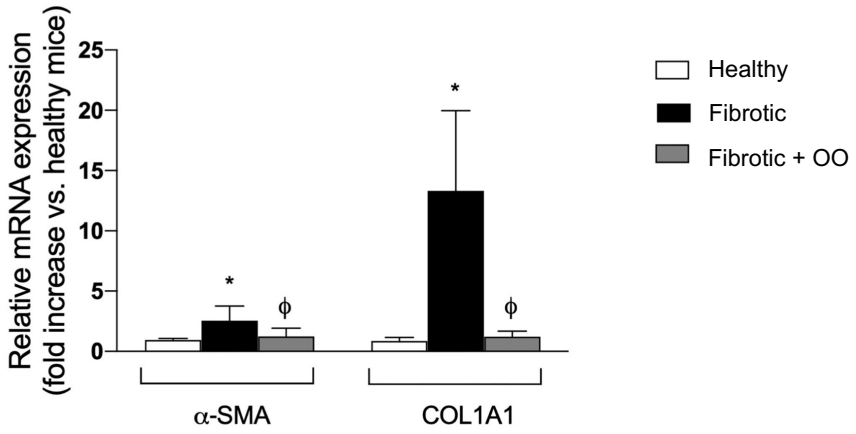

*Figure 43 – Effect of OO on the hepatic expression of the fibrogenic genes α-SMA and COL1A1 in the mouse model of fibrosis. *P < 0.05 vs. control, φ P < 0.05 vs. fibrotic mice. Results are obtained by analysing 6 animals per group in triplicate and have been analysed by one-way ANOVA followed by the Tukey's post hoc test.*[109]

Moreover, OO counteracts the increase in the hepatic expression of the pro-fibrotic miR-181-5p and miR-221-3p (Figure 44**A**), as well as the down-regulation of the two anti-fibrotic miRNAs miR-29b-3p and miR-101b-3p induced by CCl_4 in fibrotic mice (Figure 44**B**).[109]

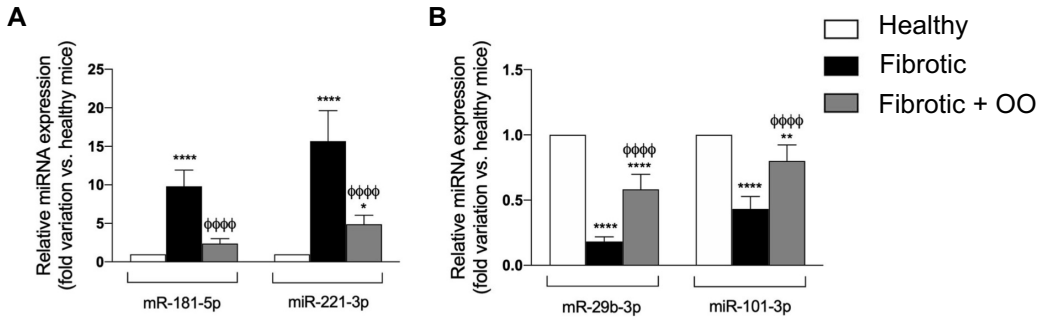

*Figure 44 – Effect of OO on the hepatic expression of pro-fibrotic (**A**) and anti-fibrotic (**B**) miRNAs in a mouse model of fibrosis. *P < 0.05, **P < 0.01, ****P < 0.0001 vs. control, φφφφ P < 0.0001 vs. fibrotic mice. Results are obtained by analysing 6 animals per group in triplicate and have been analysed by one-way ANOVA followed by the Tukey's post hoc test.*[109]

Furthermore, OO reduces the mRNA expression of pro-inflammatory ILs, up-regulated by CCl_4 administration, thus demonstrating anti-inflammatory effects (Figure 45).[109]

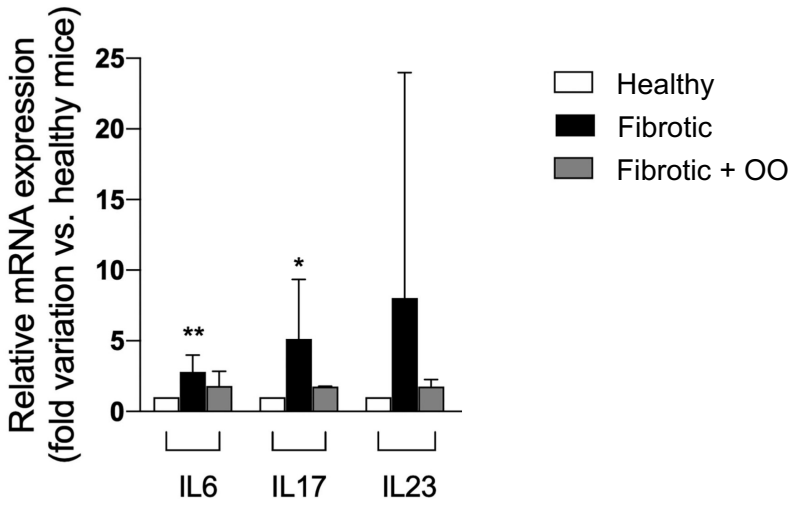

*Figure 45 – Effect of OO on hepatic gene expression of inflammatory cytokines in a mouse model of fibrosis. *P < 0.05 and **P < 0.01 vs. control mice. Results are obtained by analysing 6 animals per group in triplicate and have been analysed by one-way ANOVA followed by the Tukey's post hoc test.*[109]

In conclusion, these data have demonstrated that OO extracted from EVOO exerts a promising antifibrotic effect, both in *in vitro* an *in vivo* models of liver fibrosis, due to its capability to reduce oxidative stress and inflammation involving putative miRNAs, thus reducing HSCs activation and hepatic fibrosis.[109]

3.2.4 Conclusion

During this PhD thesis, several nutraceutical properties of OC and OO were evaluated.

The role of OC and OO in the obesity-associated adipocytes inflammation was proved, demonstrating that both secoiridoids are able to counteract the inflammation of the adipocytes by attenuating the activation of NF-κB, a signalling pathway involved in various metabolic disorders and whose stimulation can lead to insulin resistance.[110] A further study demonstrated the ability of OC to inhibit the proliferation of skin melanoma cells (501Mel cells) *in vitro* through a transcriptional modulation of genes and miRNAs, highlighting the anti-cancer potential of this compound.[108] Moreover, it was demonstrated that OO exerts a promising antifibrotic effect, both in *in vitro* an *in vivo* models of liver fibrosis, by reducing oxidative stress and inflammation involving putative miRNAs, as well as HSCs activation and thus hepatic fibrosis.[109]

3.3 Study of the variations in the phenolic and polyphenolic composition of EVOOs during storage

OO and OC in EVOOs can undergo degradation processes, like hydrolytic and oxidative reactions, influenced by factors such as light, storage time, temperature and oxygen.[12,17,18]

The hydrolysis reaction (Figure 46) occurs on the ester bond of OO and OC and leads to the formation of T and HT, respectively, which are phenolic compounds endowed with nutraceutical properties. This reaction is more closely influenced by storage time factor.

From HPLC analysis of EVOO, it was possible to observe that fresh EVOO contained high amount of OC and OO and little quantity of HT and T, as shown in the chromatogram reported in Figure 47.

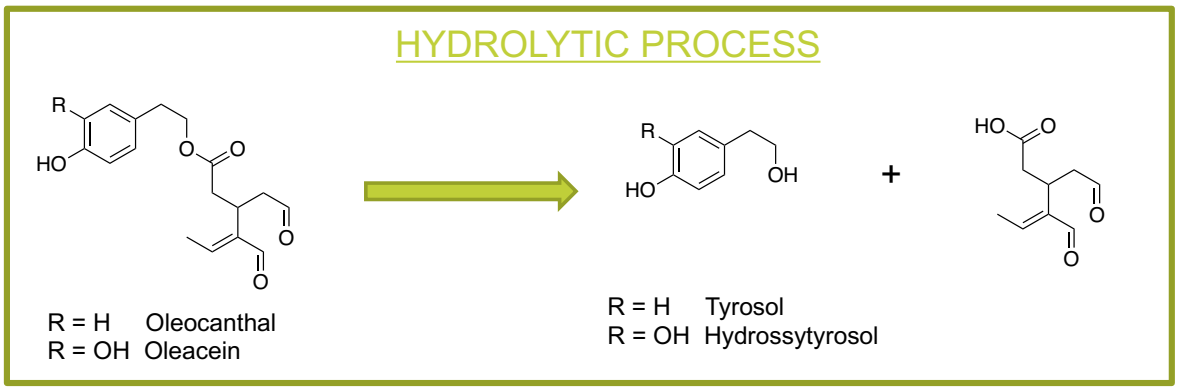

Figure 46 – Hydrolytic process that affects oleocanthal and oleacein leading to the formation of tyrosol and hydroxytyrosol, respectively.

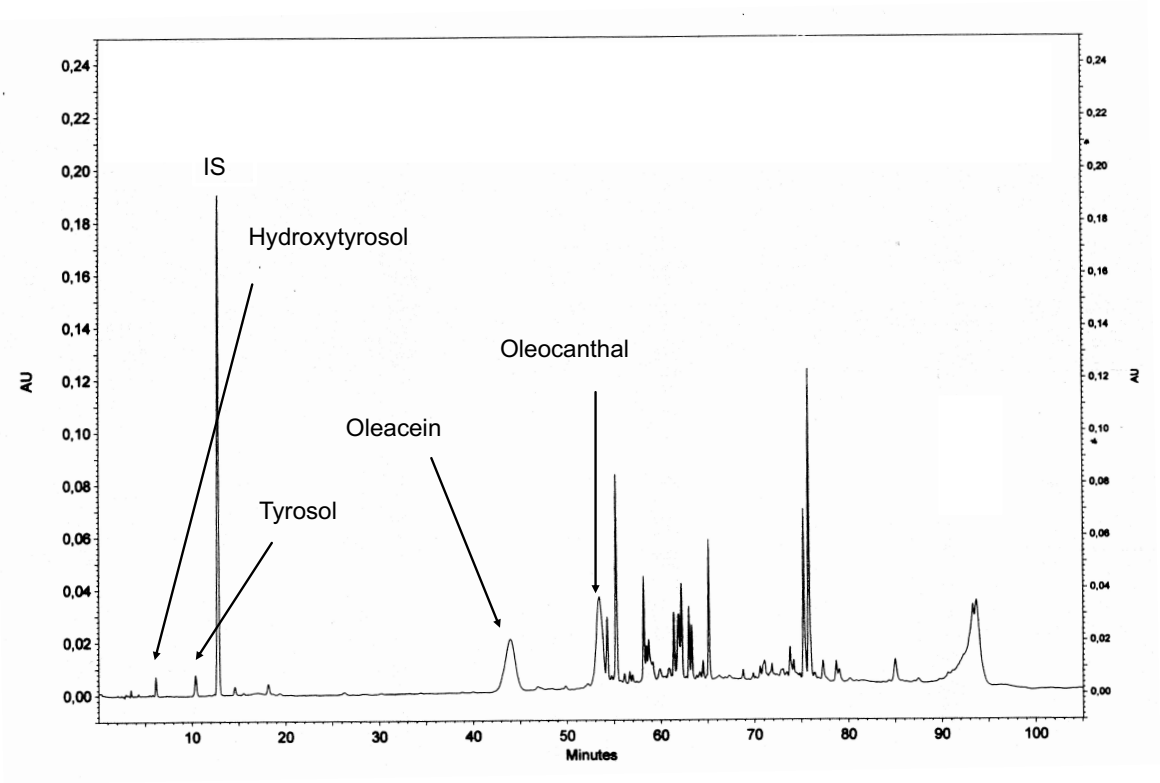

Figure 47 – HPLC chromatogram of a fresh EVOO. IS = Internal Standard.

In order to evaluate the changing in the phenolic composition in EVOOs and in particular to study the progression of hydrolytic processes that occur in EVOO during storage time, I analysed the variation of HT, T, OC and OO content in three different EVOOs for fifteen months (from December 2019 to March 2021).

The EVOOs analysed in this study were two Tuscan EVOOs of the 2019/2020 crop seasons (**A** and **B**) and an Italian EVOO of the 2018/2019 crop season (**C**). These EVOOs were stored under different conditions: an aliquot was kept at room temperature (25°C) and exposed to daylight; another aliquot was kept at the temperature of 4°C (into the fridge), in dark condition. At the time of the first analysis (December 2019), EVOOs **A** and **B** were fresh, while the EVOO **C** had already been stored for one year at room temperature in dark condition. Periodically EVOOs were extracted (method reported in section 4.2.9.1 of the experimental part) and analysed through HPLC, by exploiting the method described in section 4.2.9.2.2 of the experimental part.

3.3.1 Initial Phenolic Composition

The initial total phenolic content (TPC) in each EVOO analysed in December 2019 was evaluated by using the Folin-Ciocalteu assay, described in section 4.2.12.1 of the experimental part. The TPC in EVOOs is expressed as μg of gallic acid equivalents (GAE)/g of EVOOs (ppm). The results of the analysis, reported in Figure 48, showed that the EVOO with the higher amount of TPC was sample **C** (304.96 ± 0.29 μg GAE/g EVOO) followed by samples **B** and **A** (260.22 ± 13.92 and 233.26 ± 12.34 μg GAE/g EVOO, respectively). However, the initial TPC showed low variability among the three samples.

As concerns the quantity of the single phenols presents in each EVOO (expressed as μg of phenolic compound/g of EVOO, ppm), some differences, probably linked to the olive tree *Cultivar* and olive oil aging, could be observed. At the first month of analysis (in December 2019) the OC and OO content in the three EVOOs analysed was quite high, ranged from 94.49 to 116.09 ppm for OC and from 148.93 to 226.36 ppm for OO (Table 6). The starting concentration of HT and T in samples **A** and **B** was low (between 4.72 and 7.28 ppm), while in EVOO **C** was higher (the HT content was 34.11 ± 0.57 ppm, while the T content was 55.62 ± 3.10 ppm). These results, in accordance with the literature, could be explained with the different EVOOs starting age, in fact, EVOO **C** is one year older than EVOOs **A** and **B**.[15]

The HPLC chromatograms of the EVOOs samples **A**, **B** and **C** at the beginning of the analysis (December 2019), are reported in Figure 49, Figure 50 and Figure 51, respectively.

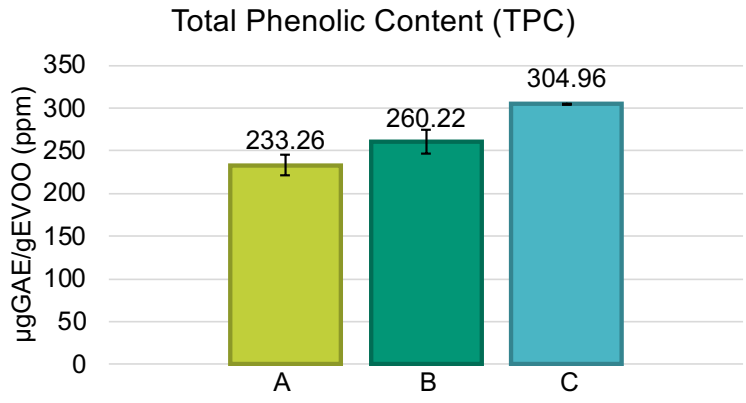

*Figure 48 – TPC content (μg GAE/g EVOO, ppm) in each EVOOs (**A**, **B** and **C**). Data are expressed as mean ± SD of an experiment performed in triplicate.*

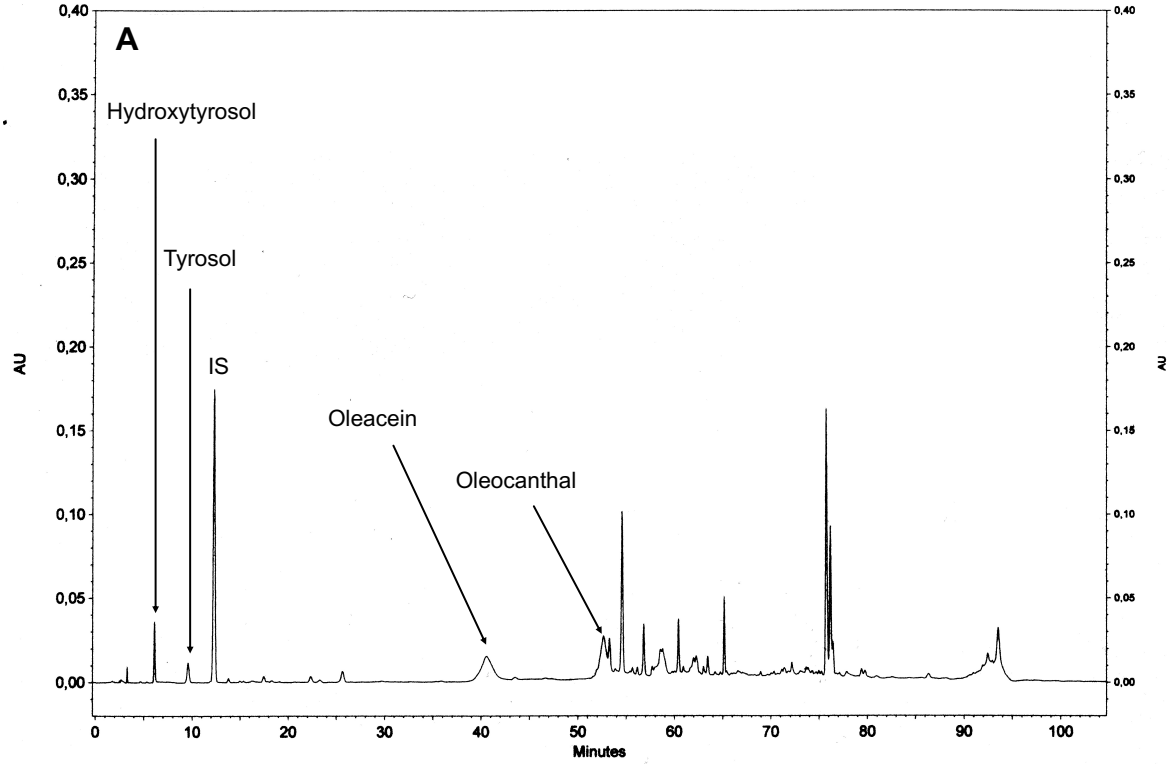

*Figure 49 – HPLC chromatogram of EVOO **A** at the beginning of the analysis (December 2019). IS = Internal Standard.*

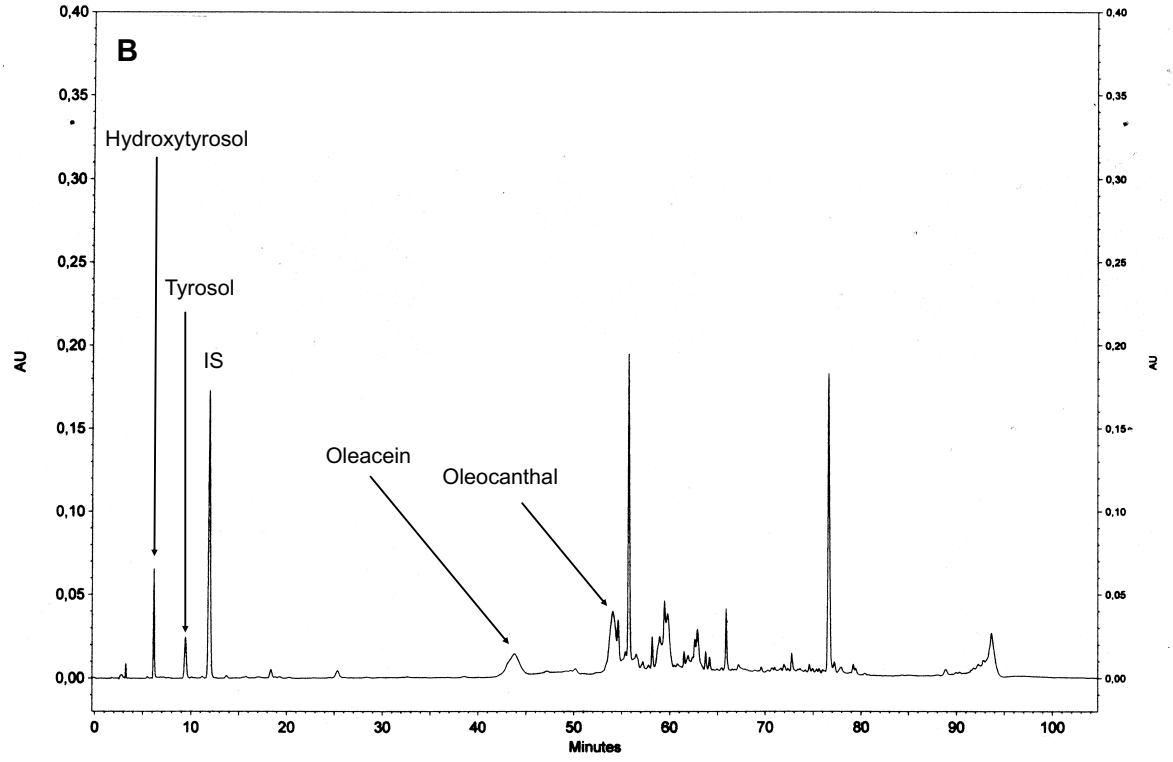

*Figure 50 – HPLC chromatogram of EVOO **B** at the beginning of the analysis (December 2019). IS = Internal Standard.*

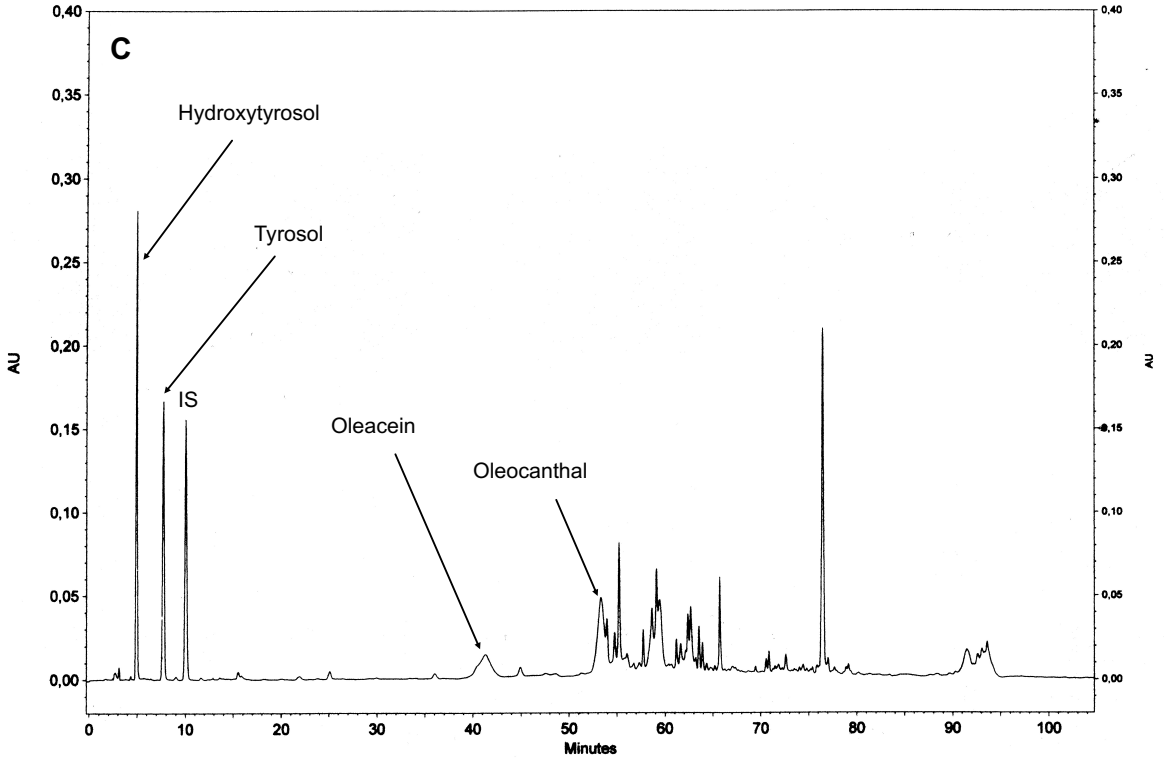

*Figure 51 – HPLC chromatogram of EVOO **C** at the beginning of the analysis (December 2019). IS = Internal Standard.*

3.3.2 Variation of Phenolic Concentration during Storage

The variation of phenolic concentration during EVOOs storage at room temperature, in light condition and at 4°C, in dark condition, was evaluated (Figure 58, Figure 59, Figure 60 and Table 7).

The retention time and the UV absorbance spectrum of the phenolic compounds present in the samples were compared with those of the pure standards and quantified by using *p*-hydroxyphenylacetic acid as IS. Each analysis was performed in triplicate and the content of each phenolic compound was expressed as µg of phenolic compound/g of EVOO (ppm).

3.3.2.1 Storage at Room Temperature and Exposed to Daylight

During storage of EVOOs at room temperature and in the light condition, OC and OO in all samples decreased but with different rates (Figure 58, Figure 59, Figure 60 red bars and Table 7). In particular, in the EVOO **A**, the reduction of the two secoiridoids was more marked than in EVOOs **B** and **C**. In fact, in EVOO **A** the quantity of OC and OO decreased rapidly and only after seven months of storage

(July 2020), they were no longer present. While for samples **B** and **C**, OC and OO were no more detectable after eleven and twelve months of storage, respectively (November and December 2020). The reduction of OC and OO was mainly due to the development of hydrolytic processes that lead to the formation of HT and T, respectively. In fact, simultaneously with the reduction of the two secoiridoids (OC and OO), an increase in simple phenols (HT and T) was observed (Figure 58, Figure 59, Figure 60 red bars and Table 7). This increase is very evident in EVOO **A** where only after two months of storage (February 2020) HT and T increase 6 and 10 times, respectively, compared to the initial content, showing a very efficient hydrolytic process. EVOO **C** showed a very little variation in the quantity of HT and T during storage. The content of HT doesn't seem to change much, while for T only a modest increase can be observed.

It is interesting to notice how in all EVOOs the T content tends to increase until it reaches a plateau phase. As regards HT content, after a first phase in which its concentration increases, it began to decrease (after eleven months of storage, October 2020) for the three EVOOs analysed. This behaviour could be due to the fact that HT molecule may be more unstable compared to T depending on its chemical structure and thus subjected to further degradation processes.

The different trend among EVOOs could depend on factors related to the physico-chemical characteristics of the EVOO or on the presence of microorganisms, which could affect EVOO itself.[18]

The HPLC chromatograms of the three EVOOs samples **A**, **B** and **C** analysed after fifteen months of storage at room temperature and in light condition (March 2021), are reported in Figure 52, Figure 53 and Figure 54, respectively.

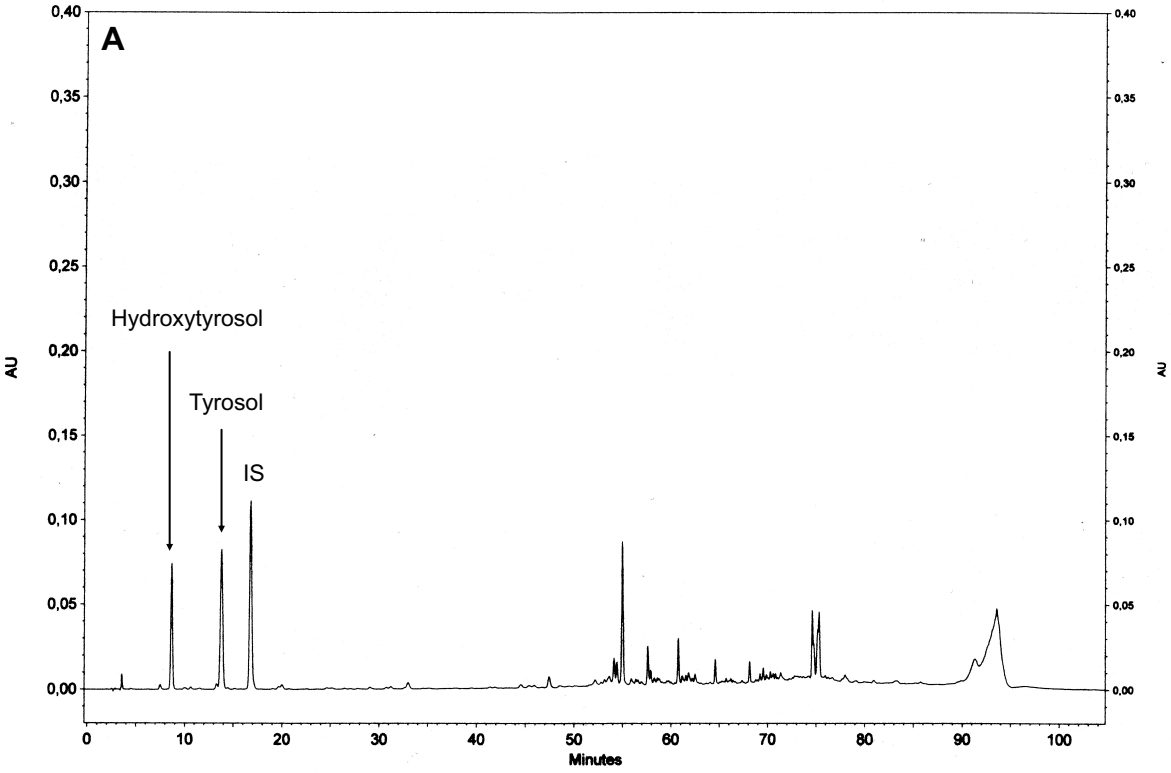

*Figure 52 – HPLC chromatogram of EVOO **A** analysed after fifteen months of storage at room temperature and in light condition (March 2021). IS = Internal Standard.*

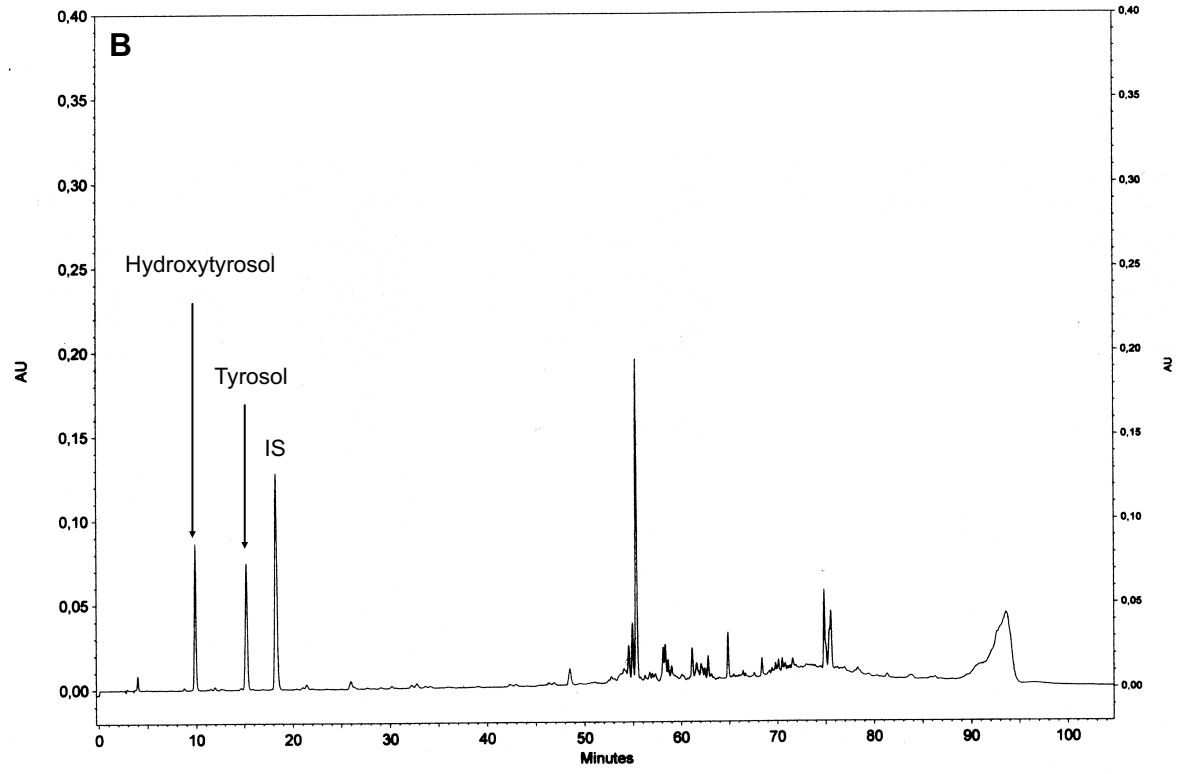

*Figure 53 – HPLC chromatogram of EVOO **B** analysed after fifteen months of storage at room temperature and in light condition (March 2021). IS = Internal Standard.*

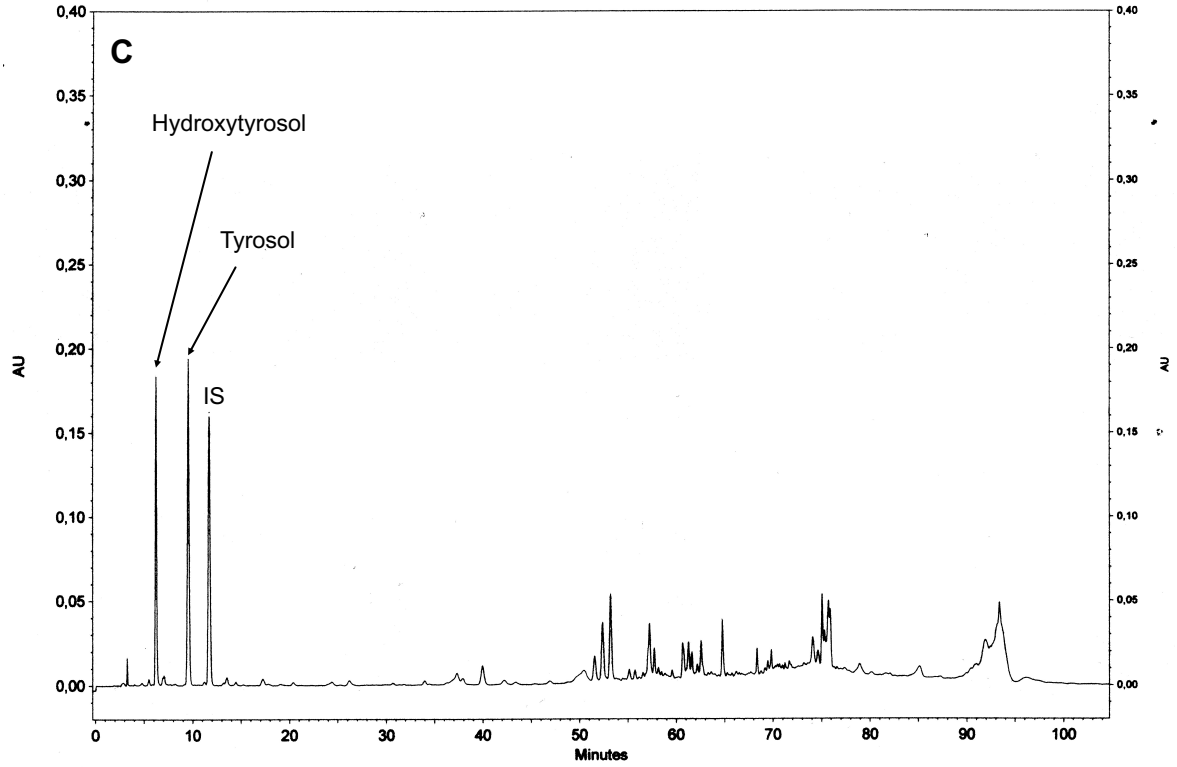

*Figure 54 – HPLC chromatogram of EVOO **C** analysed after fifteen months of storage at room temperature and in light condition (March 2021). IS = Internal Standard.*

3.3.2.2 Storage at 4°C in Dark Condition

During storage at 4°C and in dark condition (Figure 58, Figure 59, Figure 60 blue bars and Table 6) the hydrolytic process that occurs in EVOOs was less marked than in samples kept at room temperature and exposed to daylight. In all samples the variation of OC and OO was very similar, showing a gradual decrease. HT and T raised very slowly, doubling after 16 months in samples **A** and **B** and remaining almost constant in sample **C**.

The HPLC chromatograms of the three EVOOs samples **A**, **B** and **C** analysed after fifteen months of storage at 4°C and in dark condition (March 2021), are reported in Figure 55, Figure 56 and Figure 57, respectively.

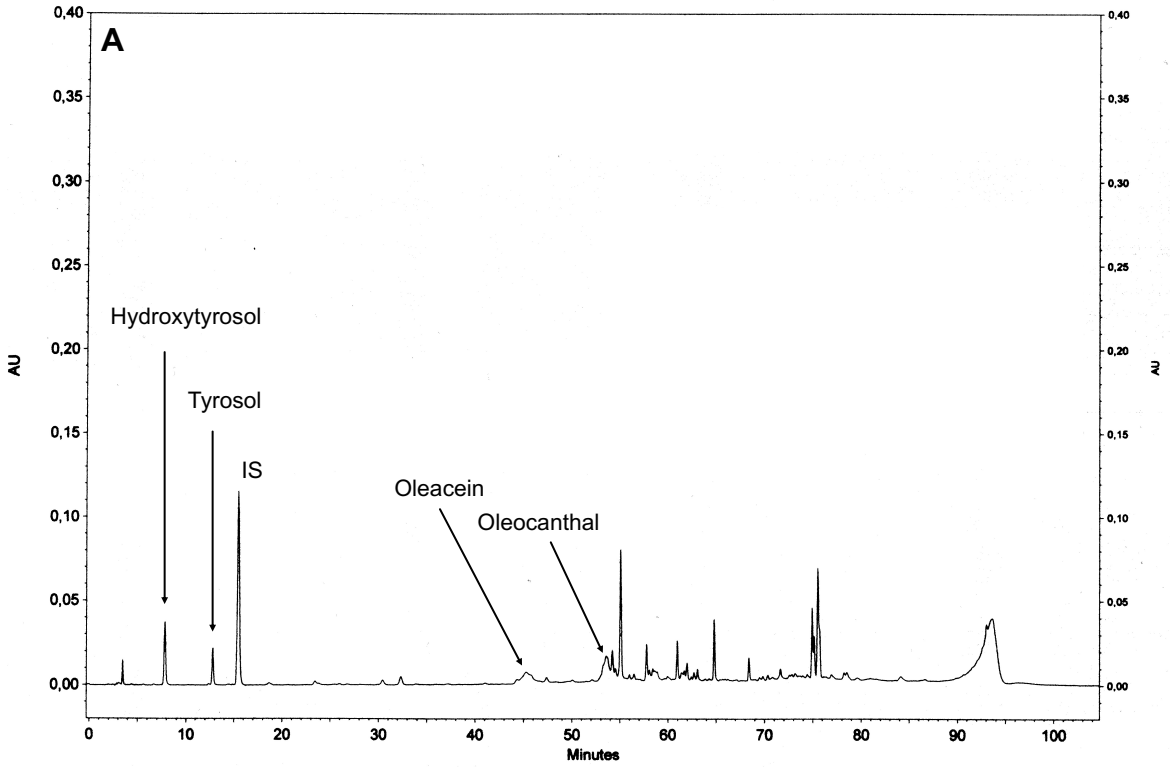

*Figure 55 – HPLC chromatogram of EVOO **A** analysed after fifteen months of storage at 4°C and in dark condition (March 2021). IS= Internal Standard.*

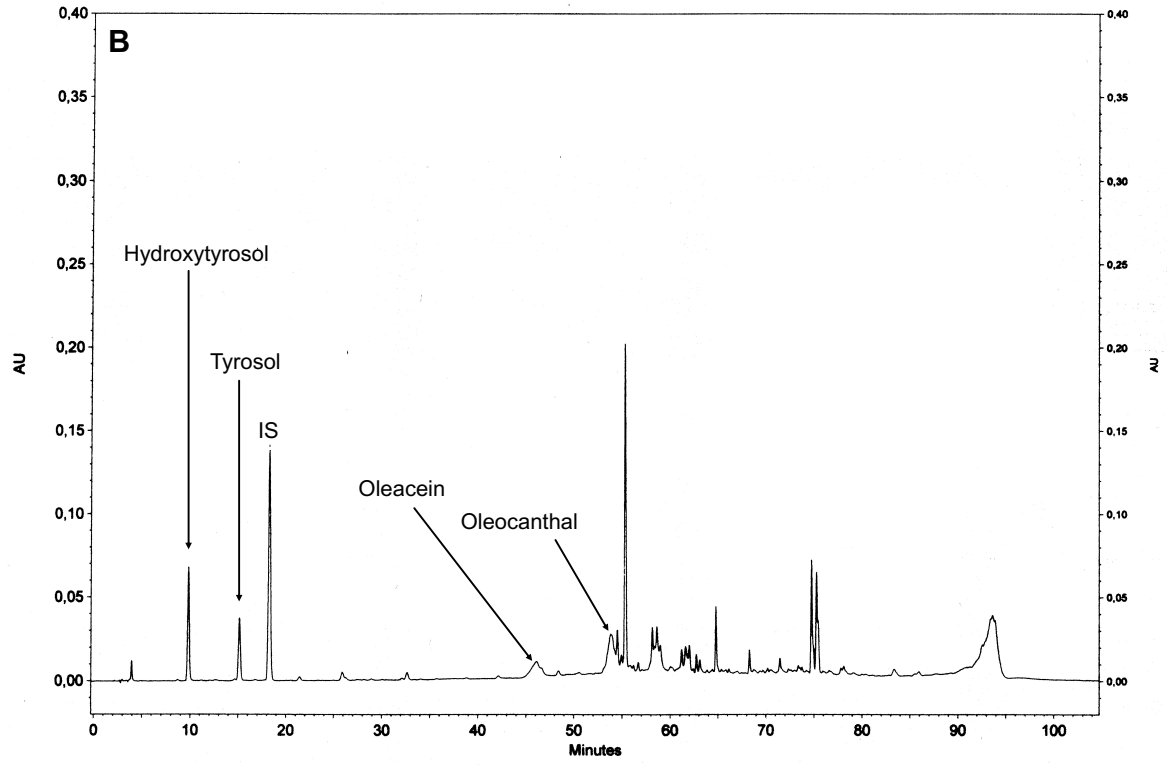

*Figure 56 – HPLC chromatogram of EVOO **B** analysed after fifteen months of storage at 4°C and in dark condition (March 2021). IS= Internal Standard.*

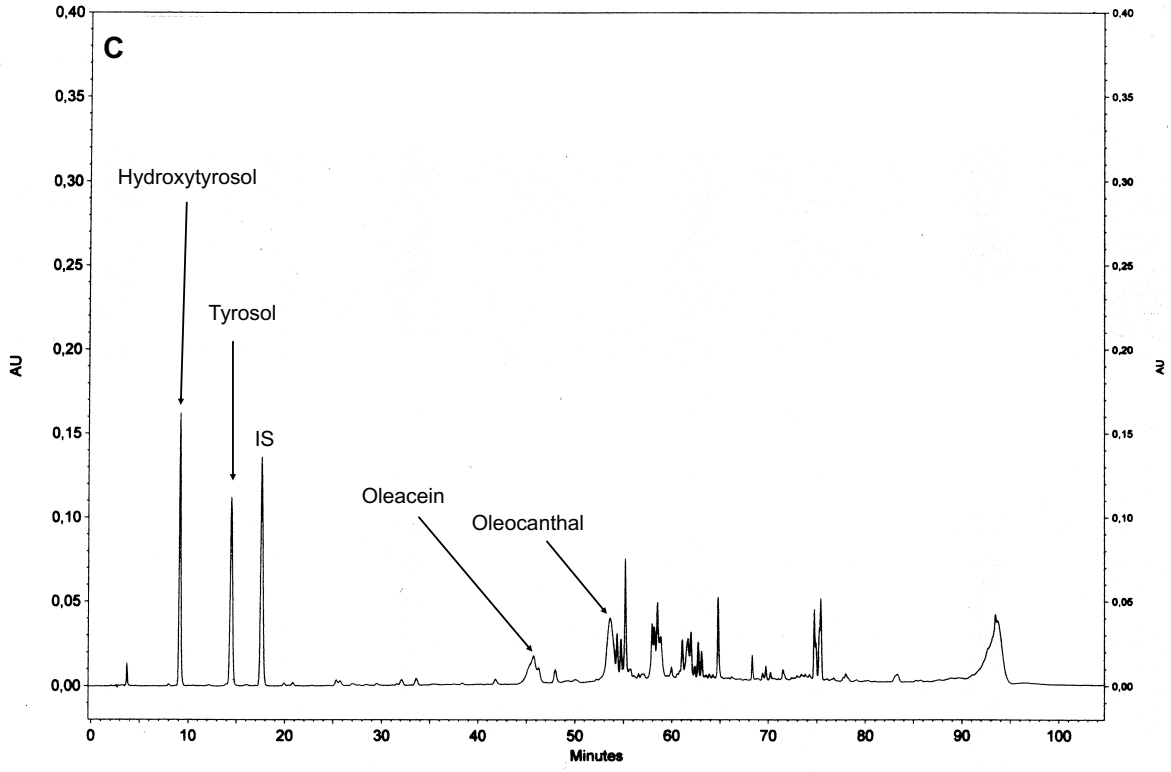

*Figure 57 - HPLC chromatogram of EVOO **C** analysed after fifteen months of storage at 4°C and in dark condition (March 2021). IS= Internal Standard.*

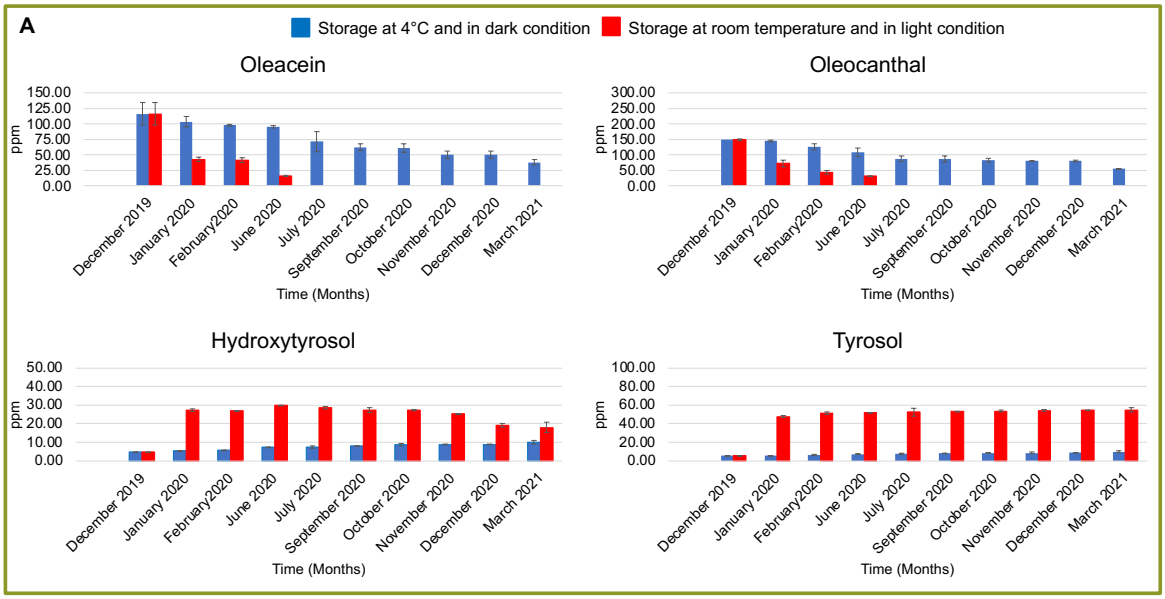

*Figure 58 – Concentration of oleacein, oleocanthal, hydroxytyrosol and tyrosol (µg of phenolic compound/g of EVOO, ppm) in EVOO **A** storage at 4°C in dark condition (blue bars) and at room temperature exposed to daylight (red bars), for 15 months.*

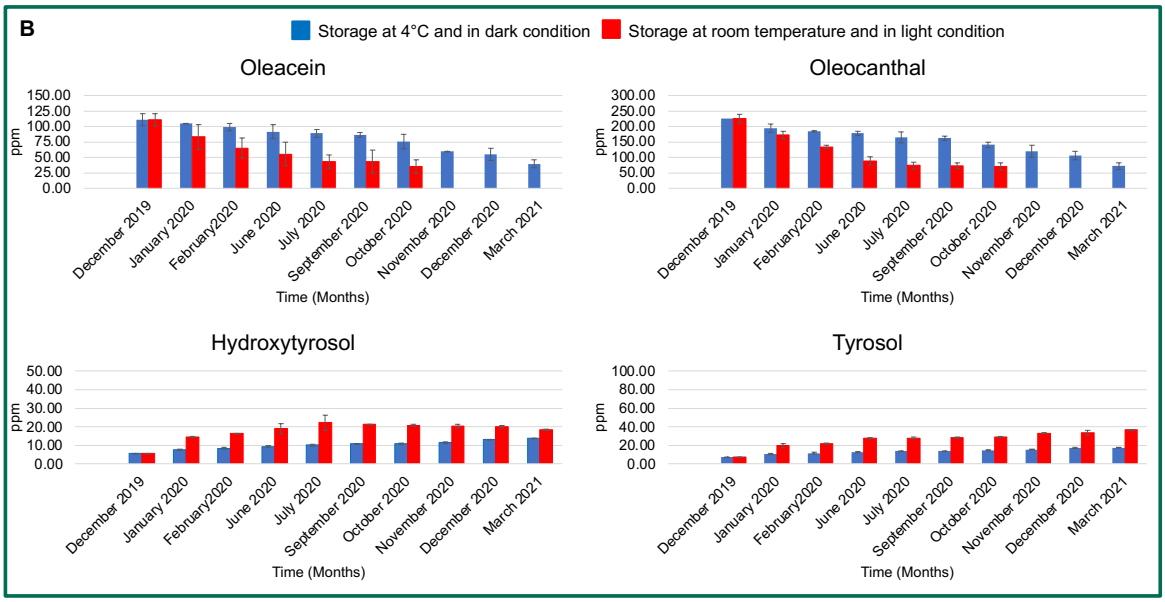

*Figure 59 – Concentration of oleacein, oleocanthal, hydroxytyrosol and tyrosol (µg of phenolic compound/g of EVOO, ppm) in EVOO **B** storage at 4°C in dark condition (blue bars) and at room temperature exposed to daylight (red bars), for 15 months.*

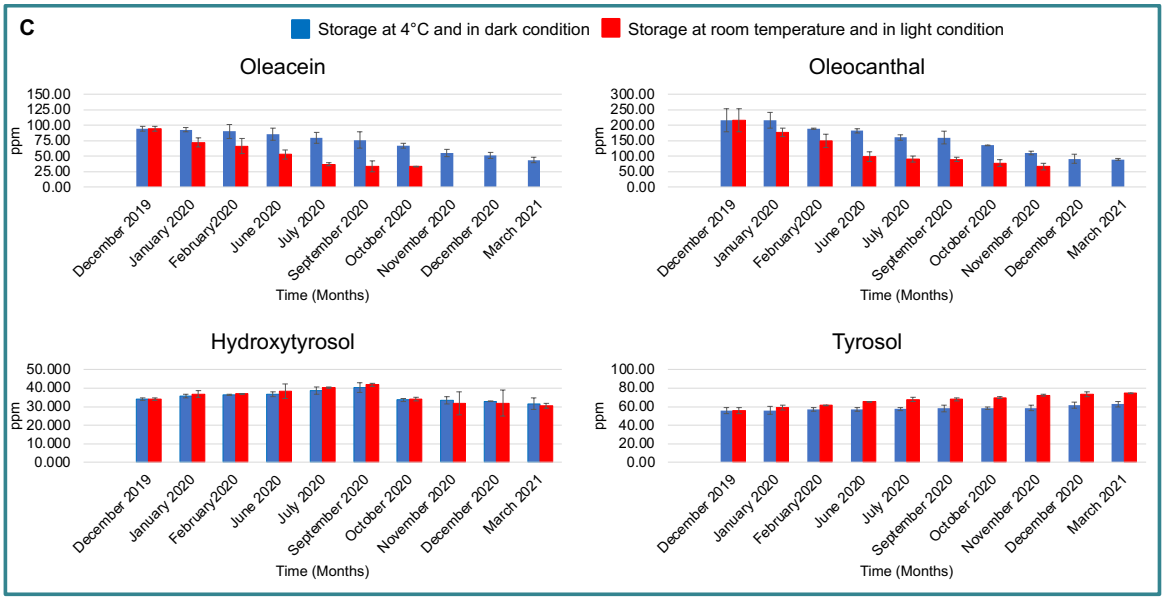

*Figure 60 – Concentration of oleacein, oleocanthal, hydroxytyrosol and tyrosol (µg of phenolic compound/g of EVOO, ppm) in EVOO **C** storage at 4°C in dark condition (blue bars) and at room temperature exposed to daylight (red bars), for 15 months.*

*Table 6 – Concentration of phenolic compounds (µg of phenolic compound/g of EVOO, ppm) in three different EVOOs (**A**, **B** and **C**) storage at 4°C and in dark condition. HT = Hydroxytyrosol; T = Tyrosol; OC = Oleacein; OO = Oleocanthal.*

Time	EVOO	HT	T	OC	OO
December 2019	A	4.72 ± 0.11	5.47 ± 0.25	116.09 ± 18.39	148.93 ± 3.04
	B	5.67 ± 0.01	7.28 ± 0.01	110.69 ± 9.80	226.36 ± 13.30
	C	34.11 ± 0.57	55.62 ± 3.10	94.49 ± 3.75	216.12 ± 36.44
January 2020	A	5.51 ± 0.12	5.86 ± 0.14	103.40 ± 8.20	144.54 ± 10.46
	B	7.58 ± 0.29	10.84 ± 0.67	105.01 ± 0.46	194.94 ± 2.73
	C	35.78 ± 0.99	55.96 ± 4.36	92.84 ± 3.00	216.00 ± 24.76
February 2020	A	5.74 ± 0.18	6.31 ± 0.59	97.67 ± 1.71	125.72 ± 13.67
	B	8.41 ± 0.48	11.71 ± 0.75	98.94 ± 5.98	184.92 ± 6.47
	C	36.40 ± 0.19	57.04 ± 1.96	90.00 ± 11.43	188.85 ± 1.99
June 2020	A	7.40 ± 0.18	7.22 ± 0.16	95.33 ± 2.26	108.82 ± 8.50
	B	9.38 ± 0.57	12.76 ± 0.91	91.73 ± 11.47	178.15 ± 17.65
	C	36.59 ± 1.31	57.17 ± 2.12	85.67 ± 9.61	182.22 ± 6.60
July 2020	A	7.52 ± 0.59	7.72 ± 0.87	71.36 ± 16.28	87.42 ± 9.13
	B	10.14 ± 0.50	13.97 ± 0.23	89.15 ± 6.18	165.78 ± 6.77
	C	38.73 ± 1.92	57.45 ± 1.89	79.76 ± 8.72	160.95 ± 8.91
September 2020	A	7.98 ± 0.12	8.03 ± 0.49	62.31 ± 5.46	86.42 ± 5.36
	B	10.77 ± 0.15	14.10 ± 0.22	86.56 ± 4.05	162.87 ± 9.20
	C	40.29 ± 2.53	58.30 ± 3.58	76.02 ± 13.20	159.92 ± 20.37
October 2020	A	8.68 ± 0.56	8.51 ± 0.23	61.05 ± 7.18	82.93 ± 0.53
	B	11.08 ± 0.34	14.46 ± 0.60	75.88 ± 11.64	140.88 ± 19.27
	C	33.71 ± 0.80	58.58 ± 1.30	66.60 ± 3.96	135.52 ± 0.06
November 2020	A	8.85 ± 0.22	8.59 ± 1.01	49.98 ± 6.12	81.20 ± 3.01
	B	11.42 ± 0.57	15.58 ± 0.48	60.02 ± 0.37	119.80 ± 13.71
	C	33.50 ± 1.98	58.60 ± 2.77	55.39 ± 5.96	110.86 ± 5.88
December 2020	A	8.90 ± 0.04	8.88 ± 0.20	49.98 ± 5.90	80.29 ± 0.40
	B	13.18 ± 0.02	17.45 ± 0.80	55.63 ± 9.77	106.64 ± 11.16
	C	32.89 ± 0.07	61.73 ± 3.28	51.24 ± 4.67	91.75 ± 15.06
March 2021	A	10.10 ± 0.91	9.80 ± 1.09	37.74 ± 4.14	55.34 ± 4.36
	B	13.74 ± 0.25	17.52 ± 0.25	39.57 ± 6.39	72.65 ± 0.53
	C	31.61 ± 3.04	62.70 ± 2.73	43.66 ± 4.57	89.27 ± 2.60

- Data are expressed as means ± SD of experiment performed in triplicate. N.D. = Not Detectable. -

*Table 7 - Concentration of phenolic compounds (μg of phenolic compound/g of EVOO, ppm) in three different EVOOs (**A**, **B** and **C**) storage at room temperature and in light conditions. HT = Hydroxytyrosol; T = Tyrosol; OC = Oleacein; OO = Oleocanthal.*

Time	EVOO	HT	T	OC	OO
December 2019	A	4.72 ± 0.11	5.47 ± 0.25	116.09 ± 18.39	148.93 ± 3.04
	B	5.67 ± 0.01	7.28 ± 0.01	110.69 ± 9.80	226.36 ± 13.30
	C	34.11 ± 0.57	55.62 ± 3.10	94.49 ± 3.75	216.12 ± 36.44
January 2020	A	27.30 ± 0.74	47.80 ± 1.21	42.72 ± 3.10	72.45 ± 10.51
	B	14.53 ± 0.34	19.73 ± 2.43	83.22 ± 19.83	173.17 ± 11.17
	C	36.85 ± 1.70	59.15 ± 2.53	72.24 ± 7.05	176.47 ± 13.33
February 2020	A	27.09 ± 0.07	51.66 ± 1.33	40.96 ± 3.99	43.38 ± 5.26
	B	16.34 ± 0.18	22.14 ± 0.63	65.30 ± 16.09	134.09 ± 4.94
	C	37.06 ± 0.04	61.43 ± 0.02	66.23 ± 12.31	149.64 ± 20.87
June 2020	A	29.89 ± 0.05	51.74 ± 0.28	16.20 ± 1.05	31.58 ± 1.15
	B	18.93 ± 2.77	27.70 ± 0.61	55.30 ± 19.06	88.56 ± 13.35
	C	38.44 ± 3.91	65.76 ± 0.03	52.96 ± 7.33	98.93 ± 15.17
July 2020	A	28.64 ± 0.54	52.63 ± 4.18	N.D.	N.D.
	B	22.20 ± 4.19	27.78 ± 1.00	43.45 ± 11.00	74.50 ± 11.13
	C	40.29 ± 0.35	67.69 ± 2.35	36.93 ± 2.29	91.33 ± 9.36
September 2020	A	27.36 ± 1.34	53.14 ± 0.13	N.D.	N.D.
	B	21.28 ± 0.17	28.43 ± 0.57	43.37 ± 18.58	73.59 ± 8.80
	C	41.78 ± 0.73	67.89 ± 1.89	33.72 ± 19.08	89.72 ± 7.23
October 2020	A	27.36 ± 0.42	53.66 ± 1.00	N.D.	N.D.
	B	20.86 ± 0.47	29.29 ± 0.71	35.62 ± 10.56	71.31 ± 11.69
	C	34.06 ± 0.88	69.77 ± 0.96	33.44 ± 0.40	77.73 ± 11.28
November 2020	A	25.30 ± 0.01	54.18 ± 0.91	N.D.	N.D.
	B	20.36 ± 0.90	33.09 ± 0.34	N.D.	N.D.
	C	31.95 ± 6.21	72.39 ± 0.90	N.D.	66.34 ± 10.36
December 2020	A	19.22 ± 0.92	54.51 ± 0.34	N.D.	N.D.
	B	20.18 ± 0.63	33.54 ± 2.72	N.D.	N.D.
	C	31.88 ± 7.04	73.47 ± 2.78	N.D.	N.D.
March 2021	A	17.91 ± 2.80	54.76 ± 2.25	N.D.	N.D.
	B	18.50 ± 0.29	36.63 ± 0.19	N.D.	N.D.
	C	30.49 ± 1.24	74.38 ± 0.06	N.D.	N.D.

- Data are expressed as means ± SD of experiment performed in triplicate. N.D. = Not Detectable. -

3.3.3 Conclusion

These results confirmed that the phenolic compounds present in EVOO underwent hydrolytic processes during storage. However, the evolution of this pathway differs in each EVOO sample. Moreover, the hydrolytic process is strongly related to storage condition. In fact, in EVOOs exposed to light and maintained at 25°C, the degradation was generally more marked than in EVOO stored in dark and at 4°C, due to the greater influence of external factors on storage conditions.

3.4 Study of novel components in EVOOs and their potential nutraceutical properties

Besides the hydrolytic process, phenolic compounds in EVOOs can undergo oxidative processes influenced by external pro-oxidizing factors, such as light (photo-oxidation), temperature, storage time and oxygen, and by natural auto-oxidation processes that occur in EVOO even if it is put into a strictly controlled environment.[15] In fact, recent studies have highlighted the presence of oxidation products of phenolic compounds.[17]

From the analysis of EVOO during storage, discussed in section 3.3, a very small, poorly detectable peak was identified in fresh EVOO (Figure 61, blue arrow) which increased after fifteen months of storage at room temperature and exposed to daylight, as reported in the Figure 62 (red arrow).

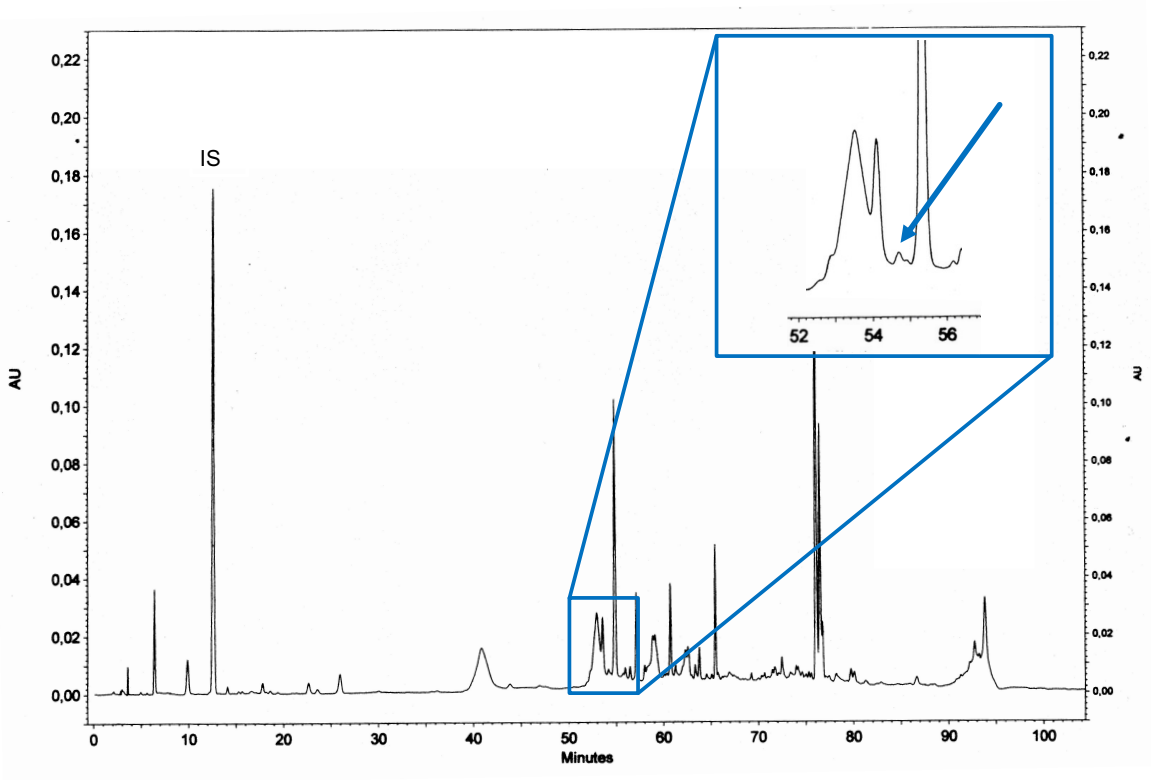

Figure 61 – HPLC chromatogram of a fresh EVOO. IS = Internal Standard.

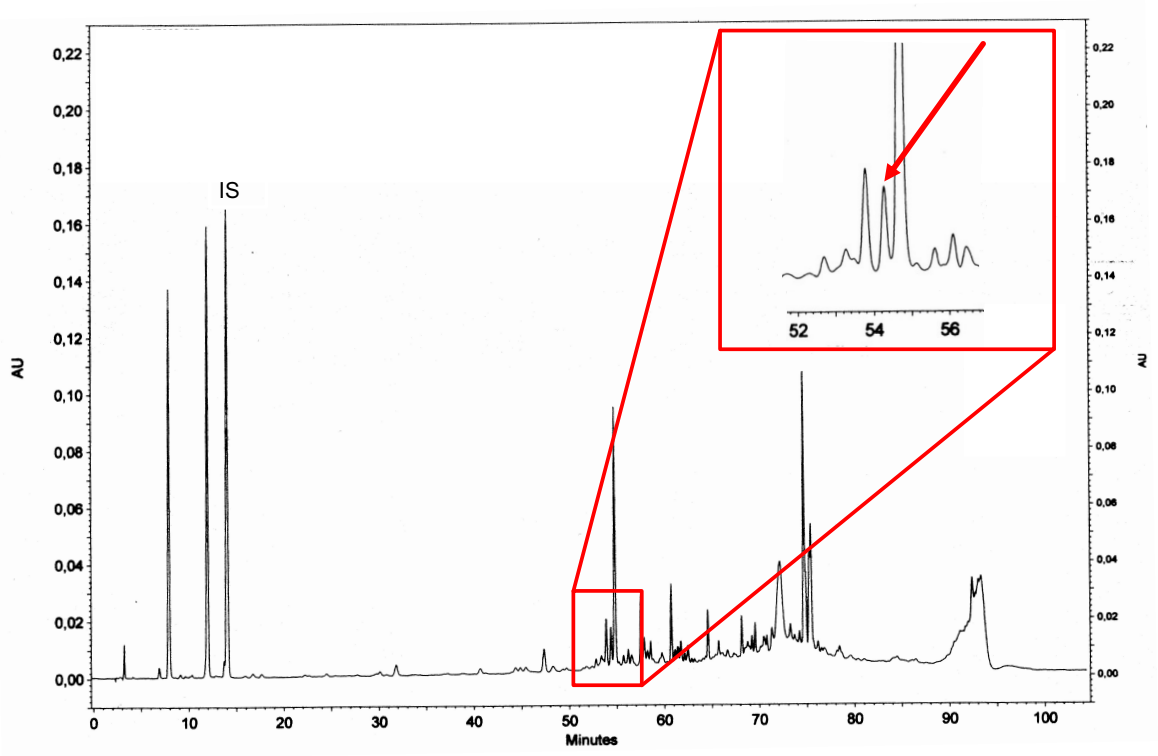

Figure 62 –HPLC chromatogram of an EVOO after fifteen months of storage at room temperature and exposed to daylight. IS = Internal Standard.

This peak was attributable to a compound named oleocanthalic acid (OA), which was recently reported by Tsolakou *et al.* as an oxidative derivative of OO.[112] These authors also showed that the content of OA in a fresh EVOO was very low and it increased after several months of EVOO storage (24 months) due to the oxidation of the OO (Figure 63), as confirmed by my analysis. Moreover, in this work the potential neuroprotective properties OA were also highlighted.[112]

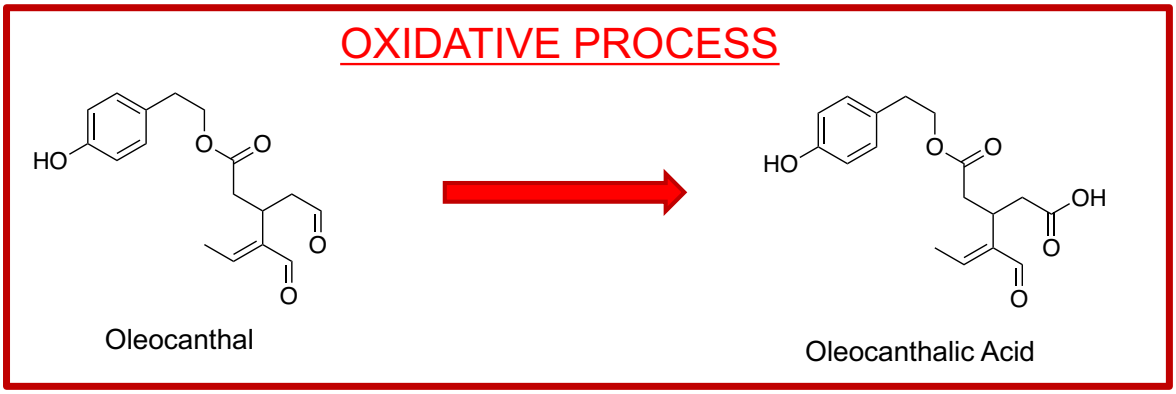

Figure 63 – Oxidative process can lead to the formation of oleocanthalic acid from oleocanthal.

Therefore, my attention was focused on the study of OA in order to obtain this compound with a high purity and then to investigate its nutraceutical properties. With these purposes, an efficient and reproducible method for the extraction and the purification of OA from Tuscan EVOOs was developed.[113]

3.4.1 Extraction and Purification of Oleocanthalic Acid from Tuscan Extra-Virgin Olive Oil

Methods reported in literature for the extraction and the purification of OA started, in one case, from 400 g of EVOO aged for a long time (two years) to get about 70 mg of OA[112] and, in another case, from a very high amount of fresh EVOO (6 L) to obtain only 4.6 mg of OA.[114]

During this PhD, a method to accelerate the oxidation of OO to OA was developed, in order to achieve significant amount of OA to be extracted from a small amount of fresh EVOOs (100g).[113]

First of all, a fresh EVOO, rich in OO, was selected through HPLC analysis of several Tuscan EVOOs, by using the Method II described in section 4.2.9.2.2 of the experimental part. The chromatogram of the selected EVOO is reported in Figure 64. This selected EVOO is characterized by a starting concentration of OO of 383 ppm, a concentration of OC of 281 ppm, while the amount of HT and T was very low (about 11 and 17 ppm, respectively) and the OA peak was not detectable.

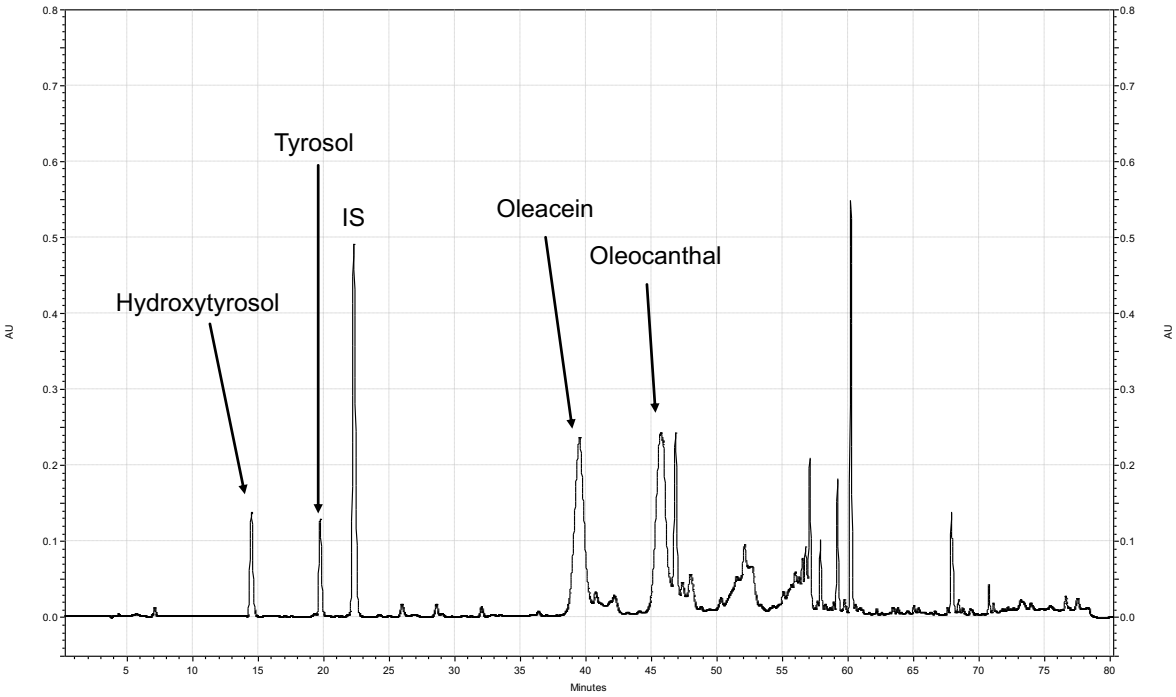

Figure 64 – HPLC chromatogram of the selected fresh EVOO. IS = Internal Standard.

Since the oxidative process may be influenced by light, storage time, temperature and oxygen, the selected fresh EVOO was subjected to different temperature and light conditions, during different times. The formation of OA was monitored through the HPLC method developed and validated in this thesis (Method II, reported in section 4.2.9.2.2 of the experimental part).

Tsolakou *et al.* observed an increase of the OA/OO ratio in an olive oil sample naturally without phenolic compounds, added with pure OO and stored at 60°C for 14 days in an open vial and in the dark. In this way they simulated the aging of an olive oil after 24 months of storage where OA was detected.[112]

Therefore, based on this evidence, the selected fresh EVOO was heated at 60°C and in dark condition, as reported in section 4.2.5.1 of the experimental part (Method I). This EVOO was constantly monitored through HPLC analysis at defined time intervals (0, 4, 7, 9, 12, 14, 21, 32, 44, 80 days) and the results were compared with those of the same EVOO kept at 4°C, used as control. In these conditions, it was possible to notice that the oxidative process was slow. In particular, the peak attributable to OA was detectable after 12 days and only after 44-80 days OA was present in significant quantities in EVOO (about 250 ppm) (Figure 65**A**); at the same time the peak corresponding to OO slowly reduced (Figure 65**B**).

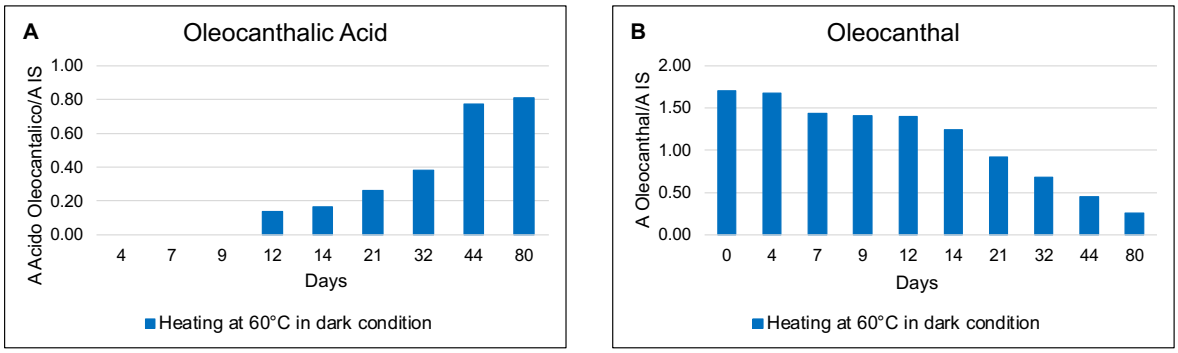

*Figure 65 – Variation of oleocanthalic acid (**A**) and oleocanthal (**B**) in time, in the EVOO subjected to heating at 60°C in dark condition. A = Peak Area; IS = Internal Standard.*

The HPLC chromatogram reported in Figure 66, related to EVOO heated at 60°C in dark condition after 80 days, shows the formation of the peak attributable to OA and the reduction of the OO peak. Moreover, both a significant reduction of OC and HT, and an increase of T content are observable.

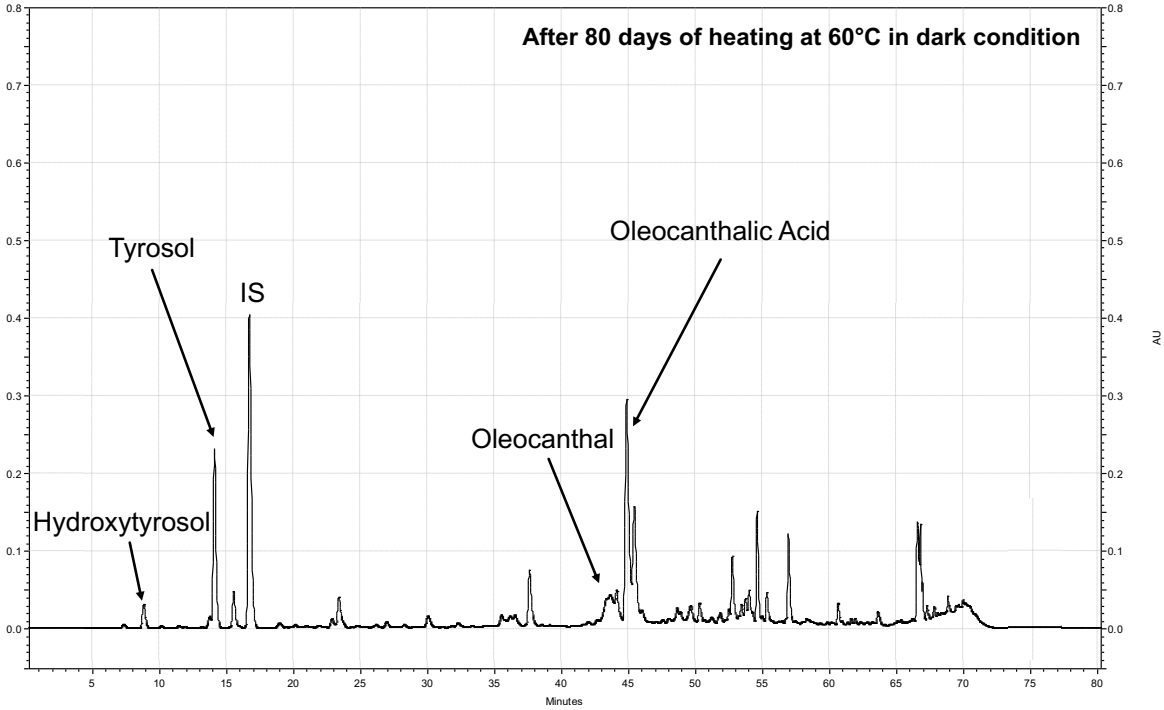

Figure 66 – HPLC chromatogram of EVOO after 80 days of heating at 60°C in dark condition. IS = Internal Standard.

Since temperature and light represent the main factors that influence the oxidative processes, a decisive improvement of the oxidation was achieved by subjecting the selected Tuscan EVOO to heating at 80°C and by exposing it to daylight, as reported in section 4.2.5.2 of the experimental part (Method II). In these conditions, OA started to form already after 4 days and after 14 days the EVOO contained significant amount of OA (about 370 ppm) (Figure 67**A**, red bars); at the same time the amount of OO reduced quite rapidly (Figure 67**B**, red bars).

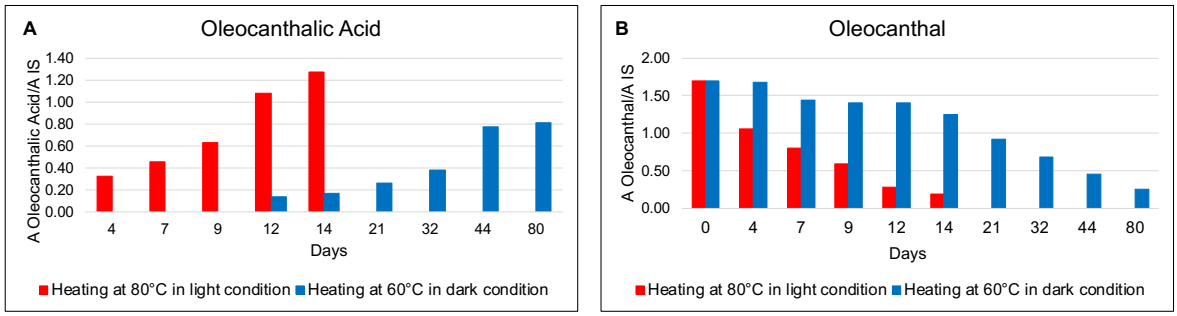

*Figure 67 - Variation of oleocanthalic acid (**A**) and oleocanthal (**B**) in time, in the EVOO subjected to heating at 80°C in light condition (red bars) and in the EVOO subjected to heating at 60°C in dark condition (blue bars). A = Peak Area; IS = Internal Standard.*

After 14 days of heating at 80°C in light condition, the formation of a very high peak attributable to OA, the significant reduction of OO, OC and HT peaks and an increase of T content were observable in the HPLC chromatogram of EVOO (Figure 68). This EVOO (heated at 80°C) was then suitable for the subsequent extraction and purification in order to obtain pure OA.

With this procedure it was possible to drastically reduce the time required for the OA formation in EVOO going from two years of the method reported in the literature[112] to just two weeks of this method.[113] It was also possible to reduce the quantity of starting EVOO to be extracted, going from the 6 L as described in the literature[114] to just 100 g of EVOO amount used in this method.[113]

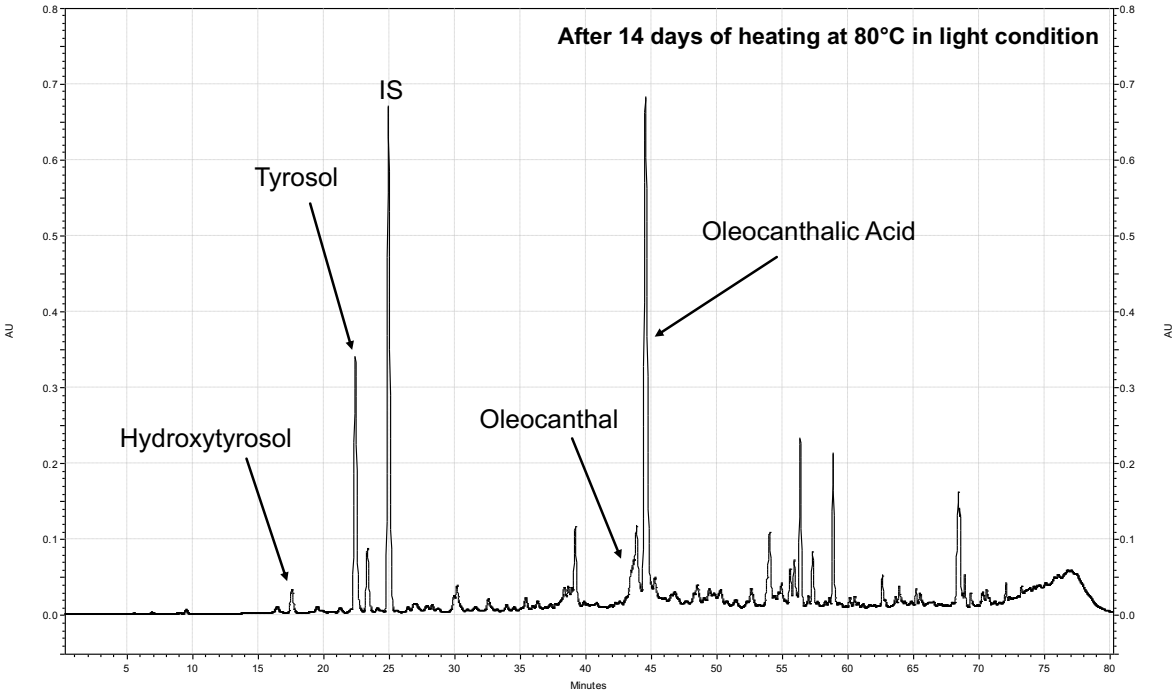

Figure 68 – HPLC chromatogram of EVOO after 14 days of heating at 80°C in light condition. IS = Internal Standard.

EVOO (100g) subjected to heating at 80°C for 14 days, was extracted through a liquid-liquid extraction, as described in section 4.2.6 of the experimental part. Successively a procedure to purify OA, was developed.[113]

Initially, based on a method reported in literature,[112] I performed a direct phase chromatography, by using the advanced automatic flash purification system and a mixture of *n*-hexane and EtOAc as mobile phase (Method I, section 4.2.7.1.1 of the experimental part). The fractions containing OA were collected. The ^{1}H-NMR spectrum of these fractions (Figure 69) showed that, although it was possible to detect the diagnostic signals of OA, the product was not sufficiently pure and needed a second step of purification.

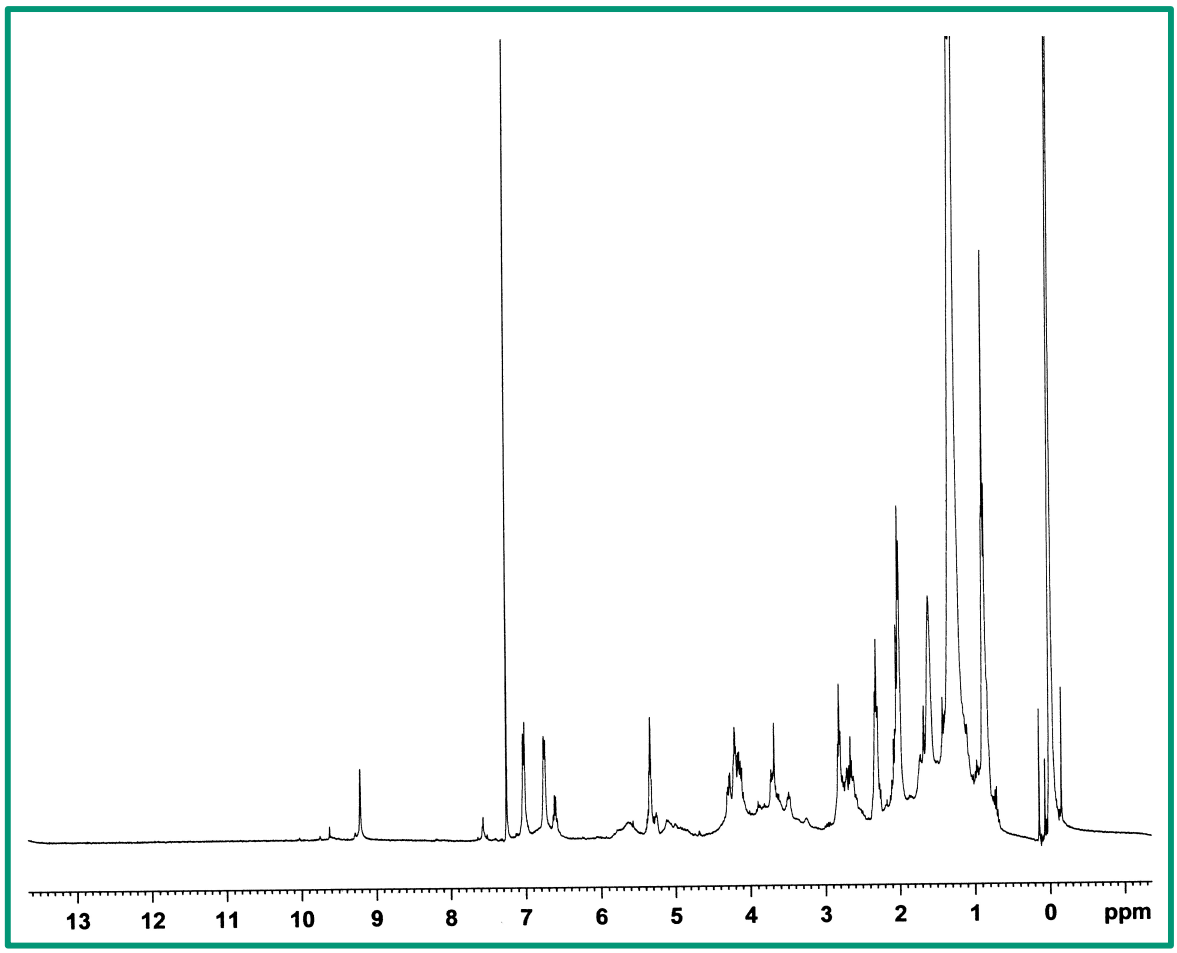

Figure 69 – ^{1}H-NMR ($CDCl_3$ - 400 MHz) of oleocanthalic acid after the first step of purification (Method I).

Then the fractions containing OA were subjected to a preparative TLC, by using *n*-hexane:EtOAc (3:7, v/v) as mobile phase, by following the method reported in literature for the OC and OO purification,[46,47] as described in the section 4.2.7.2.1 of the experimental part. However, in this condition the yield and the purity of OA obtained were low (about 5 mg from 100 g of EVOO; purity <95%). In Figure 70 the ^{1}H-NMR spectrum of the collected fractions is reported.

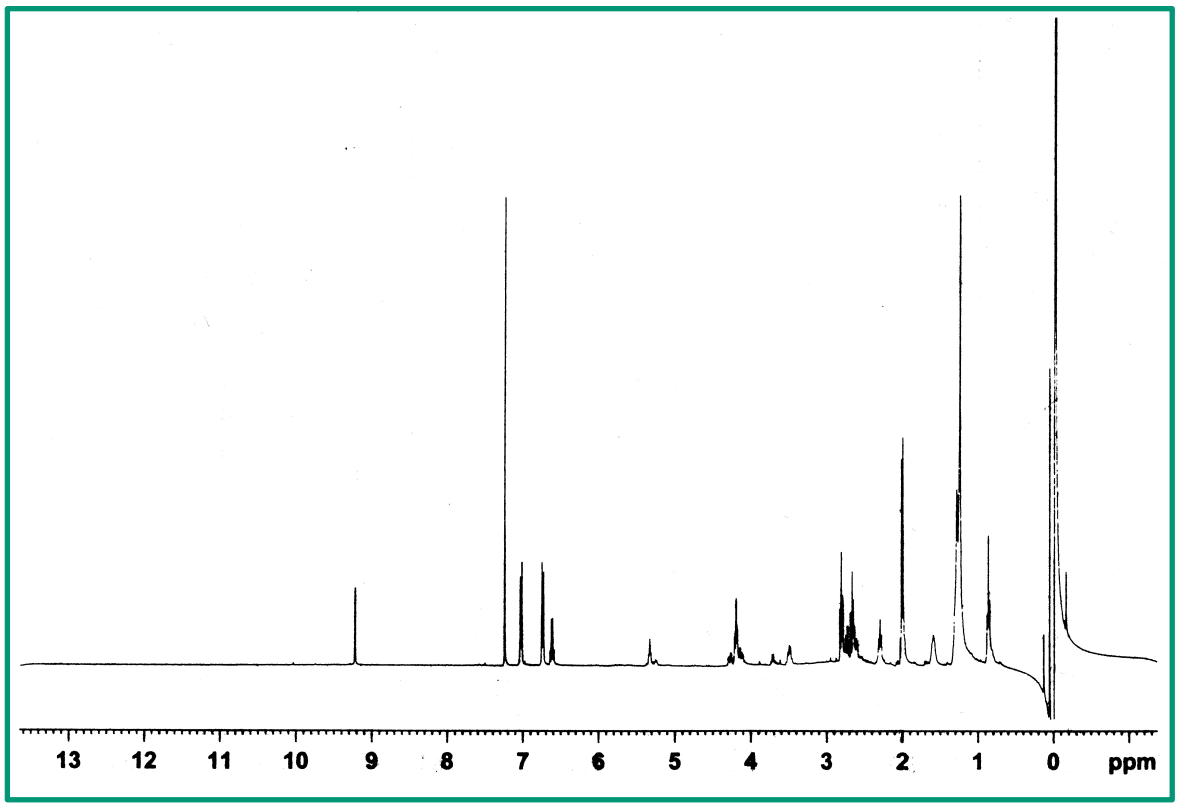

Figure 70 – ^{1}H-NMR ($CDCl_3$ - 400 MHz) of oleocanthalic acid after the second step of purification performed by exploiting preparative thin layer chromatography.

In order to improve the yield and the purity, the fractions containing OA obtained after the first step of purification (Method I), were further purified by exploiting a flash column chromatography, by using the same mobile phase of the preparative TLC. With this method (Method II), extensively described in section 4.2.7.2.2 of the experimental part, it was possible to increase the yield, but the OA obtained was not sufficiently pure, as shown in the ^{1}H-NMR spectrum (Figure 71), where some impurities are still present.

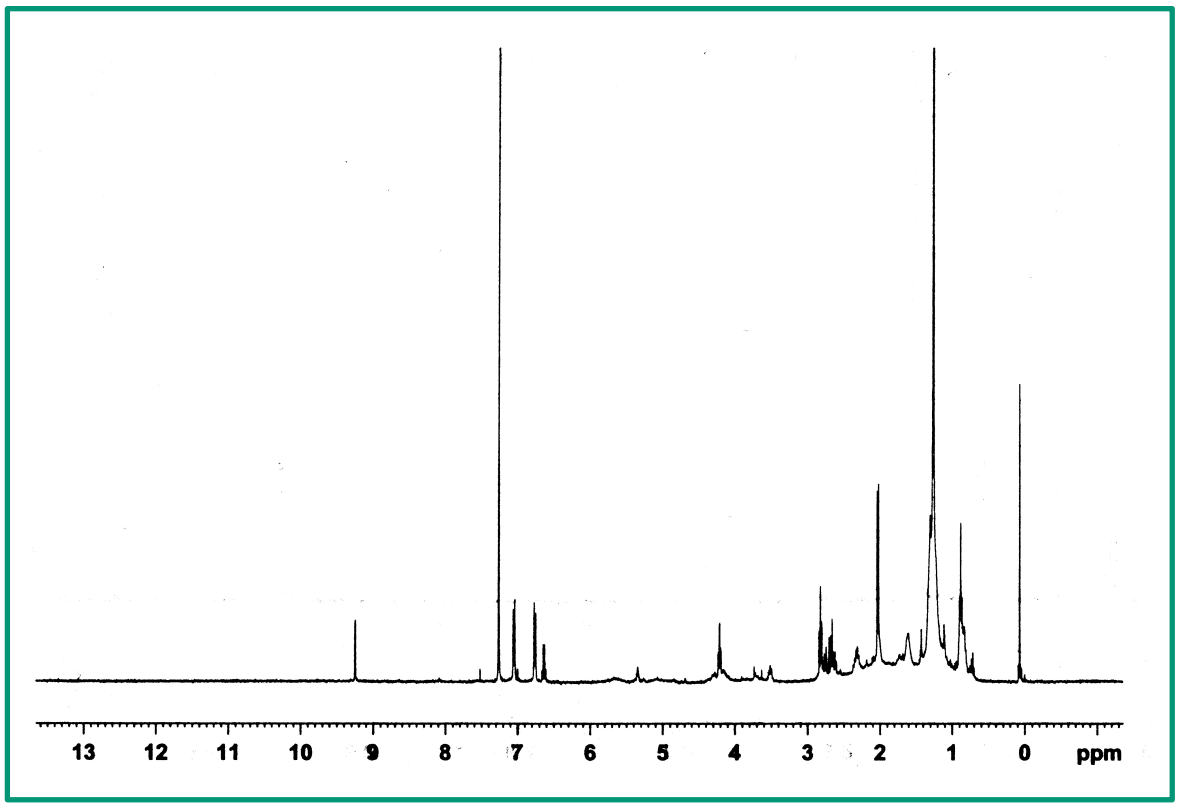

Figure 71 – ^{1}H-NMR ($CDCl_3$ - 400 MHz) of oleocanthalic acid after the second step of purification performed by exploiting flash column chromatography.

Both the first and the second steps of purification of OA were improved in order to obtain OA with the optimal grade of purity to be submitted to pharmacological investigations. In particular, the mobile phase of the Method I used as first step of purification was modified by using a preliminary elution in $CHCl_3$ followed by the same mobile phase used in the Method I (*n*-hexane:EtOAc), with the aim to remove the most apolar components. This step was performed again through the advanced automated flash purification system. This new method (Method II, described in section 4.2.7.1.2 of the experimental part), allowed to obtain higher amounts of OA than the Method I. Although, the ^{1}H-NMR spectrum of OA obtained with the Method II (Figure 72) showed an improvement of the purity compared to that obtained with the Method I, OA needed further purification.

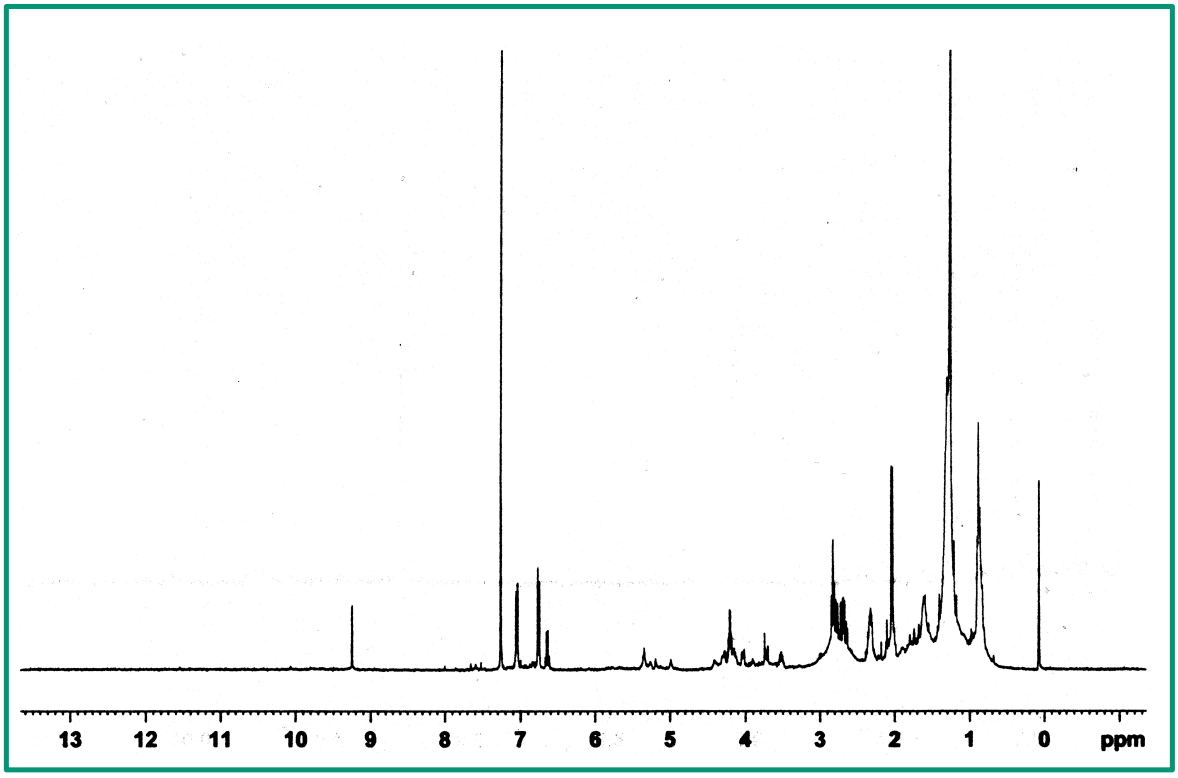

Figure 72 – ^{1}H-NMR ($CDCl_3$ - 400 MHz) of oleocanthalic acid after the first step of purification (Method II).

Therefore, the fractions containing OA were subjected to a second step of purification by exploiting a reverse phase column chromatography, carried out by advanced automated flash purification instrument and by using a C18 cartridge as stationary phase and a mixture of H_2O and ACN as mobile phase, similar to the one used in HPLC analysis of EVOOs. With this method (Method III, reported in section 4.2.7.2.3 of the experimental part), it was possible to obtain OA with a high yield (25 mg from 100g of starting EVOO) and good purity (>95%) suitable to be submitted to pharmacological investigations.

The structure of OA and its purity were confirmed by NMR spectroscopy (^{1}H-NMR, Figure 73 and ^{13}C-NMR, Figure 74) and liquid chromatography–mass spectrometry (LC-MS) (Figure 75). The LC-MS-MS spectrum of the ion at m/z 319.1, obtained by using a -20 V collision energy, displayed a fragmentation pattern compatible with the OA structure and corresponding to that reported in the literature.[114] Once the pure OA was obtained, the linearity of the HPLC method (Method II) was verified by calculating the correlation coefficient of the OA calibration curve, the limit of detection (LOD) and the limit of quantification (LOQ), as reported in section 4.2.11 of the experimental part.

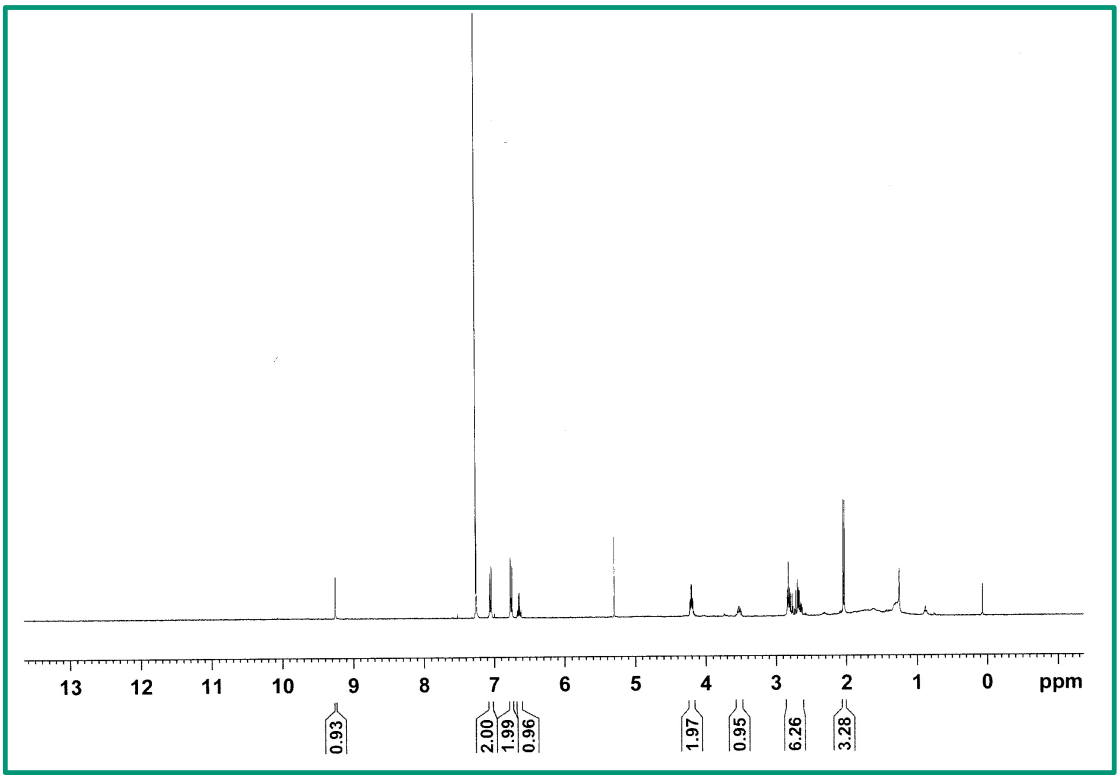

Figure 73 – ^{1}H-NMR ($CDCl_3$ - 400 MHz) spectrum of oleocanthalic acid after the second step of purification performed by exploiting reverse flash column chromatography carried out by automated flash purification instrument.

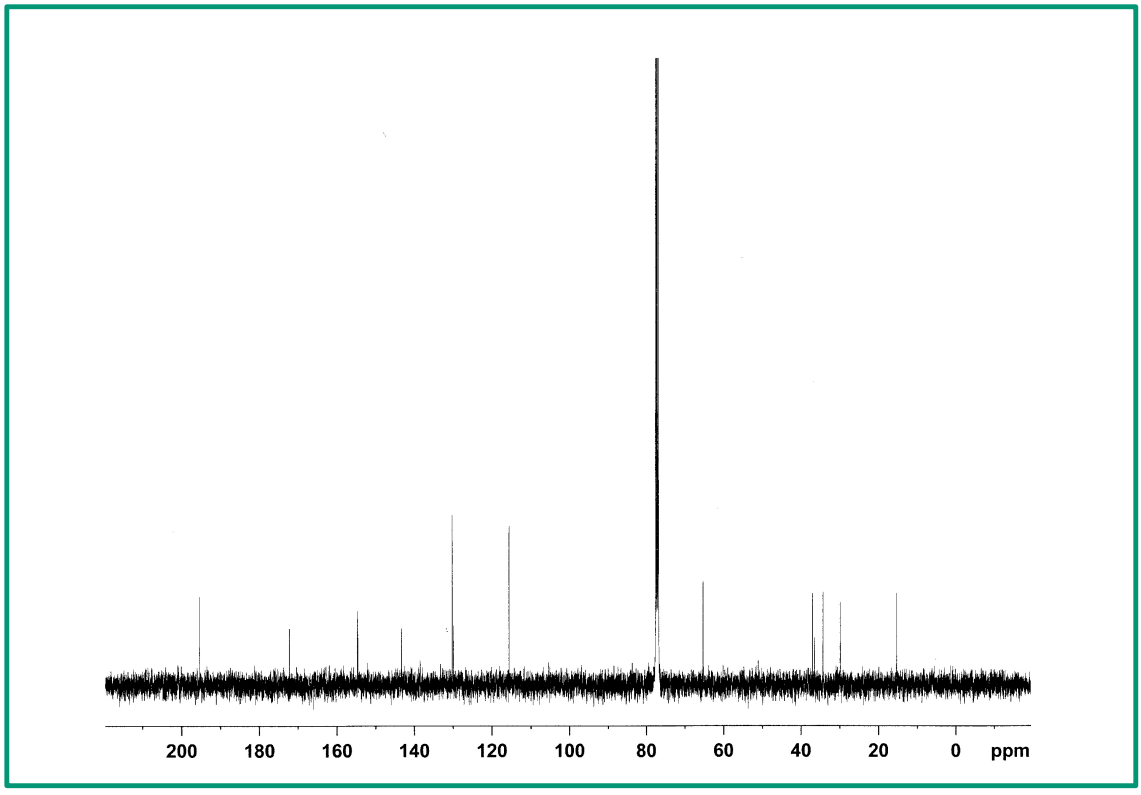

Figure 74 – ^{13}C-NMR ($CDCl_3$ - 100 MHz) spectrum of oleocanthalic acid after the second step of purification performed by exploiting reverse flash column chromatography carried out by automated flash purification instrument.

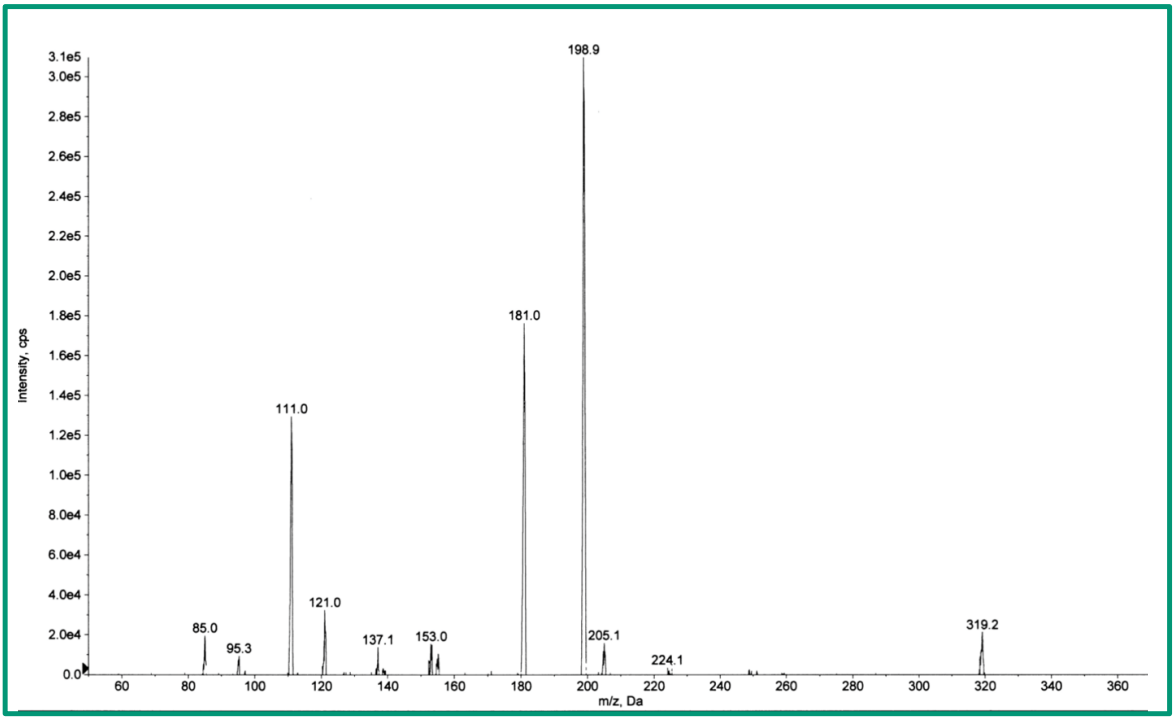

Figure 75 –LC-MS spectrum of oleocanthalic acid after the second step of purification performed by exploiting reverse flash column chromatography carried out by automated flash purification instrument.

The HPLC method (Method II) was developed improving Method I used for the quantification of OC and OO. Since with Method I it was not possible to identify the OA chromatographic peak, the gradient elution of the mobile phase was modified, obtaining Method II that exploits a reverse-phase C18 column as stationary phase and a mixture of H_2O/AcOH (97.5: 2.5 v/v) (A) and MeOH/ACN (1: 1 v/v), as mobile phase, with the gradient reported in section 4.2.9.2.2 of the experimental part. With this change it was possible to improve the resolution of the OA chromatographic peak.

3.4.2 Nutraceutical studies on Oleocanthalic Acid

Nowadays, the nutraceutical properties of OA are poorly investigated. Just a recent study has highlighted a potential neuroprotective effect of this compound.[112]

In this context, the nutraceutical properties of OA were screened in collaboration with the research group of Doctor Francisca Rodrigues (REQUIMTE/LAQV – Superior Institute of Engineering of Porto). Preliminarily, the OA scavenging potential against ROS was screened.

ROS represent biological side-products of cells metabolic reactions, but their overproduction together with an inability of the antioxidant defence system in counteracting the reactive species generated, lead to oxidative stress. This phenomenon directly induces damage on biomolecules, such as proteins, lipids, and DNA and it also interferes with metabolic pathways. Therefore, ROS are the major driving causes of oxidative stress-mediated disorders.[115]

On this basis, the scavenging potential of OA against $O_2^{\bullet-}$, HOCl and peroxyl radical ($ROO^{\bullet}$), the most important biologically relevant reactive species, was evaluated, providing a detailed assessment of the *in vitro* radicals quenching activity of OA for the first time (Table 8). For this purpose, the activity of OA was compared with two positive controls: ascorbic acid and gallic acid.[113]

3.4.2.1 Radical Scavenging Activity of Oleocanthalic Acid

As reported in Table 8, gallic acid displayed the best $O_2^{\bullet-}$ scavenging activities (IC_{50} = 13.02 µg/mL), while no significant differences were observed between OA and ascorbic acid (19.09 % and 24.01 % of inhibition, respectively). These data were in accordance with the values obtained for other natural matrices reported in the literature.[116–120]

In the HOCl quenching assay, OA showed lower efficiency (IC_{50} = 360.87 µg/mL) than ascorbic acid and gallic acid, which are better HOCl scavengers (IC_{50} values of 2.87 and 2.88 µg/mL, respectively). However, the HOCl scavenging ability of OA is comparable with the results reported in the literature for other natural matrices.[118,120]

The ROO• scavenging capacity was performed by using the oxygen radical absorbance capacity assay. The results were expressed as µmol of Trolox equivalents (TE) per mg of sample on dry weight (DW) and as a ratio between the slope of the sample or positive controls and the slope of Trolox. OA displayed a low capacity to scavenge $ROO^{\bullet}$ (0.0056 µmol TE/mg DW) comparatively to gallic acid and ascorbic acid (4.98 µmol TE/mg DW and 2.94 µmol TE/mg DW, respectively). It is interesting to notice that these data are better than the ones reported in literature for other natural matrices that did not showed capacity to quench $ROO^{\bullet}$.[119,121–124]

Table 8 – Superoxide anion radical ($O_2^{\bullet-}$), hypochlorous acid (HOCl) and peroxyl radical ($ROO^{\bullet}$) scavenging capacity of oleocanthalic acid.

	$O_2^{\bullet-}$		HOCl	ROO•	
	IC_{50} (µg/mL)	% Inhibition	IC_{50} (µg/mL)	Trolox equivalents (µmol TE/mg DW)	S_{Sample}/S_{Trolox} #
Oleocanthalic Acid	-	19.09 ± 1.20[a]	360.87 ± 8.79[a]	0.0056 ± 0.0003[a]	0.0036 ± 0.0004[a]
Positive Controls:					
Ascorbic Acid	-	24.01 ± 2.45[a]	2.87 ± 0.03[b]	2.94 ± 0.12[b]	1.04 ± 0.06[b]
Gallic Acid	13.02 ± 0.21[b]	-	2.88 ± 0.35[b]	4.98 ± 0.27[c]	1.50 ± 0.02[c]

- Values are expressed as mean ± standard error of the mean (n = 3). IC_{50} = In vitro concentration needed to reduce in 50% the reactivity of the reactive species in the tested media (mean ± standard error of the mean). # Results expressed as ratio between the slope of the sample or positive controls and the slope of Trolox. Different letters (a, b, c) in the same column indicate significant differences between substances ($p < 0.05$). -

These data suggested that OA could be a promising scavenger of reactive species, particularly HOCl.[113]

3.4.2.2 Radical Scavenging Activity of Oleocanthal and Tyrosol

Since OA represents the oxidative product of OO and considering that T is an OA metabolite derived from hydrolytic process, the *in vitro* scavenging capacity of OO and T against ROS ($O_2^{\bullet-}$, HOCl and $ROO^{\bullet}$) were then evaluated. For this purpose, the activity of OO and T was compared with two positive controls: catechin and gallic acid. The results are summarized in Table 9.

The positive controls gallic acid and catechin were the best $O_2^{\bullet-}$ quenchers (IC_{50} = 12.04 µg/mL and 48.05 µg/mL, respectively), followed by OO (IC_{50}= 919.80 µg/mL). Concerning T, it was not possible to calculate the IC_{50} due to the low scavenging efficiency. Therefore, the result for T was expressed as inhibition percentage at the highest concentration tested (1000 µg/mL), reaching 17.05% of $O_2^{\bullet-}$ inhibition.

Regarding HOCl quenching assay, T displayed lower efficiency (IC_{50} = 571.32 µg/mL) than OO (IC_{50} = 73.18 µg/mL), while catechin and gallic acid were better HOCl scavengers (IC_{50} = 0.22 µg/mL and 4.80 µg/mL, respectively).

In ROO• quenching capacity assay, OO was the most effective ROO• quencher (0.0152 µmol TE/mg DW) compared to T (0.0046 µmol TE/mg DW). However, the positive controls achieved better results, displaying the highest value for the gallic acid (1.39 µmol TE/mg DW).

Table 9 – Superoxide anion radical ($O_2^{\bullet -}$), hypochlorous acid (HOCl) and peroxyl radical ($ROO^{\bullet}$) scavenging capacities of tyrosol and oleocanthal.

	$O_2^{\bullet -}$		HOCl	$ROO^{\bullet}$
	IC_{50} (µg/mL)	% Inhibition	IC_{50} (µg/mL)	Trolox equivalents (µmol TE/mg DW)
Oleocanthal	919.80 ± 34.30[a]	-	73.18 ± 1.43[a]	0.0152 ± 0.0029[a]
Tyrosol	-	17.05 ± 0.67[c]	517.32 ± 8.50[b]	0.0046 ± 0.0007[a]
Positive Controls:				
Catechin	48.05 ± 0.78[b]	-	0.22 ± 0.01[c]	0.44 ± 0.07[b]
Gallic Acid	12.04 ± 0.03[b]	-	4.80 ± 0.06[c]	1.39 ± 0.11[c]

- Values are expressed as mean ± standard error of the mean (n = 3). IC_{50} = In vitro concentration required to decrease in 50% the reactivity of the reactive species in the tested media (mean ± standard error of the mean). Different letters (a, b, c) in the same column indicate significant differences between samples ($p < 0.05$). -

In conclusion, OO was the most effective scavenger against the ROS studied when compared to T. Moreover, the highest quenching efficiency was achieved for HOCl (IC_{50} of 73.18 and 571.32 µg/mL for OO and T, respectively). The capacity of OO and T as scavengers of ROS, in particular HOCl and $O_2^{\bullet -}$, was demonstrated.

3.4.2.3 Permeation assays of Oleocanthalic Acid

Preliminary experiments were conducted aiming to screen the effects of OA on skin cells viability, in order to find an effective safety concentration for the further permeation experiments. The positive control used was the culture medium (Dulbecco's Modified Eagle Medium, DMEM) while the negative control was 1% (w/v) Triton X-100. In Figure 76 the effect of OA treatment on the viability of Caco-2 (Figure 76**A**), HT29-MTX (Figure 76**B**), HFF-1 (Figure 76**C**) and HaCaT (Figure 76**D**) cells at different concentrations, is shown.

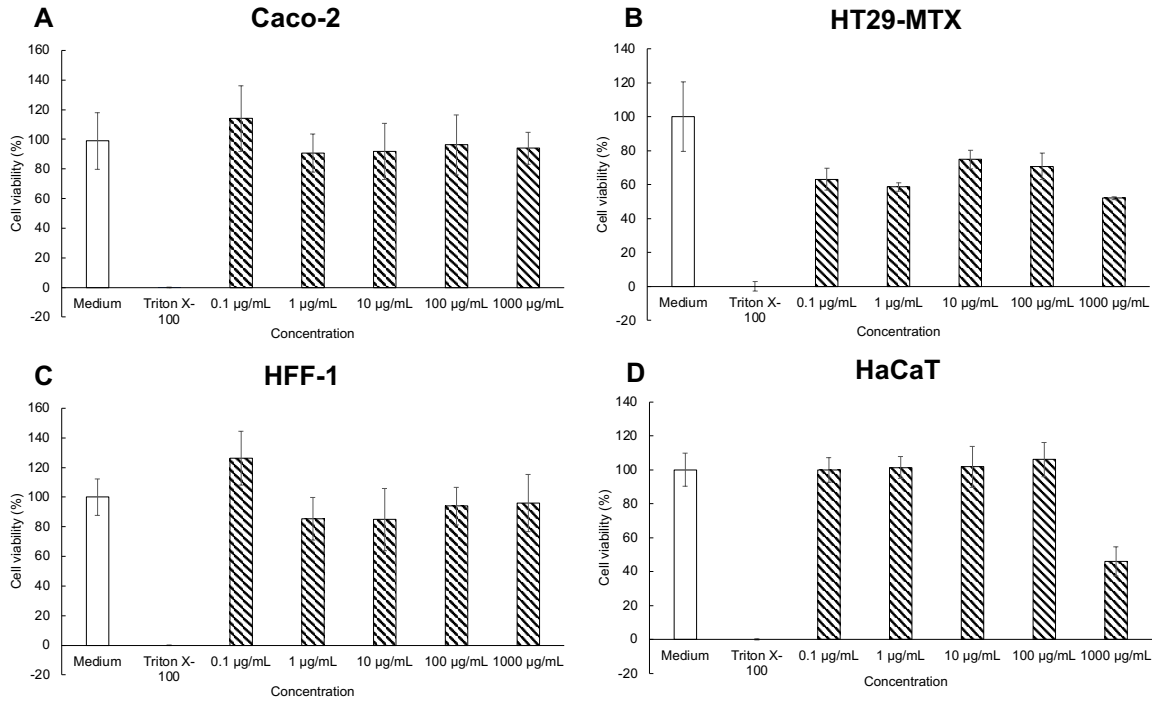

*Figure 76 – The effect of oleocanthalic acid treatment on the viability of Caco-2 (**A**), HT29-MTX (**B**), HFF-1 (**C**) and HaCaT (**D**) cells at different concentrations. Cell viability was assessed by the 3(4,5dimethylthiazolyl)-2,5-diphenyl- tetrazolium bromide (MTT) assay. Data are means ± SD (n = 3).*

Permeation assays on intestinal Caco-2 cells, at the concentration of 100 µg/mL, are ongoing.

3.4.3 Variation of Oleocanthalic Acid during EVOO Storage

The variation of OA content in EVOO during storage was evaluated by analysing EVOOs (**A**, **B** and **C**) monitored for fifteen months (from December 2019 to March 2021) (Table 10) (as reported in section 3.3). The retention time and the UV absorbance spectrum of OA present in the samples were compared with those of the pure standard and quantified by using *p*-hydroxyphenylacetic acid as IS. Each analysis was performed in triplicate and the content of OA was expressed as µg of OA/g of EVOO (ppm).

3.4.3.1 Initial Concentration

In fresh EVOOs, in December 2019, OA is not present, as in the case of sample **B**, or present in a very low amount, as in the case of sample **A** (10.61 ppm). In EVOO **C**, one year older than the other two EVOOs, OA is already detectable in

significant amount (39.72 ± 4.59 ppm) proving that the oxidative reaction has already started. The HPLC chromatograms of EVOOs samples **A**, **B** and **C** at the beginning of the analysis (December 2019) are reported in Figure 77, Figure 78 and Figure 79, respectively.

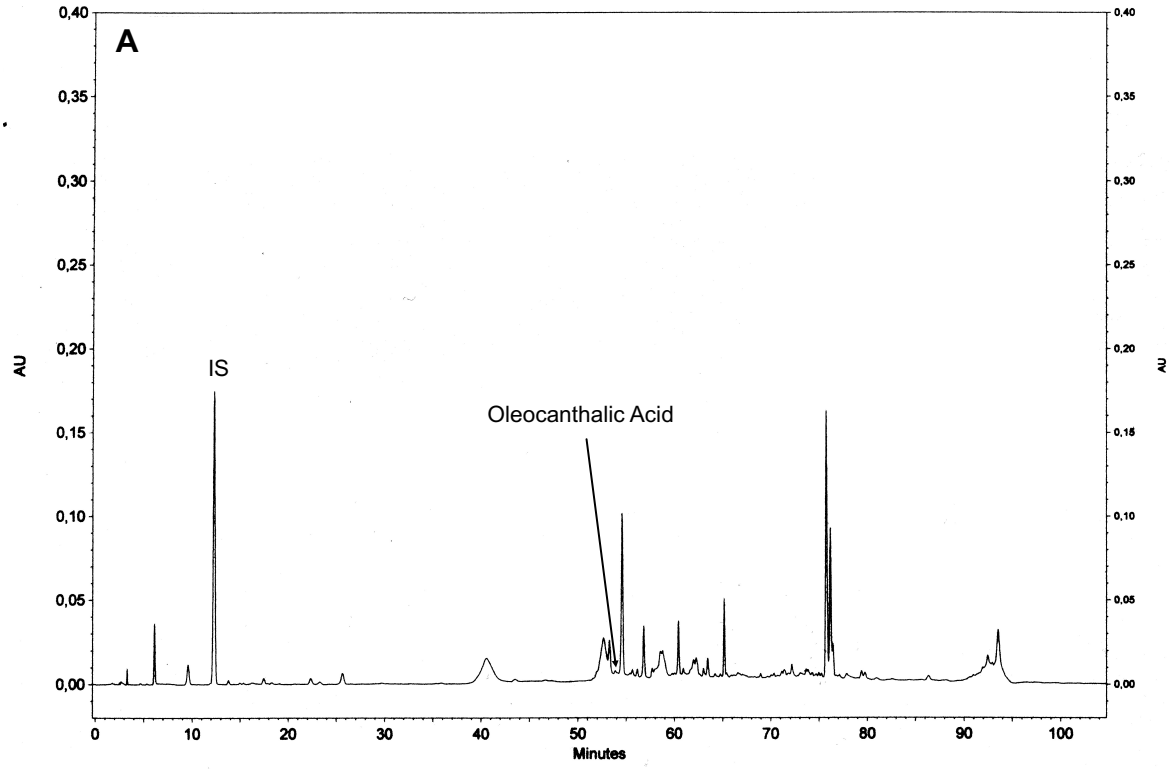

*Figure 77 – HPLC chromatogram of EVOO **A** at the beginning of the analysis (December 2019). IS = Internal Standard.*

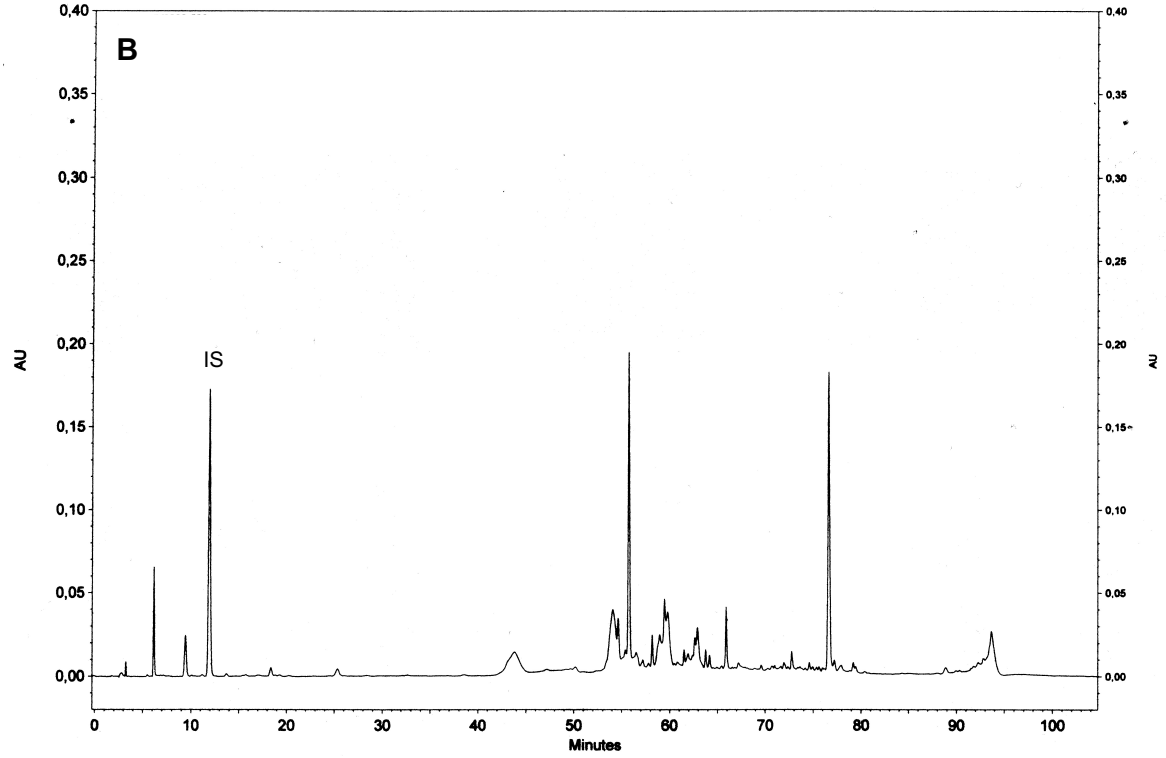

*Figure 78 – HPLC chromatogram of EVOO **B** at the beginning of the analysis (December 2019). IS = Internal Standard.*

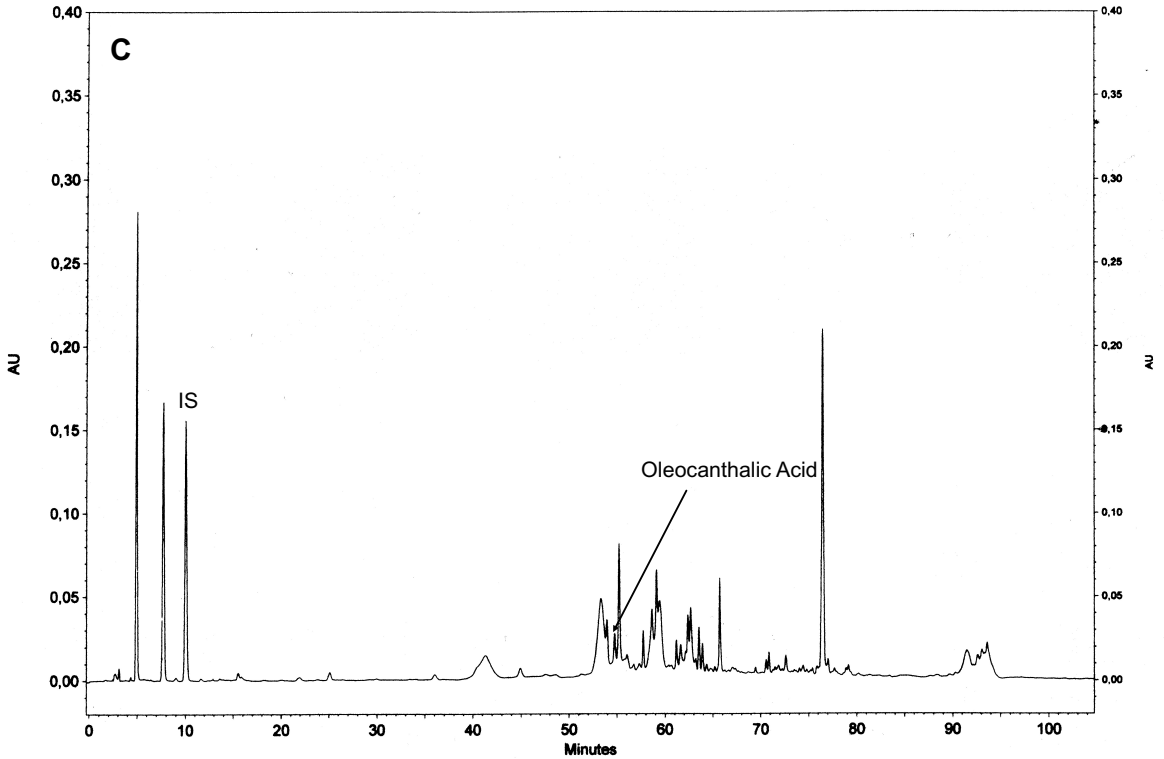

*Figure 79 – HPLC chromatogram of EVOO **C** at the beginning of the analysis (December 2019). IS = Internal Standard.*

3.4.3.2 Storage at Room Temperature and Exposed to Daylight

In all samples, OA increased during storage as shown in Table 10 and in Figure 86 (red bars). However, this trend was more pronounced in samples **B** and **C** than in sample **A**. In fact, in sample **B** OA, which initially (December 2019) was not present, increased until it reached the concentration of 67.23 ppm after fifteen months of storage (March 2021). This behaviour could be related to the higher initial amount of OO. In sample **C**, OA was already present in the initial analysis, as expected for one-year old EVOO, doubling in fifteen months. Furthermore, in this sample it was possible to observe a reduction of OA after twelve months of storage (December 2020) probably due to the hydrolytic process that occurs in OA itself. In sample **A** the concentration of OA doesn't increase significantly after fifteen months of storage (from 10.61 to 24.00 ppm) and remains at levels of approximatively 20 ppm from June 2020 to March 2021. This trend could be explained by the fact that, after seven months of storage (July 2020) the OO in EVOO **A** is no longer quantifiable and consequently it can no longer be oxidized to OA.

The HPLC chromatograms of EVOOs samples **A**, **B** and **C** analysed after fifteen months of storage at room temperature and in light condition (March 2021), are reported in Figure 80, Figure 81 and Figure 82, respectively.

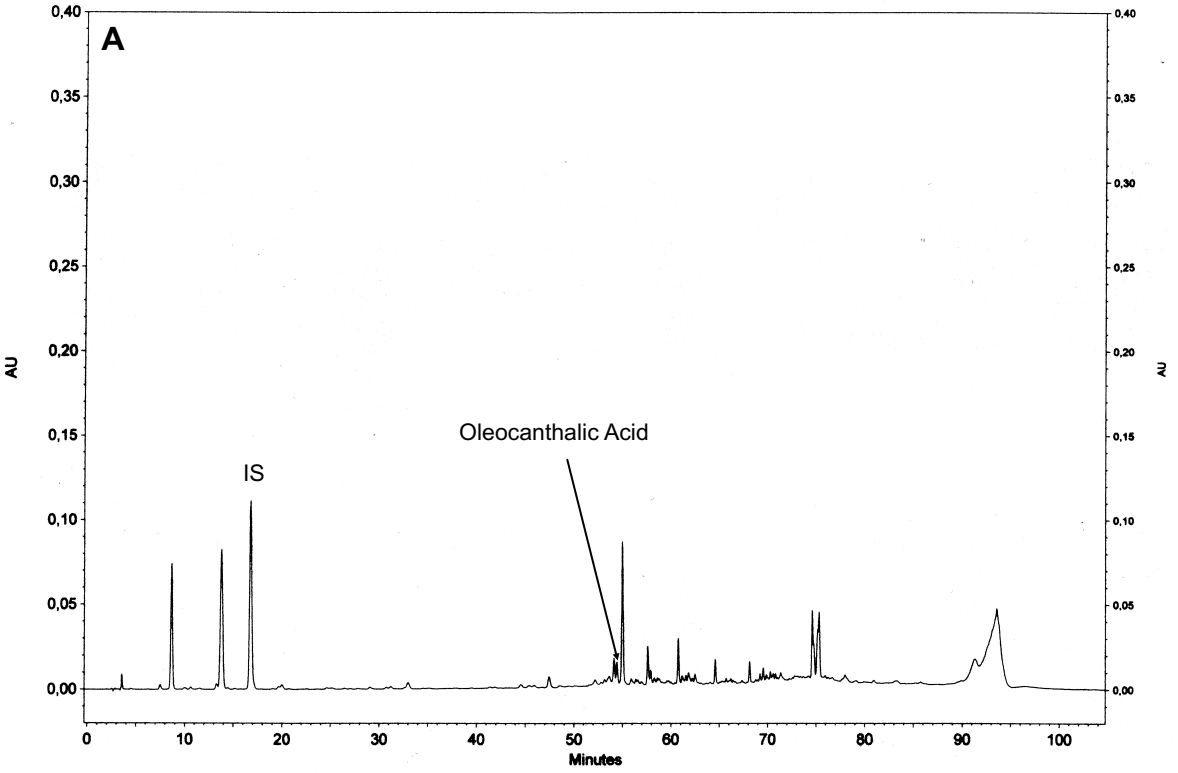

*Figure 80 – HPLC chromatogram of EVOO **A**, analysed after fifteen months of storage at room temperature and in light condition (March 2021). IS = Internal Standard*

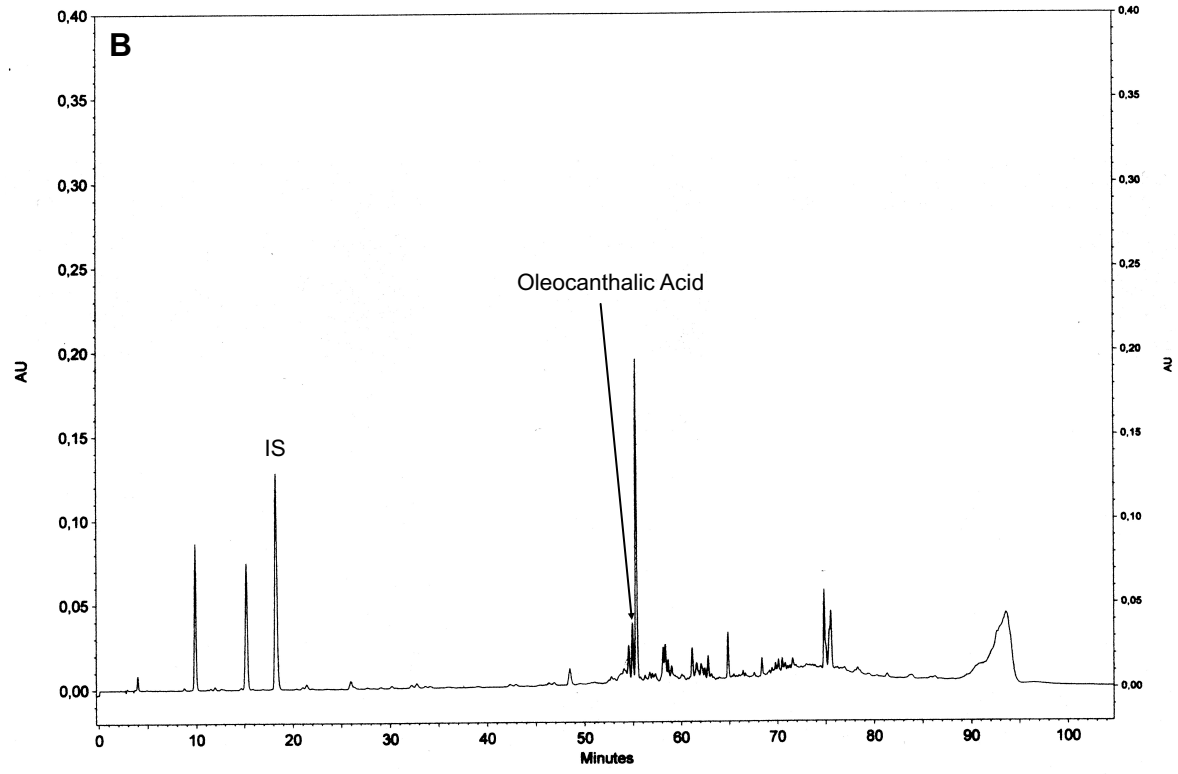

*Figure 81 – HPLC chromatogram of EVOO **B**, analysed after fifteen months of storage at room temperature and in light condition (March 2021). IS = Internal Standard*

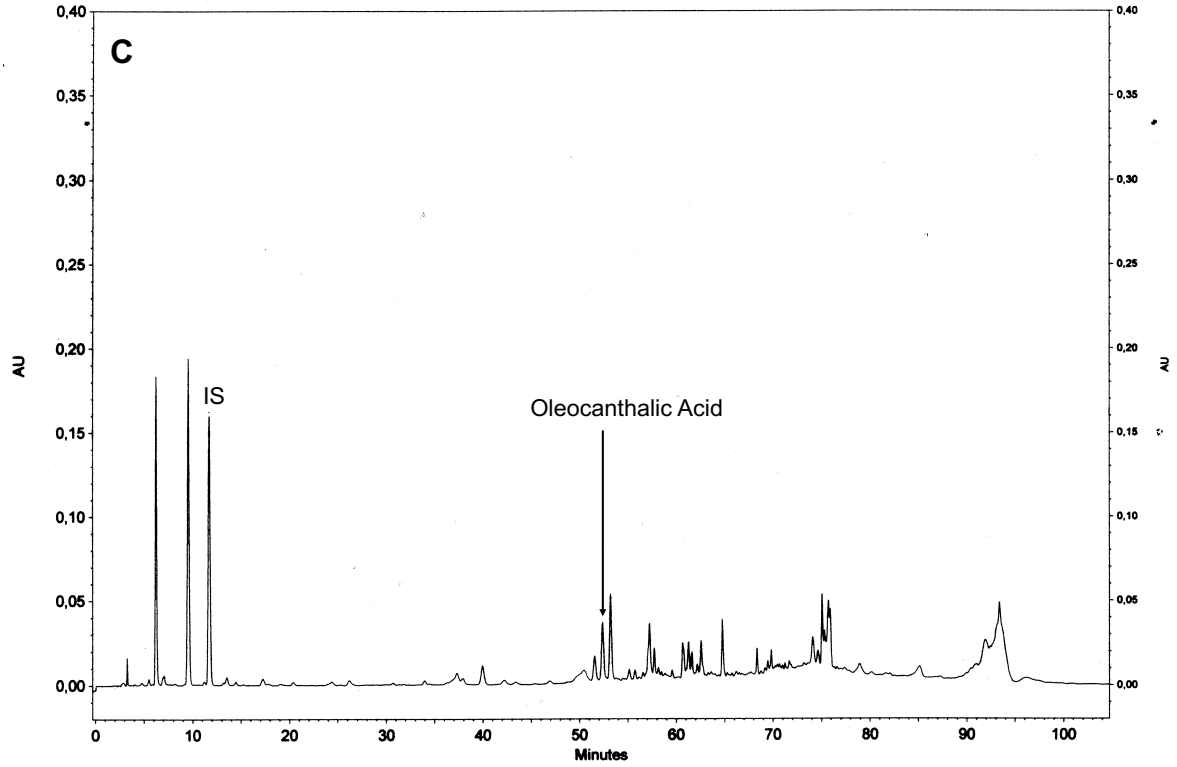

*Figure 82 – HPLC chromatogram of EVOO **C**, analysed after fifteen months of storage at room temperature and in light condition (March 2021). IS = Internal Standard.*

3.4.3.3 Storage at 4°C in Dark Condition

During storage at 4°C and in dark condition (Table 10, Figure 86-blue bars) OA increased in all samples but with some differences. Concerning **B** and **C** EVOOs, the oxidative process in these conditions were less marked than during storage at room temperature, due to the lesser effect of external factors on storage conditions. Indeed, the concentration of OA in samples **B** and **C** after fifteen months of storage at 4°C was 37.39 and 67.83 ppm, respectively, and lower than the concentration after fifteen months of storage at room temperature (67.23 and 83.27 ppm, respectively). Differently, in sample **A**, the concentration of OA increased slightly, in a similar way both during storage at 4°C and at room temperature, reaching about 20 ppm (21.16 and 24.00 ppm, respectively) after fifteen months.

The HPLC chromatograms of EVOOs samples **A**, **B** and **C**, analysed after fifteen months of storage at 4°C and in dark condition (March 2021) are reported in Figure 83, Figure 84 and Figure 85, respectively.

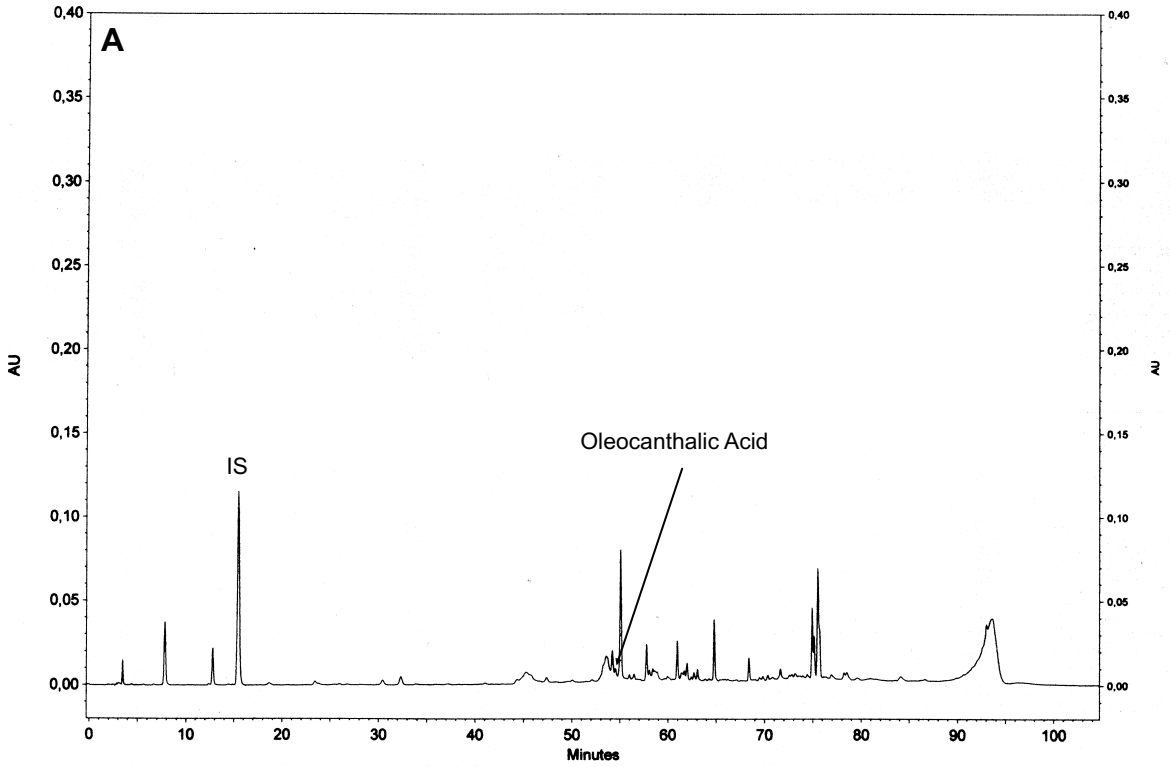

*Figure 83 – HPLC chromatogram of EVOO **A** analysed after fifteen months of storage at 4°C and in dark condition (March 2021). IS = Internal Standard.*

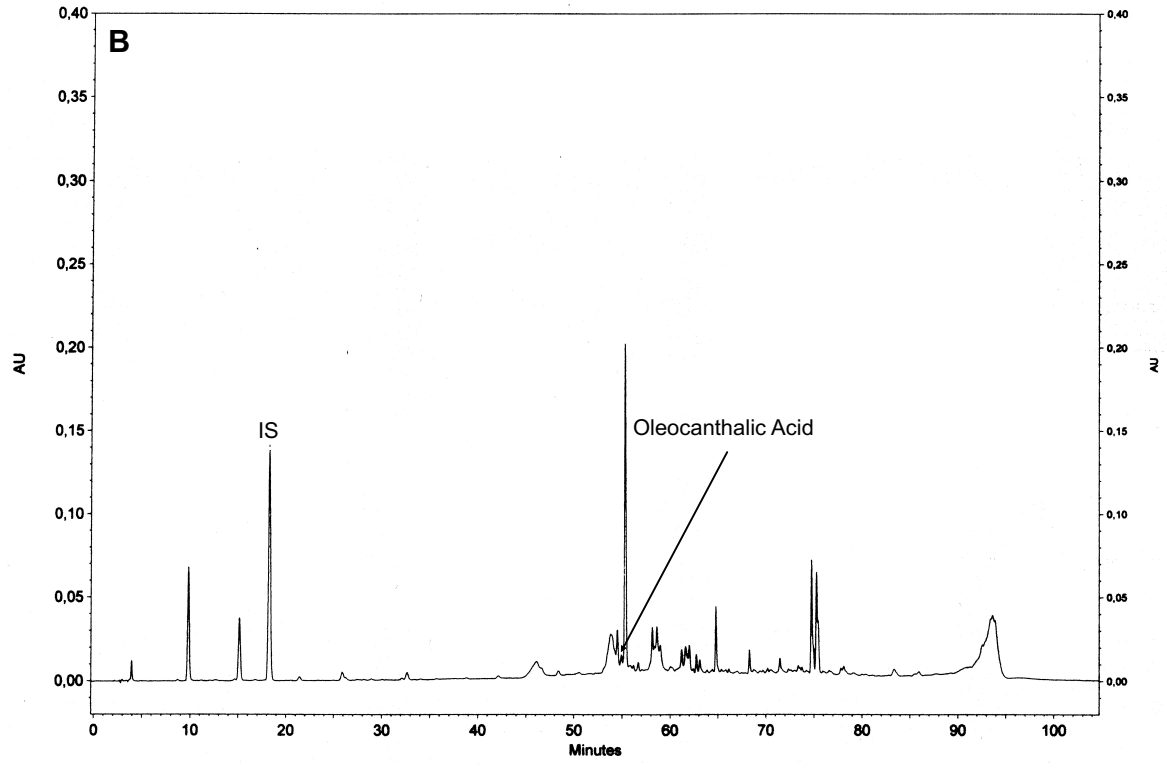

*Figure 84 – HPLC chromatogram of EVOO **B** analysed after fifteen months of storage at 4°C and in dark condition (March 2021). IS = Internal Standard.*

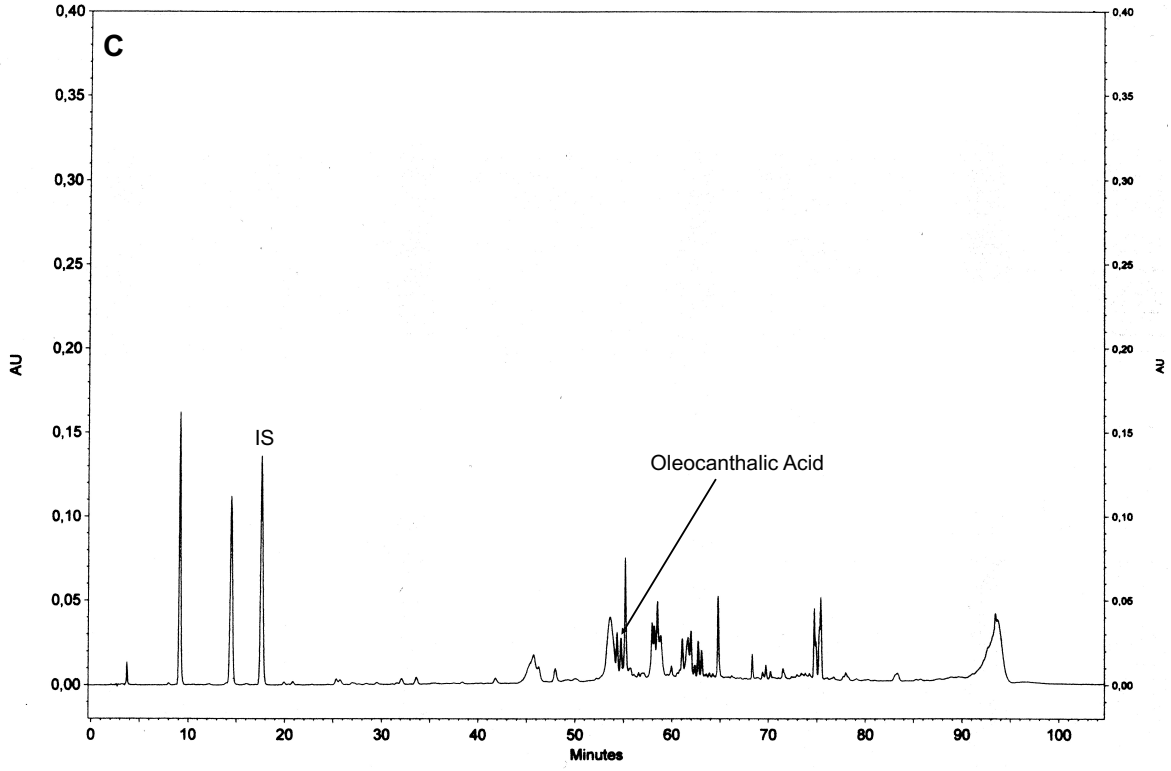

*Figure 85 – HPLC chromatogram of EVOO **C** analysed after fifteen months of storage at 4°C and in dark condition (March 2021). IS = Internal Standard.*

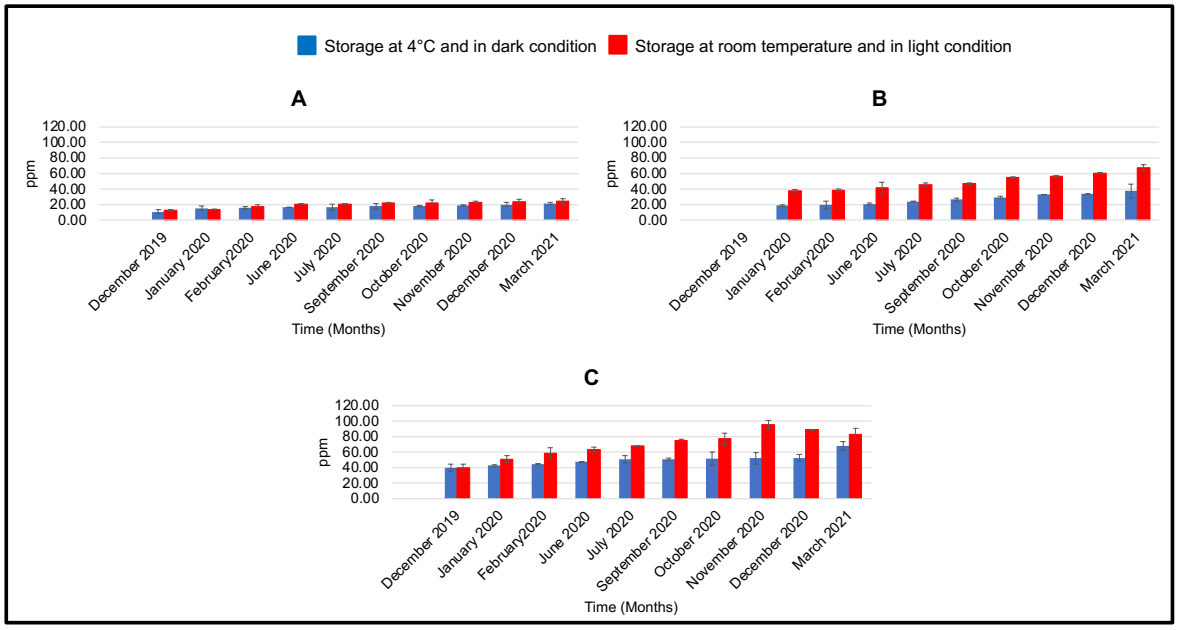

*Figure 86 – Concentration of oleocanthalic acid (µg of OA/g of EVOO, ppm) in EVOOs **A**, **B** and **C** storage at 4°C in dark condition (blue bars) and at room temperature exposed to daylight (red bars), for fifteen months.*

*Table 10 – Concentration of oleocanthalic acid (OA) (μg of OA/g of EVOO, ppm) in three different EVOOs (**A**, **B** and **C**) storage at 4°C in dark condition and at room temperature in light conditions.*

Time	EVOO	OA Storage at 4°C in dark condition	OA Storage at room temperature in light condition
December 2019	A	10.61 ± 2.96	10.61 ± 2.96
	B	N.D.	N.D.
	C	39.72 ± 4.59	39.72 ± 4.59
January 2020	A	15.20 ± 2.64	13.70 ± 0.17
	B	18.63 ± 1.20	37.54 ± 1.51
	C	42.65 ± 1.07	51.07 ± 4.20
February 2020	A	15.94 ± 1.64	17.48 ± 1.92
	B	19.40 ± 5.22	38.75 ± 1.66
	C	44.42 ± 1.00	58.72 ± 6.79
June 2020	A	16.32 ± 0.28	20.37 ± 0.95
	B	20.76 ± 1.33	41.28 ± 7.31
	C	47.25 ± 0.67	63.13 ± 3.07
July 2020	A	16.44 ± 4.12	20.64 ± 0.55
	B	23.83 ± 0.57	45.26 ± 2.39
	C	50.71 ± 4.62	67.71 ± 0.46
September 2020	A	17.85 ± 3.68	22.04 ± 0.67
	B	26.40 ± 1.81	46.70 ± 1.22
	C	50.89 ± 1.40	75.11 ± 1.23
October 2020	A	17.89 ± 0.76	22.39 ± 3.43
	B	28.90 ± 1.36	54.95 ± 0.83
	C	51.50 ± 8.51	77.16 ± 7.27
November 2020	A	19.09 ± 0.61	23.11 ± 1.25
	B	33.16 ± 0.20	56.64 ± 0.92
	C	52.00 ± 7.34	95.56 ± 5.21
December 2020	A	20.03 ± 2.43	23.96 ± 2.98
	B	33.80 ± 0.25	60.39 ± 0.68
	C	52.68 ± 4.02	89.11 ± 0.15
March 2021	A	21.16 ± 1.42	24.00 ± 6.85
	B	37.39 ± 9.10	67.23 ± 3.84
	C	67.83 ± 5.55	83.27 ± 7.56

- Data are expressed as means ± SD of experiments performed in triplicate. N.D. = Not Detectable. -

3.4.4 Conclusion

In this PhD thesis, an efficient and reproducible method for the extraction and the purification of OA from EVOOs was developed in order to obtain this compound with high purity and thus to investigate its nutraceutical properties. Moreover, the HPLC method for its qualitative and quantitative determination in EVOO was validated.[113]

A detailed assessment of the OA *in vitro* radicals quenching activity was provided for the first time, demonstrating its scavenging capacity against ROS.[113] Further studies regarding its nutraceutical properties are ongoing.

It was also possible to confirm, by monitoring EVOOs for fifteen months that the formation of OA depends on storage conditions and on EVOOs age.

3.5 Study of composition of Tuscan EVOOs for the determination of their geographical traceability

During my PhD, I analysed several Tuscan EVOOs as part of a project coordinated by Professor Stefano Loppi of the University of Siena, which aims to study the geographical traceability of EVOOs coming from Siena (Valdichiana Senese) through the multielemental fingerprinting technique, as the correlation between the elements in the soil and in EVOO. In particular, the free acidity and the TPC of forty EVOOs were evaluated. Moreover, a qualitative and quantitative analysis of EVOOs was performed by HPLC, to determine the single phenolic compounds, and a qualitative-quantitative analysis of the main FAs was also carried out by gas chromatography (GC).

The forty EVOOs analysed (reported in section 4.1.3) were produced in 2020/2021 (**1-21**), 2019/2020 (**22-37**) and 2018/2019 (**38-40**) crop seasons.

3.5.1 Determination of Free Acidity

The determination of the free acidity was performed by using an acid-base titration in presence of phenolphthalein as indicator, as reported in section 4.2.14 of the experimental part.

The analysis was performed in duplicate, and the results were expressed as molar percentage of oleic acid. In Table 11 the free acidity values for each EVOO analysed were reported.

As expected, all the samples had a free acidity parameter within the legal values for EVOOs (≤ 0.80%), with only one exception represented by the sample **22**, which had a slightly higher value (0.88%). Acidity values ranged between 0.14% and 0.24% for EVOOs produced in 2020/2021 crop season (**1-21**) and between 0.17% and 0.67% for EVOOs produced in 2019/2020 (**22-37**) and 2018/2019 (**38-39**) crop seasons. The lowest acidity value was found for sample **14** (0.13%). It was possible to observe, in agreement with the literature, that older EVOOs (**22-37** and **38-39**) had higher free acidity values than fresh EVOOs (**1-21**) and it is probably the reason why sample **22** slightly exceeded the limit.

*Table 11 – Free acidity values (% oleic acid) of EVOOs produced in in 2020/2021 (**1-21**), 2019/2020 (**22-37**) and 2018/2019 (**38-39**) crop seasons.*

Nr	Acidity (% Oleic Acid)	Nr	Acidity (% Oleic Acid)
1	0.15	**21**	0.15
2	0.21	**22**	0.88
3	0.15	**23**	0.28
4	0.17	**24**	0.22
5	0.17	**25**	0.28
6	0.16	**26**	0.17
7	0.17	**27**	0.29
8	0.22	**28**	0.47
9	0.18	**29**	0.43
10	0.21	**30**	0.33
11	0.14	**31**	0.36
12	0.17	**32**	0.31
13	0.18	**33**	0.38
14	0.13	**34**	0.51
15	0.24	**35**	0.67
16	0.18	**36**	0.31
17	0.24	**37**	0.39
18	0.20	**38**	0.42
19	0.14	**39**	0.45
20	0.17		

- Data are expressed as molar % of oleic acid of experiments performed in duplicate. -

3.5.2 Determination of Total Phenolic Content

The TPC of each EVOO analysed was evaluated by using the Folin-Ciocalteu assay, described in section 4.2.12.1 of the experimental part. The TPC in EVOOs was expressed as μg of GAE/g of EVOOs (ppm). Comparison between fresh EVOO samples (produced in 2020/2021 crop season) and old EVOO samples (produced in 2019/2020 and 2018/2019 crop seasons) was performed by using Student's t-test. $P < 0.05$ was considered statistically significant.

As reported in Figure 87, the TPC of each EVOO varied greatly according to the sample. In particular, fresh EVOOs (**1-21**) (Figure 87-blue bars) had higher TPC values, ranged between 140.84 and 678.32 ppm, than old EVOOs (**22-37** and **38-39**), ranged between 86.37 and 396.53 ppm (Figure 87-red bars) ($P < 0.05$). The highest TPC value was found for sample **3** (678.32 ppm), while the lowest TPC value was attributable to sample **22** (86.37 ppm). These differences between samples could probably be due to the different condition of storage and to the type of EVOO analysed.

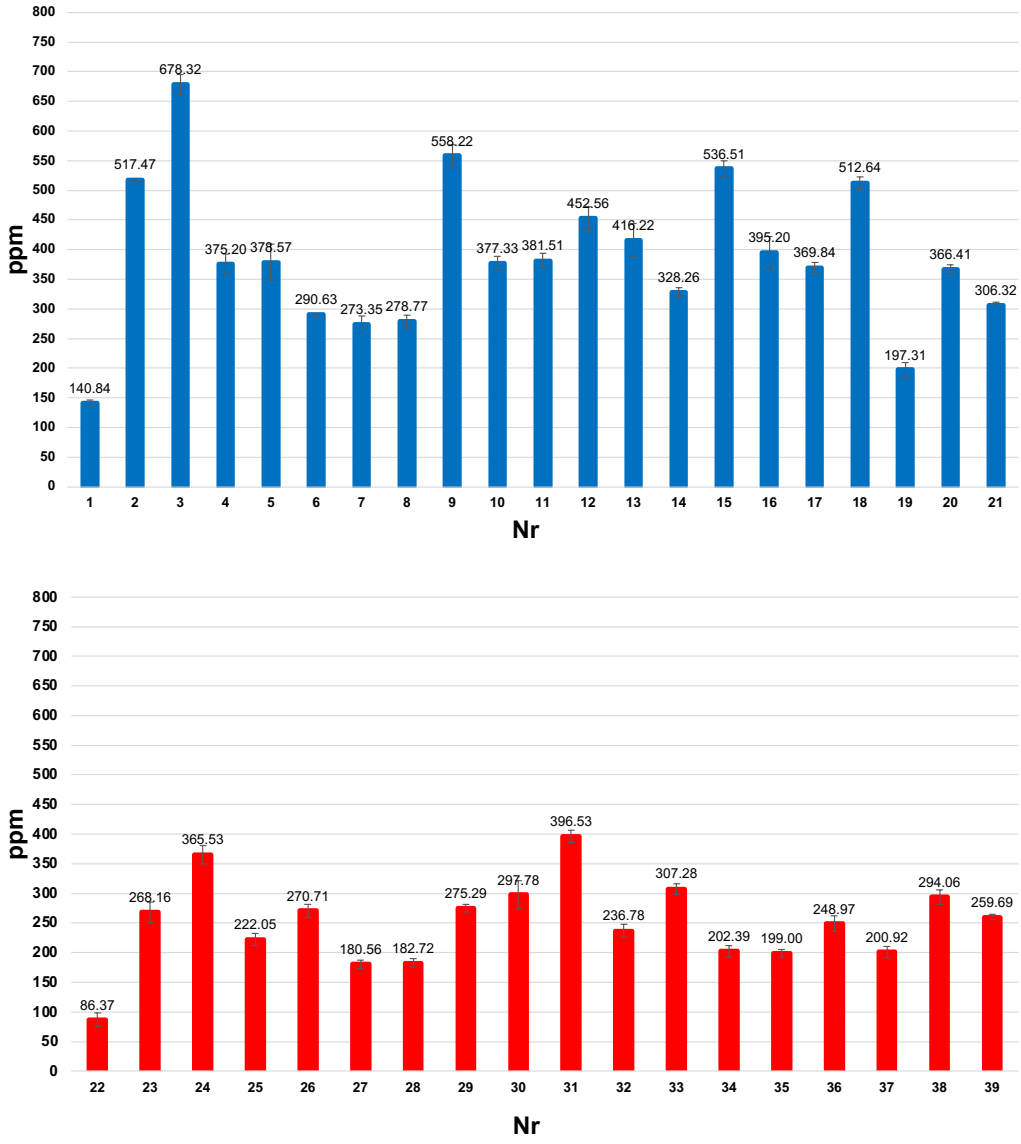

*Figure 87 – TPC content of each EVOO (μg of GAE/g of EVOOs, ppm). Data are expressed as mean ± SD of an experiment performed in triplicate. Blue bars = EVOOs produced in 2020/2021 crop season (**1-21**); Red bars = EVOOs produced in 2019/2020 (**22-37**) and 2018/2019 (**38-39**) crop seasons.*

3.5.3 Qualitative-Quantitative Determination of EVOOs Phenolic Composition

The amount of HT, T, OC, OO and OA, in each EVOO, was determined through HPLC analysis. The retention time and the UV absorbance spectrum of the phenolic compounds present in the samples were compared with those of the pure standards and quantified by using *p*-hydroxyphenylacetic acid as IS. Each analysis was performed in triplicate and the content of each phenolic compound was expressed as μg of phenolic compound/g of EVOO (ppm). Comparison between fresh EVOO samples (produced in 2020/2021 crop season) and old EVOO samples (produced in 2019/2020 and 2018/2019 crop seasons) was performed by using Student's t-test. $P < 0.05$ was considered statistically significant.

As reported in Table 12, the concentration of phenolic compounds in EVOOs varied greatly according to the sample mainly depending on storage times. In particular, fresh EVOOs (**1-21**) had higher OC and OO and lower HT, T and OA (if present) concentrations than old EVOOs (**22-37** and **38-40**) ($P < 0.05$). These values are in line with those reported in the literature and with the analysis described in section 3.3, relatively to the variation of phenolic compounds during storage.

The highest content of OC and OO was found in sample **3** (563.18 ppm and 307.50 ppm, respectively), while the lowest one was observed in sample **22** (24.08 ppm for OO, while OC was not detectable).

The concentration of HT and T is higher in older EVOOs (the average values were 9.06 ppm and 13.46 ppm, respectively), than in fresh EVOOs (the average values were 2.04 ppm and 4.21 ppm, respectively).

As regards OA, in fresh EVOOs (**1-21**) its concentration average value was 27 ppm. In samples **6** and **14** OA was not detectable. The old EVOOs (**22-37** an **38-40**) are characterized by highest OA concentration values (the average was about 40 ppm), except for sample **32** where the amount of OA was very low (9.46 ppm). The highest amount of OA was found in sample **27** (100.32 ppm).

*Table 12 – Phenolic composition (µg of phenolic compound/g of EVOO, ppm) of EVOOs produced in 2020/2021 (**1-21**), 2019/2020 (**22-37**) and 2018/2019 (**38-40**) crop seasons. HT = Hydroxytyrosol; T = Tyrosol; OC = Oleacein; OO = Oleocanthal; OA = Oleocanthalic Acid.*

Nr	HT	T	OC	OO	OA
1	0.73 ± 0.01	10.49 ± 0.19	39.78 ± 4.22	102.35 ± 13.87	14.66 ± 0.84
2	1.72 ± 0.06	1.73 ± 0.12	100.42 ± 5.56	150.78 ± 10.30	31.38 ± 2.78
3	1.46 ± 0.11	1.60 ± 0.13	563.18 ± 33.54	307.50 ± 15.72	38.15 ± 2.48
4	2.19 ± 0.23	7.79 ± 0.64	170.39 ± 12.38	245.67 ± 34.10	24.66 ± 3.52
5	1.38 ± 0.09	1.96 ± 0.06	54.78 ± 10.91	132.52 ± 25.26	55.99 ± 5.51
6	0.95 ± 0.01	2.78 ± 0.05	215.57 ± 6.02	235.03 ± 2.38	N.D.
7	1.22 ± 0.08	3.68 ± 0.11	58.78 ± 4.17	128.78 ± 24.58	30.90 ± 3.66
8	2.02 ± 0.03	4.45 ± 0.37	117.32 ± 23.66	148.70 ± 15.65	22.05 ± 0.37
9	1.31 ± 0.07	2.24 ± 0.17	411.47 ± 10.55	316.86 ± 24.77	23.76 ± 3.54
10	5.54 ± 0.40	4.15 ± 0.37	226.73 ± 15.94	216.15 ± 15.95	32.85 ± 2.38
11	2.74 ± 0.22	3.16 ± 0.30	193.16 ± 12.61	231.72 ± 6.41	37.50 ± 2.59
12	1.72 ± 0.09	2.86 ± 0.16	124.60 ± 7.41	169.60 ± 14.98	34.26 ± 2.80
13	3.84 ± 0.18	7.25 ± 0.68	206.12 ± 4.15	213.60 ± 2.94	12.41 ± 0.04
14	1.05 ± 0.14	4.47 ± 0.39	107.60 ± 8.93	224.32 ± 22.75	N.D.
15	1.98 ± 0.02	6.00 ± 0.17	227.84 ± 3.91	294.61 ± 15.98	41.61 ± 6.46
16	1.84 ± 0.24	2.72 ± 0.33	100.79 ± 13.75	138.81 ± 28.91	39.96 ± 3.97
17	1.00 ± 0.01	3.81 ± 0.10	89.98 ± 6.61	181.87 ± 4.89	14.29 ± 0.43
18	2.48 ± 0.23	3.83 ± 0.34	277.96 ± 10.83	266.32 ± 6.52	52.03 ± 4.06
19	1.03 ± 0.08	3.39 ± 0.34	122.57 ± 1.89	173.56 ± 9.10	9.34 ± 0.26
20	4.19 ± 0.04	5.39 ± 0.16	169.00 ± 5.81	187.85 ± 11.56	43.72 ± 0.46
21	2.42 ± 0.14	4.71 ± 0.12	246.77 ± 15.78	171.36 ± 1.53	16.28 ± 0.69
22	N.D.	3.06 ± 0.08	N.D.	24.08 ± 0.84	13.11 ± 2.22
23	8.80 ± 0.08	4.99 ± 0.28	76.54 ± 1.21	61.13 ± 0.84	29.57 ± 1.38
24	6.20 ± 0.16	6.45 ± 0.34	302.94 ± 10.80	207.54 ± 7.89	38.71 ± 3.36
25	42.71 ± 1.89	54.58 ± 2.19	42.22 ± 1.60	45.67 ± 4.38	23.00 ± 1.20
26	4.35 ± 0.06	7.52 ± 0.31	17.17 ± 0.17	70.69 ± 1.35	34.64 ± 2.67
27	3.91 ± 0.13	9.98 ± 0.05	29.39 ± 1.58	89.83 ± 1.56	100.32 ± 2.84
28	3.72 ± 0.13	6.25 ± 0.23	70.54 ± 5.74	104.01 ± 7.07	15.23 ± 0.68
29	6.88 ± 0.03	8.01 ± 0.43	187.69 ± 1.99	194.43 ± 4.92	49.23 ± 2.82
30	14.42 ± 0.23	28.40 ± 0.61	60.71 ± 4.86	79.59 ± 6.30	44.60 ± 1.82
31	8.83 ± 0.44	13.53 ± 0.54	153.73 ± 11.76	288.23 ± 17.36	62.28 ± 2.85
32	13.84 ± 0.54	30.07 ± 1.18	37.24 ± 0.76	63.44 ± 1.13	9.46 ± 0.31
33	6.11 ± 0.14	9.71 ± 0.31	129.77 ± 2.12	182.75 ± 12.17	54.63 ± 2.65
34	2.82 ± 0.05	7.61 ± 0.03	75.10 ± 2.68	192.66 ± 10.60	35.71 ± 3.33
35	5.24 ± 0.10	5.73 ± 0.87	87.06 ± 9.97	90.29 ± 8.34	31.60 ± 1.74

36	8.41 ± 0.27	11.56 ± 0.55	99.17 ± 9.18	157.52 ± 17.27	53.32 ± 2.13
37	4.77 ± 0.05	9.27 ± 0.52	123.74 ± 6.44	122.66 ± 2.94	34.61 ± 2.60
38	10.77 ± 0.24	12.07 ± 0.32	64.60 ± 4.92	88.65 ± 6.08	46.77 ± 2.71
39	15.38 ± 0.45	18.57 ± 0.20	51.68 ± 0.08	97.07 ± 4.10	40.31 ± 2.60
40	5.04 ± 0.10	8.32 ± 0.34	59.86 ± 0.74	95.27 ± 0.59	52.35 ± 3.28

- Data are expressed as means ± SD of experiment performed in triplicate. N.D. = Not Detectable. -

3.5.4 Qualitative-Quantitative Determination of EVOOs Fatty Acid Composition

3.5.4.1 Development of a GC Method for Fatty Acids Analysis

To analyse the FAs composition in EVOOs a GC method was developed starting from procedures reported in the literature and opportunely modified.[125,126]

At first, the GC method reported by Caporaso *et al*.[125] (reported in section 4.2.13.2.1 of the experimental part) was used. With this method (Method I) it was not possible to identify the peaks of two standards corresponding to C22:0 and C24:0, as reported in Figure 88.

Thus, another procedure was exploited, based on a method reported in literature by Yang *et al.* slightly modified.[126] With this method (Method II, described in section 4.2.13.2.2 of the experimental part), the resolution of the chromatographic peaks was improved and it was possible to identify all the chromatographic peaks corresponding to all the standards, as shown in Figure 89.

In Figure 90 a GC chromatogram of an EVOO analysed is reported, where it is possible to observe its FA profile.

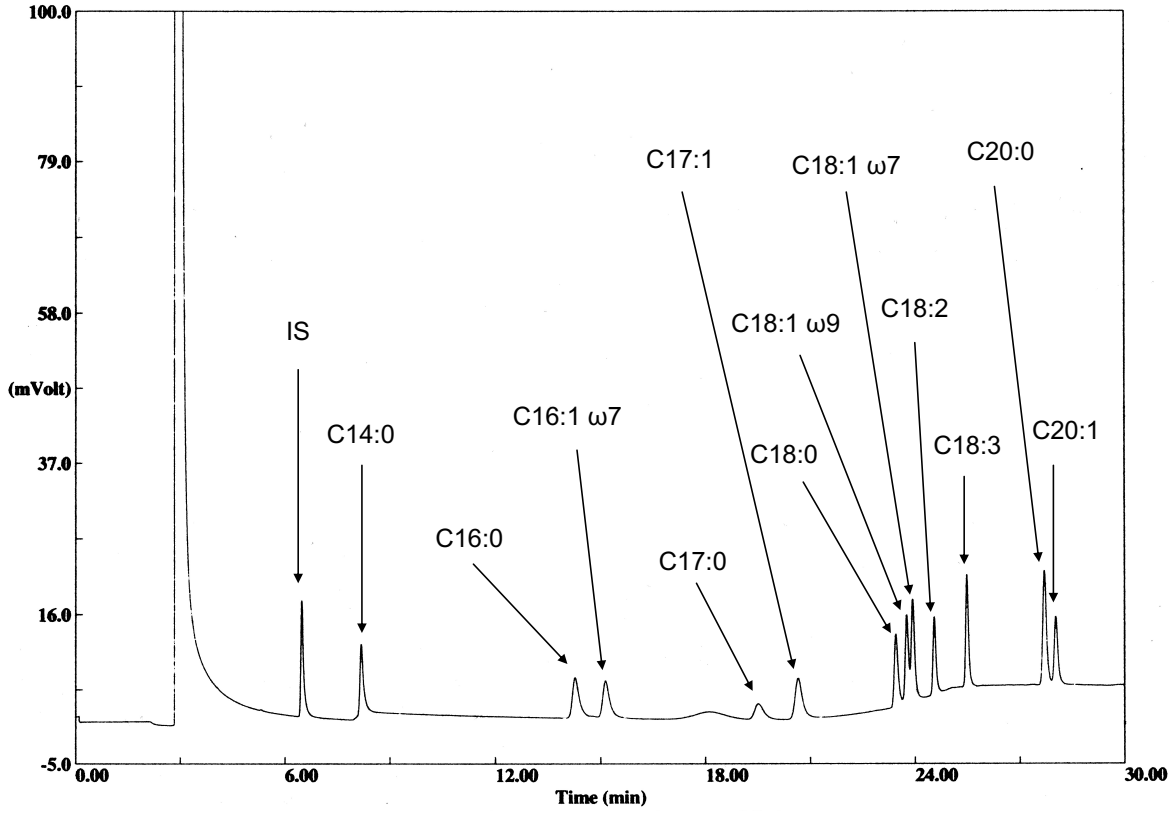

Figure 88 – GC chromatogram obtained by using the Method I. The standards were injected as a mixture dissolved in n-hexane. IS = Internal Standard.

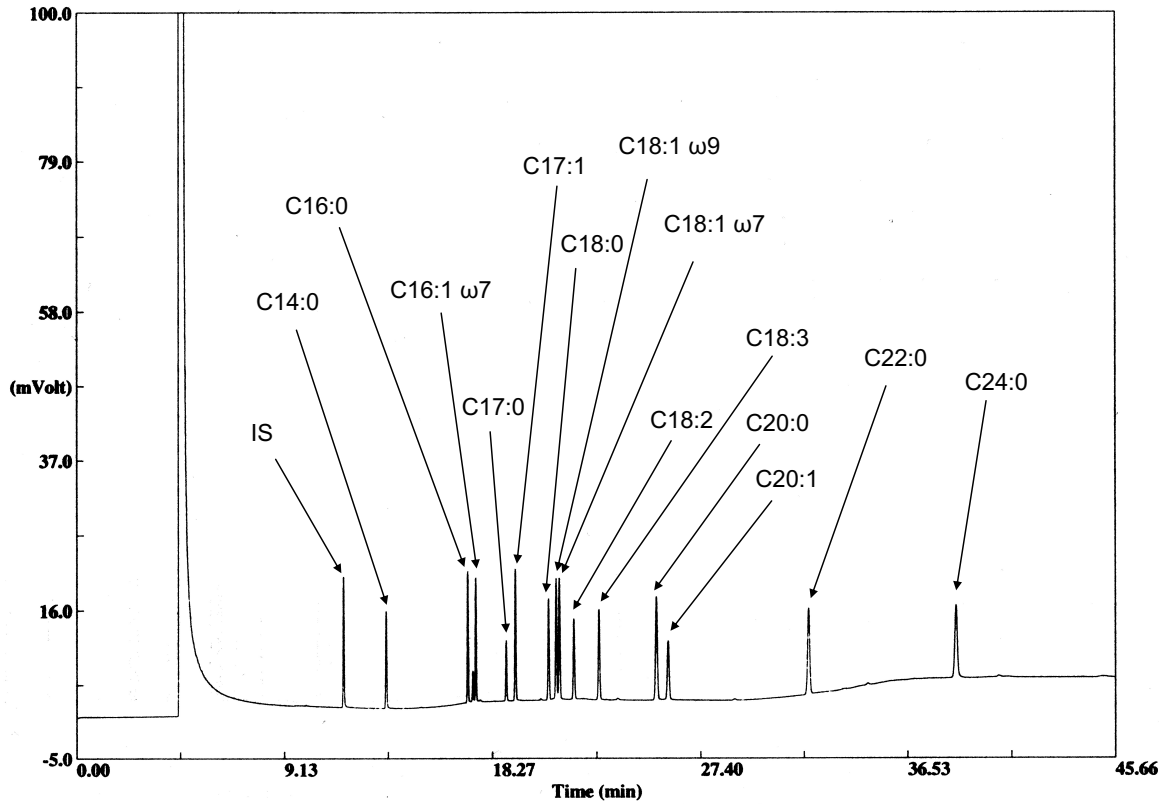

Figure 89 – GC chromatogram obtained by using the Method II. The standards were injected as a mixture dissolved in n-hexane. IS = Internal Standard.

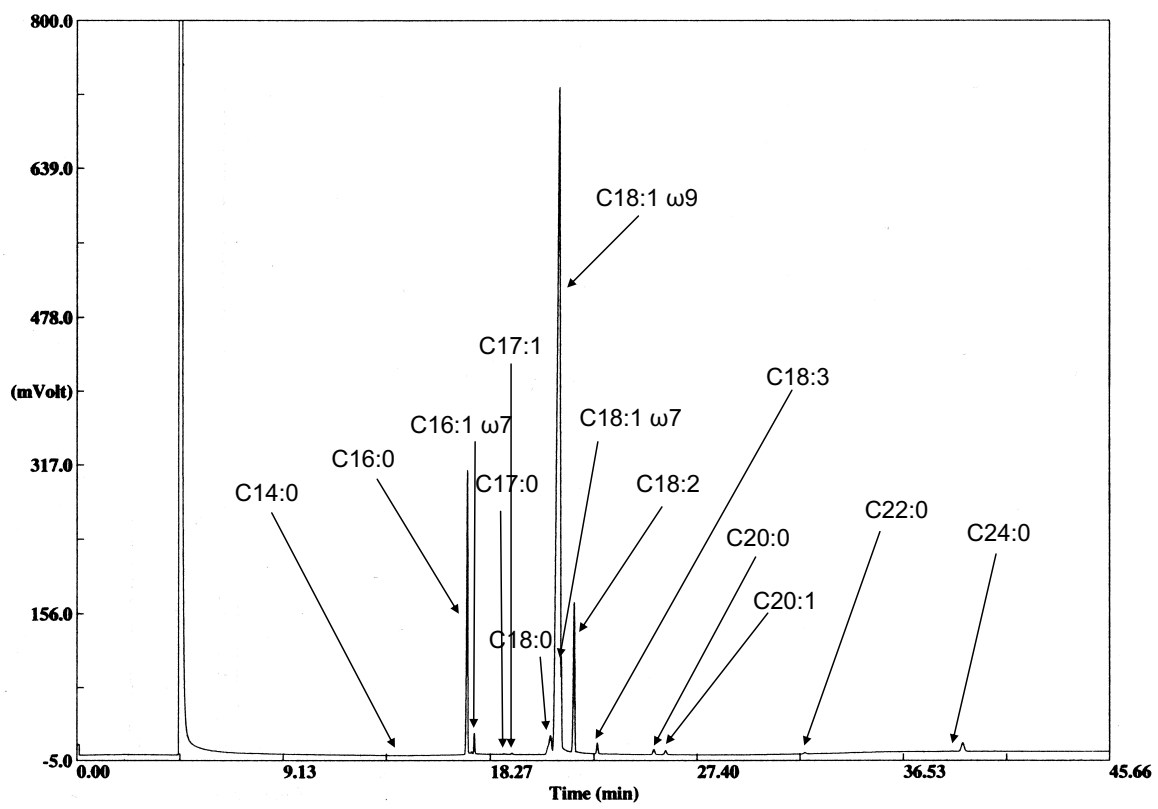

Figure 90 – GC chromatogram of an EVOO.

3.5.4.2 Fatty Acid Composition of EVOOs

In order to determine the FA composition, EVOOs samples were prepared through alkaline transmethylation by using the procedure reported in section 4.2.13.1 of the experimental part and successively injected to GC. The identification of the peaks was achieved by comparing the retention time of the FAs present in EVOO with those of the pure standards (commercial FAs methyl esters, FAMEs) and quantified by using methyl tridecanoate as internal standard (IS). The results of the analysis, performed in triplicate were expressed as g of FA/100 g of EVOO (%), as reported in Table 13 and Table 14. All EVOOs analysed showed the same FAs composition. Moreover, the concentration of each specific FA is similar in all EVOO samples, with little variability.

As expected, the most abundant FA in all EVOO samples was represented by the MUFA oleic acid (C18:1 ω9). The highest concentration of this FA was 72.09% in sample **35** and the lowest was 47.84% in sample **24**. Beside oleic acid, other unsaturated FAs in EVOOs were found such as 11-octadecenoic acid (C18:1 ω7) and palmitoleic acid (C16:1 ω7) with an average concentration of 1.93%, and

0.96%, respectively, 10-heptadecenoic acid (C17:1) and gadoleic acid (C21:1), both with an average concentration less than 1%. Moreover, linoleic acid (C18:2) and α-linolenic acid (C18:3) were quantified. The highest concentration of linoleic acid (11.40%) and α-linolenic acid (0.67%) was achieved in samples **25** and **5**, respectively.

Concerning the concentration of SFAs, those present in highest amount were palmitic acid (C16:0) (mean value = 8.53%) followed by stearic acid (C18:0) and eicosanoic acid (C20:0) (mean value = 1.21% and 0.20%, respectively). The average concentration of the other SFAs (C14:0, C17:0, C22:0 and C24:0) was less than 0.06%.

*Table 13 – Fatty acid composition (% p/p, g FA/100g EVOO) of EVOOs produced in 2020/2021 (**1**-**21**), 2019/2020 (**22**-**37**) and 2018/2019 (**38**-**40**) crop seasons.*

Nr	C14:0	C16:0	C16:1 ω7	C17:0	C17:1	C18:0	C18:1 ω9
1	0.010 ± 0.001	8.337 ± 0.034	0.839 ± 0.018	0.061 ± 0.001	0.068 ± 0.002	1.188 ± 0.023	61.063 ± 0.707
2	0.010 ± 0.001	8.854 ± 0.175	0.810 ± 0.017	0.061 ± 0.002	0.060 ± 0.002	1.258 ± 0.019	61.542 ± 1.239
3	0.009 ± 0.001	6.876 ± 0.175	0.689 ± 0.021	0.062 ± 0.002	0.067 ± 0.001	1.149 ± 0.017	61.437 ± 1.176
4	0.011 ± 0.001	8.440 ± 0.132	1.014 ± 0.016	0.046 ± 0.001	0.048 ± 0.002	1.092 ± 0.007	52.240 ± 0.823
5	0.010 ± 0.001	10.155 ± 0.020	0.868 ± 0.025	0.067 ± 0.002	0.060 ± 0.003	1.374 ± 0.074	63.839 ± 3.356
6	0.009 ± 0.001	9.123 ± 0.218	1.039 ± 0.025	0.058 ± 0.001	0.064 ± 0.003	1.168 ± 0.039	61.721 ± 1.882
7	0.010 ± 0.001	8.392 ± 0.272	0.923 ± 0.030	0.063 ± 0.001	0.068 ± 0.001	1.260 ± 0.038	57.4286 ± 1.565
8	0.009 ± 0.001	7.835 ± 0.209	0.945 ± 0.030	0.050 ± 0.001	0.059 ± 0.002	1.040 ± 0.032	54.147 ± 1.645
9	0.008 ± 0.001	8.131 ± 0.236	0.820 ± 0.020	0.060 ± 0.002	0.066 ± 0.001	1.144 ± 0.027	60.4784 ± 1.882
10	0.008 ± 0.001	8.443 ± 0.162	0.852 ± 0.015	0.059 ± 0.001	0.063 ± 0.003	1.265 ± 0.016	65.418 ± 0.672
11	0.009 ± 0.001	7.297 ± 0.203	0.775 ± 0.021	0.052 ± 0.001	0.054 ± 0.001	1.057 ± 0.021	53.214 ± 1.109
12	0.009 ± 0.001	7.532 ± 0.099	0.721 ± 0.010	0.053 ± 0.001	0.055 ± 0.001	1.053 ± 0.025	53.006 ± 0.662
13	0.008 ± 0.001	6.980 ± 0.115	0.776 ± 0.014	0.078 ± 0.002	0.087 ± 0.001	1.088 ± 0.027	55.951 ± 0.841
14	0.009 ± 0.001	8.460 ± 0.256	0.894 ± 0.029	0.060 ± 0.003	0.063 ± 0.003	1.290 ± 0.045	67.528 ± 2.212
15	0.009 ± 0.001	8.526 ± 0.320	0.833 ± 0.031	0.059 ± 0.002	0.060 ± 0.002	1.274 ± 0.041	63.833 ± 2.258
16	0.010 ± 0.001	7.959 ± 0.324	0.903 ± 0.029	0.057 ± 0.002	0.054 ± 0.001	1.276 ± 0.048	58.209 ± 1.520
17	0.009 ± 0.001	8.198 ± 0.467	0.863 ± 0.042	0.063 ± 0.003	0.074 ± 0.003	1.160 ± 0.062	65.993 ± 3.846
18	0.010 ± 0.001	8.505 ± 0.368	0.877 ± 0.048	0.059 ± 0.001	0.064 ± 0.002	1.260 ± 0.060	62.705 ± 3.111
19	0.010 ± 0.001	9.006 ± 0.278	0.949 ± 0.032	0.062 ± 0.002	0.069 ± 0.001	1.165 ± 0.019	63.272 ± 1.921
20	0.009 ± 0.001	8.456 ± 0.240	0.885 ± 0.018	0.059 ± 0.003	0.067 ± 0.001	1.084 ± 0.036	57.229 ± 1.538
21	0.009 ± 0.001	8.543 ± 0.267	0.838 ± 0.018	0.064 ± 0.003	0.065 ± 0.002	1.367 ± 0.048	62.389 ± 1.556
22	0.010 ± 0.001	7.548 ± 0.350	0.820 ± 0.038	0.053 ± 0.003	0.055 ± 0.002	1.064 ± 0.050	56.607 ± 2.000

23	0.011 ± 0.001	8.940 ± 0.098	1.039 ± 0.077	0.047 ± 0.001	0.052 ± 0.001	1.035 ± 0.004	61.515 ± 0.152
24	0.008 ± 0.001	6.778 ± 0.175	0.678 ± 0.014	0.046 ± 0.003	0.050 ± 0.002	0.840 ± 0.046	47.837 ± 1.543
25	0.011 ± 0.001	9.159 ± 0.226	1.044 ± 0.027	0.057 ± 0.001	0.050 ± 0.003	1.492 ± 0.041	56.469 ± 1.184
26	0.009 ± 0.001	9.353 ± 0.602	1.017 ± 0.060	0.054 ± 0.003	0.054 ± 0.002	1.349 ± 0.095	62.224 ± 3.992
27	0.010 ± 0.001	10.074 ± 0.221	1.354 ± 0.046	0.053 ± 0.002	0.059 ± 0.003	1.415 ± 0.041	69.073 ± 2.240
28	0.008 ± 0.001	8.644 ± 0.617	0.952 ± 0.063	0.056 ± 0.005	0.070 ± 0.004	1.078 ± 0.103	63.309 ± 4.795
29	0.013 ± 0.001	8.614 ± 0.391	1.087 ± 0.056	0.056 ± 0.003	0.066 ± 0.004	1.150 ± 0.052	63.373 ± 3.340
30	0.010 ± 0.001	9.146 ± 0.219	1.157 ± 0.018	0.049 ± 0.002	0.057 ± 0.002	1.281 ± 0.026	62.307 ± 1.727
31	0.011 ± 0.001	10.494 ± 0.104	1.475 ± 0.044	0.085 ± 0.003	0.093 ± 0.001	1.645 ± 0.033	71.795 ± 0.779
32	0.009 ± 0.001	8.203 ± 0.285	0.813 ± 0.044	0.037 ± 0.002	0.043 ± 0.001	1.209 ± 0.041	61.594 ± 2.205
33	0.009 ± 0.001	8.683 ± 0.237	1.088 ± 0.054	0.053 ± 0.001	0.056 ± 0.003	1.247 ± 0.072	58.539 ± 2.549
34	0.009 ± 0.001	7.573 ± 0.163	1.044 ± 0.030	0.048 ± 0.002	0.061 ± 0.001	1.163 ± 0.019	58.108 ± 1.494
35	0.010 ± 0.001	9.609 ± 0.612	1.116 ± 0.047	0.062 ± 0.003	0.076 ± 0.001	1.192 ± 0.053	72.094 ± 2.891
36	0.010 ± 0.001	7.867 ± 0.133	1.234 ± 0.017	0.107 ± 0.002	0.120 ± 0.003	1.104 ± 0.042	49.228 ± 1.029
37	0.009 ± 0.001	7.799 ± 0.226	1.041 ± 0.031	0.046 ± 0.004	0.063 ± 0.003	0.853 ± 0.004	54.756 ± 1.279
38	0.010 ± 0.001	8.990 ± 0.228	1.181 ± 0.040	0.061 ± 0.003	0.067 ± 0.001	1.298 ± 0.002	60.052 ± 1.175
39	0.009 ± 0.001	9.907 ± 0.173	1.078 ± 0.022	0.056 ± 0.003	0.062 ± 0.002	1.463 ± 0.025	71.392 ± 1.239
40	0.010 ± 0.001	9.303 ± 0.249	1.224 ± 0.078	0.045 ± 0.006	0.052 ± 0.001	1.359 ± 0.086	60.675 ± 1.742

- Data are expressed as means ± SD of experiment performed in triplicate. -

*Table 14 - Fatty acid composition (% p/p, g FA/100g EVOO) of EVOOs produced in 2020/2021 (**1**-**21**), 2019/2020 (**22**-**37**) and 2018/2019 (**38**-**40**) crop seasons.*

Nr	C18:1 ω7	C18:2	C18:3	C20:0	C20:1	C22:0	C24:0
1	1.791 ± 0.058	6.708 ± 0.072	0.555 ± 0.006	0.193 ± 0.003	0.334 ± 0.015	0.059 ± 0.002	0.026 ± 0.001
2	1.710 ± 0.011	6.923 ± 0.147	0.551 ± 0.011	0.201 ± 0.005	0.321 ± 0.001	0.061 ± 0.002	0.027 ± 0.001
3	1.623 ± 0.051	6.075 ± 0.136	0.555 ± 0.010	0.188 ± 0.004	0.319 ± 0.016	0.056 ± 0.001	0.024 ± 0.001
4	1.886 ± 0.038	8.229 ± 0.122	0.511 ± 0.005	0.173 ± 0.003	0.283 ± 0.009	0.049 ± 0.001	0.025 ± 0.001
5	1.949 ± 0.062	8.337 ± 0.456	0.672 ± 0.035	0.223 ± 0.015	0.371 ± 0.013	0.068 ± 0.004	0.033 ± 0.001
6	1.964 ± 0.072	6.050 ± 0.185	0.521 ± 0.015	0.185 ± 0.006	0.307 ± 0.015	0.052 ± 0.002	0.024 ± 0.002
7	1.782 ± 0.019	6.620 ± 0.181	0.523 ± 0.015	0.202 ± 0.006	0.299 ± 0.004	0.059 ± 0.001	0.028 ± 0.001
8	1.846 ± 0.095	5.755 ± 0.180	0.502 ± 0.015	0.177 ± 0.006	0.293 ± 0.009	0.054 ± 0.001	0.026 ± 0.001
9	1.765 ± 0.030	6.598 ± 0.200	0.510 ± 0.019	0.187 ± 0.010	0.329 ± 0.019	0.057 ± 0.001	0.026 ± 0.001
10	1.878 ± 0.078	6.370 ± 0.068	0.537 ± 0.005	0.207 ± 0.004	0.348 ± 0.009	0.062 ± 0.002	0.026 ± 0.001
11	1.587 ± 0.072	5.457 ± 0.114	0.466 ± 0.011	0.170 ± 0.003	0.259 ± 0.006	0.048 ± 0.002	0.021 ± 0.001
12	1.587 ± 0.083	5.849 ± 0.071	0.496 ± 0.008	0.179 ± 0.003	0.296 ± 0.006	0.053 ± 0.001	0.025 ± 0.001
13	1.705 ± 0.043	6.258 ± 0.080	0.486 ± 0.007	0.187 ± 0.001	0.318 ± 0.020	0.059 ± 0.001	0.026 ± 0.001
14	1.934 ± 0.062	6.020 ± 0.220	0.531 ± 0.022	0.201 ± 0.006	0.343 ± 0.008	0.055 ± 0.001	0.025 ± 0.001
15	1.828 ± 0.109	6.748 ± 0.237	0.545 ± 0.019	0.212 ± 0.008	0.347 ± 0.006	0.063 ± 0.002	0.028 ± 0.001
16	1.621 ± 0.019	6.469 ± 0.145	0.575 ± 0.015	0.214 ± 0.006	0.306 ± 0.020	0.068 ± 0.003	0.031 ± 0.001
17	2.012 ± 0.108	7.459 ± 0.426	0.580 ± 0.033	0.212 ± 0.013	0.403 ± 0.025	0.067 ± 0.003	0.030 ± 0.003
18	1.836 ± 0.118	6.710 ± 0.332	0.536 ± 0.023	0.203 ± 0.009	0.327 ± 0.016	0.059 ± 0.003	0.026 ± 0.001
19	2.057 ± 0.065	6.879 ± 0.210	0.574 ± 0.020	0.198 ± 0.006	0.345 ± 0.018	0.062 ± 0.002	0.028 ± 0.001
20	1.862 ± 0.072	6.597 ± 0.181	0.499 ± 0.013	0.180 ± 0.004	0.301 ± 0.024	0.055 ± 0.001	0.025 ± 0.001
21	1.675 ± 0.077	6.657 ± 0.137	0.555 ± 0.010	0.210 ± 0.009	0.315 ± 0.022	0.060 ± 0.003	0.026 ± 0.001
22	1.917 ± 0.059	6.071 ± 0.260	0.504 ± 0.023	0.182 ± 0.007	0.311 ± 0.011	0.054 ± 0.001	0.026 ± 0.001

23	2.056 ± 0.105	7.395 ± 0.008	0.520 ± 0.004	0.177 ± 0.003	0.325 ± 0.009	0.056± 0.001	0.025 ± 0.001
24	1.573 ± 0.041	4.827 ± 0.163	0.438 ± 0.013	0.141 ± 0.007	0.254 ± 0.014	0.042 ± 0.002	0.020 ± 0.001
25	2.107 ± 0.123	11.404 ± 0.341	0.602 ± 0.013	0.231 ± 0.004	0.337 ± 0.010	0.071 ± 0.003	0.033 ± 0.001
26	2.053 ± 0.112	7.312 ± 0.453	0.517 ± 0.036	0.199 ± 0.013	0.326 ± 0.020	0.057 ± 0.005	0.026 ± 0.002
27	2.298 ± 0.085	7.270 ± 0.257	0.469 ± 0.016	0.199 ± 0.010	0.309 ± 0.019	0.053 ± 0.002	0.022 ± 0.002
28	2.135 ± 0.111	6.789 ± 0.507	0.560 ± 0.041	0.190 ± 0.012	0.371 ± 0.019	0.060 ± 0.02	0.031 ± 0.002
29	2.152 ± 0.100	6.617 ± 0.353	0.507 ± 0.022	0.189 ± 0.013	0.331 ± 0.015	0.056 ± 0.004	0.024 ± 0.001
30	2.210 ± 0.175	7.036 ± 0.174	0.477 ± 0.012	0.190 ± 0.008	0.306 ± 0.019	0.053 ± 0.003	0.024 ± 0.001
31	2.492 ± 0.125	10.432 ± 0.101	0.630 ± 0.007	0.244 ± 0.002	0.376 ± 0.020 ±	0.065 ± 0.001	0.032 ± 0.002
32	1.663 ± 0.107	8.000 ± 0.295	0.426 ± 0.017	0.188 ± 0.009	0.302 ± 0.026	0.057 ± 0.001	0.020 ± 0.001
33	1.978 ± 0.043	6.863 ± 0.281	0.534 ± 0.026	0.193 ± 0.009	0.300 ± 0.014	0.054 ± 0.002	0.024 ± 0.002
34	1.998 ± 0.043	7.125 ± 0.194	0.430 ± 0.008	0.172 ± 0.004	0.289 ± 0.007	0.049 ± 0.002	0.021 ± 0.001
35	2.402 ± 0.078	8.159 ± 0.317	0.611 ± 0.025	0.208 ± 0.008	0.394 ± 0.0016	0.065 ± 0.003	0.029 ± 0.001
36	1.884 ± 0.041	5.093 ± 0.110	0.342 ± 0.006	0.171 ± 0.005	0.240 ± 0.014	0.047 ± 0.001	0.023 ± 0.001
37	2.088 ± 0.068	6.179 ± 0.157	0.430 ± 0.014	0.148 ± 0.002	0.281 ± 0.007	0.044 ± 0.001	0.020 ± 0.001
38	2.000 ± 0.020	6.210 ± 0.122	0.451 ± 0.011	0.192 ± 0.005	0.278 ± 0.019	0.055 ± 0.001	0.022 ± 0.002
39	2.353 ± 0.079	9.159 ± 0.191	0.495 ± 0.012	0.230 ± 0.005	0.370 ± 0.014	0.067 ± 0.001	0.028 ± 0.002
40	1.936 ± 0.035	8.408 ± 0.207	0.414 ± 0.012	0.234 ± 0.022	0.283 ± 0.003	0.056 ± 0.003	0.025 ± 0.001

- Data are expressed as means ± SD of experiment performed in triplicate. -

3.5.5 Conclusion

The results of these analyses will be correlated with data relating to other parameters studied, such as the concentration of macro-elements, micro-elements, essential and non-essential trace elements, as well as rare earth elements, present both in the samples of EVOOs and in those of soil where the olive trees are been cultivated, in order to create a model that allows to verify and guarantee the origin of the oil, thus indissolubly linking EVOO to its production area.

3.6 Development of devices useful in tissue regeneration fields from olive leaves phytoextracts (OLEs) obtained from autochthonous Tuscan olive trees *Cultivars*

During my PhD, I collaborated on a multidisciplinary project, coordinated by Professor Rossella Di Stefano (University of Pisa), focused on the study of OLEs obtained from leaves of autochthonous Tuscan olive trees (*Olea Europaea* L., Var. *Olivastra seggianese*), with the aim to obtain biocompatible fibers incorporating OLE as biomedical devices potentially useful in wounds healing and skin regeneration fields.

As part of this project, I provided the qualitative and quantitative analysis of the phenolic profile of the OLEs, deriving from leaves collected at different months, in order to select the appropriate OLE in terms of phenolic and polyphenolic composition, to be incorporated in the biopolymers. Once the OLE was incorporated in the biopolymers, it was necessary to verify that the system was able to release the phenolic compounds contained in the OLE for its use as a device. Thus, I have evaluated the release profile of the phenolic compounds from the biopolymers incorporating OLE.[127–129]

3.6.1 Qualitative and Quantitative Determination of Phenolic Compounds in OLEs

I analysed three kinds of OLEs obtained from leaves of autochthonous Tuscan olive trees (*Olea europaea* L., Var. *Olivastra seggianese*), collected in three different months: October 2018, March 2019 and May 2019. Initially, for the qualitative-quantitative analysis of the phenolic compounds present in OLEs, a slightly modified method for the determination of OO and OC was used. This method (Method I), extensively described in section 4.2.10.2.1 of the experimental part, exploits a mixture of H_2O/AcOH (97.5: 2.5 v/v) (A) and MeOH/ACN (1:1 v/v) (B) as mobile phase. However, Method I did not allow the identification of some phenolic compounds. In particular, there was a partial overlap of the rutin and luteolin-7-O-glucoside chromatographic peaks (red circle), as shown Figure 91.

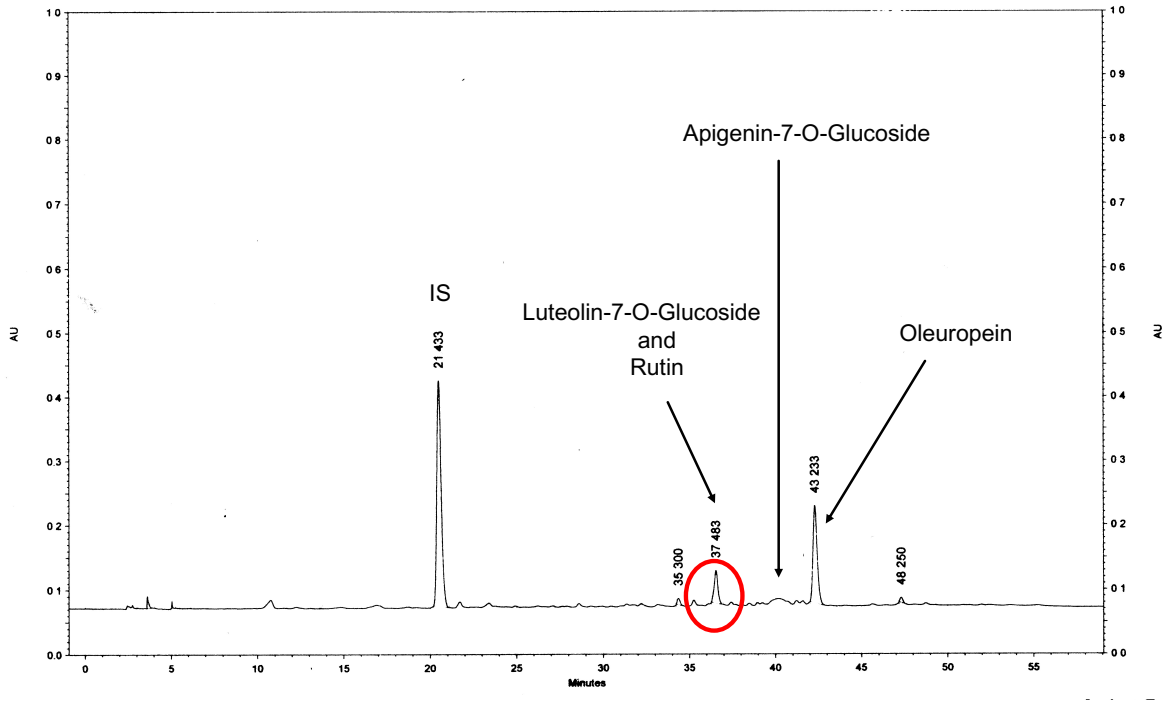

Figure 91 – HPLC chromatogram of an OLE obtained by using the Method I. Red circle = partial overlap of rutin and luteolin-7-O-glucoside peaks.

After literature review, an HPLC method for the characterization of the most widely studied phenolic compounds present in OLE was identified.[130] This new HPLC method (Method II) is reported in detail in section 4.2.10.2.2 of the experimental part and it exploits a mixture H_2O/AcOH (97.5: 2.5 v/v) (A) and ACN (B) as mobile phase. With Method II it was possible to obtain a good resolution of the chromatographic peaks related to all the phenolic compounds investigated in OLE (Figure 92).

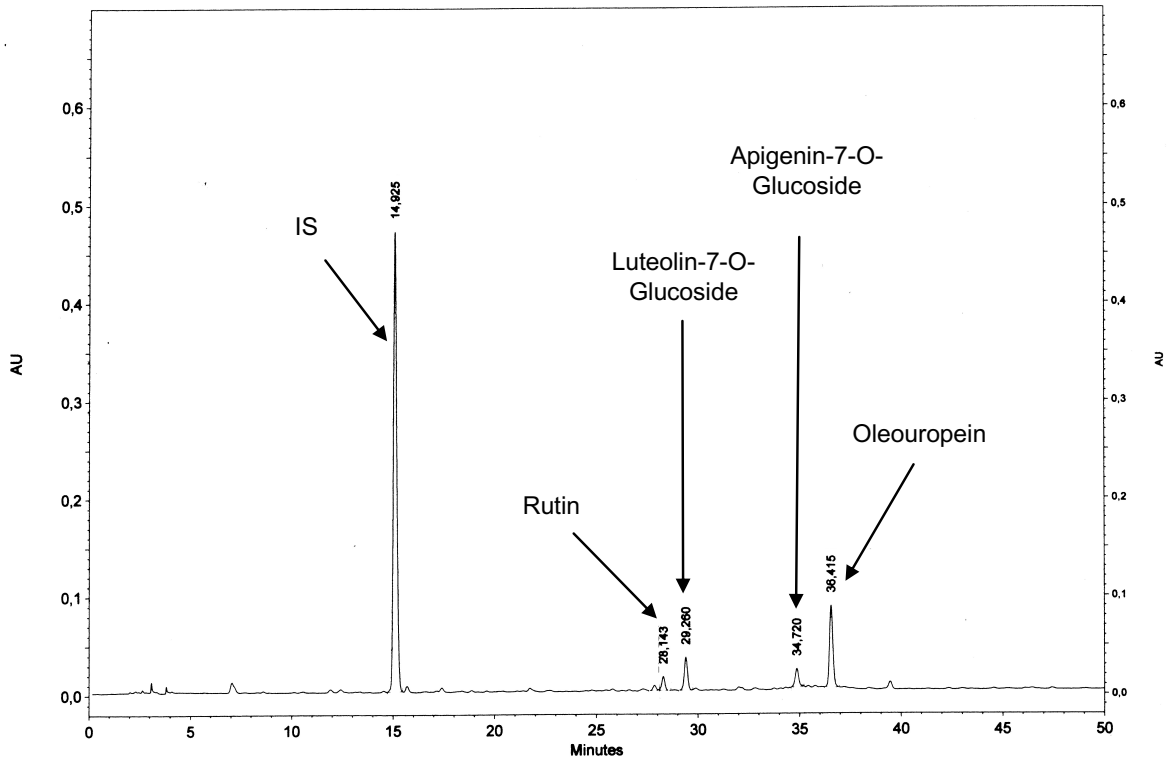

Figure 92 – HPLC chromatogram of an OLE obtained using the Method II.

The presence of OL, luteolin-7-O-glucoside, apigenin-7-O-glucoside and rutin, as well as that of other phenolic compounds such as verbascoside, T, HT, caffeic acid, *p*-coumaric acid, ferulic acid and vanillin, was evaluated. The phenolic compounds present in OLEs were identified by comparing the retention times of the chromatographic peaks with those of the standard commercial compounds.

For the quantitative determination of the phenols present in OLEs, I used the calibration curves obtained by using analyte solutions (OL, luteolin-7-O-glucoside, apigenin-7-O-glucoside, rutin, HT, caffeic acid and *p*-coumaric acid) with *p*-hydroxyphenylacetic acid, used as IS, in different concentrations, as described in section 4.2.11 of the experimental part.

OLEs were dissolved in methanol (MeOH) and then analysed through HPLC (method reported in section 4.2.10.1.1 of the experimental part). The phenols content in each OLE was expressed as mg/g of OLE as reported in Table 15.

Table 15 – Phenolic content (mg/g of OLE) of all the OLEs analysed through HPLC after solubilization in MeOH.

OLEs	Rutin	Luteolin-7-O-glucoside	Apigenin-7-O-glucoside	Oleuropein
October 2018 OLE	2.489 ± 0.163	5.330 ± 0.094	3.347 ± 0.122	17.679 ± 0.747
March 2019 OLE	-	3.764 ± 0.363	-	11.576 ± 1.179
May 2019 OLE	3.758 ± 0.067	5.748 ± 0.080	2.736 ± 0.236	38.782 ± 3.501

- Data are expressed as mean ± SD of two independent experiment each performed in duplicate. -

The most abundant phenolic compound present in all OLEs was OL, followed by luteolin-7-O-glucoside, as confirmed by the literature.[23] Furthermore, OLE contained apigenin-7-O-glucoside and rutin, as for October 2018 and May 2019 OLEs. Other phenolic compounds, such as verbascoside, ferulic acid, caffeic acid, *p*-coumaric acid, T, HT and vanillin were not detectable. The amount of OL in May 2019 OLE was about 4 times higher than that of March 2019 OLE and about 2 times higher than the October 2018 OLE. The luteolin-7-O-glucoside content was comparable in the three OLEs. The amount of rutin and apigenin-7-O-glucoside was comparable in May 2019 and October 2018 OLEs, while they are not present in March 2019 OLE. The HPLC chromatograms of October 2018, March 2019 and May 2019 OLEs are shown in Figure 93, Figure 94 and Figure 95, respectively.

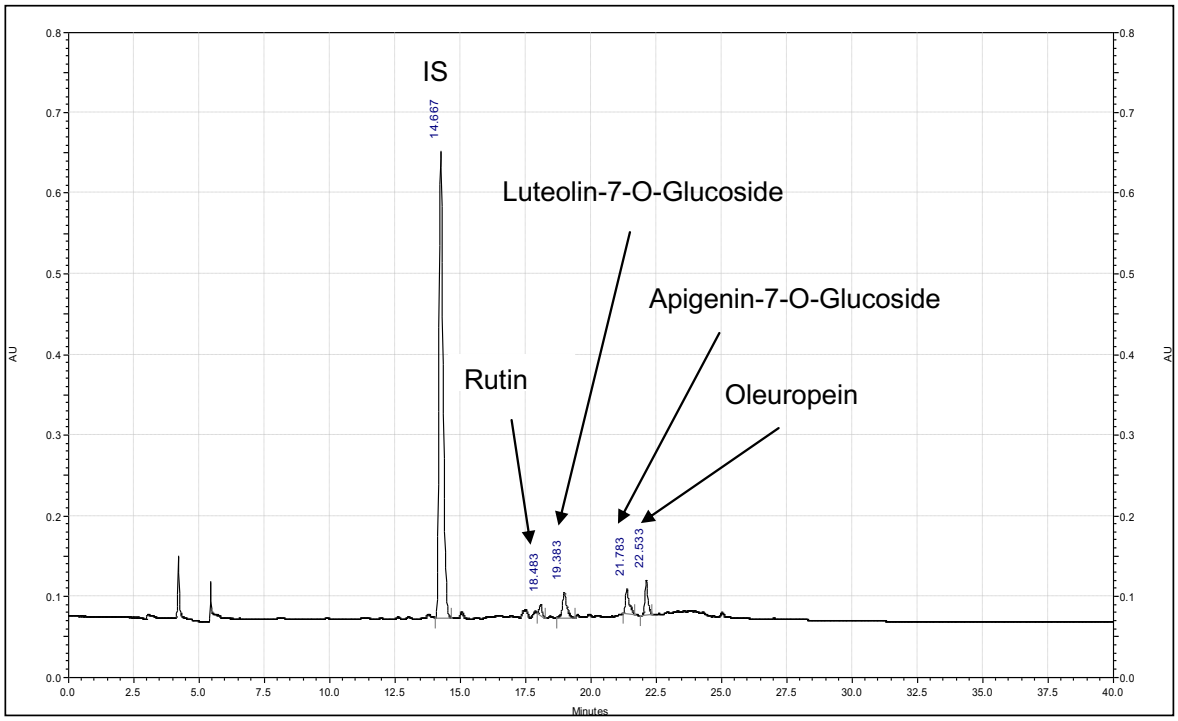

Figure 93 – HPLC chromatogram of October 2018 OLE.

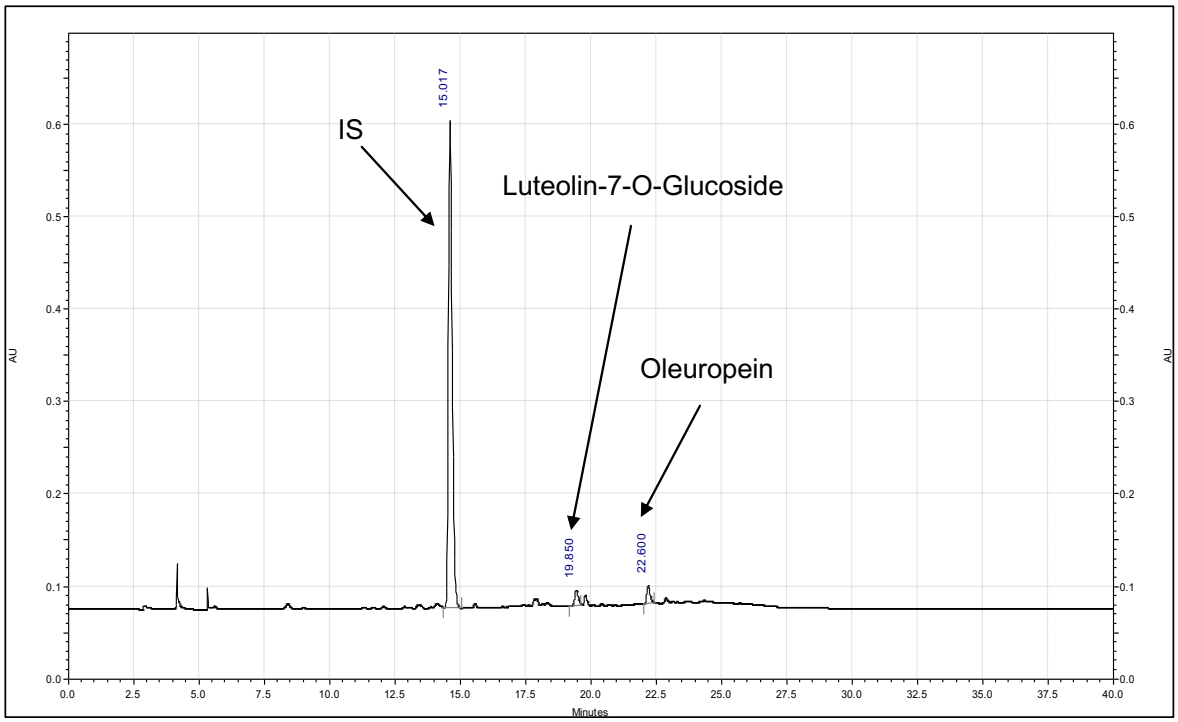

Figure 94 – HPLC chromatogram of March 2019 OLE.

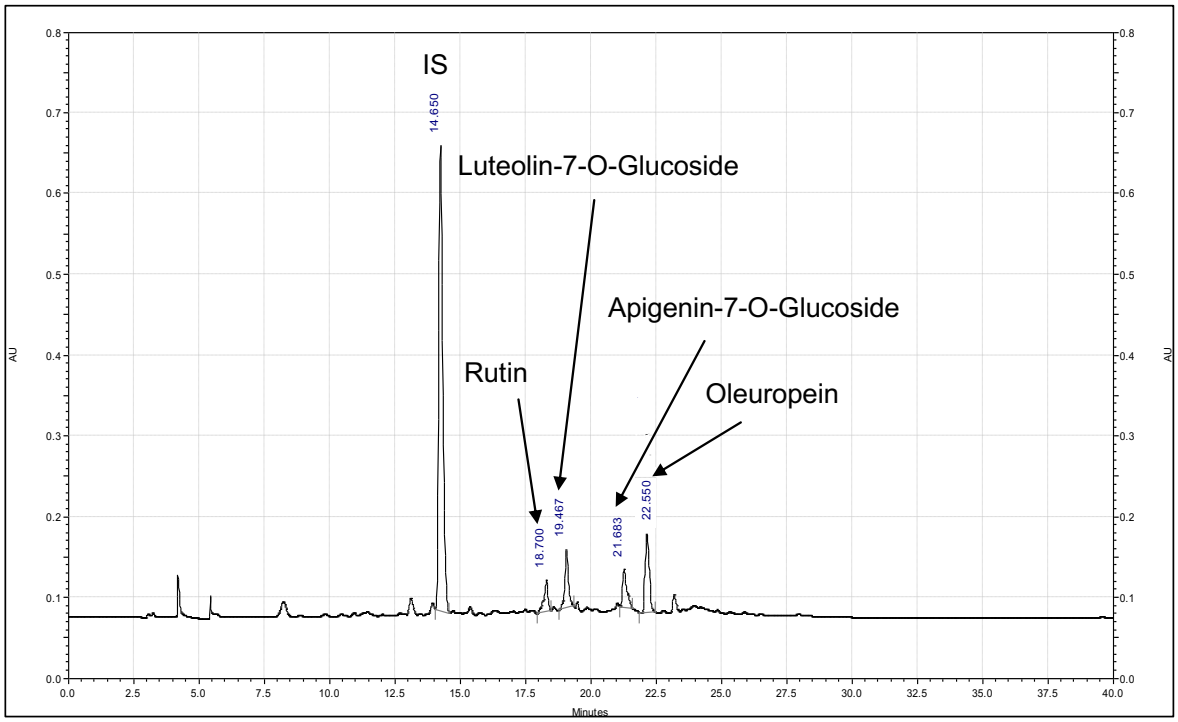

Figure 95 – HPLC chromatogram of May 2019 OLE.

The May 2019 OLE was the best in terms of phenolic and polyphenolic composition and then it was selected for the incorporation into biopolymers.

The May 2019 OLE was also analysed through HPLC after solubilization in phosphate-buffered saline (PBS) which represents the same medium where the release profile was evaluated (as reported in section 4.2.15 of the experimental part). Data are reported in Table 16.

Table 16 – Phenolic content (mg/g of OLE) of May 2019 OLE after solubilization in PBS.

Phenolic Compound	**mg/g**
HT	0.085 ± 0.078
Caffeic Acid	0.180 ± 0.024
p-Coumaric Acid	0.085 ± 0.007
Rutin	3.370 ± 0.328
Luteolin-7-O-Glucoside	6.968 ± 0.236
Apigenin-7-O-Glucoside	1.972 ± 0.167
Oleuropein	32.641 ± 3.065

- Data are expressed as mean ± SD of two independent experiment each performed in triplicate. -

The content of OL, apigenin-7-O-glucoside, luteolin-7-O-glucoside and rutin after the solubilization of May 2019 OLE in PBS was comparable to that derived after solubilization in MeOH, but in this case it was possible to identify and quantify other compounds, such as HT, caffeic acid and *p*-coumaric acid, with a concentration lower than 1 mg/g of OLE. The HPLC chromatogram of May 2019 OLE solubilized in PBS is reported in Figure 96.

I also evaluated the TPC of the selected OLE by using the Folin-Ciocalteu assay, described in section 4.2.12.2 of the experimental part. The TPC in OLE is expressed as µg GAE/mg of OLE and for May 2019 OLE correspond at 58.47 ± 2.00 µg GAE/mg.

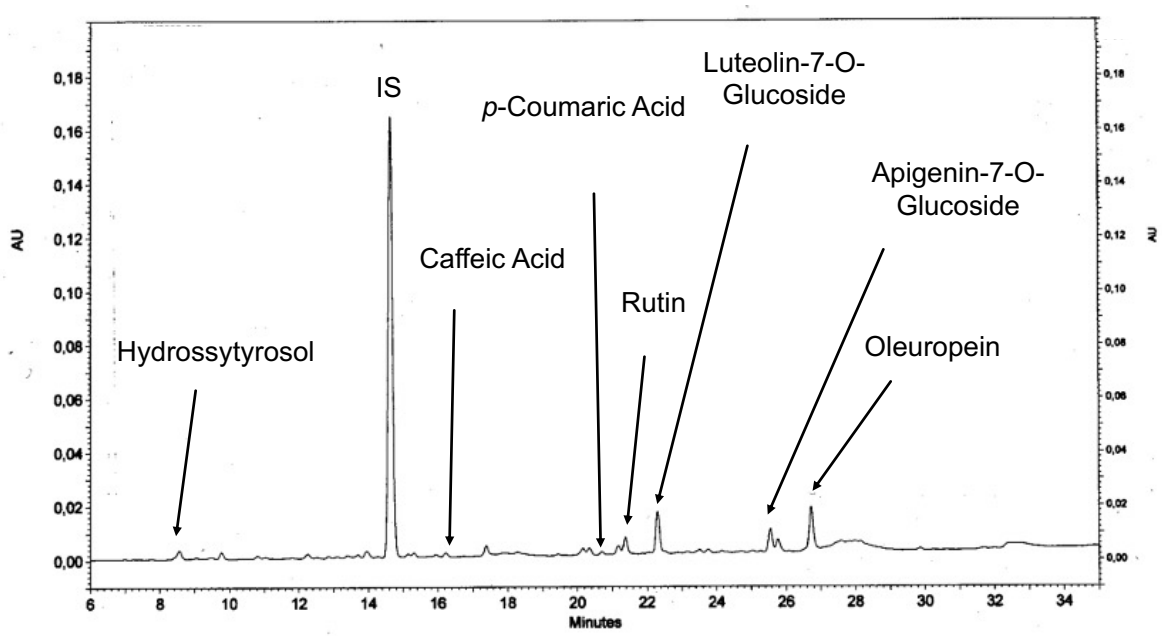

Figure 96 – HPLC chromatogram of May 2019 OLE solubilized in PBS.

3.6.2 Fibers Scaffold Incorporating OLE

The May 2019 OLE selected was incorporated into biocompatible and biodegradable biopolymers in collaboration with the group of bioengineers of University of Pisa (Professor Serena Danti's research group), through electrospinning technique.[128] The biopolymers chosen by bioengineers belong to the class of polyhydroxyalkanoates (PHA) (Figure 97).

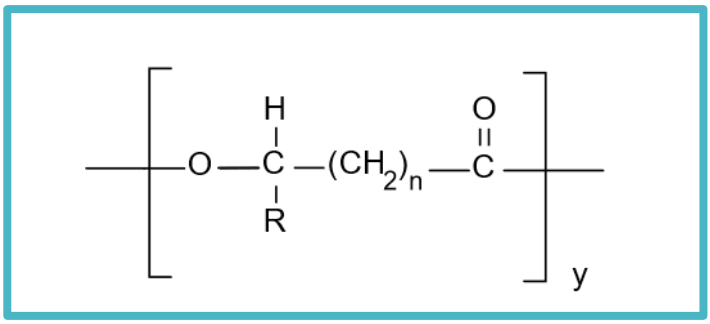

Figure 97 – General structure of PHAs.

In particular bioengineers selected two polymers: the commercial poly(3-hydroxybutyrate-co-3-hydroxyvalerate) (PHBHV) and the polyhydroxybutyrate/poly(hydroxyoctanoate-co-hydroxydecanoate) (PHB/PHOHD) developed in bioengineers' laboratory.[128]

In Figure 98 are reported the images obtained by scanning electron microscopy (SEM) of the fibers before (**A** and **C**) and after incorporating OLE (**B** and **D**). In Figure 98 **B** and **D** it was possible to observe a thickening of the fibers compared with the Figure 98 **A** and **C**, due to the incorporation of the OLE.

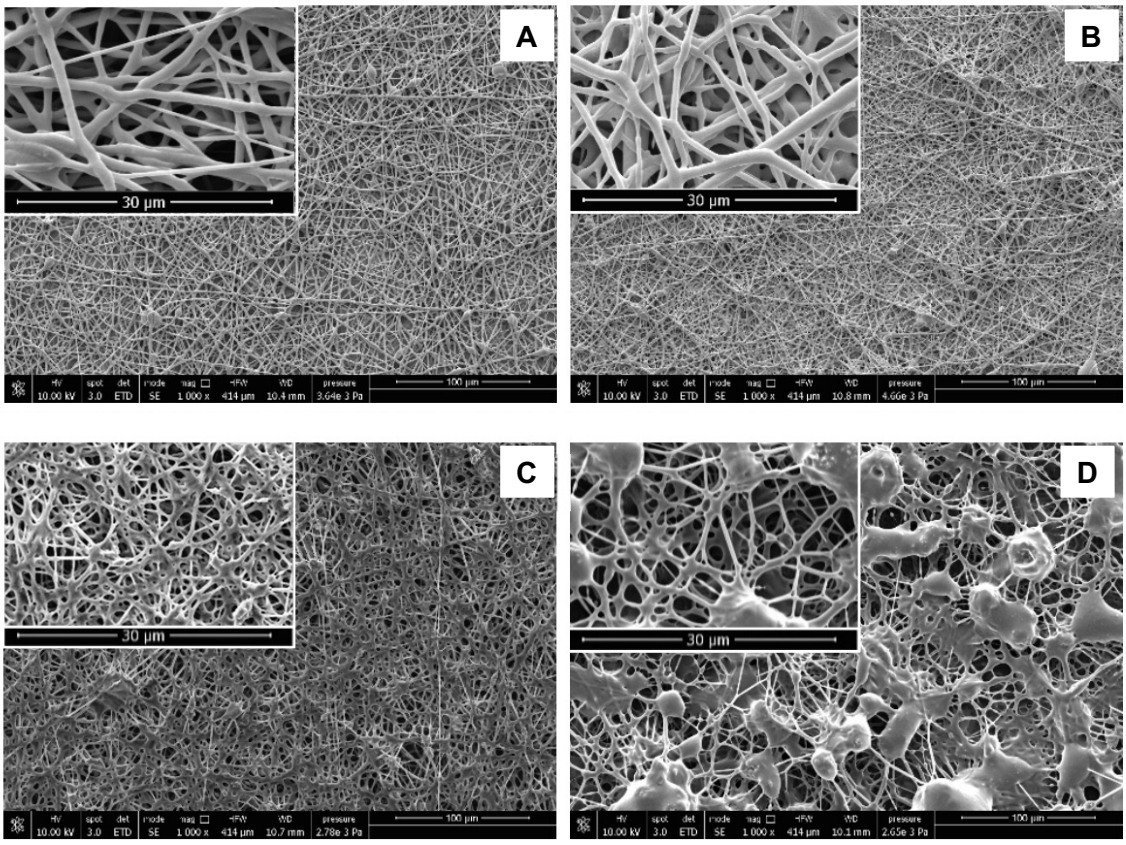

*Figure 98 – SEM images of PHA fibers: PHBHV (**A** and **B**) and PHB/PHOHD (**C** and **D**) before (**A** and **C**) and after (**B** and **D**) the OLE incorporation.*[128]

3.6.3 Release Profile Analysis

Once the OLE was incorporated into the fibers, obtaining PHBHV-OLE and PHB/PHOHD-OLE fibers, it was necessary to verify that the systems were able to release the phenolic compounds contained in the OLE for their use as devices.

Therefore, based on a procedure reported in literature,[131] a method to verify the release of the phenolic compounds from the fibers was developed. For this purpose, the diffusion of the phenolic compounds from the polymers was evaluated in a release medium by exploiting PBS at the controlled temperature of 37°C, to mimic the physiological conditions in which the device would be used. The procedure was extensively described in section 4.2.15 of the experimental part. The qualitative-quantitative evaluation of the phenols released from the fibers (luteolin-7-O-glucoside, apigenin-7-O-glucoside and OL) was performed by HPLC analysis at defined time intervals (0, 0.5, 1, 1.5, 3, 4, 6, 24, 48, 144 h) and the results were expressed as cumulative percentage of the total amount released from the fibers. From the results of the HPLC analysis it was possible to observe that the release of the phenolic compounds from PHBHV-OLE fiber was fast (Figure 99) and about 60% of the total amount of OL was released after 30 minutes. Successively the release of OL became more gradual reaching about 90% after 6 hours. Moreover, after 30 minutes the release of luteolin-7-O-glucoside and apigenin-7-O-glucoside was about 40% and 30% of the total amount in the fiber, respectively and they were both released about 80% after 6 hours (Table 17). These studies confirm that the fibers are able to significantly release the phenolic compounds of the incorporated OLE.

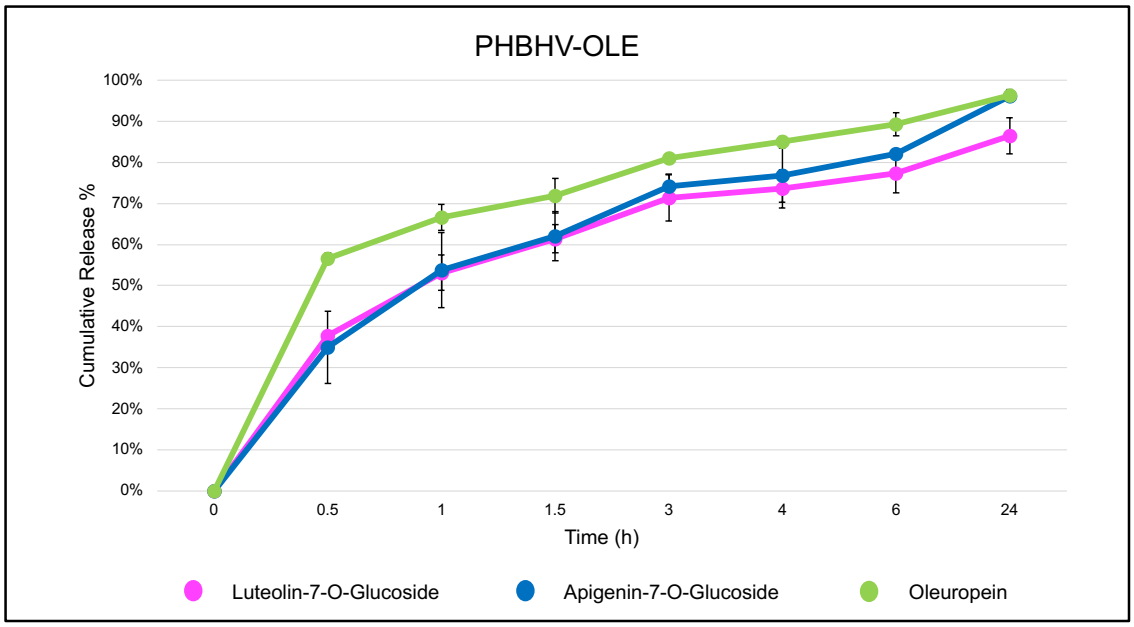

Figure 99 – Cumulative release percentage of luteolin-7-O-glucoside (pink line), apigenin-7-O-glucoside (blue line) and oleuropein (green line) from PHBHV-OLE fiber.

Table 17 - Cumulative release percentage of luteolin-7-O-glucoside, apigenin-7-O-glucoside and oleuropein from PHBHV-OLE fiber.

	CUMULATIVE RELEASE %		
Time (h)	**Luteolin-7-O-glucoside**	**Apigenin-7-O-glucoside**	**Oleuropein**
0.0	0.00 ± 0.00	0.00 ± 0.00	0.00 ± 0.00
0.5	37.68 ± 0.30	34.97 ± 8.80	56.59 ± 1.43
1.0	53.06 ± 4.30	53.79 ± 9.11	66.57 ± 3.21
1.5	61.37 ± 3.42	62.02 ± 6.00	71.87 ± 4.18
3.0	71.41 ± 5.71	74.19 ± 2.84	80.98 ± 0.96
4.0	73.58 ± 4.68	76.87 ± 6.64	85.08 ± 1.28
6.0	77.31 ± 4.65	82.01 ± 0.62	89.27 ± 2.85
24.0	86.48 ± 4.45	96.18 ± 0.25	96.31 ± 1.37

- Data are expressed as mean ± SD of an experiment performed in duplicate. -

As regards the PHB/PHOHD-OLE fiber the release profile of the phenolic compounds analysed was slower and more gradual than that of the PHBHV-OLE fiber (Figure 100). In particular, the release of luteolin-7-O-glucoside, apigenin-7-O-glucoside and OL reaches about 50-60% of the total amount contained in the fiber

after 6 hours, while about 80-90% of the release of all the compounds was reached after 48 hours (Table 18).

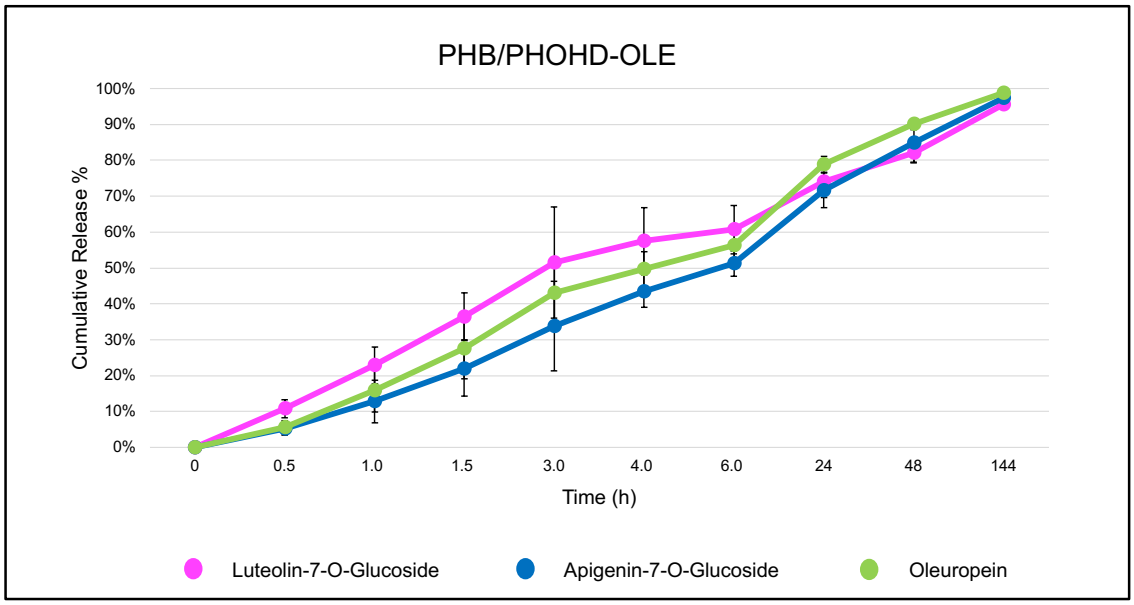

Figure 100 - Cumulative release percentage of luteolin-7-O-glucoside (pink line), apigenin-7-O-glucoside (blue line) and oleuropein (green line) from PHB/PHOHD-OLE fiber.

Table 18 - Cumulative release percentage of luteolin-7-O-glucoside, apigenin-7-O-glucoside and oleuropein from PHB/OHOHD-OLE fiber.

	CUMULATIVE RELEASE %		
Time (h)	**Luteolin-7-O-glucoside**	**Apigenin-7-O-glucoside**	**Oleuropein**
0.0	0.00 ± 0.00	0.00 ± 0.00	0.00 ± 0.00
0.5	10.80 ± 2.60	5.31 ± 1.78	5.69 ± 1.76
1.0	22.87 ± 5.12	12.83 ± 5.92	15.95 ± 6.07
1.5	36.53 ± 6.47	22.05 ± 7.68	27.50 ± 8.37
3.0	51.60 ± 15.47	33.83 ± 12.52	43.02 ± 9.85
4.0	57.52 ± 9.21	43.57 ± 4.56	49.69 ± 4.86
6.0	60.77 ± 6.73	51.30 ± 3.55	56.38 ± 3.70
24.0	73.99 ± 4.37	71.73 ± 4.84	78.90 ± 2.28
48.0	82.21 ± 2.91	85.01 ± 5.50	90.12 ± 1.52
144.0	95.56 ± 0.99	97.48 ± 0.71	98.71 ± 0.44

- Data are expressed as mean ± SD of an experiment performed in duplicate. -

3.6.4 Characterization of PHBHV-OLE Fiber

In collaboration with the research group of Professor Serena Danti, the morphological properties of the PHBHV and PHBHV/OLE fibers were investigated.[129]

In Figure 101 the SEM micrographs of the PHBHV fiber (Figure 101**A**) and PHBHV-OLE fiber (Figure 101**B**) are reported. These fibers had difference in porosity (42.22% and 63.33%, for PHBHV and PHBHV-OLE respectively) and PHBHV-OLE fiber is thicker than PHBHV fiber. Indeed, the fiber diameters were 1.29 ± 0.34 μm and 0.93 ± 0.23 μm for PHBHV-OLE and PHBHV fibers, respectively. These differences confirmed the incorporation of OLE into the fiber.[129]

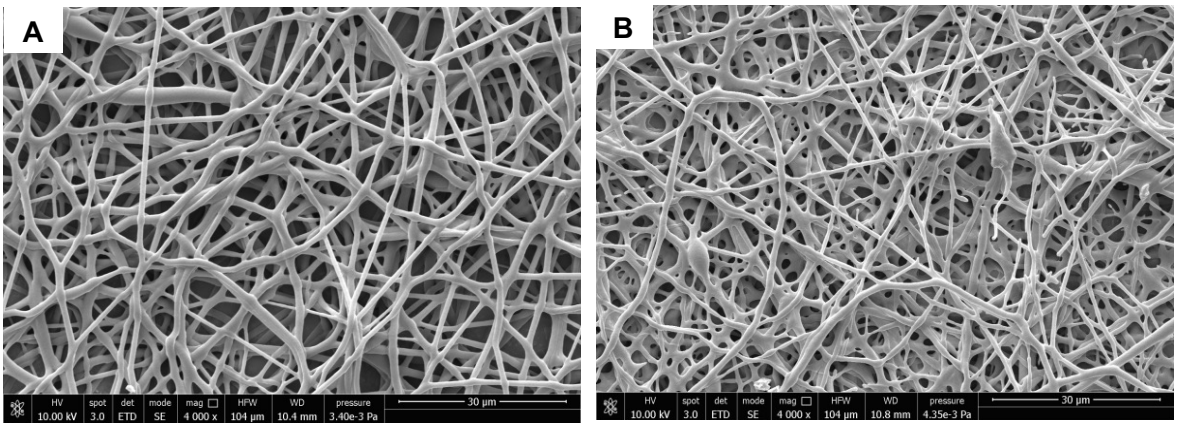

*Figure 101 – SEM micrographs of (**A**) PHBHV and (**B**) PHBHV-OLE electrospun fibers. Scale bar is 20 μm, 4000× magnification, 10 kV voltage.*

The incorporation was also confirmed by Fourier-transform infrared spectroscopy (FT-IR) analysis, as shown in Figure 102. In particular, it was possible to observe that the band at 3300 cm^{-1}, which is indicative of the presence of -OH groups typical of phenolic compounds in OLE, was not present in PHBHV fiber alone (brown line), while is marked in OLE sample (blue line) and in PHBHV-OLE fiber (red line). Moreover, in the spectra, the absorption bands between 1700-1738 cm^{-1}, related to the C=O groups of PHBHV is also shown.

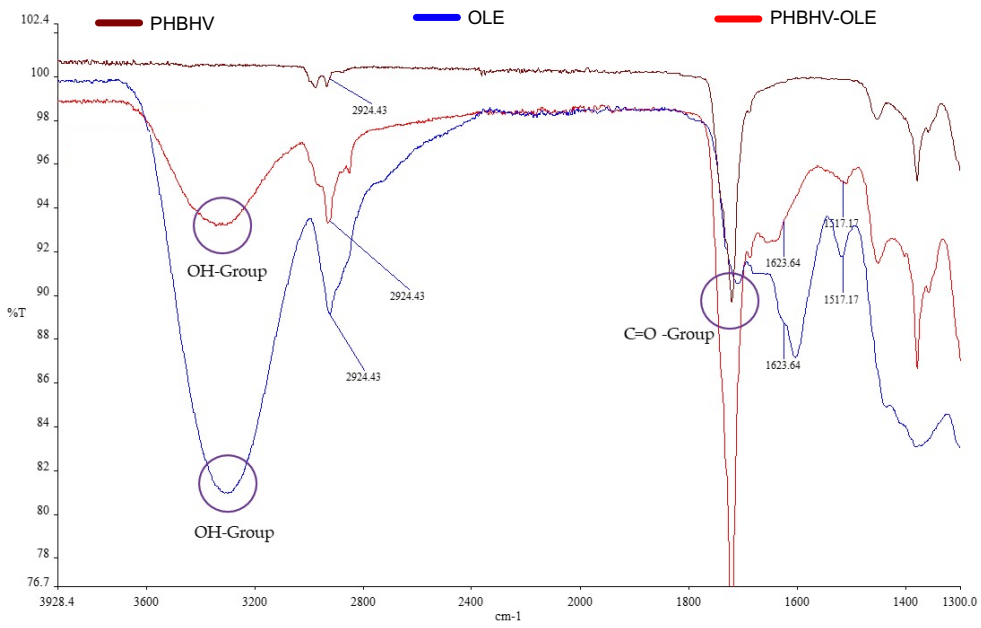

Figure 102 - FT-IR spectra of OLE (blue line), PHBHV fiber (brown line) and PHBHV/OLE fiber (red line) samples showing characteristic bands. T= Transmittance.

An *in vitro* degradation analysis on PHBHV/OLE scaffolds was carried out for a period of two months by immersing the sample in PBS and PBS added with MMP-9, in order to mimic the conditions of a normal tissue remodeling process. In fact, MMP-9 represents a proteolytic enzyme largely expressed during wound healing process, whose proteolytic activity can induce ECM degradation, thus inhibiting the healing process. At different time-points of incubation, the samples were analysed by measuring the weight loss. After 56 days, the percentage of weight loss of PHBHV-OLE fiber, after incubation in PBS and in PBS added with MMP-9 was about 4.2% and 9.6%, respectively. These results showed a very long degradation time in *in vitro* assessment also in presence of MMP-9.[129]

Furthermore, the cytocompatibility of PHBHV and PHBHV-OLE was evaluated *in vitro* by using human Caucasian foreskin fetal fibroblasts (HFFF2) cell line. For this purpose, HFFF2 cells were seeded on PHBHV and PHBHV/OLE fiber meshes and after 72 h the metabolic activity of cell/scaffold constructs was evaluated confirming a good biocompatibility.[129]

All these results suggested that PHBHV-OLE could be particularly suitable for potential use as a device in the treatment of skin wounds.[129]

3.6.5 Biological Evaluation of Fibers Incorporating OLE

3.6.5.1 Antioxidant Effect of OLE in 2D and 3D Culture Models

In collaboration with the research group of Professor Rossella Di Stefano the protective effect of OLE on human umbilical vein endothelial cells (HUVECs) was evaluated by using a conventional culture (2D model) and a novel tissue engineered culture (3D model).[127] To obtain the new 3D model, HUVECs were grown on poly(vinylidenefluoride-co-trifluoroethylene) (P(VDF-TrFE)) fiber mesh, a biocompatible polymer used in biomedical and tissue engineering fields. The scaffold, obtained by electrospinning technique, should be able to mimic the natural ECM, thus improving the native cell morphology and function.

In the 2D model, HUVECs were pre-treated with different concentrations of OLE (0, 5, 10, 50, 100, 250 µg/mL of total polyphenols (TPs)) for 2h (Figure 103**A**) and 24h (Figure 103**B**) followed by treatment with 100 µM H_2O_2 for 1h. The cells viability was thus investigated. The concentrations between 50 µg/mL and 250 µg/mL of TPs prevented the HUVECs viability reduction induced by H_2O_2 treatment confirming that OLE possesses an antioxidant effect, as shown in Figure 103.[127]

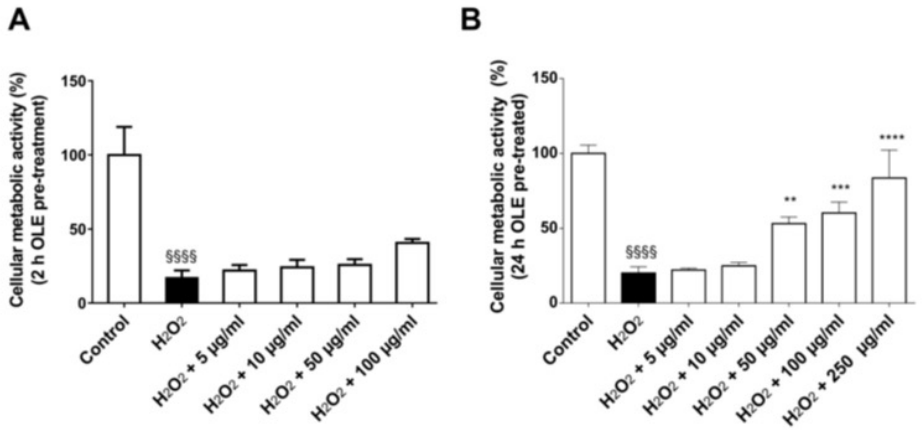

*Figure 103 – Antioxidant effect of OLE. HUVEC viability was evaluated after 2 h (**A**) and 24 h (**B**) of pre-treatment with different concentrations of OLE (i.e., 0, 5, 10, 50, 100, up to 250 µg/mL of TPs) followed by treatment with 100 µM H_2O_2 for 1 h. Data are expressed as metabolic activity percentage compared to control (untreated cells) and are representative of 3 separate experiments run in triplicate. ** $p < 0.005$, *** $p < 0.0005$ and **** $p < 0.00005$ vs. H_2O_2; §§§§ $p < 0.00001$ vs. control.*[127]

Moreover, the effect of OLE on ROS accumulation in HUVECs was investigated after 24 h of pre-treatment with different concentrations of OLE (0, 10, 25, 50, 100 and 250 µg/mL of TPs). As shown in Figure 104 OLE phenols possess a protective effect at a concentration below 250 µg/mL TP.[127]

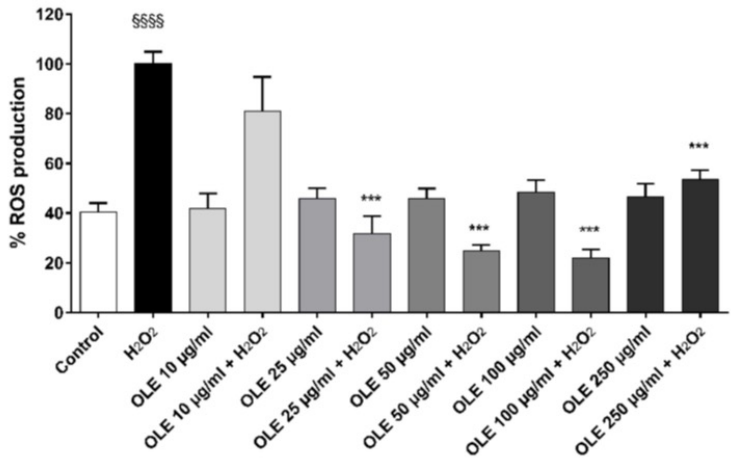

*Figure 104 – ROS production by HUVECs was evaluated after 24 h of incubation with different concentrations of OLE (i.e., 0, 10, 25, 50, 100, up to 250 µg/mL of TPs) and 100 µM H_2O_2 for 1 h. Data are expressed as ROS production% by treated cells and are representative of 3 separate experiments run in triplicate (*** $p < 0.05$ vs. H_2O_2; §§§§ $p < 0.0001$ vs. control).*[127]

These data confirmed a dose-dependent effect of OLE on cell metabolic activity (2D model) and suggested that the concentration of 250 µg/mL of TPs was enough to reduce the effect of H_2O_2-induced oxidative stress and to induce cytoprotective effects in HUVECs.[127]

The protective effect of OLE on HUVECs against the H_2O_2-induced oxidative stress was also evaluated on 3D model. With this aim, the ROS production in cell/scaffold constructs was investigated by pre-treating for 24 h with OLE at 100 µg/mL of TPs, followed by treatment with 100 µM H_2O_2 for 1 h. It was demonstrated that OLE exerts a strong protective effect against ROS accumulation induced by H_2O_2 in the 3D model of H_2O_2-stressed HUVECs.[127]

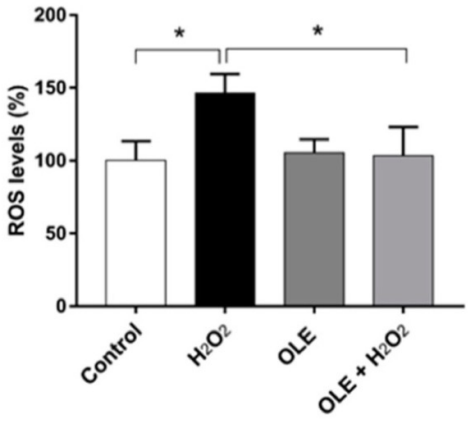

Figure 105 – Results of ROS analysis performed on the 3D model treated with OLE for 24 h followed by H_2O_2 incubation for 1 h. ROS induction percentage as from integrated optical density ($p < 0.05$ vs. control, H_2O_2, and OLE + H_2O_2).*[127]

3D model represents a better predictive model of real tissue response compared with 2D model. Moreover, in the 3D model, a 100 µg/mL OLE concentration was enough to reach a ROS-protective effect, while in 2D model a 250 µg/mL OLE dose was required.[127]

3.6.5.2 Immunomodulatory Activity of PHBHV-OLE and PHB/PHOHD Fibers

The anti-inflammatory and immunomodulatory properties of PHBHV-OLE and PHB/PHOHD-OLE fibers were investigated.[128] For this purpose, the expression of a panel of cytokines associated with the inflammatory process and innate immune response was evaluated on human dermal keratinocytes (HaCaT cells) incubated for 24 h with PHBHV fiber, PHB/PHOHD fiber, OLE, PHBHV-OLE fiber or PHB/PHOHD fiber. In particular, the pro-inflammatory cytokines investigate are the following: IL-1α, IL-1β, IL-6, IL-8, TNF-α and of the antimicrobial peptide human beta defensin (HBD)-2 (an inducible antimicrobial peptide involved in innate immunity).[128]

As shown in Figure 106, IL-1α (Figure 106**A**), IL-1β (Figure 106**B**) IL-6 (Figure 106**C**) and IL-8 (Figure 106**D**) expression levels were significantly reduced by all the fibers in 6 h and OLE modulated the IL-1α, IL-1β and IL-6 expression in 24 h.[128]

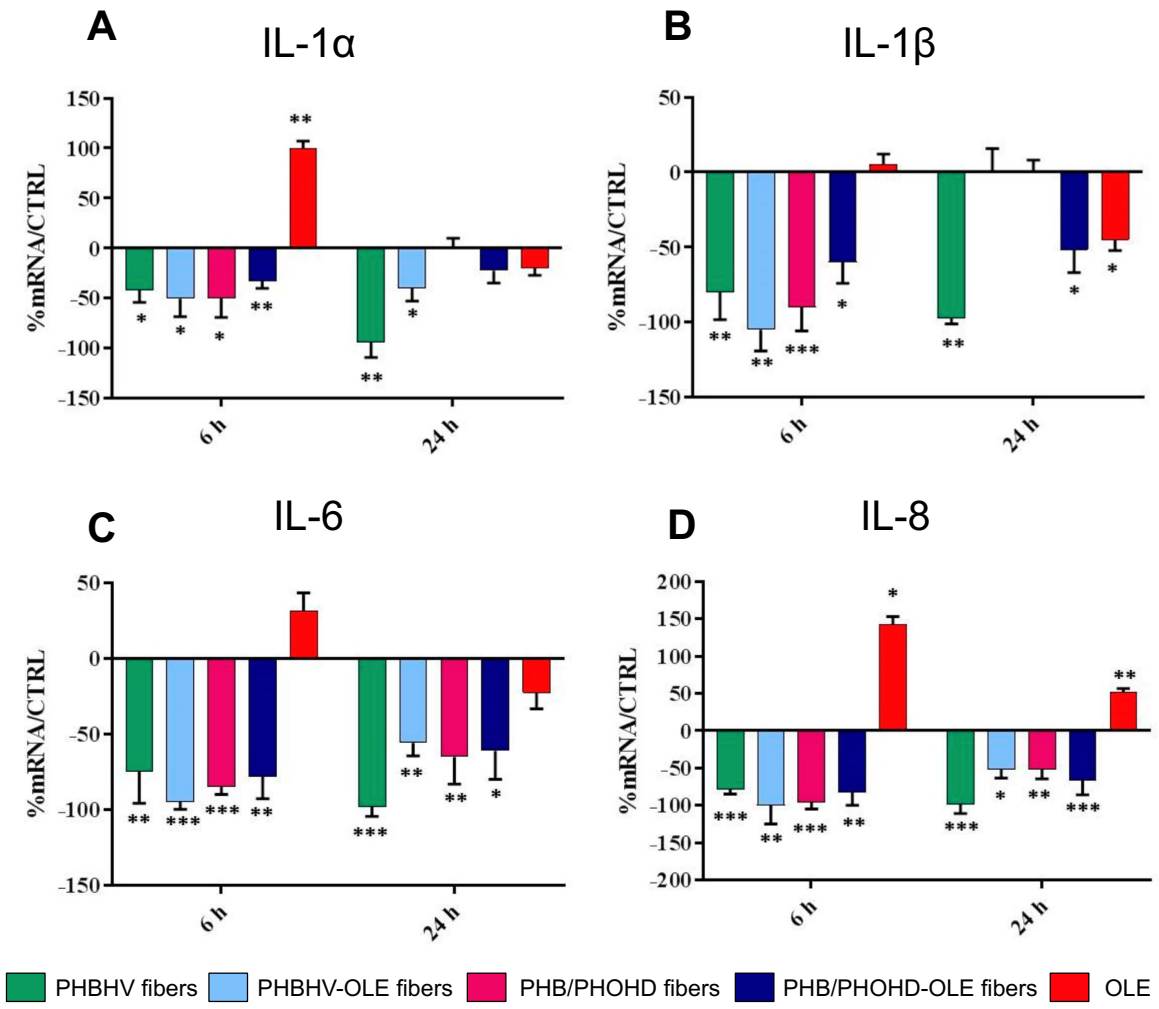

*Figure 106 – Bar graphs showing IL-1α (**A**), IL 1β (**B**), IL-6 (**C**) and IL-8 (**D**) expression by HaCaT cells after 6 h and 24 h. Comparisons between samples were analysed by Student's t-test. Data are mean ± SD and are expressed as percentage of increment relative to untreated cells (used as controls). Significant differences are indicated by * ($p < 0.05$), ** ($p < 0.01$) and *** ($p < 0.001$) for comparison between each sample and its respective control.*[128]

Concerning the TNF-α expression level, all the fibers reduce the expression of TNF-α, as reported in Figure 107.[128]

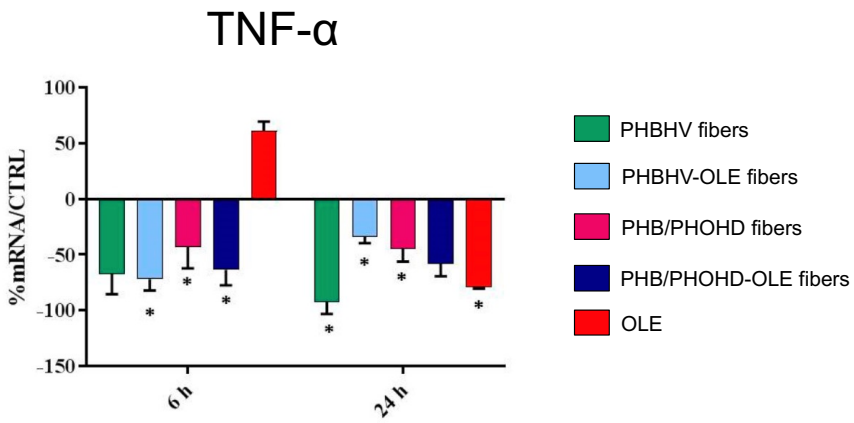

*Figure 107 – Bar graphs showing TNF-α expression by HaCaT cells after 6 h and 24 h. Comparisons between samples were analysed by Student's t-test. Data are mean ± SD and are expressed as percentage of increment relative to untreated cells (used as controls). Significant differences are indicated by * ($p < 0.05$) for comparison between each sample and its respective control.*[128]

Therefore, as regard HBD-2 expression, the formulations contained PHB/PHOHD fiber (PHB/PHOHD fiber and PHB/PHOHD-OLE fiber) and PHBHV-OLE fiber were able to promote the upregulation of HBD-2 after 6 h (Figure 108).[128]

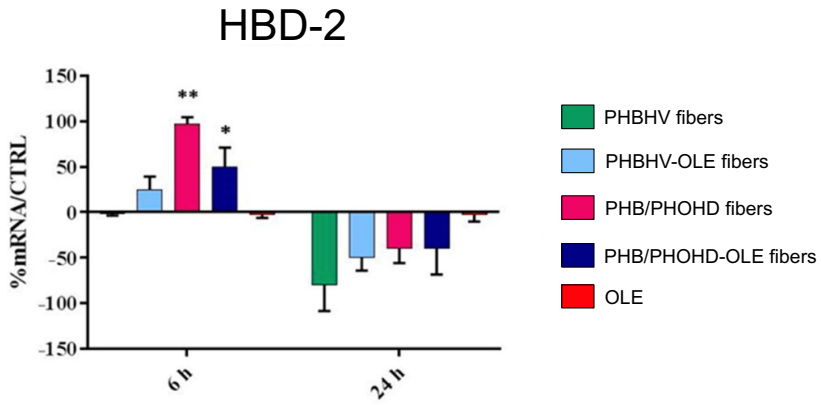

*Figure 108 – Bar graphs showing HBD-2 expression by HaCaT cells after 6 h and 24 h. Comparisons between samples were analysed by Student's t-test. Data are mean ± SD and are expressed as percentage of increment relative to untreated cells (used as controls). Significant differences are indicated by * ($p < 0.05$) and ** ($p < 0.01$) for comparison between each sample and its respective control.*[128]

These results demonstrated that PHBHV-OLE fibers and PHB/PHOHD-OLE fibers possess promising anti-inflammatory and immunomodulatory properties, able to reduce inflammation and stimulate the innate immune response useful for the development of devices for biomedical application.[128]

3.6.6 Conclusion

These results demonstrated that bio-polymers incorporating OLEs, obtained from leaves of autochthonous Tuscan olive trees, might represent a valid strategy in biomedical applications and might be used in different tissue regeneration fields such as wounds and diseases compromised by oxidative stress.

4 EXPERIMENTAL PART

4.1 Materials

4.1.1 Solvents and Analytical Standards

ACN, MeOH, H_2O, *n*-hexane, each one with HPLC grade, acetic acid (AcOH), $CHCl_3$, EtOAc, diethyl ether, absolute ethanol, potassium hydroxide (KOH, 0.1M) and phenolphthalein were purchased from Sigma-Aldrich (Milan, Italy). The standards used are the following: HT and T purchased from TCI (Belgium); *p*-hydroxyphenyl acetic acid, gallic acid, caffeic acid, ferulic acid, *p*-coumaric acid and vanillin purchased from Sigma Aldrich (Milan, Italy); verbascoside, luteolin-7-O-glucoside, apigenin-7-O-glucoside and OL purchased from Extrasynthese (Genay, France); OC, OO and OA isolated and purified, as reported in section 4.2.2 and 4.2.7 of this PhD thesis; FAMEs purchased from Larodan (Soldan, Sweden). Folin-Ciocalteu's phenol reagent (FCR) was purchased from Merck (Darmstadt, Germany). Dulbecco's phosphate buffered saline (PBS) was provided by Sigma-Aldrich (Milan, Italy) and for each analysis was diluted 10 times.

4.1.2 Instruments

Solvent evaporation was carried out under vacuum by using a rotating evaporator (Steroglass, Strike 300). The homogenization was achieved by exploiting a vortex mixer (VELP® scientifica, Zx3, Advanced Vortex Mixer) and a rotary shaker. Centrifugation was performed through a centrifuge set at 4,000 rpm. HPLC analysis was conducted with an HPLC instrument (Thermo Finnigan-Spectra System SCM1000) equipped with a Spectra System P2000 (Pumps), Spectra System UV2000, set to 280 nm, and by using a Phenomenex Gemini reverse-phase C18 column (250×4.6 mm, 5 µm particle size; Phenomenex, Castel Maggiore, Italy). Spectrophotometric analysis for the determination of TPC was performed by using a spectrophotometer (Shimadzu) set on 725 nm. Chromatographic purifications were carried out by advanced automated flash purification system (Isolera™ Prime 3.2.2, Biotage®). LC-MS runs were executed with an AB-Sciex (Concord, Ontario, Canada) API 4000 triple quadrupole mass spectrometer, equipped with Turbo V electrospray ionization source (ESI), and coupled to an Agilent Technologies (Santa Clara, CA, USA) 1290 UHPLC system, consisting of a high-pressure pump, autosampler, and column oven. TLC analysis was made by using aluminium silica gel (60 F_{254}; Sigma Aldrich srl, Milan, Italy) and aluminium silica gel 60 RP-18 F254s

(Merck srl, Darmstadt, Germany) visualized under a UV lamp (λ = 254 nm). For preparative TLC, PLC Silica gel (60 F_{254}, Merck, Darmstadt, Germany) was utilized. Silica gel flash chromatography was performed by using silica gel 60Å (0.040-0.063 mm; Merck srl, Darmstadt, Germany). The ^{1}H-NMR and ^{13}C-NMR spectra were recorded in $CDCl_3$ on a Bruker AVANCE IIITM 400 spectrometer (operating at 400 MHz for ^{1}H and at 100 MHz for ^{13}C) using solvent as IS. Chemical shifts (δ) are reported in parts per million (ppm) related to the residual solvent signal, while coupling constants (*J*) are expressed in Hertz (Hz). GC analyses were carried put through a GC instrument (Thermo Finnigan) equipped with flame ionization detector and using a Quadrex fused silica capillary column (60 m, 0.25 mm I.D., 0.25 μm film thickness; Quadrex Corporation, Woodbridge, USA). The oven (Heraesus) was set at a temperature of 25°C for the determination of the TPC and at a temperature of 37°C for the release profile analyses.

4.1.3 EVOO samples

For the extraction of OC, OO and OA two Tuscan EVOOs, were exploited.

For the evaluation of the changing in the phenolic composition during storage, three EVOOs were selected and monitored for fifteen months (from December 2019 to March 2021): two Tuscan EVOOs of the 2019/2020 crop seasons (**A** and **B**) and an Italian EVOO of the 2018/2019 crop season (**C**). These EVOOs were stored under different conditions: an aliquot was kept at room temperature (25°C) and exposed to daylight; another aliquot was kept at the temperature of 4°C (into the fridge), in dark condition. At the beginning of the analysis (December 2019), EVOOs **A** and **B** were fresh, while the EVOO **C** had already been stored for one year at room temperature in dark condition.

The forty EVOOs coming from Siena (Valdichiana Senese) analysed in terms of free acidity, TPC, as well as for the qualitative-quantitative determination of the single phenolic compounds, and qualitative-quantitative determination of the main FAs, are reported in Table 19.

Table 19 – Crop season of the analysed EVOOs. ***1-21*** *= EVOOs produced in 2020/2021 crop season;* ***22-37*** *= EVOOs produced in 2019/2020 crop season;* ***38-40*** *= EVOOs produced in 2018/2019 crop season.*

Nr	CROP SEASON	Nr	CROP SEASON
1	2020/21	**21**	2020/21
2	2020/21	**22**	2019/20
3	2020/21	**23**	2019/20
4	2020/21	**24**	2019/20
5	2020/21	**25**	2019/20
6	2020/21	**26**	2019/20
7	2020/21	**27**	2019/20
8	2020/21	**28**	2019/20
9	2020/21	**29**	2019/20
10	2020/21	**30**	2019/20
11	2020/21	**31**	2019/20
12	2020/21	**32**	2019/20
13	2020/21	**33**	2019/20
14	2020/21	**34**	2019/20
15	2020/21	**35**	2019/20
16	2020/21	**36**	2019/20
17	2020/21	**37**	2019/20
18	2020/21	**38**	2018/19
19	2020/21	**39**	2018/19
20	2020/21	**40**	2018/19

4.1.4 OLE samples

Olive leaves were obtained from autochthonous Tuscan olive trees (*Cultivar Olivastra seggianese*). The leaves collection was performed at CNR-IVALSA, Follonica (GR), Italy and it was carried out manually at different months:

- October 2018;
- March 2019;
- May 2019.

Leaves were placed in liquid nitrogen and crushed manually. To the leaves powder was added water and then the mixture was homogenized by using a

sonicator and a vortex mixer. After centrifugation at 4,000 rpm for 5 min, at 25°C, the water phase was collected and freeze-dried, obtaining OLEs.

4.2 Methods

4.2.1 Extraction of Oleacein and Oleocanthal from EVOO.

The extraction of OC and OO was executed by following the procedure reported in the literature.[47] About 100 g of fresh EVOO was mixed with *n*-hexane (400 ml) and ACN (500 ml). The mixture was homogenized by using a vortex mixer (30 sec) and a rotary shaker (30 min) and after that was centrifuged at 4,000 rpm for 5 min, at 25°C. The ACN phase was collected and then it was evaporated under reduced pressure to afford the crude residue which was purified to obtain the desired compounds.

4.2.2 Purification of Oleacein and Oleocanthal

The procedure for the purification of OC and OO was improved starting from a method previously developed in my PhD thesis laboratory and it consists of a double step of purification.[47]

4.2.2.1 First Step of Purification

The crude residue obtained from the extraction of fresh EVOO was subjected to the first step of purification by exploiting the advanced automated flash purification system (Isolera™ Prime 3.2.2, Biotage®). A Biotage® SNAP Ultra cartridge (HP-Sphere™ 25μm) was used as stationary phase, while the mobile phase consisted of a mixture of $CHCl_3$ (A) and EtOAc (B), with the gradient shown in

Table 20. The flow rate was 25 mL/min and for each tube 15 mL were collected. Fractions 40-60 (about 60 mg) containing OO or fractions 60-120 (about 60 mg) containing OC were subjected to a further step of purification.

Table 20 – Mobile phase gradient used for the first step of purification of OO and OC.

Mobile Phase (B%)	Fractions	Volume (mL)
0%	1-36	540
From 0% to 45%	37-180	2160
45%	181-186	90
From 45% to 100%	187-192	90
100%	193-198	90

4.2.2.2 Second Step of Purification

4.2.2.2.1 Method I

OC and OO obtained after the first step of purification (4.2.2.1) were further purified by exploiting a preparative TLC. The mobile phase was a mixture of EtOAc:*n*-hexane 4:6 (v/v) for OO and EtOAc:*n*-hexane 5:5 (v/v) for OC. The corresponding zones were extracted from the stationary phase by using EtOAc under sonication for 15 min. This procedure was performed twice until maximum purity was achieved, obtaining 8 mg of OO and 5 mg of OC.

4.2.2.2.2 Method II

OC and OO obtained after the first step of purification (4.2.2.1) were further purified by flash column chromatography on silica gel. The mobile phase was mixture of EtOAc:*n*-exane 4:6 (v/v) for OO and EtOAc:*n*-exane 5:5 (v/v) for OC. The amount of OC and OO purified was 10 mg for both the compounds, but the purity was low.

4.2.2.2.3 Method III

The second step of purification was performed by using the advanced automated flash purification system (Isolera™ Prime 3.2.2, Biotage®). A Biotage® SNAP Ultra C18 12g cartridge was used as stationary phase, while the mobile phase consisted of a mixture of H_2O (A) and ACN (B) with the gradient shown in Table 21. The flowrate was 10 mL/min and for each tube 5 mL were collected. Fractions 20-30 (about 10 mg) and fractions 30-40 (about 15 mg) contained pure OC and OO, respectively.

Table 21 - Mobile phase gradient used for the second step of purification of OO and OC (Method III).

Mobile Phase (B%)	Fractions	Volume (mL)
From 5% to 10%	1-10	51
From 10% to 100%	11-61	255
100%	62-75	68

4.2.3 Characterization of Oleacein

The characterization and the purity of OC were established on ^{1}H-NMR, ^{13}C-NMR, LC-MS and HPLC analyses.

^{1}H-NMR ($CDCl_3$-400 MHz) δ: 2.06 (d, 3H, *J* = 7.2 Hz, CH_3); 2.58-2.97 (m, 6H, CH_2); 3.60-3.68 (m, 1H, CH); 4.12-4.26 (m, 2H, CH_2); 6.60-6.80 (m, 4H, Ar, =CH); 9.21 (d, 1H, *J* = 2.0 Hz, CHO); 9.66 (d, 1H, CHO) ppm.

^{13}C-NMR ($CDCl_3$-100 MHz) δ: 15.47; 29.85; 34.34; 37.09; 46.46; 65.31; 115.36; 116.51; 121.52; 130.81; 142.87; 143.38; 155.43; 171.92; 195.63; 201.98 ppm.

The HPLC and the LC-MS analyses revealed that OC purity was > 95 %.

4.2.4 Characterization of Oleocanthal

The characterization and the purity of OO were established on ^{1}H-NMR, ^{13}C-NMR, LC-MS and HPLC analyses.

^{1}H-NMR ($CDCl_3$-400 MHz) δ: 2.07 (d, 3H, J = 7.2 Hz, CH_3); 3.00-2.58 (m, 6H, CH_2); 3.57-3.65 (m, 1H, CH); 4.17-4.24 (m, 2H, CH_2); 6.63 (q, 1H, *J* = 7.2 Hz, =CH); 6.76 (d, 2H, *J* = 8.4 Hz, Ar); 7.04 (d, 2H, *J* = 8.4 Hz, Ar); 9.23 (d, 1H, *J* = 2.0 Hz, CHO); 9.63 (s, 1H, CHO) ppm.

^{13}C-NMR ($CDCl_3$-100 MHz) δ: 15.42; 27.34; 34.29; 36.97; 46.29; 65.30; 115.48; 115.55; 129.91; 130.18; 143.38; 154.58; 154.44; 154.61; 172.11; 195.28; 200.44 ppm

The HPLC and the LC-MS analyses revealed that OO purity was > 95 %.

4.2.5 Method to Accelerate the Oxidative Process of Oleocanthal to Oleocanthalic Acid in EVOO

4.2.5.1 Method I

An EVOO (200 mL) rich in OO (383 ppm) was heated at 60°C for 80 days in an open pyrex® glass beaker (500mL) and in dark conditions, on the basis of a procedure reported in literature.[112] This EVOO was periodically extracted and analysed in terms of phenolic composition through HPLC. In particular, samples of 3 g were taken from EVOO heated at 60°C after 4, 7, 9, 12, 14, 21, 32, 44, 80 days. Each aliquot was cooled and extracted as reported in section 4.2.9.1. The data were compared with those derived from an aliquot of the same EVOO kept at 4°C, used as control.

4.2.5.2 Method II

An EVOO (100 mL) rich in OO (383 ppm) was heated at 80°C for 14 days in an open pyrex® glass round-bottom boiling flask (500 mL), under stirring (300 rpm) and exposed to daylight. This EVOO was periodically extracted and analysed in terms of phenolic composition through HPLC. In particular, samples of 3 g were taken from EVOO heated at 80°C after 4, 7, 9, 12, 14 days. Each aliquot was cooled and extracted as reported in section 4.2.9.1. The data were compared with those derived from an aliquot of the same EVOO kept at 4°C, used as control. In these conditions an EVOO rich in OA to be extracted, was obtained.

4.2.6 Extraction of Oleocanthalic Acid from EVOO.

The extraction of OA was performed by following the procedure reported for the extraction of OO and OC (section 4.2.1). About 100 g of EVOO subjected to heating at 80°C for 14 days (as reported in section 4.2.5.2) were mixed with *n*-hexane (400 mL) and ACN (500 mL). The mixture was homogenized by using a vortex mixer (30 sec) and a rotary shaker (30 min) and after that was centrifuged at 4,000 rpm for 5 min, at 25°C. The ACN phase was collected and then it was evaporated under reduced pressure to afford the crude residue which was purified in order to obtain the desired compound.

4.2.7 Purification of Oleocanthalic Acid

4.2.7.1 First step of purification

Based on a procedure reported in the literature slightly modified,[112] the first step of purification was performed by using the advanced automated flash purification system (Isolera™ Prime 3.2.2, Biotage®) and by exploiting a Biotage® SNAP Ultra cartriage (HP-Sphere™ 25μm) as stationary phase.

4.2.7.1.1 Method I

The mobile phase consisted of a mixture of EtOAc and *n*-hexane, with the gradient shown in Table 22. The flow rate was 25 mL/min and for each tube 15 mL were collected. Based on TLC (rf 0.15 in *n*-hexane:AcOEt 4:6) the fractions 100-130 were selected, resulting in a residue containing OA (about 40 mg). This residue was subjected to further purification.

Table 22 – Mobile phase gradient used for the first step of purification of OA (Method I).

Mobile Phase	Fractions	Volume (mL)
5:95% EtOAc:*n*-Hexane	1-21	315
10:90% EtOAc:*n*-Hexane	22-42	315
20:80% EtOAc:*n*-Hexane	43-63	315
30:70% EtOAc:*n*-Hexane	64-84	315
40:60% EtOAc:*n*-Hexane	85-105	315
50:50% EtOAc:*n*-Hexane	106-126	315
100% EtOAc	127-147	810

4.2.7.1.2 Method II

The mobile phase consisted of a mixture of $CHCl_3$, EtOAc and *n*-hexane with the gradient shown in Table 23. The flow rate was 25 mL/min and for each tube 15 mL were collected. Based on TLC (rf 0.15 in *n*-hexane:AcOEt 4:6) the fractions 160–210 were selected, resulting in a residue containing OA (90 mg). This residue was subjected to further purification.

Table 23 - Mobile phase gradient used for the first step of purification of OA (Method II).

Mobile Phase	Fractions	Volume (mL)
100% $CHCl_3$	1-30	450
5:95% EtOAc:*n*-Hexane	31-51	315
10:90% EtOAc:*n*-Hexane	52-72	315
20:80% EtOAc:*n*-Hexane	73-93	315
30:70% EtOAc:*n*-Hexane	94-114	315
40:60% EtOAc:*n*-Hexane	115-135	315
50:50% EtOAc:*n*-Hexane	136-156	315
100% EtOAc	157-222	990

4.2.7.2 Second step of purification

4.2.7.2.1 Method I

OA derived from the first step of purification (Method I, section 4.2.7.1.1) was further purified through a preparative TLC, by using *n*-hexane:EtOAc 3:7 (v/v) as mobile phase. The corresponding zones were extracted from the stationary phase by using EtOAc under sonication for 15 min. This procedure was performed twice until maximum purity was achieved, obtaining 5.0 mg of OA.

4.2.7.2.2 Method II

OA obtained after the first step of purification (Method I, reported in section 4.2.7.1.1) was further purified by using a flash column chromatography. The mobile phase consisted of a mixture of *n*-hexane and EtOAc, with a gradient shown in Table 24. Fractions 93–113 containing OA (about 2 mg), were selected.

Table 24 - Mobile phase gradient used for the second step of purification of OA, method II.

Mobile Phase (%)	Fractions	Volume (mL)
30:70% EtOAc:*n*-Hexane	1-10	200
50:50% EtOAc:*n*-Hexane	11-59	100
70:30% EtOAc:*n*-Hexane	60-167	300
100% EtOAc	168-180	200

4.2.7.2.3 Method III

OA derived from the first step of purification (Method II, reported in section 4.2.7.1.2) was further purified by exploiting the advanced automated flash purification system (Isolera™ Prime 3.2.2, Biotage®). A Biotage® SNAP Ultra C18 12g cartridge was used as stationary phase, while the mobile phase consisted of a mixture of H2O (A) and ACN (B) with a gradient shown in Table 25. The flowrate was 10 mL/min and for each tube 5 mL were collected. The fractions 25-32 were collected, affording pure OA (25 mg). The trend of purification and the presence of OA was monitored through TLC (mobile phase H_2O:ACN 6:4; rf of OA = 0.32).

Table 25 - Mobile phase gradient used for the second step of purification of OA, method III.

Mobile Phase (B%)	Fractions	Volume (mL)
From 5% to 10%	1-10	51
From 10% to 100%	11-61	255
100%	62-71	51

4.2.8 Characterization of Oleocanthalic Acid

The characterization and the purity of OA were established on ^{1}H-NMR, ^{13}C-NMR, LC-MS and HPLC analyses

^{1}H-NMR ($CDCl_3$-400 MHz) δ: 2.02 (d, 3H, *J* = 7.2 Hz, CH_3); 2.61-2.84 (m, 6H, CH_2); 3.47-3.55 (m, 1H, CH); 4.18-4.24 (m, 2H, CH_2); 6.63 (q, 1H, *J* = 7.2 Hz, =CH); 6.76 (d, 2H, *J* = 8.4 Hz, Ar); 7.04 (d, 2H, *J* = 8.4 Hz, Ar); 9.24 (d, 1H, *J* = 2.0 Hz, CHO) ppm.

^{13}C-NMR ($CDCl_3$-100 MHz) δ: 15.32; 29.85; 34.30; 36.45; 36.98; 65.32; 115.54; 129.86; 130.17; 143.27; 154.58; 154.68; 172.21; 195.31 ppm.

The HPLC analysis revealed that OA purity was > 95 %.

LC-MS, carried out with a Turbo V electrospray source, in negative ion mode and flow injection, provided a full scan spectrum containing a $[M-H]^-$ ion at m/z 319.1.

4.2.9 HPLC analysis of EVOO

4.2.9.1 EVOOs Extraction

The extraction of EVOO was performed by using a method reported in literature.[47] About 3 g of EVOO was mixed with *n*-hexane (12 mL) and ACN (15 mL). The mixture was homogenized by using a vortex mixer (30 sec) and a rotary shaker (30 min) and after that was centrifuged at 4,000 rpm for 5 min, at 25°C. The ACN phase was collected and 1 mL of a solution of *p*-hydroxyphenylacetic acid (IS 0.20 mg/mL in ACN) was added. Then it was evaporated under reduced pressure to afford the crude residue which was injected in HPLC instrument as a mixture of MeOH:H_2O (1:1 v/v).

The stock solution of IS 0.20 mg/mL in ACN was prepared by dissolving 20 mg of commercial *p*-hydroxyphenylacetic acid in 100 mL of ACN.

4.2.9.2 HPLC Method

4.2.9.2.1 Method I

EVOO extracts were analysed through HPLC by using the method previously developed to quantify the OO, in my PhD thesis laboratory.[18] The mobile phase consisted of a mixture of H_2O/AcOH (97.5: 2.5 v/v) (A) and MeOH/ACN (1:1 v/v) (B)

with a gradient reported in Table 26. The flow rate was 1 mL/min and the injected volume was 50.0 µL.

Table 26 – HPLC method previously developed for the quantification of oleocanthal in EVOO (Method I).

Total Time (min)	A %	B %
0.0	95	5
25.0	70	30
50.0	65	35
65.0	30	70
70.0	-	100
85.0	95	5
80.0	95	5

4.2.9.2.2 Method II

The mobile phase consisted of a mixture of H_2O/AcOH (97.5: 2.5 v/v) (A) and MeOH/ACN (1: 1 v/v) (B) with a gradient shown in Table 27. The flow rate was 1 mL/min and the injected volume was 50.0 µL.

Table 27 – HPLC method II.

Total Time (min)	A %	B %
0.0	95	5
45.0	70	30
65.0	30	70
70.0	20	80
85.0	20	80
90.0	-	100
95.0	95	5
105.0	95	5

The retention time and the UV absorbance spectrum of the phenolic compounds present in the samples were compared with those of the pure standards and quantified at the wavelength of 280 nm by using *p*-hydroxyphenylacetic acid as IS. The EVOO samples were injected as a mixture of MeOH:H_2O (1:1 v/v).

4.2.10 HPLC analysis of OLEs

4.2.10.1 Preparation of OLE samples for HPLC analysis

4.2.10.1.1 Method I

To a mixture of 10 mg of OLE in MeOH (3 mL), 2 mL of a solution of *p*-hydroxyphenylacetic acid, as IS (1 mg/mL in MeOH), were added. The mixture was homogenized by using a vortex mixer (30 sec) and a rotary shaker (30 minutes) and then it was centrifugated for 5 minutes at 4,000 rpm and at 25°C. The liquid phase was collected and was injected to HPLC as a mixture of MeOH/H_2O (1:1 v/v) and the injected volume was 50 µL. For each OLE analysed the solution was prepared in duplicate and for each duplicate the HPLC analysis was performed three times.

The stock solution of IS 1 mg/mL in MeOH was prepared by dissolving 100 mg of commercial *p*-hydroxyphenylacetic acid in 100 mL of MeOH.

4.2.10.1.2 Method II

10 mg of OLE were solubilized in 5 mL of PBS. The solution was homogenized by using a vortex mixer (30 seconds) and a rotary shaker (30 minutes) in order to obtain a stock solution. Subsequently, 50 µL of a solution of *p*-hydroxyphenyl acetic acid (IS 1 mg/mL in MeOH) and 50 µL of MeOH were added to 100 µL of the stock solution, which was then injected in HPLC (50 µL) as a mixture of MeOH/PBS (1:1 v/v). The stock solution was prepared in duplicate, and for each duplicate the HPLC analysis was performed three times.

The stock solution of IS (1 mg/mL in MeOH) was prepared by dissolving 100 mg of commercial *p*-hydroxyphenylacetic acid in 100 mL of MeOH.

4.2.10.2 HPLC Method

4.2.10.2.1 Method I

The mobile phase consisted of a mixture of H_2O/AcOH (97.5: 2.5 v/v) (A) and MeOH/ACN (1:1 v/v) (B) with the gradient reported in Table 28. The flow rate was 1 mL/min and the volume injected was 50 µL.

Table 28 – Mobile phase gradient of the HPLC method I.

Total Time (min)	A%	B%
0.0	95	5
45.0	70	30
50.0	70	30
55.0	95	5
60.0	95	5

4.2.10.2.2 Method II

The mobile phase consisted of a mixture of H_2O/AcOH (97.5: 2.5 v/v) (A) and ACN (B) with the gradient showed in Table 29, according to the procedure reported in the literature.[130] The flow rate was 1 mL/min and the volume injected was 50 µL.

Table 29 – Mobile phase gradient of the HPLC method II.

Total Time (min)	A%	B%
0.0	95	5
20.0	75	25
40.0	50	50
50.0	20	80
60.0	95	5
65.0	95	5

The retention time and the UV absorbance spectrum of the phenolic compounds present in the samples were compared with those of the pure standards and quantified at the wavelength of 280 nm using *p*-hydroxyphenylacetic acid as IS. The OLE samples were injected as a mixture of MeOH:H_2O (1:1 v/v) or MeOH:PBS (1:1 v/v).

4.2.11 Calibration Curves, LOD and LOQ

For each compound which was quantified, the calibration curve was built by using mixture of IS and the proper analyte at different concentrations and the correlation coefficients (r^2) were > 0.9979. The calibration curve of HT, T, OC, OO were previously reported,[18] while the calibration curves of the other compounds are reported in Table 30.

Table 30 – Calibration curves and r^2 of the phenolic compound quantify in EVOOs and OLEs.

Compound	Calibration Curve	r^2
Oleocanthalic Acid (OA)	y = 0.2237x	0.9995
Caffeic Acid	y = 5.5090x	0.9985
p-Coumaric Acid	y = 8.8685x	0.9996
Rutin	y = 1.5201x	0.9995
Luteolin-7-O-Glucoside	y = 1.7242x	0.9979
Apigenin-7-O-Glucoside	y = 3.4282x	0.9998
Oleuropein (OL)	y = 0.4990x	0.9988

Moreover, for OA the HPLC Method II (sections 4.2.9.2.2) was validated through the determination of the LOD and the LOQ. The data are reported in Table 31. LOD and LOQ were set based on signal-to-noise ratio (S/Ns); 3:1 and 10:1 for LOD and LOQ, respectively.

Table 31 – LOD and LOQ of oleocanthalic acid.

Compound	LOD (µg/mL)	LOQ (µg/mL)
Oleocanthalic Acid (OA)	1.95	4.55

4.2.12 Folin-Ciocalteu Assays

Folin-Ciocalteu assay was performed by following a procedure reported in the literature, opportunely modified.[132]

4.2.12.1 TPC in EVOOs

2.5 g of EVOO was mixed with 5 mL of *n*-hexane and extracted with 5 mL MeOH (80% v/v). The mixture was homogenized by using a vortex mixer for 2 minutes, a rotary shaker for 15 minutes and centrifugated for 5 minutes at 4,000 rpm and at 25°C, then methanolic phase was collected. This procedure was repeated twice (the final methanolic solution collected was 10 mL). Successively, 0.25 mL of FCR and 1.5 mL of a Na_2CO_3 solution (20% w/v) were added to the methanolic solution (1 mL) in a volumetric flask and then distilled water was added to reach the final volume of 10 mL. The blank solution was prepared by replacing the methanolic solution (1 mL), with distilled water (1 mL). Each sample was stored at the controlled temperature of 25°C and in the dark for 45 minutes. After this period, the samples were analysed by using a spectrophotometer set on λ = 725 nm. Each analysis was performed in triplicate and the TPC of each EVOO was expressed as μg of GAE/g of EVOO (ppm).

4.2.12.2 TPC in OLEs

10 mg of OLE were solubilized in 5 mL of MeOH (80% v/v). The solution thus obtained was homogenized with a vortex mixer for 30 seconds and a rotary shaker for 30 minutes. 0.25 mL of FCR and 1.5 mL of a Na_2CO_3 solution (20% w/v) were added to 1 mL of the OLE methanolic solution in a volumetric flask and then distilled water was added to reach the final volume of 10 mL. The blank solution was prepared by replacing the methanolic solution (1 mL) with distilled water (1 mL). Each sample was stored at the controlled temperature of 25°C and in the dark for 45 minutes. After this period, the samples were analysed by using a spectrophotometer set on λ = 725 nm. Each analysis was performed in duplicate and the TPC of each OLE was expressed as μg of GAE/mg of OLE.

4.2.12.3 Gallic Acid Calibration Curve

The stock solution of gallic acid was prepared by solubilizing 2.00 mg of commercial gallic acid in 10 mL of MeOH (80% v/v). This stock solution was then diluted to obtain solutions with different final concentrations: 1, 5, 7.5, 10 and 15 μg/mL. 0.25 mL of FCR and 1.5 mL of a of Na_2CO_3 solution (20% w/v) were added to 1 mL of each methanolic solution of gallic acid in a volumetric flask and then distilled water was added to reach the final volume of 10 mL. The blank solution was

prepared by replacing the methanolic solution of gallic acid (1 mL), with distilled water (1 mL). Each solution was stored at the controlled temperature of 25°C and in the dark for 45 minutes. After this period, the samples were analysed by using a spectrophotometer set on λ = 725 nm. For each dilution of the standard, the absorbance was evaluated thus the gallic acid calibration curve was built with a correlation coefficient (r^2) > 0.9947, as reported in Table 32.

Table 32 – Calibration curve and r^2 of gallic acid.

Compound	Calibration Curve	r^2
Gallic Acid	y = 0.0098x + 0.0983	0.9947

4.2.13 GC analysis of Fatty Acids Composition in EVOO

4.2.13.1 EVOO Samples Preparation

The EVOO samples were prepared through alkaline transmethylation by using a procedure reported in literature.[125] EVOO was solubilized in *n*-hexane in order to obtain a 1% solution of EVOO. This solution (0.8 mL) was added to a methanolic solution of KOH 2M (0.4 mL), and then shaken by using a vortex mixer for 1 minute and a rotary shaker for 10 minutes. After the separation of the phases through decantation, the organic phase was collected and 10 µL of a solution of methyl tridecanoate (IS 10 mg/mL in *n*-hexane) were added to 100 µL of this solution. 1 µL of this final solution was injected in GC. For each EVOO the analysis was performed in triplicate.

The stock solution of IS (10 mg/mL in *n*-hexane) was prepared by dissolving 10 mg of commercial methyl tridecanoate in 10 mL of *n*-hexane.

4.2.13.2 GC Method

4.2.13.2.1 Method I

Based on a method reported by Caporaso *et al*.,[125] the oven temperature was set at 170°C and held at this temperature for 20 min; it increased until 220°C with a rate of 10°C/min and held at this temperature for 5 min, as reported in Table 33. The FID temperature was kept at 250°C, the carrier was N_2, the column flow was 2 mL/min, the split ratio was 1/12 and the injected volume was 1µL.

Table 33 – GC method reported by Caporaso et al.

Total Time (min)	Rate (°C/min)	Temperature (°C)	Hold Time (min)
0.00	-	170	20.00
20.00	-	170	0.00
30.00	10.0	220	5.00

4.2.13.2.2 Method II

Based on the method reported by Yang *et al*.,[126] a method to analyse the FAs composition of EVOOs was developed. The oven temperature was set at 120°C and it increased until 160°C with a rate of 10°C/min; subsequently from 160°C to 190°C with a rate of 3°C/min; then from 190°C to 220°C held for 12 min, with a rate of 10°C/min; finally, from 220°C to 240°C, held for 10 min, with a rate of 3°C/min. Total time was 45.67 min as reported in Table 34. The FID temperature was kept at 250°C, the carrier was N_2, the column flow was 1mL/min, the split ratio was 1/12 and the injected volume was 1µL.

Table 34 – GC method II.

Total Time (min)	Rate (°C/min)	Temperature (°C)	Hold Time (min)
0.00	-	120	0.00
4.00	10.0	160	0.00
14.00	3.0	190	0.00
29.00	10.0	220	12.00
45.67	3.0	240	10.00

The identification of the peaks was achieved by comparing the retention time of the FAs present in EVOO with those of the pure standards (commercial FAMEs) and quantified by using methyl tridecanoate as IS. The retention times of each commercial FAME were reported in Table 35.

Table 35 – Retention time of the IS (methyl tridecanoate) and the commercial FAMEs and corresponding FAs quantified in EVOOs.

FAMEs	Corresponding FAs	Retention Time (min)
Methyl Tridecanoate (IS)	C13:0	11.72
Methyl Tetradecanoate	C14:0	13.60
Methyl Hexadecanoate	C16:0	17.18
Methyl 9(Z)-Hexadecenoate	C16:1 ω7	17.53
Methyl Heptadecanoate	C17:0	18.86
Methyl 10(Z)-Heptadecenoate	C17:1	19.26
Methyl Octadecanoate	C18:0	20.72
Methyl 9(Z)-Octadecenoate	C18:1 ω9	21.06
Methyl 11(Z)-Octadecenoate	C18:1; ω7	21.20
Methyl 9(Z),12(Z)-Octadecadienoate	C18:2	21.83
Methyl 9(Z),12(Z),15(Z)-Octadecatrienoate	C18:3	22.92
Methyl Eicosanoate	C20:0	25.45
Methyl 11(Z)-Eicosenoate	C20:1	25.96
Methyl Docosanoate	C22:0	32.15
Methyl Tetracosanoato	C24:0	38.65

4.2.13.3 Fatty Acids Composition of EVOOs

For each FA which was quantified, the calibration curve was built by using mixture of IS and the proper analyte at different concentrations and the correlation coefficients (r^2) were >0.9990, as reported in Table 36.

Table 36 – Calibration curves and r^2 of the fatty acids quantified in EVOOs.

FAs	Calibration Curve	r^2
C14:0	y = 1.0332x	0.9993
C16:0	y = 1.2530x	0.9990
C16:1 ω7	y = 0.7540x	0.9993
C17:0	y = 0.6323x	0.9998
C17:1	y = 1.1298x	0.9999
C18:0	y = 1.3714x	0.9993
C18:1 ω9	y = 1.0294x	0.9993
C18:1; ω7	y = 1.1950x	0.9992
C18:2	y = 0.7942x	0.9993
C18:3	y = 1.0993x	0.9990
C20:0	y = 1.5738x	0.9997
C20:1	y = 0.7792x	0.9992
C22:0	y = 1.6823x	0.9996
C24:0	y = 1.6363x	0.9998

4.2.14 Determination of free acidity

The determination of the free acidity was performed by using an acid-base titration in presence of phenolphthalein, as indicator. In particular, 10 g of EVOO was dissolved in 150 mL of a mixture of diethyl ether: absolute ethanol (2:1, v/v), which was previously neutralized with few drops of a solution of KOH 0.1M in the presence of phenolphthalein. The final solution was then titrated with a solution of KOH 0.1 M in the presence of phenolphthalein until the indicator changes colour and by using a burette with 0.05 mL divisions. The analyses were performed in duplicate, and the results were expressed as molar percentage of oleic acid.

4.2.15 Release Profile of the Phenols from the Fibers

The diffusion of phenolic compounds in a release medium (PBS) was determined, based on a procedure reported in literature.[131] A 4 cm^2 square of the fiber was inserted into a 3 cm diameter well of a multi-well plate and 2 mL of PBS was added to each well. Then the plate containing the solutions was incubated in

the oven at the controlled temperature of 37°C. At defined time intervals (0, 0.5, 1, 1.5, 3, 4, 6, 24, 48, 144 h) the medium was removed, the well was washed with 1 mL of PBS and an equal amount of the fresh medium (2 mL) was replaced each time. The qualitative and the quantitative evaluation of the phenols released from the fiber was carried out by HPLC analysis, as described in section 4.2.10.2.2. For each kind of fiber the experiment was performed in duplicate. The results were expressed as cumulative percentage of the total amount released from the fiber.

5 REFERENCES

(1) Klonaris, S.; Agiangkatzoglou, A. Competitiveness of Greek Virgin Olive Oil in the Main Destination Markets. *Br. Food J.* **2018**.

(2) Juan, M. E.; Wenzel, U.; Daniel, H.; Planas, J. M. Olive Fruit Extracts and HT-29 Human Colon Cancer Cells. In *Olives and Olive Oil in Health and Disease Prevention*; Elsevier, 2010; pp 1301–1310.

(3) Peri, C. *The Extra-Virgin Olive Oil Handbook*; John Wiley & Sons, 2014.

(4) Rodríguez-López, P.; Lozano-Sanchez, J.; Borrás-Linares, I.; Emanuelli, T.; Menéndez, J. A.; Segura-Carretero, A. Structure-Biological Activity Relationships of Extra-Virgin Olive Oil Phenolic Compounds: Health Properties and Bioavailability. *Antioxidants* **2020**, *9* (8), 685.

(5) Bellumori, M.; Cecchi, L.; Innocenti, M.; Clodoveo, M. L.; Corbo, F.; Mulinacci, N. The EFSA Health Claim on Olive Oil Polyphenols: Acid Hydrolysis Validation and Total Hydroxytyrosol and Tyrosol Determination in Italian Virgin Olive Oils. *Molecules* **2019**, *24* (11), 2179.

(6) on Dietetic Products, N.; (NDA), A. Scientific Opinion on the Substantiation of Health Claims Related to Olive Oil and Maintenance of Normal Blood LDL-Cholesterol Concentrations (ID 1316, 1332), Maintenance of Normal (Fasting) Blood Concentrations of Triglycerides (ID 1316, 1332), Maintenan. *EFSA J.* **2011**, *9* (4), 2044.

(7) on Dietetic Products, N.; (NDA), A. Scientific Opinion on the Substantiation of Health Claims Related to Oleic Acid Intended to Replace Saturated Fatty Acids (SFAs) in Foods or Diets and Maintenance of Normal Blood LDL-Cholesterol Concentrations (ID 673, 728, 729, 1302, 4334) and Maintenanc. *EFSA J.* **2011**, *9* (4), 2043.

(8) on Dietetic Products, N.; (NDA), A. Scientific Opinion on the Substantiation of Health Claims Related to Linoleic Acid and Maintenance of Normal Blood Cholesterol Concentrations (ID 489) Pursuant to Article 13 (1) of Regulation (EC) No 1924/2006. *EFSA J.* **2009**, *7* (10), 1276.

(9) Gaforio, J. J.; Sánchez-Quesada, C.; López-Biedma, A.; del Carmen Ramírez-Tortose, M.; Warleta, F. Molecular Aspects of Squalene and Implications for Olive Oil and the Mediterranean Diet. In *The Mediterranean Diet*; Elsevier, 2015; pp 281–290.

(10) Micera, M.; Botto, A.; Geddo, F.; Antoniotti, S.; Bertea, C. M.; Levi, R.; Gallo, M. P.; Querio, G. Squalene: More than a Step toward Sterols. *Antioxidants*

2020, *9* (8), 688.

(11) Lee, G. Y.; Han, S. N. The Role of Vitamin E in Immunity. *Nutrients* **2018**, *10* (11), 1614.

(12) Esposto, S.; Taticchi, A.; Urbani, S.; Selvaggini, R.; Veneziani, G.; Di Maio, I.; Sordini, B.; Servili, M. Effect of Light Exposure on the Quality of Extra Virgin Olive Oils According to Their Chemical Composition. *Food Chem.* **2017**, *229*, 726–733.

(13) on Dietetic Products, N.; (NDA), A. Scientific Opinion on the Substantiation of Health Claims Related to Vitamin E and Protection of DNA, Proteins and Lipids from Oxidative Damage (ID 160, 162, 1947), Maintenance of the Normal Function of the Immune System (ID 161, 163), Maintenance of Norm. *EFSA J.* **2010**, *8* (10), 1816.

(14) on Dietetic Products, N.; (NDA), A. Scientific Opinion on the Substantiation of a Health Claim Related to Polyphenols in Olive and Maintenance of Normal Blood HDL Cholesterol Concentrations (ID 1639, Further Assessment) Pursuant to Article 13 (1) of Regulation (EC) No 1924/2006. *EFSA J.* **2012**, *10* (8), 2848.

(15) Mousavi, S.; Mariotti, R.; Stanzione, V.; Pandolfi, S.; Mastio, V.; Baldoni, L.; Cultrera, N. G. M. Evolution of Extra Virgin Olive Oil Quality under Different Storage Conditions. *Foods* **2021**, *10* (8), 1945.

(16) Mishra, P.; Lleó, L.; Cuadrado, T.; Ruiz-Altisent, M.; Hernández-Sánchez, N. Monitoring Oxidation Changes in Commercial Extra Virgin Olive Oils with Fluorescence Spectroscopy-Based Prototype. *Eur. Food Res. Technol.* **2018**, *244* (3), 565–575.

(17) Kotsiou, K.; Tasioula-Margari, M. Monitoring the Phenolic Compounds of Greek Extra-Virgin Olive Oils during Storage. *Food Chem.* **2016**, *200*, 255–262.

(18) Palla, M.; Digiacomo, M.; Cristani, C.; Bertini, S.; Giovannetti, M.; Macchia, M.; Manera, C.; Agnolucci, M. Composition of Health-Promoting Phenolic Compounds in Two Extra Virgin Olive Oils and Diversity of Associated Yeasts. *J. Food Compos. Anal.* **2018**, *74*, 27–33.

(19) Berbel, J.; Posadillo, A. Review and Analysis of Alternatives for the Valorisation of Agro-Industrial Olive Oil by-Products. *Sustainability* **2018**, *10* (1), 237.

(20) Talhaoui, N.; Taamalli, A.; Gómez-Caravaca, A. M.; Fernández-Gutiérrez, A.; Segura-Carretero, A. Phenolic Compounds in Olive Leaves: Analytical Determination, Biotic and Abiotic Influence, and Health Benefits. *Food Res. Int.* **2015**, *77*, 92–108.

(21) Romani, A.; Ieri, F.; Urciuoli, S.; Noce, A.; Marrone, G.; Nediani, C.; Bernini, R. Health Effects of Phenolic Compounds Found in Extra-Virgin Olive Oil, by-Products, and Leaf of Olea Europaea L. *Nutrients* **2019**, *11* (8), 1776.

(22) Mallamaci, R.; Budriesi, R.; Clodoveo, M. L.; Biotti, G.; Micucci, M.; Ragusa, A.; Curci, F.; Muraglia, M.; Corbo, F.; Franchini, C. Olive Tree in Circular Economy as a Source of Secondary Metabolites Active for Human and Animal Health beyond Oxidative Stress and Inflammation. *Molecules* **2021**, *26* (4), 1072.

(23) Medina, E.; Romero, C.; García, P.; Brenes, M. Characterization of Bioactive Compounds in Commercial Olive Leaf Extracts, and Olive Leaves and Their Infusions. *Food Funct.* **2019**, *10* (8), 4716–4724.

(24) Guinda, Á.; Castellano, J. M.; Santos-Lozano, J. M.; Delgado-Hervás, T.; Gutiérrez-Adánez, P.; Rada, M. Determination of Major Bioactive Compounds from Olive Leaf. *LWT-Food Sci. Technol.* **2015**, *64* (1), 431–438.

(25) Romani, A.; Mulas, S.; Heimler, D. Polyphenols and Secoiridoids in Raw Material (Olea Europaea L. Leaves) and Commercial Food Supplements. *Eur. Food Res. Technol.* **2017**, *243* (3), 429–435.

(26) Montedoro, G.; Servili, M.; Baldioli, M.; Selvaggini, R.; Miniati, E.; Macchioni, A. Simple and Hydrolyzable Compounds in Virgin Olive Oil. 3. Spectroscopic Characterizations of the Secoiridoid Derivatives. *J. Agric. Food Chem.* **1993**, *41* (11), 2228–2234.

(27) Beauchamp, G. K.; Keast, R. S. J.; Morel, D.; Lin, J.; Pika, J.; Han, Q.; Lee, C.-H.; Smith, A. B.; Breslin, P. A. S. Ibuprofen-like Activity in Extra-Virgin Olive Oil. *Nature* **2005**, *437* (7055), 45–46.

(28) Lozano-Castellón, J.; López-Yerena, A.; de Alvarenga, J. F.; del Castillo-Alba, J.; Vallverdú-Queralt, A.; Escribano-Ferrer, E.; Lamuela-Raventós, R. M. Health-Promoting Properties of Oleocanthal and Oleacein: Two Secoiridoids from Extra-Virgin Olive Oil. *Crit. Rev. Food Sci. Nutr.* **2020**, *60* (15), 2532–2548.

(29) Vougogiannopoulou, K.; Lemus, C.; Halabalaki, M.; Pergola, C.; Werz, O.;

Smith III, A. B.; Michel, S.; Skaltsounis, L.; Deguin, B. One-Step Semisynthesis of Oleacein and the Determination as a 5-Lipoxygenase Inhibitor. *J. Nat. Prod.* **2014**, *77* (3), 441–445.

(30) Rosignoli, P.; Fuccelli, R.; Fabiani, R.; Servili, M.; Morozzi, G. Effect of Olive Oil Phenols on the Production of Inflammatory Mediators in Freshly Isolated Human Monocytes. *J. Nutr. Biochem.* **2013**, *24* (8), 1513–1519.

(31) Scotece, M.; Gómez, R.; Conde, J.; Lopez, V.; Gómez-Reino, J. J.; Lago, F.; Smith III, A. B.; Gualillo, O. Further Evidence for the Anti-Inflammatory Activity of Oleocanthal: Inhibition of MIP-1α and IL-6 in J774 Macrophages and in ATDC5 Chondrocytes. *Life Sci.* **2012**, *91* (23–24), 1229–1235.

(32) Cicerale, S.; Lucas, L. J.; Keast, R. S. J. Antimicrobial, Antioxidant and Anti-Inflammatory Phenolic Activities in Extra Virgin Olive Oil. *Curr. Opin. Biotechnol.* **2012**, *23* (2), 129–135.

(33) Medina, E.; De Castro, A.; Romero, C.; Brenes, M. Comparison of the Concentrations of Phenolic Compounds in Olive Oils and Other Plant Oils: Correlation with Antimicrobial Activity. *J. Agric. Food Chem.* **2006**, *54* (14), 4954–4961.

(34) Medina, E.; De Castro, A.; Romero, C.; Ramírez, E.; Brenes, M. Effect of Antimicrobial Compounds from Olive Products on Microorganisms Related to Health, Food and Agriculture. *Sci. Technol. Educ* **2013**, 1087–1094.

(35) Pang, K.-L.; Chin, K.-Y. The Biological Activities of Oleocanthal from a Molecular Perspective. *Nutrients* **2018**, *10* (5), 570.

(36) Takashima, T.; Sakata, Y.; Iwakiri, R.; Shiraishi, R.; Oda, Y.; Inoue, N.; Nakayama, A.; Toda, S.; Fujimoto, K. Feeding with Olive Oil Attenuates Inflammation in Dextran Sulfate Sodium-Induced Colitis in Rat. *J. Nutr. Biochem.* **2014**, *25* (2), 186–192.

(37) Khanfar, M. A.; Bardaweel, S. K.; Akl, M. R.; El Sayed, K. A. Olive Oil-Derived Oleocanthal as Potent Inhibitor of Mammalian Target of Rapamycin: Biological Evaluation and Molecular Modeling Studies. *Phyther. Res.* **2015**, *29* (11), 1776–1782.

(38) Elnagar, A. Y.; Sylvester, P. W.; El Sayed, K. A. (-)-Oleocanthal as a c-Met Inhibitor for the Control of Metastatic Breast and Prostate Cancers. *Planta Med.* **2011**, *77* (10), 1013–1019.

(39) Akl, M. R.; Ayoub, N. M.; Mohyeldin, M. M.; Busnena, B. A.; Foudah, A. I.; Liu,

Y.-Y.; Sayed, K. A. E. I. Olive Phenolics as C-Met Inhibitors:(-)-Oleocanthal Attenuates Cell Proliferation, Invasiveness, and Tumor Growth in Breast Cancer Models. *PLoS One* **2014**, *9* (5), e97622.

(40) LeGendre, O.; Breslin, P. A. S.; Foster, D. A. (-)-Oleocanthal Rapidly and Selectively Induces Cancer Cell Death via Lysosomal Membrane Permeabilization. *Mol. Cell. Oncol.* **2015**, *2* (4), e1006077.

(41) Ayoub, N. M.; Siddique, A. B.; Ebrahim, H. Y.; Mohyeldin, M. M.; El Sayed, K. A. The Olive Oil Phenolic (-)-Oleocanthal Modulates Estrogen Receptor Expression in Luminal Breast Cancer in Vitro and in Vivo and Synergizes with Tamoxifen Treatment. *Eur. J. Pharmacol.* **2017**, *810*, 100–111.

(42) Khanal, P.; Oh, W.-K.; Yun, H. J.; Namgoong, G. M.; Ahn, S.-G.; Kwon, S.-M.; Choi, H.-K.; Choi, H. S. P-HPEA-EDA, a Phenolic Compound of Virgin Olive Oil, Activates AMP-Activated Protein Kinase to Inhibit Carcinogenesis. *Carcinogenesis* **2011**, *32* (4), 545–553.

(43) Cusimano, A.; Balasus, D.; Azzolina, A.; Augello, G.; Emma, M. R.; Di Sano, C.; Gramignoli, R.; Strom, S. C.; McCubrey, J. A.; Montalto, G.; Cervello, M. Oleocanthal Exerts Antitumor Effects on Human Liver and Colon Cancer Cells through ROS Generation. *Int. J. Oncol.* **2017**, *51* (2), 533–544.

(44) Pei, T.; Meng, Q.; Han, J.; Sun, H.; Li, L.; Song, R.; Sun, B.; Pan, S.; Liang, D.; Liu, L. (-)-Oleocanthal Inhibits Growth and Metastasis by Blocking Activation of STAT3 in Human Hepatocellular Carcinoma. *Oncotarget* **2016**, *7* (28), 43475.

(45) Fabiani, R.; De Bartolomeo, A.; Rosignoli, P.; Servili, M.; Selvaggini, R.; Montedoro, G. F.; Di Saverio, C.; Morozzi, G. Virgin Olive Oil Phenols Inhibit Proliferation of Human Promyelocytic Leukemia Cells (HL60) by Inducing Apoptosis and Differentiation. *J. Nutr.* **2006**, *136* (3), 614–619.

(46) Fogli, S.; Arena, C.; Carpi, S.; Polini, B.; Bertini, S.; Digiacomo, M.; Gado, F.; Saba, A.; Saccomanni, G.; Breschi, M. C.; Nieri, P.; Manera, C.; Macchia, M. Cytotoxic Activity of Oleocanthal Isolated from Virgin Olive Oil on Human Melanoma Cells. *Nutr. Cancer* **2016**, *68* (5), 873–877.

(47) Polini, B.; Digiacomo, M.; Carpi, S.; Bertini, S.; Gado, F.; Saccomanni, G.; Macchia, M.; Nieri, P.; Manera, C.; Fogli, S. Oleocanthal and Oleacein Contribute to the in Vitro Therapeutic Potential of Extra Virgin Oil-Derived Extracts in Non-Melanoma Skin Cancer. *Toxicol. Vitr.* **2018**, *52*, 243–250.

(48) Gu, Y.; Wang, J.; Peng, L. (-)-Oleocanthal Exerts Anti-Melanoma Activities and Inhibits STAT3 Signaling Pathway. *Oncol. Rep.* **2017**, *37* (1), 483–491.

(49) Qosa, H.; Batarseh, Y. S.; Mohyeldin, M. M.; El Sayed, K. A.; Keller, J. N.; Kaddoumi, A. Oleocanthal Enhances Amyloid-β Clearance from the Brains of TgSwDI Mice and in Vitro across a Human Blood-Brain Barrier Model. *ACS Chem. Neurosci.* **2015**, *6* (11), 1849–1859.

(50) Shinde, P.; Vidyasagar, N.; Dhulap, S.; Dhulap, A.; Hirwani, R. Natural Products Based P-Glycoprotein Activators for Improved β-Amyloid Clearance in Alzheimer's Disease: An in Silico Approach. *Cent. Nerv. Syst. Agents Med. Chem. (Formerly Curr. Med. Chem. Nerv. Syst. Agents)* **2016**, *16* (1), 50–59.

(51) Abuznait, A. H.; Qosa, H.; O'Connell, N. D.; Akbarian-Tefaghi, J.; Sylvester, P. W.; El Sayed, K. A.; Kaddoumi, A. Induction of Expression and Functional Activity of P-Glycoprotein Efflux Transporter by Bioactive Plant Natural Products. *Food Chem. Toxicol.* **2011**, *49* (11), 2765–2772.

(52) Batarseh, Y. S.; Kaddoumi, A. Oleocanthal-Rich Extra-Virgin Olive Oil Enhances Donepezil Effect by Reducing Amyloid-β Load and Related Toxicity in a Mouse Model of Alzheimer's Disease. *J. Nutr. Biochem.* **2018**, *55*, 113–123.

(53) Abuznait, A. H.; Qosa, H.; Busnena, B. A.; El Sayed, K. A.; Kaddoumi, A. Olive-Oil-Derived Oleocanthal Enhances β-Amyloid Clearance as a Potential Neuroprotective Mechanism against Alzheimer's Disease: In Vitro and in Vivo Studies. *ACS Chem. Neurosci.* **2013**, *4* (6), 973–982.

(54) Pitt, J.; Roth, W.; Lacor, P.; Smith, A. B.; Blankenship, M.; Velasco, P.; De Felice, F.; Breslin, P.; Klein, W. L. Alzheimer's-Associated Aβ Oligomers Show Altered Structure, Immunoreactivity and Synaptotoxicity with Low Doses of Oleocanthal. *Toxicol. Appl. Pharmacol.* **2009**, *240* (2), 189–197. https://doi.org/10.1016/j.taap.2009.07.018.

(55) Monti, M. C.; Margarucci, L.; Riccio, R.; Casapullo, A. Modulation of Tau Protein Fibrillization by Oleocanthal. *J. Nat. Prod.* **2012**, *75* (9), 1584–1588.

(56) Li, W.; Sperry, J. B.; Crowe, A.; Trojanowski, J. Q.; Smith III, A. B.; Lee, V. M.-Y. Inhibition of Tau Fibrillization by Oleocanthal via Reaction with the Amino Groups of Tau. *J. Neurochem.* **2009**, *110* (4), 1339–1351.

(57) Giusti, L.; Angeloni, C.; Barbalace, M. C.; Lacerenza, S.; Ciregia, F.; Ronci, M.; Urbani, A.; Manera, C.; Digiacomo, M.; Macchia, M.; Mazzoni, M. R.;

Lucacchini, A.; Hrelia, S. A Proteomic Approach to Uncover Neuroprotective Mechanisms of Oleocanthal against Oxidative Stress. *Int. J. Mol. Sci.* **2018**, *19* (8), 2329.

(58) Iacono, A.; Gómez, R.; Sperry, J.; Conde, J.; Bianco, G.; Meli, R.; Gómez-Reino, J. J.; Smith III, A. B.; Gualillo, O. Effect of Oleocanthal and Its Derivatives on Inflammatory Response Induced by Lipopolysaccharide in a Murine Chondrocyte Cell Line. *Arthritis Rheum.* **2010**, *62* (6), 1675–1682.

(59) Widmer, R. J.; Freund, M. A.; Flammer, A. J.; Sexton, J.; Lennon, R.; Romani, A.; Mulinacci, N.; Vinceri, F. F.; Lerman, L. O.; Lerman, A. Beneficial Effects of Polyphenol-Rich Olive Oil in Patients with Early Atherosclerosis. *Eur. J. Nutr.* **2013**, *52* (3), 1223–1231.

(60) Agrawal, K.; Melliou, E.; Li, X.; Pedersen, T. L.; Wang, S. C.; Magiatis, P.; Newman, J. W.; Holt, R. R. Oleocanthal-Rich Extra Virgin Olive Oil Demonstrates Acute Anti-Platelet Effects in Healthy Men in a Randomized Trial. *J. Funct. Foods* **2017**, *36*, 84–93.

(61) Naruszewicz, M.; E Czerwinska, M.; K Kiss, A. Oleacein. Translation from Mediterranean Diet to Potential Antiatherosclerotic Drug. *Curr. Pharm. Des.* **2015**, *21* (9), 1205–1212.

(62) Czerwińska, M.; Kiss, A. K.; Naruszewicz, M. A Comparison of Antioxidant Activities of Oleuropein and Its Dialdehydic Derivative from Olive Oil, Oleacein. *Food Chem.* **2012**, *131* (3), 940–947.

(63) Paiva-Martins, F.; Pinto, M. Isolation and Characterization of a New Hydroxytyrosol Derivative from Olive (Olea Europaea) Leaves. *J. Agric. Food Chem.* **2008**, *56* (14), 5582–5588.

(64) Hansen, K.; Adsersen, A.; Christensen, S. B.; Jensen, S. R.; Nyman, U.; Smitt, U. W. Isolation of an Angiotensin Converting Enzyme (ACE) Inhibitor from Olea Europaea and Olea Lancea. *Phytomedicine* **1996**, *2* (4), 319–325.

(65) Parzonko, A.; Czerwińska, M. E.; Kiss, A. K.; Naruszewicz, M. Oleuropein and Oleacein May Restore Biological Functions of Endothelial Progenitor Cells Impaired by Angiotensin II via Activation of Nrf2/Heme Oxygenase-1 Pathway. *Phytomedicine* **2013**, *20* (12), 1088–1094.

(66) Endtmann, C.; Ebrahimian, T.; Czech, T.; Arfa, O.; Laufs, U.; Fritz, M.; Wassmann, K.; Werner, N.; Petoumenos, V.; Nickenig, G.; Wassmann, S. Angiotensin II Impairs Endothelial Progenitor Cell Number and Function in

Vitro and in Vivo: Implications for Vascular Regeneration. *Hypertension* **2011**, *58* (3), 394–403.

(67) Baetta, R.; Corsini, A. Role of Polymorphonuclear Neutrophils in Atherosclerosis: Current State and Future Perspectives. *Atherosclerosis* **2010**, *210* (1), 1–13.

(68) Czerwińska, M. E.; Kiss, A. K.; Naruszewicz, M. Inhibition of Human Neutrophils NEP Activity, CD11b/CD18 Expression and Elastase Release by 3, 4-Dihydroxyphenylethanol-Elenolic Acid Dialdehyde, Oleacein. *Food Chem.* **2014**, *153*, 1–8.

(69) Sindona, G.; Caruso, A.; Cozza, A.; Fiorentini, S.; Lorusso, B.; Marini, E.; Nardi, M.; Procopio, A.; Zicari, S. Anti-Inflammatory Effect of 3, 4-DHPEA-EDA [2-(3, 4-Hydroxyphenyl) Ethyl (3S, 4E)-4-Formyl-3-(2-Oxoethyl) Hex-4-Enoate] on Primary Human Vascular Endothelial Cells. *Curr. Med. Chem.* **2012**, *19* (23), 4006–4013.

(70) Filipek, A.; Mikołajczyk, T. P.; Guzik, T. J.; Naruszewicz, M. Oleacein and Foam Cell Formation in Human Monocyte-Derived Macrophages: A Potential Strategy against Early and Advanced Atherosclerotic Lesions. *Pharmaceuticals* **2020**, *13* (4), 64.

(71) Visioli, F.; Bellomo, G.; Montedoro, G.; Galli, C. Low Density Lipoprotein Oxidation Is Inhibited in Vitro by Olive Oil Constituents. *Atherosclerosis* **1995**, *117* (1), 25–32.

(72) Juli, G.; Oliverio, M.; Bellizzi, D.; Gallo Cantafio, M. E.; Grillone, K.; Passarino, G.; Colica, C.; Nardi, M.; Rossi, M.; Procopio, A.; Tagliaferri, P.; Tassone, P. Anti-Tumor Activity and Epigenetic Impact of the Polyphenol Oleacein in Multiple Myeloma. *Cancers (Basel).* **2019**, *11* (7), 990.

(73) Cirmi, S.; Celano, M.; Lombardo, G. E.; Maggisano, V.; Procopio, A.; Russo, D.; Navarra, M. Oleacein Inhibits STAT3, Activates the Apoptotic Machinery, and Exerts Anti-Metastatic Effects in the SH-SY5Y Human Neuroblastoma Cells. *Food Funct.* **2020**, *11* (4), 3271–3279.

(74) Lombardo, G. E.; Lepore, S. M.; Morittu, V. M.; Arcidiacono, B.; Colica, C.; Procopio, A.; Maggisano, V.; Bulotta, S.; Costa, N.; Mignogna, C.; Britti, D.; Brunetti, A.; Russo, D.; Celano, M. Effects of Oleacein on High-Fat Diet-Dependent Steatosis, Weight Gain, and Insulin Resistance in Mice. *Front. Endocrinol. (Lausanne).* **2018**, *9*, 116.

(75) Gutiérrez-Miranda, B.; Gallardo, I.; Melliou, E.; Cabero, I.; Álvarez, Y.; Magiatis, P.; Hernández, M.; Nieto, M. L. Oleacein Attenuates the Pathogenesis of Experimental Autoimmune Encephalomyelitis through Both Antioxidant and Anti-Inflammatory Effects. *Antioxidants* **2020**, *9* (11), 1161.

(76) Hassen, I.; Casabianca, H.; Hosni, K. Biological Activities of the Natural Antioxidant Oleuropein: Exceeding the Expectation--A Mini-Review. *J. Funct. Foods* **2015**, *18*, 926–940.

(77) Kotyzová, D.; Hodková, A.; Eybl, V. The Effect of Olive Oil Phenolics--Hydroxytyrosol and Oleuropein on Antioxidant Defence Status in Acute Arsenic Exposed Rats. *Toxicol. Lett.* **2011**, No. 205, S222.

(78) Jemai, H.; Bouaziz, M.; Fki, I.; El Feki, A.; Sayadi, S. Hypolipidimic and Antioxidant Activities of Oleuropein and Its Hydrolysis Derivative-Rich Extracts from Chemlali Olive Leaves. *Chem. Biol. Interact.* **2008**, *176* (2–3), 88–98.

(79) Al-Azzawie, H. F.; Alhamdani, M.-S. S. Hypoglycemic and Antioxidant Effect of Oleuropein in Alloxan-Diabetic Rabbits. *Life Sci.* **2006**, *78* (12), 1371–1377.

(80) Domitrović, R.; Jakovac, H.; Marchesi, V. V.; Šain, I.; Romić, Ž.; Rahelić, D. Preventive and Therapeutic Effects of Oleuropein against Carbon Tetrachloride-Induced Liver Damage in Mice. *Pharmacol. Res.* **2012**, *65* (4), 451–464.

(81) Lee, O.-H.; Lee, B.-Y. Antioxidant and Antimicrobial Activities of Individual and Combined Phenolics in Olea Europaea Leaf Extract. *Bioresour. Technol.* **2010**, *101* (10), 3751–3754.

(82) Hamdi, H. K.; Castellon, R. Oleuropein, a Non-Toxic Olive Iridoid, Is an Anti-Tumor Agent and Cytoskeleton Disruptor. *Biochem. Biophys. Res. Commun.* **2005**, *334* (3), 769–778.

(83) Acquaviva, R.; Di Giacomo, C.; Sorrenti, V.; Galvano, F.; Santangelo, R.; Cardile, V.; Gangia, S.; D'Orazio, N.; Abraham, N. G.; Vanella, L. Antiproliferative Effect of Oleuropein in Prostate Cell Lines. *Int. J. Oncol.* **2012**, *41* (1), 31–38.

(84) Han, J.; Talorete, T. P. N.; Yamada, P.; Isoda, H. Anti-Proliferative and Apoptotic Effects of Oleuropein and Hydroxytyrosol on Human Breast Cancer MCF-7 Cells. *Cytotechnology* **2009**, *59* (1), 45–53.

(85) Sepporta, M. V.; Fuccelli, R.; Rosignoli, P.; Ricci, G.; Servili, M.; Morozzi, G.;

Fabiani, R. Oleuropein Inhibits Tumour Growth and Metastases Dissemination in Ovariectomised Nude Mice with MCF-7 Human Breast Tumour Xenografts. *J. Funct. Foods* **2014**, *8*, 269–273.

(86) Hassan, Z. K.; Elamin, M. H.; Daghestani, M. H.; Omer, S. A.; Al-Olayan, E. M.; Elobeid, M. A.; Virk, P.; Mohammed, O. B. Oleuropein Induces Anti-Metastatic Effects in Breast Cancer. *Asian Pacific J. cancer Prev.* **2012**, *13* (9), 4555–4559.

(87) Hassan, Z. K.; Elamin, M. H.; Omer, S. A.; Daghestani, M. H.; Al-Olayan, E. S.; Elobeid, M. A.; Virk, P. Oleuropein Induces Apoptosis via the P53 Pathway in Breast Cancer Cells. *Asian Pacific J. Cancer Prev.* **2013**, *14* (11), 6739–6742.

(88) Ruzzolini, J.; Peppicelli, S.; Andreucci, E.; Bianchini, F.; Scardigli, A.; Romani, A.; La Marca, G.; Nediani, C.; Calorini, L. Oleuropein, the Main Polyphenol of Olea Europaea Leaf Extract, Has an Anti-Cancer Effect on Human BRAF Melanoma Cells and Potentiates the Cytotoxicity of Current Chemotherapies. *Nutrients* **2018**, *10* (12), 1950.

(89) Grawish, M. E.; Zyada, M. M.; Zaher, A. R. Inhibition of 4-NQO-Induced F433 Rat Tongue Carcinogenesis by Oleuropein-Rich Extract. *Med. Oncol.* **2011**, *28* (4), 1163–1168.

(90) Andreadou, I.; Iliodromitis, E. K.; Mikros, E.; Constantinou, M.; Agalias, A.; Magiatis, P.; Skaltsounis, A. L.; Kamber, E.; Tsantili-Kakoulidou, A.; Kremastinos, D. T. The Olive Constituent Oleuropein Exhibits Anti-Ischemic, Antioxidative, and Hypolipidemic Effects in Anesthetized Rabbits. *J. Nutr.* **2006**, *136* (8), 2213–2219.

(91) Andreadou, I.; Sigala, F.; Iliodromitis, E. K.; Papaefthimiou, M.; Sigalas, C.; Aligiannis, N.; Savvari, P.; Gorgoulis, V.; Papalabros, E.; Kremastinos, D. T. Acute Doxorubicin Cardiotoxicity Is Successfully Treated with the Phytochemical Oleuropein through Suppression of Oxidative and Nitrosative Stress. *J. Mol. Cell. Cardiol.* **2007**, *42* (3), 549–558.

(92) Tsoumani, M.; Georgoulis, A.; Nikolaou, P.-E.; Kostopoulos, I. V; Dermintzoglou, T.; Papatheodorou, I.; Zoga, A.; Efentakis, P.; Konstantinou, M.; Gikas, E.; Kostomitsopoulos, N.; Papapetropoulos, A.; Lazou, A.; Skaltsounis, A.-L.; Hausenloy, D. J.; Tsitsilonis, O.; Tseti, I.; Di Lisa, F.; Iliodromitis, E. K.; Andreadou, I. Acute Administration of the Olive Constituent,

Oleuropein, Combined with Ischemic Postconditioning Increases Myocardial Protection by Modulating Oxidative Defense. *Free Radic. Biol. Med.* **2021**, *166*, 18–32.

(93) Fuentes, E.; Palomo, I. Antiplatelet Effects of Natural Bioactive Compounds by Multiple Targets: Food and Drug Interactions. *J. Funct. Foods* **2014**, *6*, 73–81.

(94) Jemai, H.; Mahmoudi, A.; Feryeni, A.; Fki, I.; Bouallagui, Z.; Choura, S.; Chamkha, M.; Sayadi, S. Hepatoprotective Effect of Oleuropein-Rich Extract from Olive Leaves against Cadmium-Induced Toxicity in Mice. *Biomed Res. Int.* **2020**, *2020*.

(95) Kim, S. W.; Hur, W.; Li, T. Z.; Lee, Y. K.; Choi, J. E.; Hong, S. W.; Lyoo, K.-S.; You, C. R.; Jung, E. S.; Jung, C. K.; Park, T.; Um, S.-J.; Yoon, S. K. Oleuropein Prevents the Progression of Steatohepatitis to Hepatic Fibrosis Induced by a High-Fat Diet in Mice. *Exp. Mol. Med.* **2014**, *46* (4), e92--e92.

(96) Larussa, T.; Oliverio, M.; Suraci, E.; Greco, M.; Placida, R.; Gervasi, S.; Marasco, R.; Imeneo, M.; Paolino, D.; Tucci, L.; Gulletta, E.; Fresta, M.; Procopio, A.; Luzza, F. Oleuropein Decreases Cyclooxygenase-2 and Interleukin-17 Expression and Attenuates Inflammatory Damage in Colonic Samples from Ulcerative Colitis Patients. *Nutrients* **2017**, *9* (4), 391.

(97) Giner, E.; Recio, M.-C.; Rios, J.-L.; Giner, R.-M. Oleuropein Protects against Dextran Sodium Sulfate-Induced Chronic Colitis in Mice. *J. Nat. Prod.* **2013**, *76* (6), 1113–1120.

(98) Vezza, T.; Algieri, F.; Rodríguez-Nogales, A.; Garrido-Mesa, J.; Utrilla, M. P.; Talhaoui, N.; Gómez-Caravaca, A. M.; Segura-Carretero, A.; Rodríguez-Cabezas, M. E.; Monteleone, G.; Galvez, J. Immunomodulatory Properties of Olea Europaea Leaf Extract in Intestinal Inflammation. *Mol. Nutr. Food Res.* **2017**, *61* (10), 1601066.

(99) Ranieri, M.; Di Mise, A.; Difonzo, G.; Centrone, M.; Venneri, M.; Pellegrino, T.; Russo, A.; Mastrodonato, M.; Caponio, F.; Valenti, G.; Tamma, G. Green Olive Leaf Extract (OLE) Provides Cytoprotection in Renal Cells Exposed to Low Doses of Cadmium. *PLoS One* **2019**, *14* (3), e0214159.

(100) Jemai, H.; Feryéni, A.; Mahmoudi, A.; Fki, I.; Bouallagui, Z.; Sayadi, S. Oleuropein Protects Kidney against Oxidative and Histopathological Damages in Subchronic Cadmium Intoxicated Mice. **2019**.

(101) Flemmig, J.; Kuchta, K.; Arnhold, J.; Rauwald, H. W. Olea Europaea Leaf (Ph. Eur.) Extract as Well as Several of Its Isolated Phenolics Inhibit the Gout-Related Enzyme Xanthine Oxidase. *Phytomedicine* **2011**, *18* (7), 561–566.

(102) Santiago-Mora, R.; Casado-Díaz, A.; De Castro, M. D.; Quesada-Gómez, J. M. Oleuropein Enhances Osteoblastogenesis and Inhibits Adipogenesis: The Effect on Differentiation in Stem Cells Derived from Bone Marrow. *Osteoporos. Int.* **2011**, *22* (2), 675–684.

(103) Perugini, P.; Vettor, M.; Rona, C.; Troisi, L.; Villanova, L.; Genta, I.; Conti, B.; Pavanetto, F. Efficacy of Oleuropein against UVB Irradiation: Preliminary Evaluation. *Int. J. Cosmet. Sci.* **2008**, *30* (2), 113–120.

(104) Cvjetićanin, T.; Miljković, D.; Stojanović, I.; Dekanski, D.; Stošić-Grujičić, S. Dried Leaf Extract of Olea Europaea Ameliorates Islet-Directed Autoimmunity in Mice. *Br. J. Nutr.* **2010**, *103* (10), 1413–1424.

(105) Zheng, S.; Huang, K.; Tong, T. Efficacy and Mechanisms of Oleuropein in Mitigating Diabetes and Diabetes Complications. *J. Agric. Food Chem.* **2021**.

(106) Mehraein, F.; Sarbishegi, M.; Aslani, A. Evaluation of Effect of Oleuropein on Skin Wound Healing in Aged Male BALB/c Mice. *Cell J.* **2014**, *16* (1), 25.

(107) Gado, F.; Digiacomo, M.; Esposito Salsano, J.; Macchia, M.; Manera, C. Phenolic Compounds in Prevention and Treatment of Skin Cancers: A Review. *Curr. Med. Chem.* **2021**.

(108) Carpi, S.; Polini, B.; Manera, C.; Digiacomo, M.; Esposito Salsano, J.; Macchia, M.; Scoditti, E.; Nieri, P. MiRNA Modulation and Antitumor Activity by the Extra-Virgin Olive Oil Polyphenol Oleacein in Human Melanoma Cells. *Front. Pharmacol.* **2020**, *11*, 1490.

(109) Gabbia, D.; Carpi, S.; Sarcognato, S.; Cannella, L.; Colognesi, M.; Scaffidi, M.; Polini, B.; Digiacomo, M.; Esposito Salsano, J.; Manera, C.; Macchia, M.; Nieri, P.; Carrara, M.; Russo, F. P.; Guido, M.; De Martin, S. The Extra Virgin Olive Oil Polyphenol Oleocanthal Exerts Antifibrotic Effects in the Liver. *Front. Nutr.* **2021**, *8*.

(110) Carpi, S.; Scoditti, E.; Massaro, M.; Polini, B.; Manera, C.; Digiacomo, M.; Esposito Salsano, J.; Poli, G.; Tuccinardi, T.; Doccini, S.; Santorelli, F. M.; Carluccio, M. A.; Macchia, M.; Wabitsch, M.; De Caterina, R.; Nieri, P. The Extra-Virgin Olive Oil Polyphenols Oleocanthal and Oleacein Counteract Inflammation-Related Gene and MiRNA Expression in Adipocytes by

Attenuating NF-KB Activation. *Nutrients* **2019**, *11* (12), 2855.

(111) Scheja, L.; Heeren, J. The Endocrine Function of Adipose Tissues in Health and Cardiometabolic Disease. *Nat. Rev. Endocrinol.* **2019**, *15* (9), 507–524.

(112) Tsolakou, A.; Diamantakos, P.; Kalaboki, I.; Mena-Bravo, A.; Priego-Capote, F.; Abdallah, I. M.; Kaddoumi, A.; Melliou, E.; Magiatis, P. Oleocanthalic Acid, a Chemical Marker of Olive Oil Aging and Exposure to a High Storage Temperature with Potential Neuroprotective Activity. *J. Agric. Food Chem.* **2018**, *66* (28), 7337–7346.

(113) Esposito Salsano, J.; Pinto, D.; Rodrigues, F.; Saba, A.; Manera, C.; Digiacomo, M.; Macchia, M. Oleocanthalic Acid from Extra-Virgin Olive Oil: Analysis, Preparative Isolation and Radical Scavenging Activity. *J. Food Compos. Anal.* **2022**, *105*, 104160.

(114) Angelis, A.; Antoniadi, L.; Stathopoulos, P.; Halabalaki, M.; Skaltsounis, L. A. Oleocanthalic and Oleaceinic Acids: New Compounds from Extra Virgin Olive Oil (EVOO). *Phytochem. Lett.* **2018**, *26*, 190–194.

(115) Uddin, M. S.; Al Mamun, A.; Kabir, M. T.; Ahmad, J.; Jeandet, P.; Sarwar, M. S.; Ashraf, G. M.; Aleya, L. Neuroprotective Role of Polyphenols against Oxidative Stress-Mediated Neurodegeneration. *Eur. J. Pharmacol.* **2020**, 173412.

(116) Barizao, E. O.; Visentainer, J. V.; de Cinque Almeida, V.; Ribeiro, D.; Chiste, R. C.; Fernandes, E. Citharexylum Solanaceum Fruit Extracts: Profiles of Phenolic Compounds and Carotenoids and Their Relation with ROS and RNS Scavenging Capacities. *Food Res. Int.* **2016**, *86*, 24–33.

(117) Berto, A.; Ribeiro, A. B.; de Souza, N. E.; Fernandes, E.; Chisté, R. C. Bioactive Compounds and Scavenging Capacity of Pulp, Peel and Seed Extracts of the Amazonian Fruit Quararibea Cordata against ROS and RNS. *Food Res. Int.* **2015**, *77*, 236–243.

(118) Chisté, R. C.; Freitas, M.; Mercadante, A. Z.; Fernandes, E. The Potential of Extracts of Caryocar Villosum Pulp to Scavenge Reactive Oxygen and Nitrogen Species. *Food Chem.* **2012**, *135* (3), 1740–1749.

(119) Chisté, R. C.; Mercadante, A. Z.; Gomes, A.; Fernandes, E.; da Costa Lima, J. L. F.; Bragagnolo, N. In Vitro Scavenging Capacity of Annatto Seed Extracts against Reactive Oxygen and Nitrogen Species. *Food Chem.* **2011**, *127* (2), 419–426.

(120) Gomes, A.; Fernandes, E.; Silva, A. M. S.; Santos, C. M. M.; Pinto, D. C. G. A.; Cavaleiro, J. A. S.; Lima, J. L. F. C. 2-Styrylchromones: Novel Strong Scavengers of Reactive Oxygen and Nitrogen Species. *Bioorg. Med. Chem.* **2007**, *15* (18), 6027–6036.

(121) Pinto, D.; de la Luz Cadiz-Gurrea, M.; Sut, S.; Ferreira, A. S.; Leyva-Jimenez, F. J.; Dall'Acqua, S.; Segura-Carretero, A.; Delerue-Matos, C.; Rodrigues, F. Valorisation of Underexploited Castanea Sativa Shells Bioactive Compounds Recovered by Supercritical Fluid Extraction with CO2: A Response Surface Methodology Approach. *J. CO2 Util.* **2020**, *40*, 101194.

(122) Pinto, D.; Franco, S. D.; Silva, A. M.; Cupara, S.; Koskovac, M.; Kojicic, K.; Soares, S.; Rodrigues, F.; Sut, S.; Dall'Acqua, S.; Oliveira, M. B. P. P. Chemical Characterization and Bioactive Properties of a Coffee-like Beverage Prepared from Quercus Cerris Kernels. *Food Funct.* **2019**, *10* (4), 2050–2060.

(123) Almeida, D.; Pinto, D.; Santos, J.; Vinha, A. F.; Palmeira, J.; Ferreira, H. N.; Rodrigues, F.; Oliveira, M. B. P. P. Hardy Kiwifruit Leaves (Actinidia Arguta): An Extraordinary Source of Value-Added Compounds for Food Industry. *Food Chem.* **2018**, *259*, 113–121.

(124) Boeing, J. S.; Ribeiro, D.; Chisté, R. C.; Visentainer, J. V.; Costa, V. M.; Freitas, M.; Fernandes, E. Chemical Characterization and Protective Effect of the Bactris Setosa Mart. Fruit against Oxidative/Nitrosative Stress. *Food Chem.* **2017**, *220*, 427–437.

(125) Caporaso, N.; Savarese, M.; Paduano, A.; Guidone, G.; De Marco, E.; Sacchi, R. Nutritional Quality Assessment of Extra Virgin Olive Oil from the Italian Retail Market: Do Natural Antioxidants Satisfy EFSA Health Claims? *J. Food Compos. Anal.* **2015**, *40*, 154–162.

(126) Yang, Y.; Ferro, M. D.; Cavaco, I.; Liang, Y. Detection and Identification of Extra Virgin Olive Oil Adulteration by GC-MS Combined with Chemometrics. *J. Agric. Food Chem.* **2013**, *61* (15), 3693–3702.

(127) De la Ossa, J. G.; Felice, F.; Azimi, B.; Esposito Salsano, J.; Digiacomo, M.; Macchia, M.; Danti, S.; Di Stefano, R. Waste Autochthonous Tuscan Olive Leaves (Olea Europaea Var. Olivastra Seggianese) as Antioxidant Source for Biomedicine. *Int. J. Mol. Sci.* **2019**, *20* (23), 5918.

(128) De la Ossa, J. G.; Fusco, A.; Azimi, B.; Esposito Salsano, J.; Digiacomo, M.; Coltelli, M.-B.; De Clerck, K.; Roy, I.; Macchia, M.; Lazzeri, A.; Donnarumma,

G.; Danti, S.; Di Stefano, R. Immunomodulatory Activity of Electrospun Polyhydroxyalkanoate Fiber Scaffolds Incorporating Olive Leaf Extract. *Appl. Sci.* **2021**, *11* (9), 4006.

(129) De la Ossa, J. G.; Danti, S.; Esposito Salsano, J.; Azimi, B.; Tempesti, V.; Barbani, N.; Digiacomo, M.; Macchia, M.; Uddin, M. J.; Cristallini, C.; Di Stefano, R.; Lazzeri, A. Electrospun Poly(3-Hydroxybutyrate-Co-3-Hydroxyvalerate)/Olive Leaf Extract Fiber Mesh as Bio-Based Scaffold for Wound Healing. **2021**, *Submitted.*

(130) Benavente-García, O.; Castillo, J.; Lorente, J.; Ortuño, A.; Del Rio, J. A. Antioxidant Activity of Phenolics Extracted from Olea Europaea L. Leaves. *Food Chem.* **2000**, *68* (4), 457–462.

(131) Chuysinuan, P.; Thanyacharoen, T.; Techasakul, S.; Ummartyotin, S. Electrospun Characteristics of Gallic Acid-Loaded Poly Vinyl Alcohol Fibers: Release Characteristics and Antioxidant Properties. *J. Sci. Adv. Mater. Devices* **2018**, *3* (2), 175–180.

(132) Alessandri, S.; Ieri, F.; Romani, A. Minor Polar Compounds in Extra Virgin Olive Oil: Correlation between HPLC-DAD-MS and the Folin-Ciocalteu Spectrophotometric Method. *J. Agric. Food Chem.* **2014**, *62* (4), 826–835.